86TH ANNUAL
Field Conference of Pennsylvania Geologists

DATING IN THE PLEISTOCENE

Establishing a Glacial Chronology in Northwestern Pennsylvania

October 6 — 8, 2022
Titusville, PA

HEADQUARTERS: Cross Creek Resort
3815 State Route 8, Titusville, PA 16354
814-827-9611

FEATURING • Erie Bluffs • Edinboro Lake • Conneaut Lake-Marsh system • Vincent Pit • McConnells Mill • Slippery Rock Gorge HIGHLIGHTING • OSL & thermoluminescence dating • kames & eskers • sand & gravel pits • paleoshorelines & ancient deltas • buried bedrock valleys • moraines & more

WWW.FCOPG.ORG

TRIP LEADERS
& GUIDEBOOK CONTRIBUTORS

Gary Fleeger • Pennsylvania Geological Survey *(retired)*

Frank Pazzaglia • Lehigh University

Eric Straffin • PennWest University Edinboro Campus

Fred Zelt • Earth Science Excursions LLC

Aaron Bierly • Pennsylvania Geological Survey

Duane Braun • Prof Emeritus Bloomsburg University

Jocelyn Spencer • Glacial Sand & Gravel Co.

Gary D'Urso

Todd Grote • Indiana University SE

Brian Zimmerman • PennWest University Edinboro Campus

Katie Tamulonis • Allegheny College

Michael Simoneau

SPONSORS

Pennsylvania Geological Survey
Lehigh University • PennWest University Edinboro Campus
Allegheny College • Indiana University SE

PRE-CONFERENCE
Field Trips & Registration
Thursday, October 6, 2022

ROCK SWAP

Silent Auction
BENEFITING
Student scholarship fund

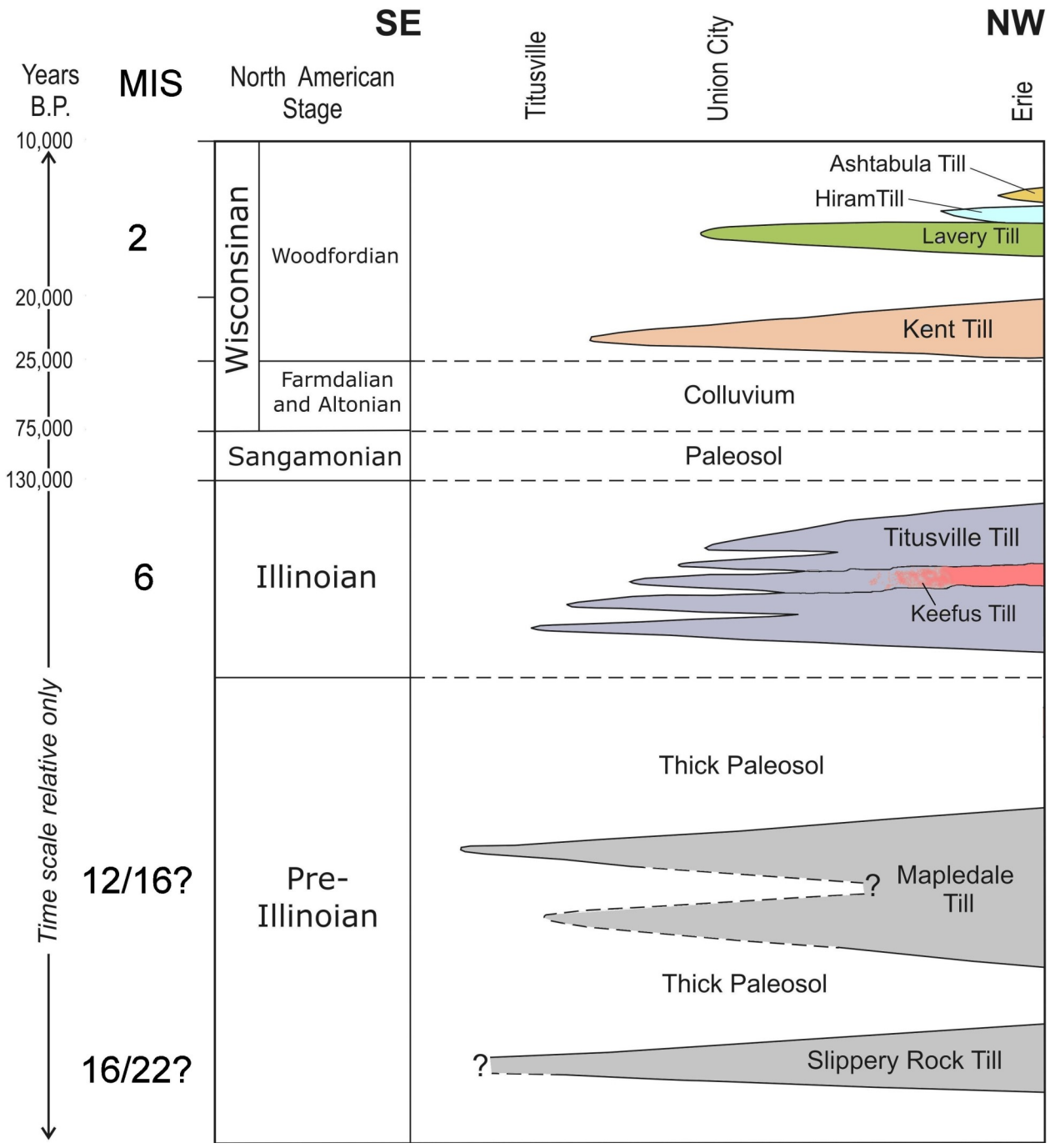

NW PA Glacial Time-Distance Diagram

modified from White, et.al., 1969

GUIDEBOOK

DATING IN THE PLEISTOCENE

ESTABLISHING A GLACIAL CHRONOLOGY IN NORWESTERN PENNSYLVANIA

86TH FIELD CONFERENCE OF PENNSYLVANIA GEOLOGISTS – 2022

Figure 1. *Map of Day 1 and Day 2 Stops.*

ACKNOWLEDGEMENTS

When I agreed to organize this Field Conference, I realized that I would have to rely heavily on others to contribute to it. They have come through spectacularly. So many thanks to leaders Aaron Bierly, Gary D'Urso, Todd Grote, Frank Pazzaglia, Mike Simoneau, Jocelyn Spencer, Eric Straffin, Katie Tamulonis, and Brian Zimmerman. Duane Braun also contributed significantly to stop descriptions and articles, but could not attend the Field Conference.

I also thank stop owners/managers/superintendents for granting permission to use their facilities for stops - Don May (ACA), Mathew D. Greene, manager Erie Bluffs SP, Boroughs of Edinboro and Conneaut Lake, John Vincent, Mike Mortimer (McClymonds), Dustin Drew, manager of McConnells Mill State Park, Vic and Daniel Cheeseman, Jocelyn Spencer (Glacial Sand and Gravel).

Robin Anthony, guidebook editor, put up with numerous late submissions, making her job more difficult. After having been the guidebook editor for many years, I can relate working with people who don't understand the concept of deadlines. I am now one of them.

The Field Conference officers thank supervisors of Worth, Muddy Creek and Brady Townships, Kaylin Hudson from West Liberty Borough; Jason Bishop from Plain Grove Township; Joe Sporer, manager of Sugarcreek Borough; Road Foreman of Slippery Rock Township for giving us permission to travel the roads for one-time passing.

In addition to the field trip stop leaders and other guidebook contributors, we wish to thank the following for their assistance in the preparation of this year's Filed Conference:

- PennDOT - Anthony P. Pioli, P.E. and Mike Mattis of Engineering District 10-0 in Indiana for clarifying questions about local roads and bridges
- Natalie Simon, Environmental Education Specialist at McConnell's Mill
- Karissa from Cross Creek Resort, who has helped us with the reservations and food
- Clarks Donuts for providing Donuts and Coffee orders
- Stewart's Catering for boxed lunches
- Janet Polka for permission access to her private land for Bill Bragonier's pre-conference trip
- Pre-Conference Leaders

  Bill Bragonier
  Fred Zelt
  Bill Kochanov
  Gary Fleeger
  Ivy Kuberry
  Katie Schmid

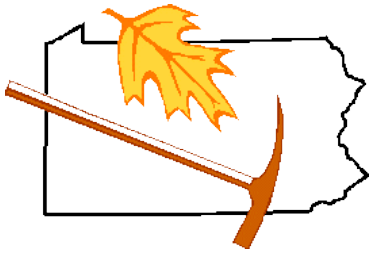

There are undoubtedly others who have been omitted, and we apologize for these omissions.

Gary M Fleeger

INTRODUCTION AND TRIP GOALS

GARY M FLEEGER

Welcome to Titusville, best known as the location where the modern oil industry began. Less well known is that it was the home of the Heisman Trophy namesake, John Heisman, and muckraker author, Ida Tarbell, who helped bring down Rockefeller's Standard Oil with her books, The Rise of the Standard Oil Company, in 1902, and The History of The Standard Oil Company: the Oil War of 1872, in 1908.

This is the third Field Conference headquartered at Cross Creek Resort. We were here previously in 1976 and 2009. Titusville, before Cross Creek, also hosted the 1959 Field Conference for the Drake Well centennial. All four Titusville Field Conferences looked at glacial geology, but this is the first that is exclusively concerned with glacial geology.

The Grand River sublobe of the Erie Lobe of the Laurentide ice sheet invaded northwestern Pennsylvania a number of times. An article in the 2005 Field Conference guidebook provides a summary of the various glaciations. The time-distance diagram on the inside of the front cover of this guidebook shows the known glacial advances into northwestern Pennsylvania, and their probable ages. Deposits from the Slippery Rock glaciation have infrequently been found, and some additional old tills have been found, but not enough to identify, name, and place in the glacial sequence. The Keefus Till, as defined (red, high carbonate), has been found only within 20 miles of Lake Erie on the Lake Plain in Ohio. The representation of the Keefus being within the Titusville on the time-distance diagram is based on my interpretation of Stop 5 of the 2005 Field Conference. To my knowledge, no additional work has been done on this problem to verify, refine, or refute that interpretation. The approximate distribution of the various tills at the surface is shown in Figure 2 of this year's guidebook article on previous published dates. Some modifications have been made since that map was published in 1969 (PaGS General Geology Report 55).

Over the next 2 days, we will look at the glacial geology of northwestern Pennsylvania, concentrating on attempting to establish a chronology. We have had a paucity of published absolute dates established in northwestern Pennsylvania, and not much more in northeastern Ohio and western New York. Most have been radiocarbon dates, but in recent years, other methods, specifically OSL (Optically Stimulated Luminescence) and TCN (Terrestrial Cosmogenic Nuclides) have been used. These methods have the benefit of being able to determine ages much older than can be done with radiocarbon, which can be used only for Wisconsinan dates. They also do not require the preservation of organic material.

This Field Conference will introduce a number of OSL dates in our attempt to develop a chronology. In recent years, Eric Straffin and Todd Grote have been using OSL and ^{14}C and detailed lidar imagery to refine the glacial margins and date the glaciation in northwestern Pennsylvania in Erie and Crawford Counties. Likewise, after his work in the Ohiopyle area, visited during last year's Field Conference, Frank Pazzaglia with Mike Simoneau investigated the Slippery Rock Gorge and West Liberty areas, obtaining additional OSL and IRSL (Infrared Stimulated Luminescence) dates. Gary D'Urso and I (as well as Frank Preston in the 1940s and 50s) have also studied the origin of the Slippery Rock Gorge. Gary and I will discuss our interpretations at Stops 7 (McConnells Mill) and 8 (Cheeseman delta).

Several of the stops have been visited by the Field Conference in previous meetings. Stop 5 parallels a stop from 1976, in that it is in the same kame deposit, but a different quarry. We took a couple of samples for OSL dating, but unfortunately, did not receive the results in time for inclusion

in the guidebook. Perhaps we will have them before the Field Conference so we can discuss them at the stop. Our interpretation is that the deposits are related to the Mapledale Till. If so, we will have our first absolute date of the Mapledale glaciation. Stop 8 was visited way back in 1950. Frank Preston, the driving force behind the creation of nearby Moraine State Park in the 1960s, discussed this site in relation to the origin of the Slippery Rock Gorge. We will do likewise, but we also have our first absolute date for the Titusville glaciation in Pennsylvania from this site. Stop 9 was a stop in 2009, when we looked at the sedimentology of the kame delta. This year, we will look at more detailed quantitative analysis of the deposits, by Katie Tamulonis and students, as well as discuss some new OSL dates obtained here.

SPEAKERS

Al Guiseppe, PG
Geoscience Manager
aguiseppe@pa.gov

Craig Ebersole, PG
Senior Geoscientist
craebersole@pa.gov

Geologic & Geographic Information Services
PA Department of Conservation and Natural Resources
Bureau of Geological Survey
3240 Schoolhouse Road
Middletown, PA 17057-3534

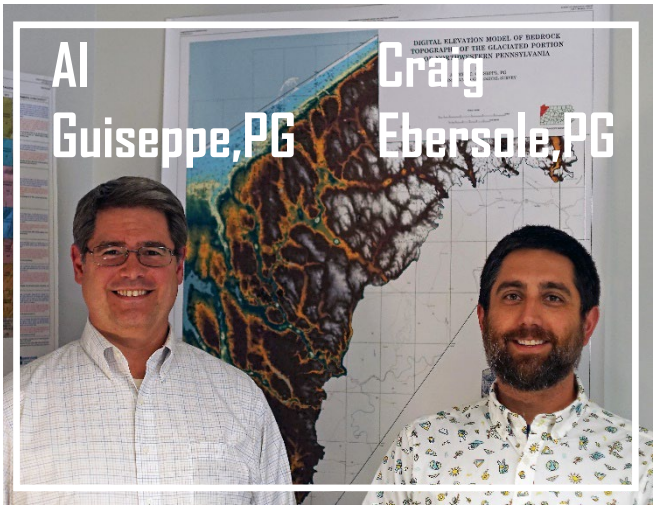

The Pennsylvania Geological Survey is embarking on a new endeavor to create a 3D geologic model of Pennsylvania as part of the US GeoFramework Initiative. Spearheading the effort is Al Guiseppe, the newly hired Geoscience Manager of the Geologic and Geographic Information Services Division at the Survey. With over 20 years of professional experience working at the intersection of geologic sciences and GIS technology, Al aims to bring a computer-aided 3D modeling perspective to traditional geologic mapping projects. Craig Ebersole, a professional geologist of 5 years, is a core member of the GIS team to bring about the 3D revolution at the Survey. In addition to wrestling with raster math to generate geologic surfacing in GIS software, Craig captures 3D point cloud data of geologically significant field locations using an unmanned aerial vehicle, or drone.

As a first step towards this ambitious goal of creating a 3D geologic model of Pennsylvania, the Survey has set out to create digital elevation models of major bounding surfaces. Towards this end, the Survey has developed a surface that represents the bedrock elevation beneath the unconsolidated sediments of the northwest glaciated portion of the state. Over the years, geologists have used subsurface data found in water wells, geotechnical borings, and seismic surveys to map the bedrock elevation in this area. Contouring the data by hand, the process of generating a bedrock elevation contour map is a laborious process and subject to radical changes in interpretation whenever new data is collected. Using digital mapping techniques, geostatistical analysis, and GIS workflow models, the Survey is striving to create a method to generate the bedrock elevation surface that relies more on automated computer processing than time-consuming manual efforts to allow for rapidly updating surfaces as new data is collected.

Guidebook for the
86th ANNUAL FIELD CONFERENCE OF PENNSYLVANIA GEOLOGISTS
October 6 — 8, 2022
DATING IN THE PLEISTOCENE
Establishing a Glacial Chronology in Northwestern Pennsylvania

Editors
Robin Anthony, Pennsylvania Geological Survey, Pittsburgh, PA
Ellen Fehrs, Pennsylvania Geological Survey, Middletown, PA
with contributions from Craig Ebersole

Field Trip Organizers
Gary Fleeger, Pennsylvania Geological Survey *(retired)*
Frank Pazzaglia, Lehigh University
Eric Straffin, PennWest University – Edinboro Campus

Field Trip Leaders and Guidebook Contributors
Gary Fleeger
Frank Pazzaglia
Eric Straffin
Fred Zelt
Aaron Bierly
Duane Braun
Gary D'Urso
Jocelyn Spencer
Todd Grote
Katie Tamulonis
Michael Simoneau
Brian Zimmerman
Christopher Laughrey
Tamara Misner
Lara Homsey-Messer
Andy Myers
Allan C. Ashworth
Dorothy M. Peteet
Margaret A. Davis
Brendan J. Culleton
Noelle Kid
Zachary Cole
Fred Baldassare

Hosts
Pennsylvania Geological Survey
Lehigh University
PennWest University – Edinboro Campus

Headquarters: Cross Creek Resort, 3815 State Route 8, Titusville, PA 16354

MEMORIAL TO EDWARD COTTER

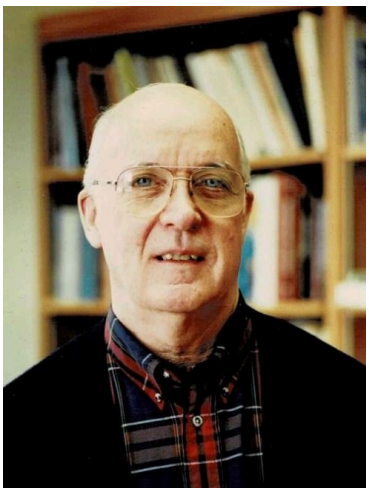

On May 13, 2022, Ed Cotter, professor emeritus at Bucknell University, passed away at age 85 in Shrewsbury, Massachusetts. Ed was a past attendee and leader of the Field Conference. He was also my first geology professor, when I took his Physical Geology class at Bucknell in 1974. It was after that class that I decided to switch my major to Geology, so it's all his fault. He was the last survivor of the "big three" professors from my years at Bucknell- Ed, Dick Nickelsen, and Jack Allen. I last saw him in 2014 at Nick's memorial service.

Ed did sedimentological research in Montana, Utah, Mexico, Ireland, Australia, and South Africa. But with the wealth of geological exposures available, he spent years studying the rocks in his own backyard in central Pennsylvania.

As with the other professors at Bucknell, Ed was very field oriented. Our classes always included almost weekly field trips, learning methods of field observation. Ed was known for his hand signals out the car window at 65 mph to indicate geologic features. Ed also organized and ran student field trips to the western US during Bucknell's January Program, that was a month-long, between semester program that existed at that time.

Ed Cotter reading a map on a Jan Plan trip about 1975. Roger Kerr, Robin Glaspey, and 2 unidentified students.

That field emphasis and central Pennsylvania research certainly translated well into Ed's participation in the Field Conference. He and Nickelsen organized and ran the 1983 Field Conference, Silurian Depositional History and Alleghanian Deformation in the Pennsylvania Valley and Ridge. This remains the largest Field Conference trip with 235 registrants, a 5-bus trip, if I recall correctly, at a time when undergraduate student participation was discouraged and was prior to the need for education credits now needed for geologist licensing. At the 1983 Field Conference, Ed presented years of research on the sedimentology of the Devonian and Silurian succession in central PA. At each of the 8 stops, Ed and Nick provided a thorough sedimentological and structural analysis of the rocks we were seeing.

Ed also was a co-leader of the 1986 Field Conference, in commemoration of the 150th anniversary of the Pennsylvania Geological Survey. He co-authored (with Jon Inners) an article on Silurian stratigraphy and sedimentology, and co-led (again with Jon) a stop at Allenport.

Ed, Nick and Jack are largely responsible for the high-quality geological education at Bucknell that continues today. Their reputation and department-building are responsible for Bucknell seeming to be one of the few separate Geology departments remaining at liberal arts schools. When I attended in the mid-1970s, Geology was combined with Geography. As opposed to the current trend of combining Geology with other departments, at Bucknell, Geology separated as a separate department in the early 1980s, and remains a separate department, now Geology and Environmental Geosciences.

Gary M Fleeger

TABLE OF CONTENTS

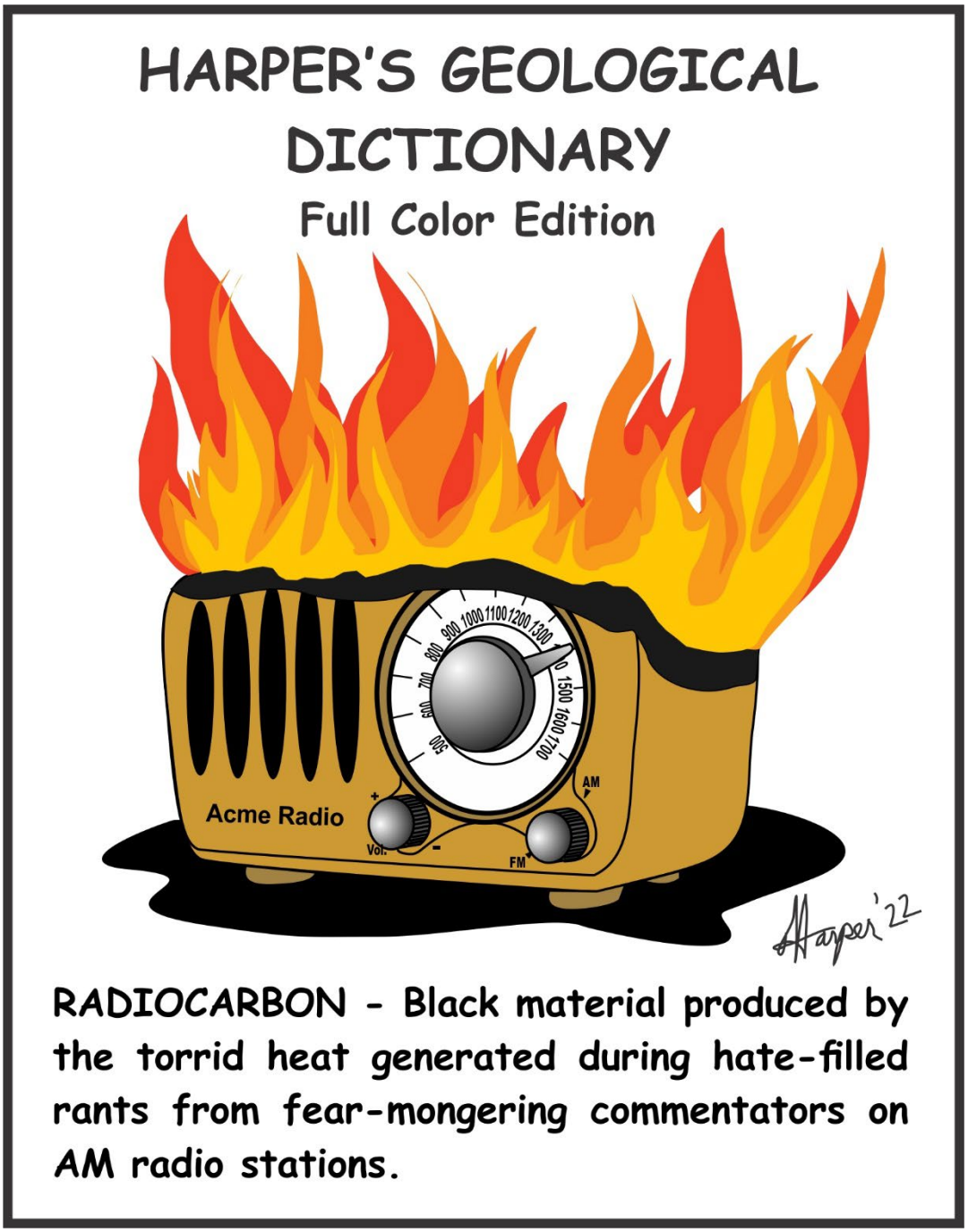
HARPER'S GEOLOGICAL DICTIONARY
Full Color Edition
Acme Radio
Vol.
AM
FM
Harper '22
RADIOCARBON - Black material produced by the torrid heat generated during hate-filled rants from fear-mongering commentators on AM radio stations.

BUT IS THERE REALLY A SLIPPERY ROCK?

VIRGINIA AND WILLIAM LYTLE

Note: This article was originally published in Pennsylvania Geology, volume 5, no. 1 (1974). It is reprinted here, slightly modified.

The fame of the Slippery Rock football team, the Rockets, dates back to 1936, when a playful sports writer "proved" that this team deserved the title of Best in the Nation. The Rockets beat Westminster 14-0, which beat West Virginia Wesleyan 7 -6, which beat Duquesne 2-0, which in turn beat Pittsburgh 7-0, which beat Notre Dame 26-0, which beat Northwestern 26- 6, which beat Minnesota 6-0.

The question, through the years, as Slippery Rock football scores are broadcast across the nation, has been, "Is there really a Slippery Rock?"

Slippery Rock State College [now Slippery Rock University of PA] was named for the town of Slippery Rock, which was named for Slippery Rock Creek. Town and college are located about fifteen miles northwest of Butler, Pennsylvania. Slippery Rock Creek originates near Murrinville in northern Butler County, circles around the town of Slippery Rock, is joined by Wolf Creek below Slippery Rock, tumbles down the scenic gorge through McConnell's Mill State Park, joins the Connoquenessing Creek before entering the Beaver River below Ellwood City - a distance altogether of about thirty-five miles.

One morning this spring I asked my husband, "Do you suppose there really is one special slippery rock, and, if there is, does anyone know where it is?"

I asked the right person. Bill Lytle is in charge of oil and gas studies with the Pennsylvania Geological Survey. "I have the information at the office," he said. "It's on an old map."

Seeing it on a map is one thing. Seeing it on location is another. On a Sunday in June, we drove to Wurtemburg in Lawrence County and walked as close as we could get to the tangle of cliff and brush that lined the eastern bank of the creek just below the map location of "The Slippery Rock" on J.P. Lesley's Slippery Rock Creek map of 1864. Now, more than a century later, the meanders of the creek bed still match those on the map.

Bill approached the owner of the house on the east side of the creek just south of the Slippery Rock location according to the Lesley map. "I have reason to believe that the rock this creek was named for is just a few hundred feet upstream from here," he said to John Eicholtz.

"I've had people come here trying to sell me things, wanting to buy my horses, asking me questions - but you're the first person ever came here to tell me that I own the original Slippery Rock!" Eicholtz replied.

Bill asked if we might walk upstream and check it out by the map.

"The water's too high now. Walking would be plenty slippery. Come back later - after we've had a spell of dry weather. Come back in September and I'll go along upstream with you," Eicholtz suggested.

Between June and September Bill and I read all we could find of the area folklore. In Sipe's History of Butler County, Pennsylvania, we read of an incident dating back to the American Revolution. "Hassler, in his 'Old Westmoreland,' says that Slippery Rock Creek received its name from an incident that occurred while Brodhead's expedition was crossing this stream. The troops crossed the creek at a place where there were many large, smooth, level rocks in the bed of the stream. On one of these rocks, the horse of John Ward slipped and fell, severely injuring the rider. Then the soldiers are said to have called this 'branch of the Beaver' Slippery Rock."

But John Ward wasn't the first man to find the rocks slippery. Further in the same chapter: "The Moravian missionary, John Heckewelder, who was in the Slippery Rock region many years before the time of Brodhead's expedition, says that the Delaware Indians called this stream 'Wescha-cha cha-pohka,' that is, a slippery rock."

Reading on, we learned: "On Hector St. John Crevecoeur's "Map of the Old West," published in 1787 - Slippery Rock Creek is designated as Riviere de la Pierre Platte "

With all three names - Slippery Rock, Wescha-cha-cha-pohka, and Pierre Platte (Flat Rock) - the singular is used. Is there a particular slippery flat rock, or are the rocks in the creek bed slippery and flat in a general sort of way?

Lesley, whose map and profile of a line of levels along Slippery Rock Creek is appended to the Second Geological Survey, Special Report J on the Petroleum of Pennsylvania, was State Geologist at the time of the report's publication in 1874. Lesley's information about the origin of the name of the creek probably came from old- timers in the area.

If it is a particular rock, what makes it so slippery? Ralston, in Early Life Along the Slippery Rock, noted that the rocks along the stream tend to collect and hold a quantity of mud - "Some would hold an inch of it, and sloping ice or soft soap was scarcely as slippery. One had to walk circumspectly to avoid falling, It was doubtless always called Slippery Rock. Whatever fanciful meaning someone may have given, it is not an Indian name. It was not named because one of Brodhead's men fell down in its water; the difficulty was to cross it at all without falling down."

So - back where we started - with a hint of an answer to another question. Why, of all the more or less slippery rocks along thirty-five miles of stream - why this particular rock? Brodhead's men were crossing the stream. Ralston says, “The difficulty was to cross it at all without falling down." Could the Slippery Rock have been located at a ford - a place where Indians, early settlers, and soldiers, before there were bridges, crossed the stream on foot or horseback?

What should we expect to find in September when the creek would be low enough to allow passage to the Rock? Lesley, in his report, says: "The Slippery Rock, which gave name to this fine stream at the first settlement of the country, is a plate of sandstone lying in place on the east bank, about a mile above Van Gordon's bridge, where there was a natural exudation of petroleum."

Bill researched the following information: "This "Natural exudation of petroleum" or oil seep, was located in Lawrence County about a mile and a half north of Wurtemburg, along the Slippery Rock Creek, and was the reason the area was drilled originally for oil and gas. The oil seeped out of the Upper Connoquenessing sandstone at stream level. Wells drilled in the

area found oil in paying quantities at approximately 200 feet below stream level in the Shenango sandstone. The productive oil pay in the Shenango sandstone was named the Slippery Rock oil sand. The Lawrence well was probably the first commercial well in the area, with an initial production of fifty barrels of oil per day, drilled soon after the Drake well. The oil field discovered by the Lawrence well was named the Slippery Rock oil field.

September. With Eicholtz guiding us, we hop carefully from stone to stone along a gently sloping stream bank. The east wall of the gorge rises abruptly a few feet beyond the shoreline. There is no place to fall except into the creek. It is each-man-for-himself as we pick our footing in quiet concentration. I am carrying the 1874 collector's item, Report J with its 1864 map of Slippery Rock Creek (**Plate 1**) and wishing with all my heart that I had left it in the car.

The main difference in the terrain when we reach the Rock is, to my untrained eye, that, instead of hopping from slippery stone to slippery stone, we are standing now on one flat, gently sloping, moist rock. It is covered (as are the smaller stones) with algae and moss - that glistens with an oily appearing iridescence. The sloping rock had been resistant to the rushing force of the stream and now provides the creek with a deceptively almost level bank and bed. The exposed portion of the solid rock extends along the edge of the creek for at least 25 feet. The dampness that covers the rock comes from a trickle of water seeping from between strata of shale and coal along the wall of the gorge. For the length of the exposed slippery rock there is no dry bank to walk on - just the creek, the moist, sloping slippery rock, and the gorge. "Well, what did you expect?" I ask myself. "This is The Slippery Rock!"

"No," I hear Bill saying. "The iridescence adhering to the algae and moss is not oil.

When oil on water is disturbed, it re-forms in one mass. The substance here, when disturbed, fragmentizes. This is an iron oxide film - not an oil film."

I've rough-sketched the picture. Bill can fill in the geological details. "Although no oil was seen seeping out of the sandstone, none was expected, since the gas pressure which used to force the oil out had been depleted long ago by the oil wells of the area. A sheen of color now seen near the contact of the Mercer and Upper Connoquenessing, was identified as an iron oxide film. The evidence points to this plate of rock as being that described by Lesley and designated at The Slippery Rock (Figure 1).

Figure 1. *The Slippery Rock?*

"From the description by Lesley of the location of the Slippery Rock, it is determined that it is just above the Glasser bridge on the Van Gorder road about one and a half miles north of its junction, at Wurtemburg, with Route 488. The Van Gordon (Van Gorder) bridge shown on Lesley's map is no longer standing. Above the Glasser bridge, for about three hundred feet, can be seen what appears to be shales and coals of the Mercer formation, extending from the edge of the creek, on up the steep hillside. At one place the underlying Upper Connoquenessing sandstone can be seen at stream level lying under the Mercer. This is apparently the "plate of sandstone lying...on the east bank," described by Lesley. It dips beneath stream level downstream before the stream reached the bridge."

Wallace notes in his *Indian Paths of Pennsylvania*, p. 82, that the Indian path, "the Kuskusky-Ohio Forks Path, from Pittsburgh to New Castle...crossed Slippery Rock Creek in the vicinity of Wurtemburg..." Could this ford have been at the Slippery Rock described by Lesley? If so, then this particular rock - excessively slippery due to an oil seep at the point where the stream was forded on foot or horseback - could be the name Slippery Rock given to it by Indians and early settlers as a warning, "Cross here but watch your footing!"?

This isn't Plymouth Rock or the Rock of Gibraltar. But how many rocks have named a creek, a town, an oil field, an oil sand, a college, and a favorite football team?

The Rock is on the John Eicholtz property [it is no longer the Eicholtz property]. It can be seen along the east bank of the creek from the Glasser bridge - or from the west bank, looking across and downstream, from the southern tip of Camp Allegheny, the Pittsburgh Salvation Army Camp. Most of the rock is under water. All of it is algae, moss, and mud-covered - treacherous, and beautiful in its rustic setting.

Plate 1. 1864 Map of Slippery Rock Creek

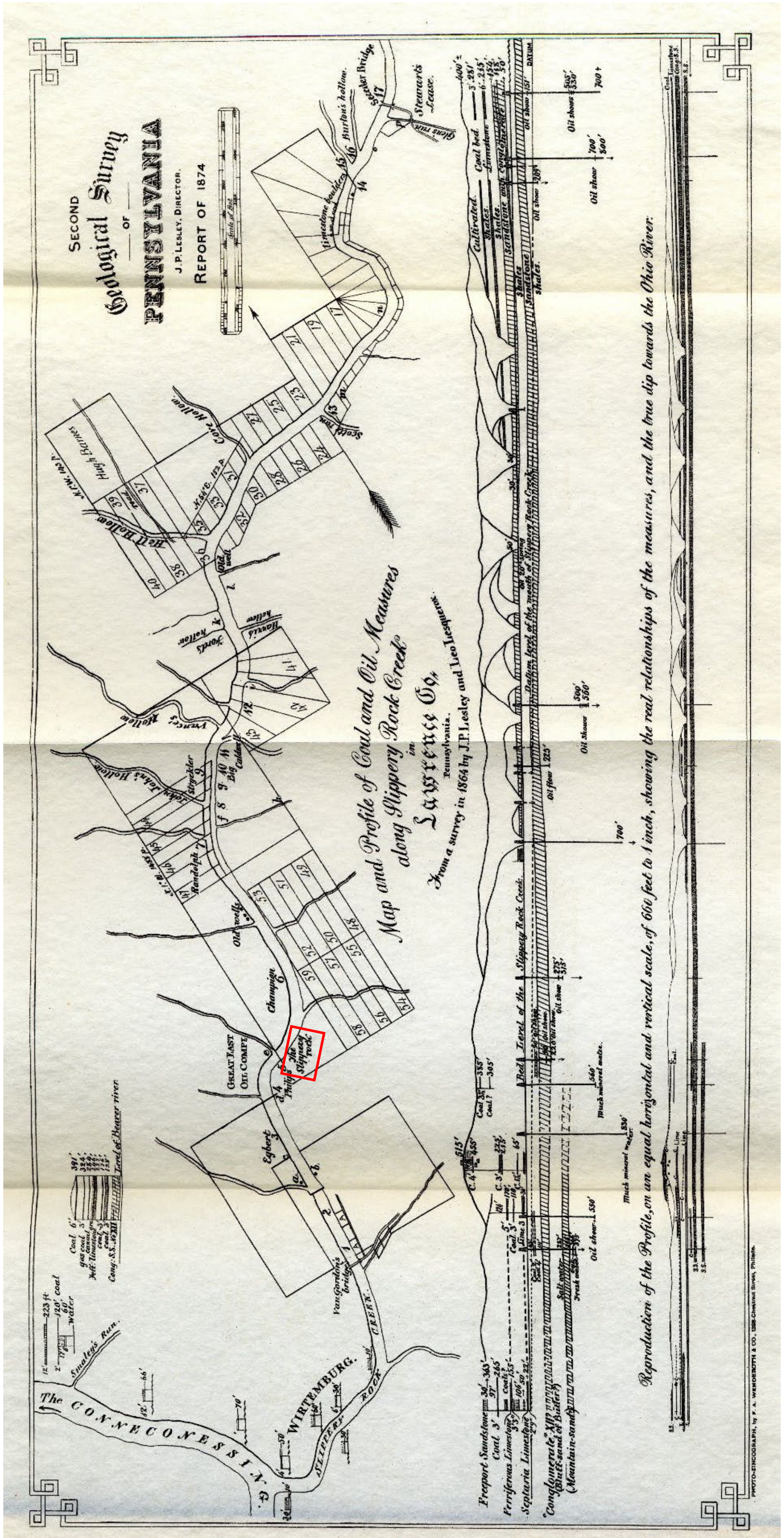

References

Lesley, J. P. (1874) Map and profile of a line of levels along Slippery Rock Creek, in, Special report on the petroleum of Pennsylvania : its production, transportation, manufacture and statistics, Second Pennsylvania Geological Survey, Report J.

Wallace, Paul A.W. (1965) Indian Paths of Pennsylvania, Pennsylvania Historical and Museum Commission.

Ralston, William A. (1945) Early life along the Slippery Rock.

Sipe, C. Hale. (1927) History of Butler County, Pennsylvania. Topeka: Historical Pub. Co.

DATING PLEISTOCENE DEPOSITS OF NORTHWESTERN PENNSYLVANIA AND NORTHEASTERN OHIO

GARY FLEEGER – PENNSYLVANIA GEOLOGICAL SURVEY *(RETIRED)*

Introduction

This article will provide a brief review of the published dates for the glacial sediments of the Grand River sublobe and correlative sediments in the Cuyahoga, Killbuck, and Scioto sublobes of the Erie Lobe in northwestern Pennsylvania and northeastern Ohio (**Figure 1**). It will serve as a background for the more recent work started in the last few years that will supplement and expand upon the early work. This Field Conference (**Figure 2**) will present some preliminary age dating completed in the last four years, and tie it in with these earlier dates to attempt to improve our understanding of the glacial chronology of northwestern Pennsylvania.

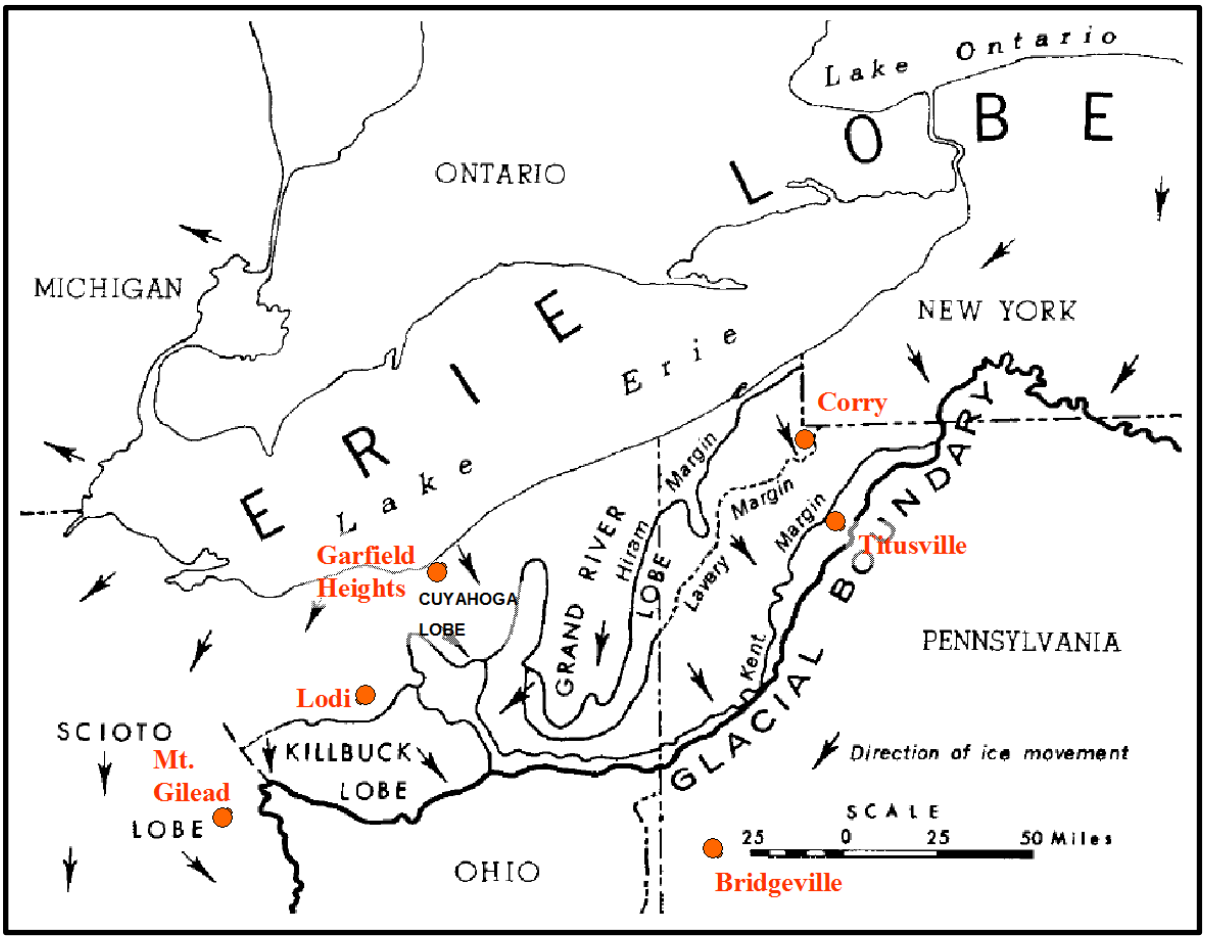

Figure 1. Outlines of the various sublobes of the Erie Lobe. *Only the Grand River sublobe extends into northwestern Pennsylvania. Correlative tills are given different stratigraphic names in different sublobes (Table 5). Locations of date sites are noted (orange dots).*

modified from Figure 1 of White et al, 1969

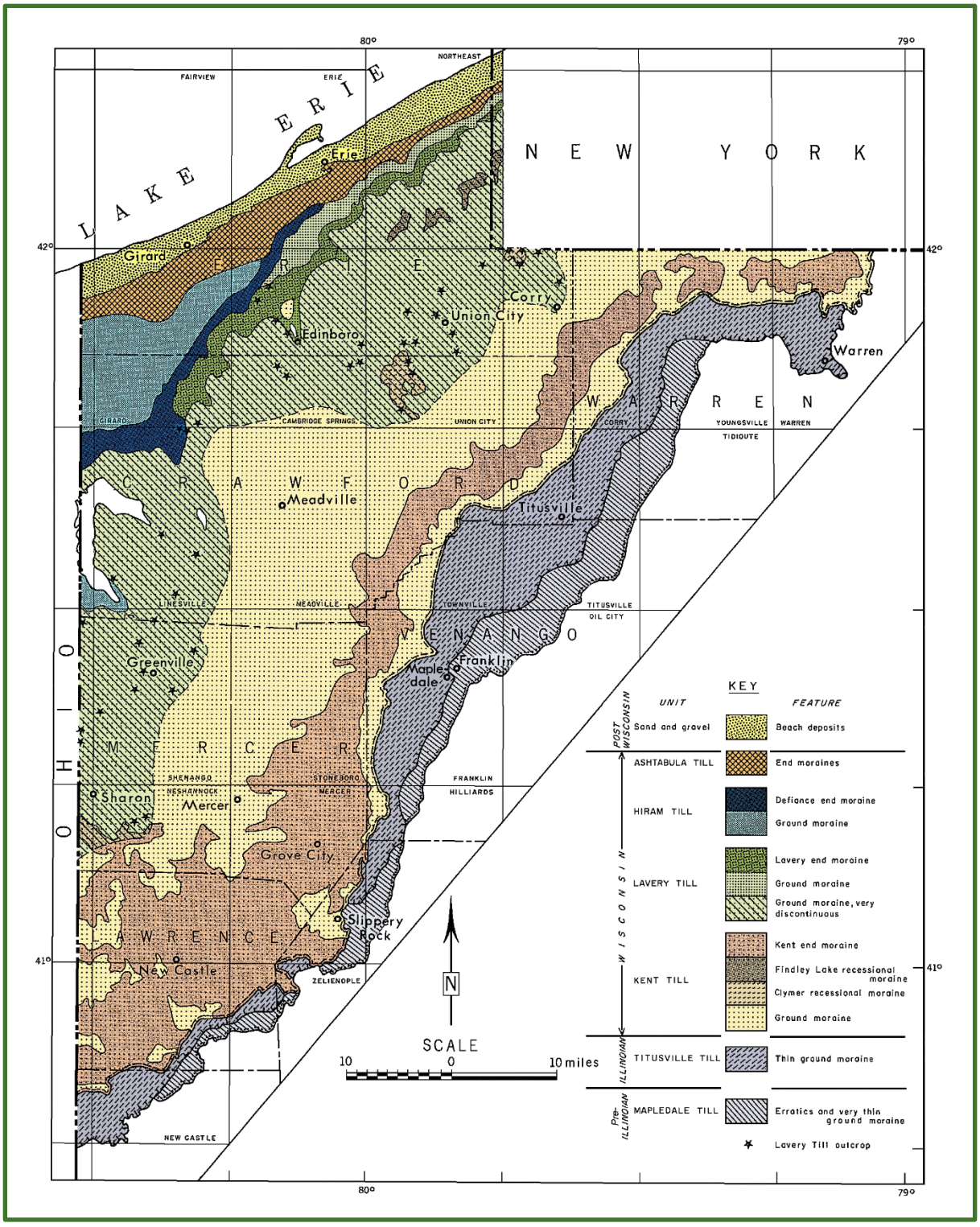

Figure 2. Map of the extent of glacial deposits of northwestern PA. *colorized from White et al, 1969*

Background

The glacial history of the Appalachian Plateau of northwestern Pennsylvania and northeastern Ohio has been well documented by the decades of study by George W. White and his many students and associates starting in the 1940s and continuing into the 1980s. Since then, there have been a few

restricted area studies done (e.g.- Ward et al, 1976; Straffin and Grote, 2010). The glacial deposits of northwestern PA were summarized in Fleeger (2005).

One aspect of the glacial history that has not been well documented is the determination of absolute ages associated with the various glacial advances and retreats. For many years, radiocarbon dating was the primary, if not sole method of absolute dating. Rarely has adequate organic material been found that would allow for dating and developing a glacial chronology for the Plateau of Pennsylvania and Ohio. After the work of White and his associates, other dating methods were developed that could be applied to the glacial sediments, but except for one instance, until recently, those methods have not been employed. For a review of the more recent dating methods used in northwestern PA, see Simoneau et al (2022).

All of the radiocarbon dates reported in these studies are uncalibrated ages. A calibration curve (**Figure 3**) can be used to convert to calendar years.

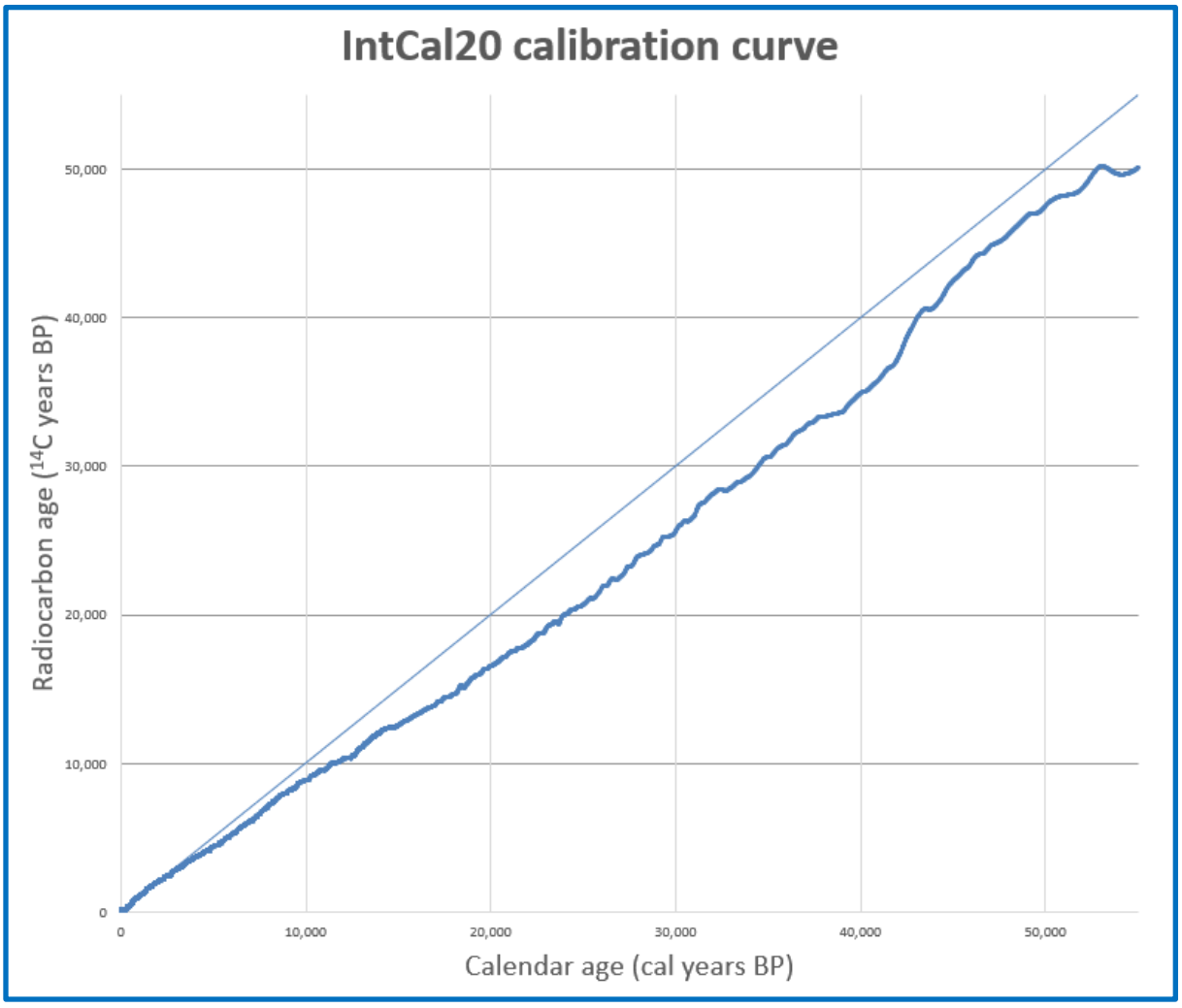

Figure 3. Calibrated ages in calendar years BP. *The thin top thin line indicates C^{14} ages. The lower line indicates calibrated ages. The divergence of the lines indicates the amount of difference in the ages.*

from Heaton, et al (2020)

Summary of earlier dating studies

Corry, PA –

(Droste, Rubin, and White, 1959; Shepps, Sitler, Droste, and White, 1959; White, Totten, and Gross, 1969): The precise location of this sample is not known. None of Droste's field maps have been located, nor has White's for the Corry 7½' quad. Droste et al (1959) described the location as 9 miles northwest from the Kent border, and 7 miles southeast from the southwest corner of New York state. Using aerial photos, what appears to be an abandoned excavation fitting that location description, just northwest of Corry (Figure 1), and currently owned by Corry Peat Products, is the likely location at 41.940333°, -79.658775 °.

At this first site where glacial sediments were dated in northwestern PA, material was extracted from a peat bog in a kettle hole, using a hand auger. Organic material from peat, as well as the underlying marl was sampled and dated (**Table 1**).

At the time of the dating, the mapping (Shepps et al, 1959) placed this site within the Kent border, and beyond the Lavery border. Therefore, they associated the oldest date at the base of the marl (14,000 radiocarbon years) as the earliest that the Kent ice retreated from this position, and the kettle was available for the accumulation of organic material. Later work by White et al (1969) extended the Lavery border past this location (Figure 3). White et al (1969) therefore reassigned this date to be the earliest time that Lavery ice retreated from the location. As a result of still later work in Ohio (see Lodi, below), this is now considered to be a minimum date for the Hiram (Totten, 1976).

Table 1. Descriptions of auger boring at Corry (Droste, et al, 1959)

Sample	Ft	Inches
Peat, brown to greenish brown, with leaves, grasses, seeds, and wood. Sample W-347 from lowest 8 in., age **9,430 ± 300** years.	9	9
Marl, light to medium gray, rich in plant material, highly calcareous, very fossiliferous, contains pelecypods, gastropods, and ostracods. Sample W-346 from top 8 in., age **13,000 ± 300** years; Sample W-365 from bottom 8 in., age **14,000 ± 150** years.	3	0
Clay, blue gray, silty, laminated, highly calcareous.	9	0
Sand and fine gravel, gray, calcareous.	1	6
Bottom of auger hole.		

Garfield Heights (Cleveland), OH –

(White, 1968, 1982; Fullerton and Groenewold, 1974; Fullerton, 1986; Szabo, 1992): Garfield Heights site is within the Cuyahoga Lobe (Figure 1) of the glaciated Allegheny Plateau (41.424671°, -81.588693°), and dates glacial sediments also exposed in northwestern PA (**Figure 4**). This site is probably the most complicated dated site discussed in this article, because it continued to be studied by numerous workers over a number of years as the exposure advanced, exposing progressively different stratigraphy (**Table 2**). The section has also been extensively studied for the flora and fauna

remains found (Leonard, 1953, Coope, 1968, Miller and Wittine, 1972, Berti, 1971 and 1975, Morgan and others, 1982).

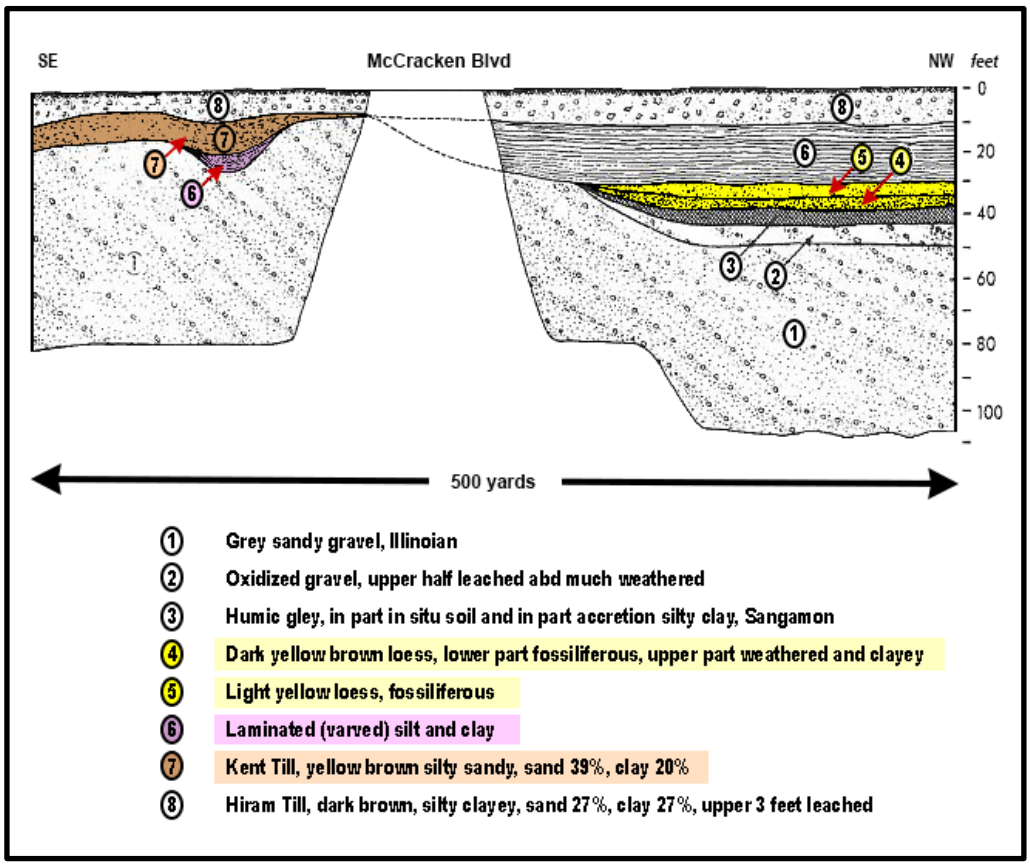

Figure 4. Sketch of sections. *modified from White, 1968*

Table 2. Composite stratigraphy* found at the site and the radiocarbon dates.

*No one section exposes all of these units. They are a composite stratigraphy developed by observations through time as mining progressed and new pits opened.

Stratigraphic unit	Dates
Hiram Till (Woodfordian)	
Lavery Till (Woodfordian)	
Kent Till (Woodfordian)	
Laminated lacustrine silt and clay	**24,600 ± 800'; 23,313 ± 391** (White, 1968) **23,560, 23,430, 22,210** (Fullerton and Groenwold (1974) **24,520 +695/-760** (Szabo, 1992)
Colluvium	
Upper loess (Farmdalian)	**28,195 ± 535** (White, 1968)
Lower loess	**27,390 ± 350** at contact between loesses (Szabo, 1992)
Accretion gley (Altonian)	
Garfield Heights Till with paleosol	
Gravel with paleosol (Sangamonian)	

The dated lacustrine sediments were interpreted as being pro-Kent, and therefore a maximum age for the Kent glaciation.

Titusville, PA –
(White and Totten, 1965; White, Totten, and Gross, 1969; Totten and Szabo, 1987; Szabo,1992):
The dated deposit at Titusville, PA (Figures 1 and 5) was a peat within gravels, that White and Totten (1965) interpreted as stratigraphically below Titusville Till and gravels exposed in a gravel pit at 41.615562°, -79.641390° (**Figure 5a**). The peat dates were **31,400 ± 2,100** years, **39,900 + 4,900 - 2,900** years, and **40,500 ± 1,000** years, placing it in the Altonian (early Wisconsinan) rather than the previous assignment as Illinoian.

However, there was a covered interval of 600 feet between the Titusville exposure and the dated sediment (Figure 5a). Subsequent work in Ontario (Eyles and Eyles, 1983; Eyles and Westgate, 1987), Illinois (Kempton and others, 1985), and northeastern PA (Braun, 1985, 1989, 1994) demonstrated that no glacier advanced beyond the Great Lakes during the Altonian, or was very restricted in extent. So the relationship between site sediments was reinterpreted to be interstadial (**Figure 5b**) alluvium and pro-Kent outwash (Braun, 1996).

Later dating of correlative sediments in NE Ohio (Mt. Gilead) indicated that the Titusville was an Illinoian glaciation (see below). This illustrates the benefit of assigning a lithostratigraphic name to the till, rather than designating it by age. The unit identification remains constant as the age interpretations change.

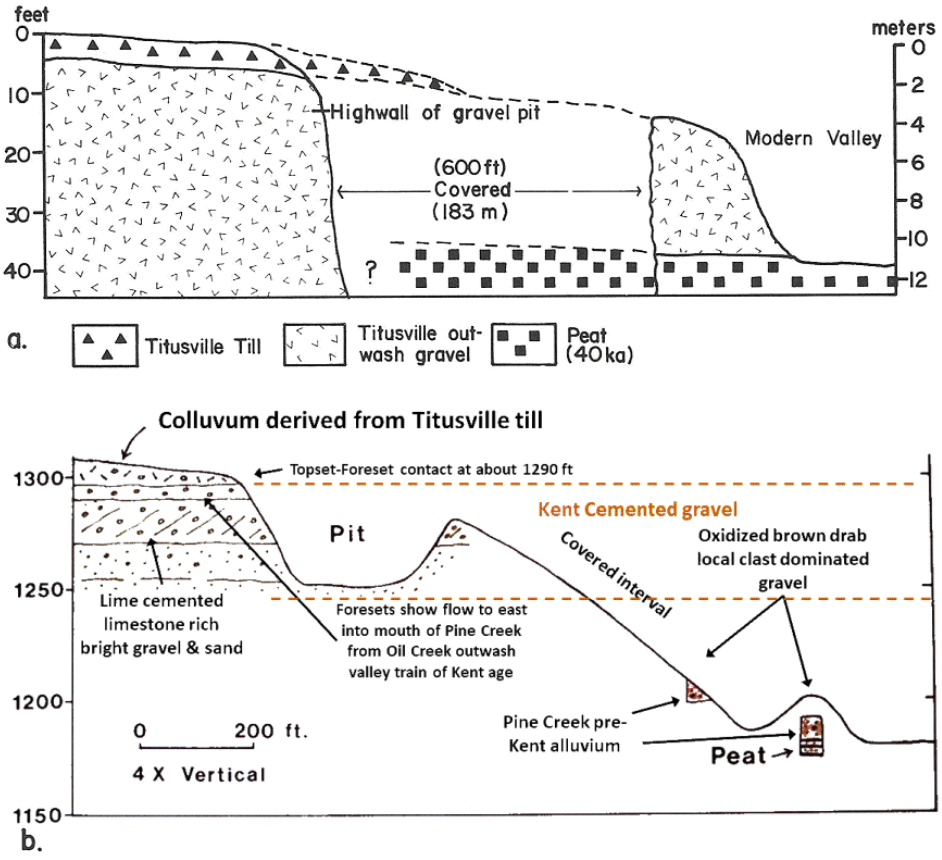

Figure 5. Two possible interpretations of the section at Titusville, PA.
a. Interpretation of White, et al (1969). From Szabo (1992).
b. Interpretation of gravel exposed in present valley as post-Titusville Till alluvium.
from Braun (unpublished)

Mt. Gilead, OH –

(Totten and Szabo, 1987; Szabo,1992): The Mt. Gilead section (40.544696°, -82.836604° ; **Figures 1** and **6**), like Garfield Heights, describes sediments that correlate with glacial sediments in northwestern PA, and showed that the age determined at Titusville was not associated with the Titusville Till. Mt. Gilead is the only published date that was not determined by carbon 14 dating, but by thermoluminesence.

Loess above 4 sheets of Millbrook Till (Millbrook Till is the name applied to the till in the Killbuck and Scioto sublobes of Ohio (Figure 1) that correlates with the Titusville Till in the Grand River sublobe), and below Kent Till correlative Navarre Till (Figure 6) was sampled, and yielded dates of **145,000 ± 25,000** years and **125,000 ± 16,000** years, establishing the Millbrook Till, and by correlation, the Titusville Till, as Illinoian.

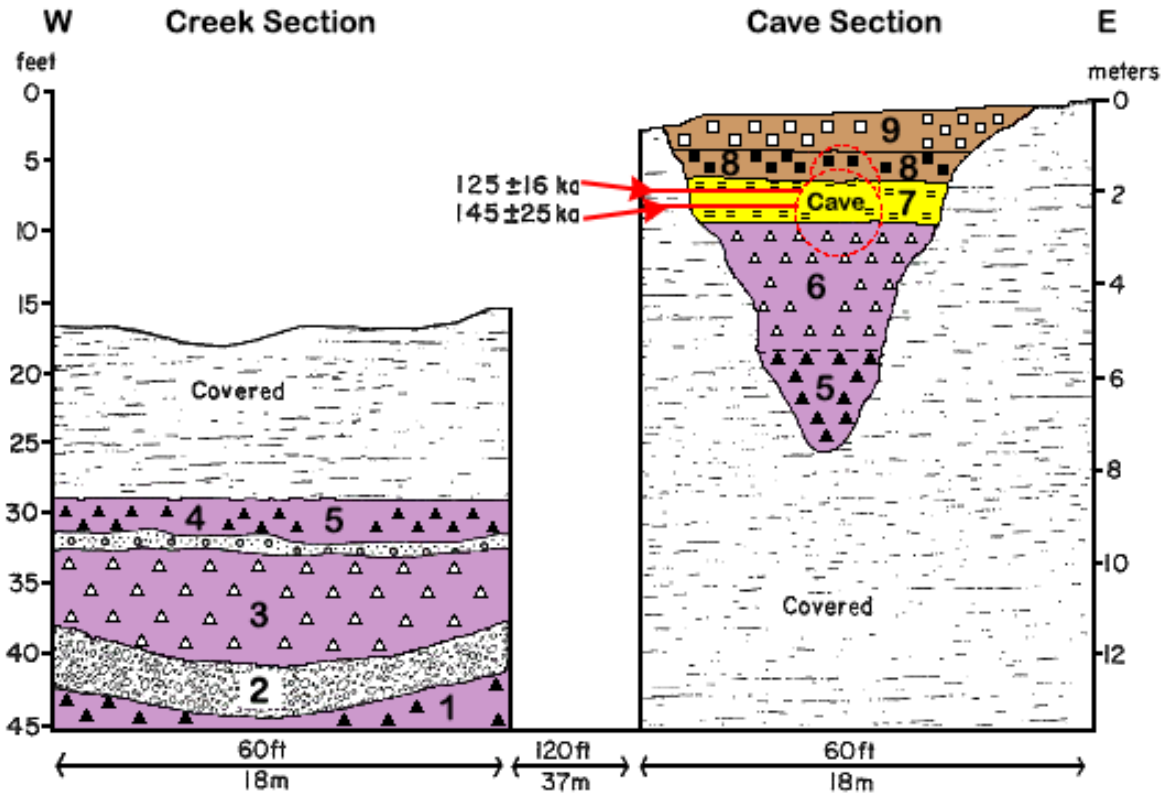

Figure 6. Section Diagram from Szabo, 1992. *The sections exposed along the north bank of Whetstone Creek at the fairgrounds at Mt. Gilead, Ohio (modified from Szabo and Totten, 1987).*

Units: 1 – Millbrook till BIV; 2 – gravel; 3 – Millbrook till BIII; 4 – sand and gravel; 5 – Millbrook till BII; 6 – Millbrook till BI; 7 – silt (loess?); 8 – Navarre till; 9 – covered Navarre till?

modified/colorized from Szabo, 1992

Bridgeville, PA –

(Schopf and Cross, 1947; Kollar and Harper, 2019): Bridgeville, in Allegheny County, southwestern PA, southwest of Pittsburgh (Figure 1), is not within the glaciated area. It is a peat

deposit associated with glacial outwash in the Ohio River valley, located at 40. 353563°, -80.121568° and supports the date of the Kent glaciation (**Table 3**).

Table 3. Radiocarbon dates established for the Bridgeville peat deposit.

Age	Reference
> 16,000	Arnold and Libby, 1951
31,390 ±86	Volman, 1981
23,340 ±600	Volman, 1981
23,170 ± 270	Volman, 1981
23,000 ± 800	Suess, 1954; Flint and Rubin, 1955
24,720 ± 130	Kollar, pers comm., Nov 21, 2019

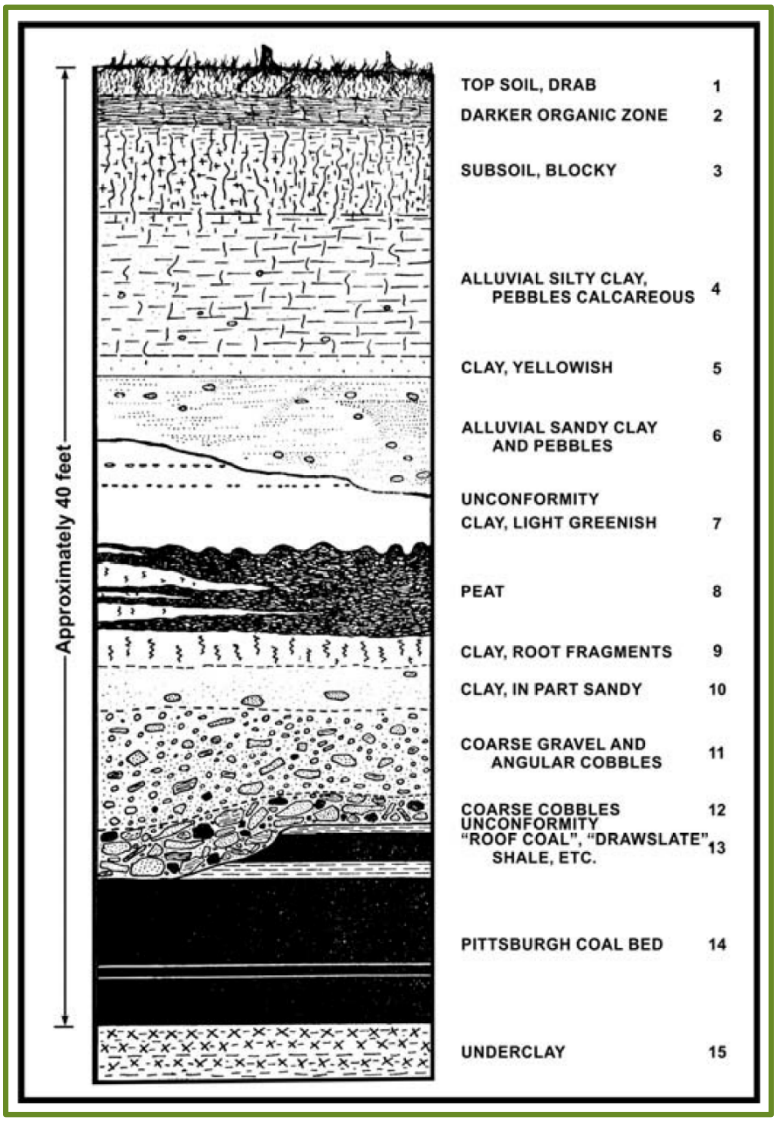

(Left) The peat is conformably sandwiched between two lacustrine clay beds (**Figure 7**), and has been interpreted as a slackwater ponding caused by damming of Chartiers Creek (tributary to the Ohio River) by active outwash aggradation in the Ohio River 8 miles downstream.

The lower clay overlain by peat may well have been deposited in an abandoned meander of Millers Run or Chartiers Creek. The site has also been studied for flora, pollen, and fauna, including mastodon bones.

Figure 7. Section exposed at Bridgeville Pleistocene bog site.
from Schopf and Cross, 1947

Lodi, OH –

(Totten, 1976): The Lodi site (Figure 1) is a filled kettle hole southwest of Cleveland (41.005675°, -81. 964415°). Because White (1982) mapped the Hiram Till at the site, the date (**Table 4**) indicates the earliest date of sediment accumulation in the kettle after the retreat of the Hiram glacier. The sediments also contain abundant plant megafossils and insects.

Table 4. Stratigraphy and dates of the Lodi, OH site.

Description	Thickness	Age (Totten, 1976)
Silt, sand, gravel (tailings pond deposits)	12 ft	
Peat	7 ft	
Clay, silt, sand, gravel, wood-bearing	12 ft	**14,050** RC YBP
Titusville Till		

Conclusion

Based on the dates in the above descriptions, White (1982) estimated the ages of the various advances (**Table 5**). The dates rarely were directly for the glacial diamicts, but with adjacent sediment that establish a minimum or maximum possible age, as discussed in each site discussion. Refer to **Figure 8** (Braun, 1994), for Marine Isotope Stages, which are alternating warm and cool periods in the Earth's paleoclimate, deduced from oxygen isotope data reflecting changes in temperature derived from data from deep sea core samples. Working backwards from the present, which is MIS 1 in the scale, stages with even numbers have high levels of oxygen-18 and represent cold glacial periods, while the odd-numbered stages are lows in the oxygen-18 figures, representing warm interglacial intervals. The data are derived from pollen and foraminifera (plankton) remains in drilled marine sediment cores, sapropels, and other data that reflect historic climate (Andrews, 2000; Wright, 2000).

Table 5. Estimated ages of the ice advances in northwestern PA. The **bolded** ice advance names are those for which published dates of associated sediments exists.

Grand River Sublobe Till Unit	White (1982) Correlative Till Unit (Sublobe)	Estimated Uncalibrated Age (White, 1982)	Marine Isotope Stage (see Figure 8)
Ashabula		15,000 (Woodfordian)	2
Hiram		17,000 (Woodfordian)	2
Lavery	Haysville (Killbuck)	19,000 (Woodfordian)	2
Kent	Navarre (Killbuck)	23,000 (Woodfordian)	2
Titusville	Mogadore (Cuyahoga) **Millbrook** (Killbuck)	40,000 (Altonian)	6
Keefus		(Illinoian)	6/12?
Mapledale	Butler (Killbuck)	(pre-Illinoian)	12/16?
Slippery Rock		(pre-Illinoian)	22?

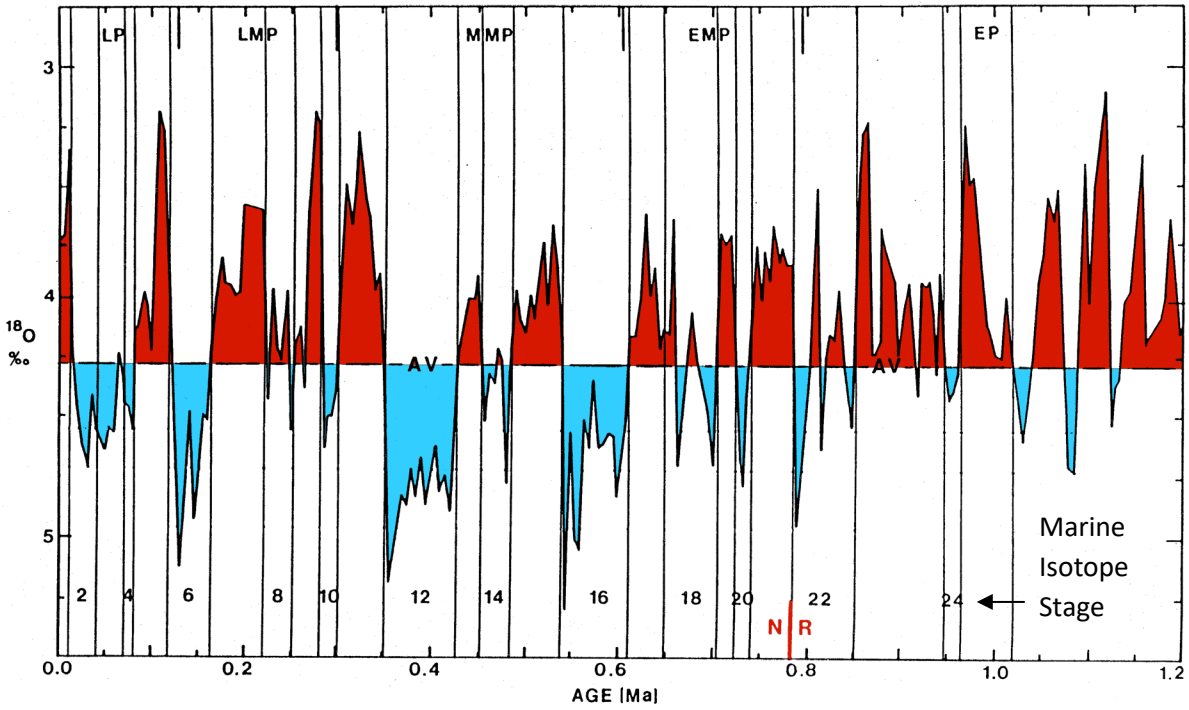

Figure 8. O^{18} percentage per age (Ma) with Marine Isotope Stage from Braun, 1994.

EP – Early Pleistocene; EMP – Early Middle Pleistocene; MMP – Middle Middle Pleistocene; LMP – Late Middle Pleistocene; LP – Late Pleistocene; N|R – Normal | Reversed Polarity. AV – Average conditions

colorized from Braun, 1994

References Cited

Andrews, John T., "Dating Glacial Events and Correlation to Global Climate Change", in Noller, Jay S., Sowers, Janet M., Lettis, William R. (eds), Quaternary geochronology: methods and applications, 2000, American Geophysical Union, ISBN 0-87590-950-7, ISBN 978-0-87590-950-9.

Arnold, J. R, and W. F. Libby, Jr., 1951, Radiocarbon dates. Science, v. 113, no.2927, p. 111-120.

Berti, A.A., 1971, Palynology and stratigraphy of the mid-Wisconsin in the eastern Great Lakes region, North America, PhD dissertation, London, Ontario, University of Western Ontario, 160 p.

Berti, A.A., 1975, Paleobotany of Wisconsin interstadials, eastern Great Lake region, North America, Quaternary Research, v. 5, p. 591 - 619.

Braun, D.D, (1985), Pre late-Wisconsinan glaciation in the Valley and Ridge of northeastern Pennsylvania, GSA Abstracts with Programs, v. 19, no. 1, p. 7.

Braun, D.D. (1989), A revised Pleistocene glaciation sequence in eastern Pennsylvania: support for limited early Wisconsinan ice and a single late Illinoian advance beyond the late Wisconsinan border, Abstracts 28th International Geological Congress, v.1, p. 196 – 197.

Braun, D.D. (1994), Late Wisconsinan to pre-Illinoian (G?) glacial events in eastern Pennsylvania, *in* Late Late Wisconsinan to pre-Illinoian (G?) glacial events in eastern Pennsylvania, USGS Open-file Report 94-434, p. 1 – 20.

Braun, D.D. (1996), The NW Pennsylvania Titusville peat site, a record of rapid climate change near to but not within the middle Wisconsin glacial limit, GSA Abstracts with Programs, v.28, no.3, p.41

Coope, G.R., 1968, Insect remains from silts below till at Garfield Heights, Ohio, GSA Bulletin, v. 79, p. 753 – 755.

Droste, John B., Meyer Rubin, and George W. White, 1959, Age of marginal Wisconsin drift at Corry, Northwestern Pennsylvania, Science, v. 130, Issue 3391, p. 1760.

Eyles, C and N. Eyles (1983) Sedimentation in a large lake: a reinterpretation of the late Pleistocene stratigraphy at Scarborough Bluffs, Ontario, Canada,. Geology, v. 11, p. 146 - 152.

Eyles, N and and J.A. Westgate (1987) Restricted regional extent of the Laurentide ice sheet in the Great Lakes basin during early Wisconsin glaciation, Geology, v. 15, p. 537 - 540.

Fleeger, G.M. (2005) Summary of the glacial geology of northwestern PA, in, Fleeger, G.M. and J.A. Harper, eds., Type sections and stereotype sections; glacial and bedrock geology in Beaver, Lawrence, Mercer, and Crawford Counties, Guidebook, 70th Annual Field Conference of Pennsylvania Geologists, Sharon, PA, p. 1-11.

Flint, R.F. and Meyer Rubin, 1955, Radiocarbon dates of pre-Mankato events in eastern and central North America, Science, v. 121 no. 3149, p. 649 – 658.

Fullerton, D.S. and Groenewold, G.H., 1974, Quaternary stratigraphy at Garfield Heights (Cleveland), Ohio, additional observations, GSA Abstracts with Programs, p. 509 – 510.

Heaton, Timothy J.; Blaauw, Maarten; Blackwell, Paul G.; Ramsey, Christopher Bronk; Reimer, Paula J.; Scott, E. Marian, 2020, The IntCal20 Approach to Radiocarbon Calibration Curve Construction: A New Methodology Using Bayesian Splines and Errors-in-Variables, Radiocarbon. 62 (4): 821–863. doi:10.1017/RDC.2020.46. ISSN 0033-8222.

Kempton, J.P., R.C. Berg, and L.R. Follmer, 1985, Revision of the stratigraphy and nomenclature of glacial deposits in central northern Illinois, *in* R.C. Berg, J.P Kempton, L.R. Follmer, and D.P. McKenna, Illinoian and Wisconsinan stratigraphy and environments in northern Illinois: the Altonian revised, Illinois State Geological Survey Guidebook 19, p.1 – 19.

Kollar and Harper, 2019, Stop 5, former Pleistocene bog site, *in* Geology and archeology of Meadowcroft Rockshelter, and the multiple ice ages of southwestern Pennsylvania, Pittsburgh Geological Society, field trip guidebook, p. 44 – 49.

Leonard, A.B., 1953, Molluscan faunules in Wisconsin loess at Cleveland, OH, American Journal of Science, v. 251, p. 369 – 376.

Miller, B.B. and Wittine, A.H., 1972, The origin of late Pleistocene deposits at Garfield Heights, Cuyahoga County, Ohio, Ohio Journal of Science, v. 76, p. 305 – 313.

Morgan, A.V., Morgan, A., and Miller, R.F., 1982, Late Farmdalian and Early Woodfordian insect assemblages from Garfield Heights, Ohio, GSA Abstracts with Programs, v. 14, p. 267.

Schopf, James F. and Aureal T. Cross, 1947, A glacial age peat deposit near Pittsburgh, American Journal of Science, v. 245, no. 7, p. 421-433.

Simoneau, M., F.J. Pazzaglia, and G.M. Fleeger, 2022, Pleistocene drainage reversals and gorge cutting at the Laurentide ice margin in northwestern Pennsylvania interpreted from new cosmogenic exposure and luminescence ages, *in* Dating in the Pleistocene, guidebook, 86th Annual Field Conference of Pennsylvania Geologists, Titusville, PA, p. ___-___.

Straffin, E. C., and Grote, Todd, 2010, Surficial geology of the Sugar Lake 7.5-minute quadrangle, Crawford and Venango Counties, Pennsylvania: Pennsylvania Geological Survey, 4th ser., Open-File Report OFSM 10–05.0, 23 p., Portable Document Format (PDF).

Suess, H.E., 1954, US Geological Survey radiocarbon dates 1, Science, v. 120, p. 467 – 473.

Szabo, J.P., 1992, Reevaluation of early Wisconsinan stratigraphy of northern Ohio, *in* Clark, P.U. and Lea, P.D., eds., The last interg;lacial – glacial transition in North America, Boulder, Colorado, GSA Special Paper 270, p. 99 – 107.

Totten, S.M., 1976, The "up-in-the-air" late Pleistocene beaver pond near Lodi, Medina County, northern Ohio, GSA Abstracts with Programs, v. 8, no. 4, p. 514.

Totten, Stanley M. and John P. Szabo, 1987, Stop 5: Mt. Gilead Fairgrounds section, in, Pre-Woodfordian stratigraphy of north-central, Ohio, Midwest Friends of the Pleistocene, 34th Field Conference, p. 63 – 67.

Volman, K. C., 1981, Paleoenvironmental implications of botanical data from Meadowcroft Rockshelter, Pennsylvania. Unpublished Ph.D. dissertation, Texas A & M University, College Station, TX.

Ward, A.N., Jr., M.T. Lukert, and W.F. Chapman, 1976, Geology and mineral resources of the Oil City quadrangle, Venango County, Pennsylvania, Pennsylvania Geological Survey, 4th series, Atlas 33a.

White, G.W., 1982, Glacial geology of northeastern Ohio, Ohio Division of Geological Survey, Bulletin 68, 75 p.

White, George W. and Stanley M. Totten, 1965, Wisconsinan age of the Titusville Till (formerly called "Inner Illinoian"), northwestern Pennsylvania, Science, v. 148, Issue 3667, p. 234 – 235.

White, George W, Stanley M. Totten, and David L. Gross, 1969, Pleistocene stratigraphy of northwestern Pennsylvania, Pennsylvania Geological Survey, 4th series, General Geology Report 55, 88 p.

White, George W., 1968, Age and correlation of Pleistocene deposits at Garfield Heights (Cleveland), Ohio, GSA Bulletin, v. 79, p. 749-752.

Wright, James D., "Global Climate Change in Marine Stable Isotope Records", in Noller, Jay S., Sowers, Janet M., Lettis, William R. (eds), Quaternary geochronology: methods and applications, 2000, American Geophysical Union, ISBN 0-87590-950-7, ISBN 978-0-87590-950-9.

PLEISTOCENE DRAINAGE REVERSALS AND GORGE CUTTING AT THE LAURENTIDE ICE MARGIN IN NORTHWESTERN PENNSYLVANIA INTERPRETED FROM NEW COSMOGENIC EXPOSURE AND LUMINESCENCE AGES

MICHAEL SIMONEAU[1,2], FRANK J. PAZZAGLIA[2] AND GARY FLEEGER[3]

Abstract

The Laurentide ice margin in western Pennsylvania locally blocked north or west-flowing, pre-glacial drainages, resulting in proglacial lakes that overtopped pre-glacial divides, carving gorges and new pathways for reversed drainages. Slippery Rock Gorge (SRG) is a ~120 m deep, 19 km long canyon incised through Pennsylvanian clastic sedimentary rocks generally thought to result from one of these reversed drainages. New terrestrial cosmogenic nuclide (TCN) ^{10}Be exposure and infrared-stimulated luminescence (IRSL) ages from bedrock and delta deposits, respectively, in the SRG indicate initial cutting was in the middle Pleistocene or older, and further deepening during the late Pleistocene, as one or more proglacial lakes formed and drained. A proglacial lake delta perched at the gorge lip near its deepest reach marks the former location of glacial Lake Prouty. An IRSL age from this delta of 140±23 ka supports the hypothesis that Lake Prouty formed at and subsequently overflowed the former drainage divide at Cleland Rock during the Illinoian (Titusville; MIS 6) ice advance. The overflow channel lowered and retreated northward, capturing portions of the formerly north-flowing McConnell's Run (paleo-Slippery Rock Creek) as other pro-glacial lakes drained, progressively reversing that drainage to the south. We model exposure ages of four ^{10}Be concentrations accounting for local topographic shielding and a slow background bedrock erosion rate of 1 m/Myr, consistent with findings of nearby published studies. We find that the model exposure ages are relatively insensitive to initial assumptions of sample thickness, density, and erosion rate, and become younger towards the river ranging from 12±1.3 and 27±2.5 ka near the gorge lip to 6.0±0.7 ka at a mid-canyon position, to 1.7±0.3 ka at modern river level. The long profile of Slippery Rock Creek has two major knickzones related to the base level fall created by the drainage reversal and resulting increase in drainage area. The long-term mean rate of incision at the location of the dated delta is 0.7 mm/yr (0.7 m/ka), but gorge deepening likely has been unsteady over the past 140 ka. Collectively, these results indicate that the gorge initiated in the middle Pleistocene, and it was deepened and its walls widened during and since the last glaciation, supporting other published hypothesis of multiple phases of gorge cutting and overflows of proglacial lakes.

Introduction

Pleistocene incursion of continental ice sheets into the northern third of the United States is thought to have had a dramatic impact on the landscape by impounding and reversing formerly north-flowing rivers, resulting in the over-topping of divides, potentially catastrophic floods, and rapid incision of newly integrated river channels. For example, assembly of the Ohio River and many of its tributaries including the Allegheny River (**Figure 1**) was recognized by the first generation of American geomorphologists, who set out to map the glacial boundary in western Pennsylvania and Ohio (Carll, 1880; Wright, 1890; Foshay, 1890; Chamberlin and Leverett, 1894; Leverett, 1902; Leverett, 1934), engendering decades of debate and speculation on the cause and effects of glaciation on the assembly of ice-marginal streams. Interest in this topic ebbed in the late 1930's, in part because hypotheses

[1] Verina Consulting Group, LLC, 1011 US Highway 22, Ste 302, Bridgewater, NJ 08807 *(current)*
[2] Department of Earth and Environmental Sciences, Lehigh University, Bethlehem, PA 18055
[3] Pennsylvania Geological Survey, *retired*, 3240 Schoolhouse Rd., Middletown, PA 17057-3534

could not be further tested in the absence of numeric age models for the mapped glacial and non-glacial deposits. For the next several decades, incremental progress was made in developing age models through direct numerical dating (e.g. radiocarbon), and inferred correlation to the marine isotopic record (Wright, 2000). In the past several decades with detailed mapping and provenance studies (e.g. D'Urso, 2000) and growing access to luminescence (Rittenour, 2018) and terrestrial cosmogenic nuclide (TCN; Granger et al., 2013) the debate has been reignited, and hypotheses posed over a century ago can now be tested.

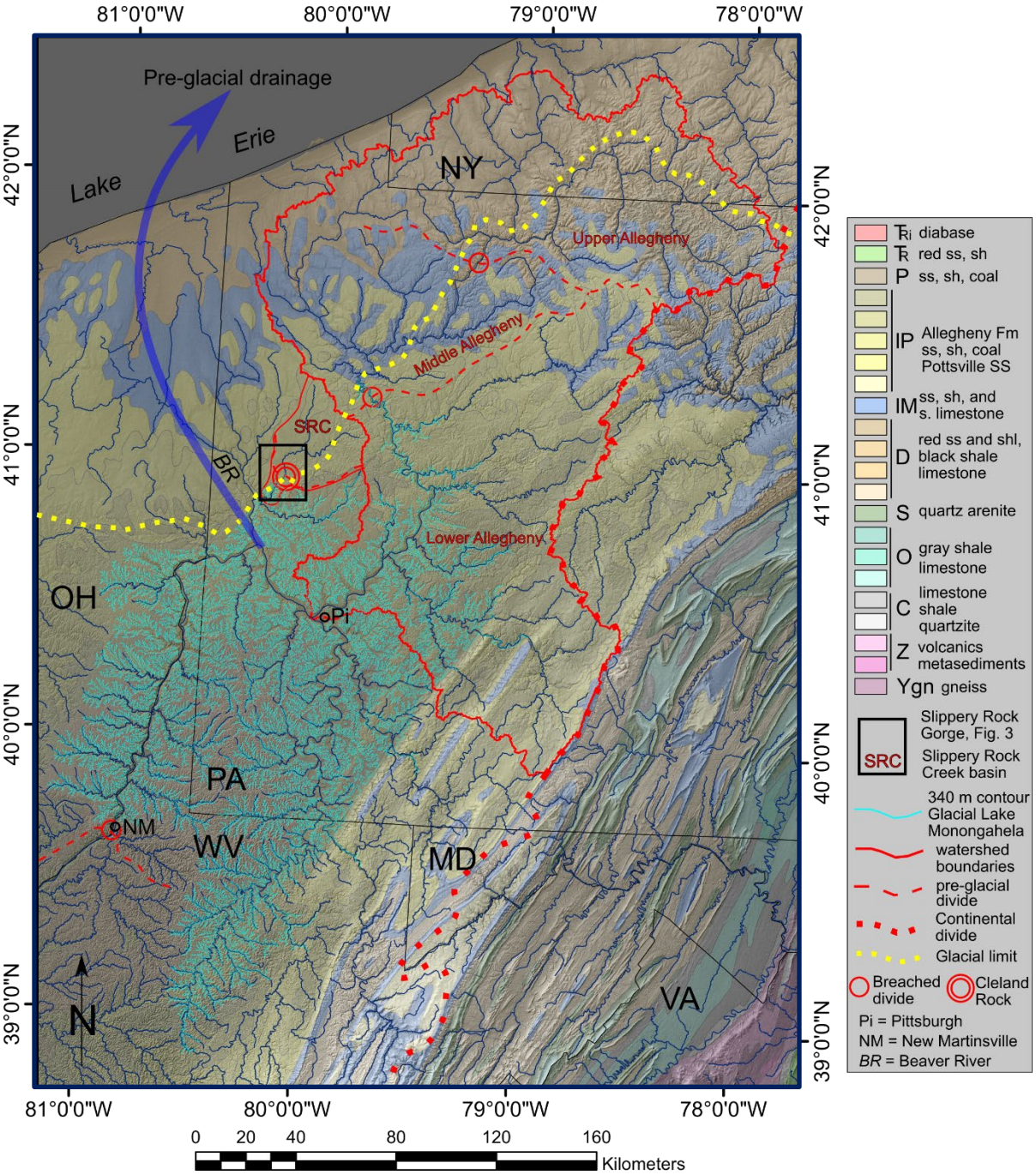

Figure 1. *Geologic map of western Pennsylvania (PA) and surrounding states showing the modern drainage, basins relevant to this study, the glacial boundary, and proposed locations of glacially-reversed drainages across local drainage divides. Assembly of the Ohio River was accomplished by impounding a formerly north-flowing drainage that occupied the modern valley of the Beaver River into Glacial Lake Monongahela and the subsequent over-topping of Glacial Lake Monongahela at the New Martinsville (NM) col. The modern Slippery Rock Creek (SRC) was a former tributary of the pre-glacial, north-flowing Beaver River that is now tributary to the Ohio.*

Northwestern Pennsylvania has comparatively less relief than the Ridge and Valley region to the east and is characterized by the glacial deposits that unconformably overlie gently-dipping late Paleozoic sedimentary rocks composed of alternating shale, sandstone, coal, and limestone (Figure 1). Several large rivers, including Slippery Rock Creek, drain the region to the south and west to the Ohio River, and ultimately to the Mississippi River. Slippery Rock Creek has incised a narrow inner gorge, here called Slippery Rock Gorge (SRG) ~19 km long with a maximum depth of ~120 m inset into a wider, more gently-sloped outer valley (Figures 1 and 2). The gorge is cut through three primary siliciclastic units of the Pottsville Formation (**Figure 2**), with the lip of the gorge supported by the Homewood Sandstone cliff-former, the mid-elevations underlain by the slope-forming Mercer Shale, and the base constituted by the Connoquenessing Sandstone. The gorge walls are covered by landslide, slump, and creep colluvial debris. The deepest part of the gorge coincides with a regional topographic high, Cleland Rock, the summit of a roughly east-west oriented ridge that marks a local paleo-drainage divide hypothesized to have been breached during gorge formation (Figure 1).

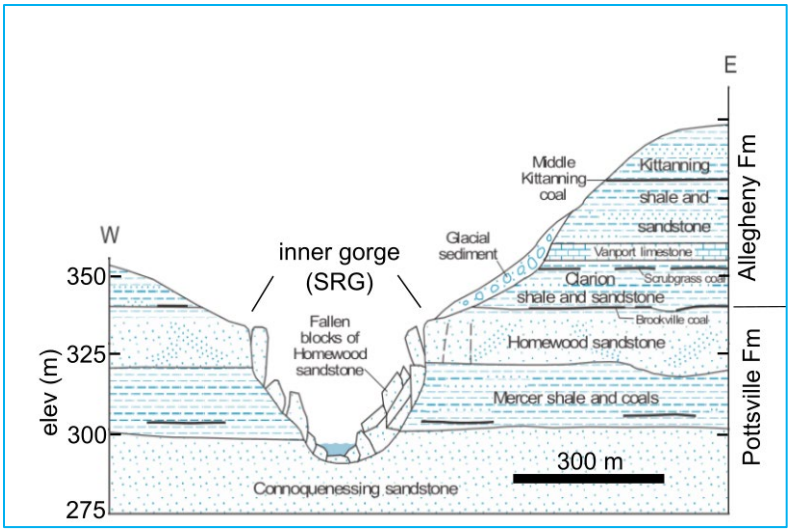

Figure 2. *Cross section of the Slippery Rock valley at McConnell's Mill showing major rock units. Slippery Rock inner gorge (SRG) refers mostly to the steep-walled gorge cut through the Homewood Sandstone, the Mercer Shale, and the Connoquenessing Sandstone. However, at Cleland Rock, the steep inner gorge extends up into the Kittanning Sandstone of the Allegheny Formation.*

Modified from Fleeger et al. (2003)

Previous studies (Preston, 1977; Fleeger et al., 2003, Fleeger et al., 2011) suggest that the SRG (Figure 2 and **Figure 3**) was initiated by draining of proglacial lakes, potentially characterized by outburst floods, that had ponded between the ancestral drainage divide and the ice margin during the LGM or in one or more pre-Wisconsinan (pre-LGM) glaciations, and subsequently deepened by floods of Wisconsinan (LGM) age. Other studies numerically modeled flood discharges of Slippery Rock Creek and its major tributaries pointing out the possibility that the gorge may be mostly pre-glacial (pre-Pleistocene) in age, being carved largely to its current configuration before the LGM, partially filled by sediment derived from that ice margin, and then re-excavated by discharges of similar magnitude to the flood of record (~500 m^3/s; D'Urso, 2000; 2022). All of these studies are well-reasoned but generally lack numeric dates for erosional or depositional landforms that can constrain the initiation and rates of gorge cutting. The main goal in this research is to create an age model, based on numeric ages that can test gorge formation hypotheses, the rates at which the gorge has been carved, and assess whether the gorge was cut by one or more episodic lake overflow events separated by significant periods of time.

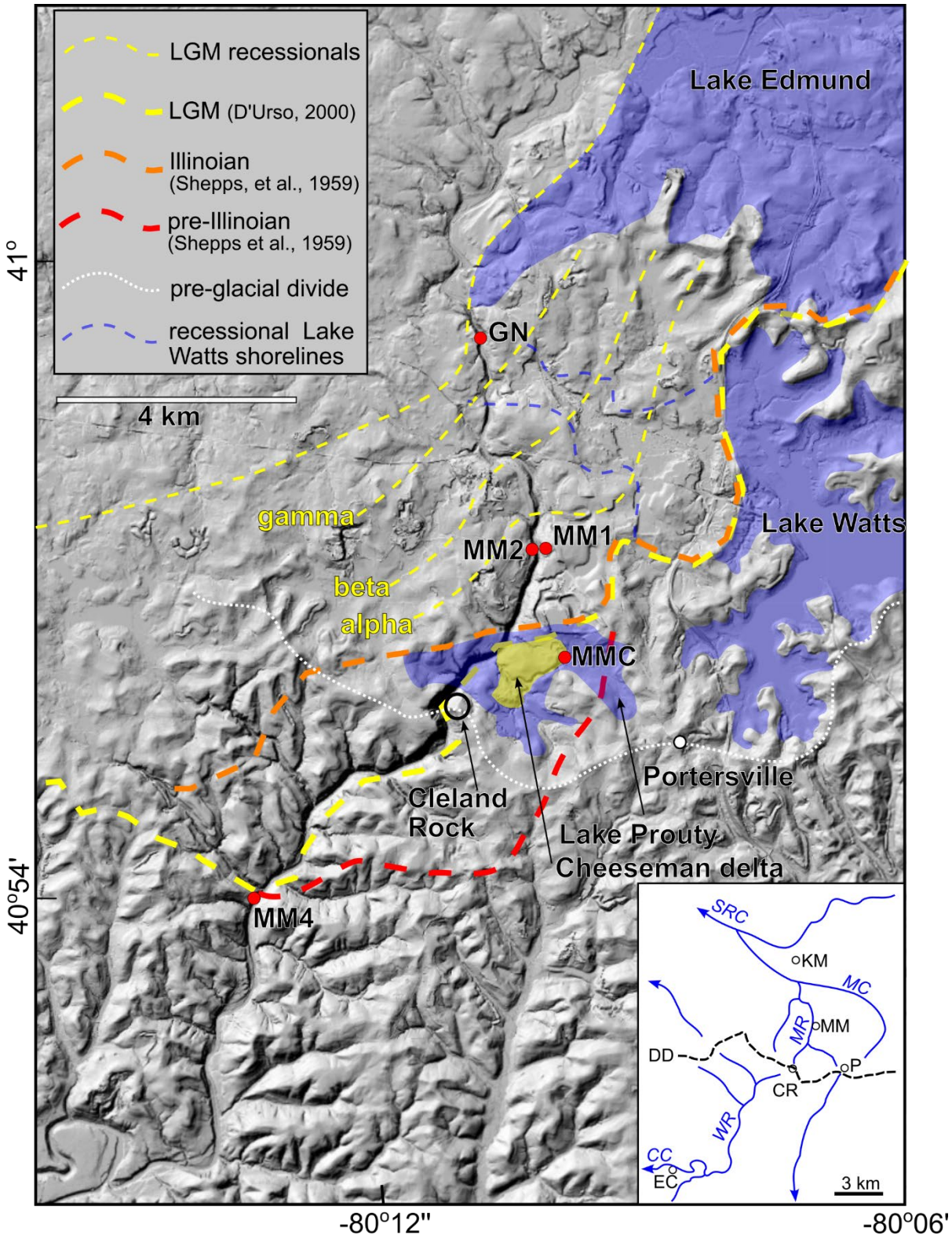

Figure 3. *Shaded relief topographic map showing major geomorphic features of the SRG region, and the locations of the one luminescence (MMC) and four cosmogenic sample locations (MM1, MM2, MM4, and GN). Inset map showing the general, pre-SRG drainage (Modified from Fleeger et al., 2003). DD=drainage divide, CR=Cleland Rock, MM=McConnells Mill, P=Portersville, KM=Kennedy Mill, EC=Elwood City, SRC=Slippery Rock Creek, MC=Muddy Creek, MR=McConnells Run, WR=Wurtemburg Run, CC=Connoquenessing Creek.*

Geologic and Geomorphic Setting

Northwestern Pennsylvania is underlain by gently-dipping Pennsylvanian and Mississippian age siliciclastic sedimentary rocks (Figure 1). Across the Slippery Rock Creek watershed, these rocks are folded into a broad anticline, with a NE-trending fold axis that passes through the center of the Slippery Rock Valley (**Figure 4**). As a result, Slippery Rock Creek is mostly incised onto an inner gorge (SRG) that includes the lower part of the Pottsville Formation called the Connequenessing sandstone, whereas the lip of the SRG is held up by the overlying Homewood sandstone, the upper part of the Pottsville Formation. Both upstream and downstream of the SRG, the Homewood sandstone intersects the channel, resulting in locally steep channel reaches. Outside of the gorge and away from Cleland Rock, the Slippery Rock Creek valley broadens, slopes recline, and the stream gradient shallows considerably. This part of the watershed is underlain mostly by the Allegheny Formation, comprised of the Clarion shale, Vanport Limestone, and Kittanning coals (Figure 2).

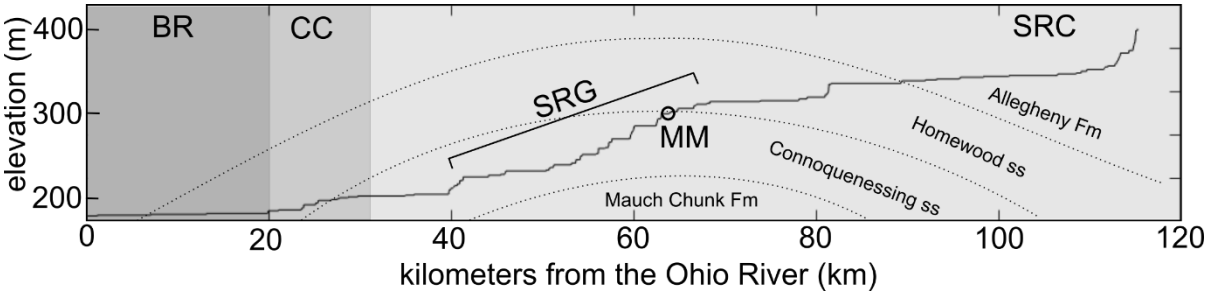

Figure 4. *Long profile of the Slippery Rock Creek made using Matlab TopoToolBox (Schwanghart and Scherler, 2014). BR=Beaver River reach, the local base level for Slippery Rock Creek. CC = Connoquenessing Creek reach. SRC = Slippery Rock Creek Reach. SRG=Slippery Rock Gorge. MM = McConnells Mill. Contacts of the main geologic units are approximate.*

Slippery Rock Creek has a steep longitudinal profile, particularly through the SRG reach (Figure 4). The ultimate base level for Slippery Rock Creek is the Ohio River, via Connoquenessing Creek and the Beaver River (Figures 1, 4). There are knickpoints at the major confluences, and where the channels intersect resistant rock units. The pre-glacial drainage in the SRG area is envisioned to have been dominated by the former east-west oriented local drainage divide centered on Cleland Rock (Figure 3). From this divide, a southwest flowing paleo-Wurtemburg Run (Fig 3., inset) crudely followed the course of the present day lower Slippery Rock Creek to the Connoquenessing Creek. On the north side of the divide, a north or northwest flowing paleo-McConnells Run followed the current course of Slippery Rock Creek through the McConnells Mill reach before turning to the northwest to join with Muddy Creek, and the paleo-Slippery Rock Creek drainage out to the former Lake Erie lowlands (Figure 3., inset). The long profiles of paleo-Wurtemburg Run and McConnells Run are envisioned to have been better graded, lacking major knickzones in comparison to the modern long profile of Slippery Rock Creek.

Northwestern Pennsylvania was glaciated by the Grand River sub lobe of the Erie lobe of the Laurentide ice sheet. At least four major ice advances may have reached this area (Shepps et al., 1959). Other mapping and provenance studies definitively document the LGM and Illinoian advances (Leverett, 1934; D'Urso, 2000) at least in the Slippery Rock Creek watershed (Figure 3). Two other possible pre-Illinoian advances left scattered remnants of till and other glacio-fluvial debris southeast of the current Illinoian glacial boundary mapped as the Mapledale and Slippery Rock tills. The Illinoian advance (marine oxygen isotope stage MIS 6, terminating ~140 Ka) produced several local landforms and deposits including the Titusville till. The more recent major advance of the Grand River sub-lobe

occurred during the Wisconsin glaciation (MIS 2, ~ 25-19 Ka). This glaciation left behind four major tills, the Kent, Lavery, Hiram, and Ashtabula tills, whose extent mostly overlaps with the Titusville till within the earlier Illinoian advance (Figure 3). Because the Illinoian and LGM ice margins cross and locally overlap the SRG, it is difficult to ascribe constructional landforms like proglacial lake deltas to either glaciation in the absence of numeric or relative (weathering, soils) age data.

The Proglacial Lake Systems and Proposed Drainage Assembly and Reversal of Slippery Rock Creek

Incision of Slippery Rock Gorge is widely thought to be related to the ice-margin blockage of the former north and northwest flowing streams, resulting in the formation of a series of proglacial lakes during both the advancing and retreating phases of glaciation. These lakes filled, overflowed to the south, and cut new courses through old drainage divides leading to the reversal of drainage direction (Figure 3). Three pro-glacial lakes may have contributed to the drainage reversal of Slippery Rock Creek (Preston, 1977). These lakes, from largest to smallest and north to south, were Lake Edmund in the Slippery Rock/ Wolf Creek basin, Lake Watts in the Muddy Creek basin, and Lake Prouty in the McConnell's Run basin. Lake Prouty in the McConnell's Run basin is interpreted to have been impounded against the paleo-drainage divide at Cleland Rock (Preston, 1977; Fleeger et al., 2011) or by ice that filled an already existing SRG (D'Urso, 2022; Braun, 2022; Figure 3). The overflow of this lake at a col near Cleland Rock is thought to have initiated the formation of the gorge (Preston, 1977) or deepened a col already breached by earlier glaciations (Braun, 2022). From this point, the recession of the Laurentide ice margin began to expose a series of lower cols that led to the drainage of Lake Watts and Lake Edmund. These lakes also now drained to the south through the now south-flowing Slippery Rock Creek. The scale of the flows and the role that they played in deepening and widening the gorge remains a topic of investigation (D'Urso, 2000; 2022; Fleeger et al., 2011; Braun, 2022).

A consequence of the reversed drainage is that the newly-formed SRG had occupied the former steep, and smaller channels of paleo-Wurtemburg Run and McConnells Run. As a result, the south-flowing Slippery Rock Creek was over-fit to these channels and their former valley gradients, with respect to its now much larger drainage area. This over-fit condition triggered a phase of relatively rapid, but transient incision that continues to the present, carving the gorge, and resulting in a stepped long profile with knickpoints accentuated by differences in rock hardness (Figure 4; Braun and Inners, 1998).

Methods

Topographic Analysis. Topographic data for this study was assembled from the SRTM 30 m resolution digital elevation model (DEM; https://earthexplorer.usgs.gov/). A river long profile is the elevation of a channel plotted against distance, effectively producing a cross section for the stream. The long profiles used in this study were created using ArcGIS and TopoToolbox and TAK scripts in MatLab (Schwanghart and Scherler, 2014; Forte and Whipple, 2019). ArcGIS is used to stitch together the DEM, and output it as an ASCII text file. This file is then used in the MatLab scripts to delineate the watershed boundaries and channels, construct long profiles, and extract topographic swath profiles. The interactive flowpathapp.m script was then used to manually select the stream of interest, Slippery Rock Creek. Next, using a script called Maplateral, the topography surrounding the long profile was extracted and used to generate a topographic swath. This tool creates a swath of a user-defined distance on both sides of the profile and projects topographic envelopes of the maximum and

minimum topography coincident with the long profile. The swath profiles (Figure 5) used in this study employed a lateral distance of 2 km.

Luminescence dating. Luminescence dating is based on the principle of time-dependent accumulation of ionizing radiation of buried materials in common mineral phases like quartz (optically-stimulated luminescence, OSL) and feldspar (infrared-stimulated luminescence, IRSL). An accessible full description of the physics and applications of luminescence dating is provided in Rittenour (2018) and references therein, and summarized here for its application to the SRG.

Luminescence dating provides an age estimate of the last time siliciclastic sediment was exposed to heat or light. When fully exposed to heat or light before being buried, a condition colloquially referred to as being "bleached," the energy levels of electrons in their orbitals are in their ground state. Upon burial, quartz and feldspar begin absorbing ionizing radiation from ambient concentrations of co-buried radioactive elements such as uranium and thorium. The absorbed ionizing radiation causes electrons to become elevated or trapped into higher energy orbitals. The amount of absorbed or trapped ionizing radiation is measured in units called a Gray (Gy; 1 Joule/kg) and is a function of the concentration of radioactive elements measured independently, and the time of sediment burial. When removed from burial and exposed to heat or light for ~7 seconds, the trapped electrons return to their ground state, and in the process the absorbed ionizing radiation is released as a flash of light. Measurement of the intensity and energy of that light is straight-forward, providing a target from which to generate an equivalent dose (De) of ionizing radiation that would be scaled to the time of burial.

For example, a buried sample is analyzed for both the concentration of radioactive elements and its luminescence signal. Then, using a known source of ionizing radiation, the same sample is dosed with the radiation for a range of time intervals. For each time interval, a luminescence signal is generated and measured and, in this way, an equivalent dose (De), measured in Gray, calculation or plot can be made. The De-luminescence signal that matches the buried sample luminescence signal indicates the dose of ionizing radiation that must have been acquired by the buried sample. Because the concentration of radioactive elements in the buried sample is known, then it becomes straight-forward to calculate the amount of time that the sample must have been buried to accumulate that dose,

$$\text{Burial Age (ka)} = \text{equivalent dose (De, in Gy)} \,/\, \text{dose rate in the sediment} \quad \left(\frac{Gy}{ka}\right) \qquad (1).$$

As with all dating methods, there are several assumptions and considerations dictated by the specific geologic setting that need to be taken into account in order to correctly interpret a luminescence age. First, not all quartz and feldspar are equally conditioned for luminescence dating. Quartz and feldspar that have been bleached and buried repeatedly, as they are in aeolian deposits, develop many electron traps that maximizes the time range and lowers the uncertainty of the technique. In this case, and considering usual concentrations of ambient ionizing radiation, quartz develops enough electron traps to effectively date buried sediments up to ~250 ka. Using IRSL, feldspar can extend the range of the technique to ~600 ka. In contrast, first-cycle sediments have poorly-developed electron traps and their luminescence signals tend to be more dispersed with higher uncertainties. Furthermore, sediments that only have been partially bleached, such as those

transported and deposited by fluvial processes, or worse, by sub-glacio-fluvial processes, may carry an inherited luminescence signal that increases their apparent burial age.

For these reasons, luminescence dating adopts either a mean age model, typically for well-bleached sediment, or a minimum age model, typically for sediment that is suspected of being partially bleached. In either case, the technique can be applied to single grains of sand or aliquots of several sand grains. In this study, we collected sediment from the Cheeseman pro-glacial lake delta, so IRSL and minimum age model techniques were applied. The goal in a minimum age model approach is to repeatedly date aliquots of the sample searching for those aliquots that have the lowest luminescence signal, meaning that they have the lowest possible inheritance from incomplete bleaching. As multiple aliquots repeatedly define a luminescence signal floor, with virtually no grains appearing to be younger, that luminescence signal floor is taken to correspond to the apparent burial age. That luminescence floor, however, could similarly be interpreted to mean that all of the grains being dated simply have the same, non-zero inheritance, and the calculated age is a combination of the time of burial, as well as that inheritance from some prior burial.

Acquiring a luminescence sample is accomplished by using a steel tube that ensures that from the time the sample is taken to the time it is analyzed, the sample is shielded from sunlight to preserve the ionized radiation burial signal. The tube is hammered into the sediments of interest and then capped. Then a second sediment sample is taken in an area surrounding the main sample to be analyzed for moisture content and radioactive isotopes such as uranium and thorium in order to determine the sediment dose rate. We collected one sample from the Cheeseman kame delta in October, 2018 and three from the West Liberty delta in October, 2019 (discussed elsewhere in this guidebook) and all four samples were analyzed at the Utah State University Luminescence Lab.

Terrestrial Cosmogenic Nuclide (TCN) Dating. TCN complements luminescence dating in that it provides an independent measure of how long rock surfaces have been exposed, the rate at which exposed rock surfaces are being eroded, and how long sediment has been buried and shielded from cosmogenic radiation. A full and accessible treatment of the physics behind TCN dating and its various applications can be found in Granger et al. (2013) and references therein, and is summarized here for its application to the SRG.

TCN dating is based on the observation that extra-solar system, high energy cosmic rays penetrate the Earth's atmosphere and into exposed surfaces, including rock and soil. The cosmic ray penetration length depends on the density of the material encountered. For the densities of rocks and soils, the effective penetration distance is measured by a few meters, and falls-off exponentially. Analogous in some ways to receiving a suntan, most of the cosmic rays interact with minerals right at the surface of the rock or soil, with less interactions for the material below the surface. Those interactions with the elements that compose common minerals, like quartz, lead to the *in-situ* production of new, commonly radioactive elements, such as ^{10}Be or ^{36}Cl. So, continuing the suntan analogy further, the accumulation of ^{10}Be in quartz (your suntan or sunburn) is directly proportional to the cosmic ray flux (a sunny or cloudy day) and the amount of time (how long you were laying out in the sun) that the mineral surface has been exposed. In reality, a cosmogenic element like ^{10}Be can accumulate in soils and rock surfaces by both *in-situ* production, as well as meteoric (rainwater) precipitation from the atmosphere. Furthermore, the technique can be used in a variety of ways to determine soil production, sample burial ages, and paleoerosion rates. Although a useful cross-check on our luminescence ages, we have not analyzed sediment from the Cheeseman kame delta to determine a

burial age. In our study, we used only *in-situ* produced ^{10}Be to determine exposure ages or surface erosion rates from the walls of SRG.

The master equation for application of TCN dating provides a good foundation for discussing the technique and its interpretation of measured cosmogenic concentrations as numeric ages,

$$\frac{dN_i}{dt} = P_i(R_c, h, z, t) - \frac{N_i}{\tau_i} \quad (2)$$

where N_i is the concentration of the in-situ cosmogenic nuclide (^{10}Be in our case) measured in atoms/g, t is time (yrs), P is ^{10}Be production in atoms/g-yr that varies as a function of R_c, the Earth's magnetic field, a latitude-dependent measurement; h, atmospheric depth or surface elevation (meters); z, the depth of the sample below the surface (meters) that is also called shielding; and t (time in yrs); less N_i divided by τ_i, the mean half-life (yrs). **Equation (2)** describes the conditions for the change in concentration of ^{10}Be in a sample based solely on the production and subsequent radioactive decay. The mean half-life of ^{10}Be means that in the case of no surface erosion, there will be an accumulation of ^{10}Be atoms for ~12 Myrs until decay balances production. In the more geologically-realistic setting where there is surface erosion, the ^{10}Be atoms that are produced are removed by both radioactive decay and erosion leading to an equation,

$$N_i = N_{inh}e^{\frac{-t}{\tau_i}} + P_i(R_c, h)(1/\tau_i + \rho E/\Lambda)^{-1}\left(1 - e^{-t[1/\tau_i + \rho E/\Lambda]}\right) \quad (3)$$

that looks more intimidating than it really is. In summary, the first term accounts for any inherited ^{10}Be (N_{inh}) that may have been acquired by a previous exposure. In practice, the sampling should be planned to minimize this term. The second term accounts for production of ^{10}Be and its removal by erosion and radioactive decay, considering Λ, the mass attenuation length typically taken to be 160 g/cm^2. If erosion is zero, then this second term simply reduces to production less radioactive decay. The third term describes the time dependency to equilibrium. In **equation (3)**, N_i is measured by extracting ^{10}Be from quartz in a chemical lab, and then determining its concentration using an accelerator mass spectrometer at a lab like the AMS facility at the University of Purdue.

Everything in equation (3), including the measured amount of ^{10}Be is known except for time (t) and erosion rate (E). So, this is the classic problem of having one equation, with two unknowns. One way to resolve this problem is to assume that $E = 0$ and then solve the equation just for time. This circumstance is what is called simple exposure and it reports a minimum age. Alternatively, secular equilibrium could be assumed meaning that time = infinity, the concentration of ^{10}Be has reached a constant value based on production, decay, and erosion, and the equation can be solved for E. Accordingly, in this study, we report minimum exposure ages based on no erosion, as well as erosion rates based on secular equilibrium between production, erosion, and decay.

We collected five TCN samples from the walls of the SRG to generate an age and erosion rate model of the gorge. When collecting the TCN samples, areas were chosen to represent the top, middle and bottom of the gorge at different locations along the longitudinal profile (Figures 3 and 5). Four of these samples, MM1-MM4 were collected in October of 2018. The first two samples, MM1 and MM2 were taken very near McConnells Mill near the top of the inner gorge on Homewood sandstone, while MM2 was taken down almost at the level of the present-day stream in the Connoquenessing sandstone. The third sample, MM3 was collected from the proposed Lake Prouty outlet slot canyon beneath Breakneck Bridge (not analyzed), whereas the fourth sample, MM4 was taken at a mid-canyon level along the west bank, near Armstrong Bridge, in the downstream part of the gorge. A fifth sample, GN, was taken at a mid-canyon level in the Homewood sandstone upstream of McConnells Mill (Kennedy gorge) in Nov, 2018.

Approximately 1-2 kg of sample was chipped from the outer 2 cm of the exposed surface. Because that samples were collected from steep, nearly vertical faces, we needed to account for natural topographic shielding of the cosmic rays in order to provide the correct production rates. All of the samples except MM3 were crushed, washed, and sieved. The size fraction between 200-800µm was retained and brought to the University of Vermont Cosmogenic Nuclide Lab, where the quartz was isolated, and ^{10}Be extracted. The concentration of ^{10}Be was then measured at the PRIME accelerator. With the ^{10}Be concentrations, we modeled both exposure ages assuming zero erosion rates and erosion rates assuming steady-state exposure using the online CRONUS calculator (Balco et al., 2008; https://hess.ess.washington.edu/).

Data

The luminescence burial age and TCN exposure ages/erosion rates are reported in **Tables 1 and 2** and shown in **Figure 5**. Sample MMC collected from the Cheeseman kame delta at the lip of the SRG near Cleland rock has an IRSL minimum age model age of 140±23 ka. This delta was deposited into Lake Prouty that has alternately been interpreted to be an Illinoian (Fleeger et al., 2011) or Wisconsinan (Preston, 1977; D'Urso, 2000) lake and deposit. The MMC material is mineralogically similar to samples WL-1 and WL-3 taken from an LGM-margin proglacial lake delta at West Liberty (Table 1.) The quartz from MMC, however, had a luminescence signal indicating that it had reached equilibrium with the ambient ionizing radiation resulting in completely full quartz electron traps. That is, the sample generated a minimum OSL age > 160 ka that is insensitive and incapable of constraining a true minimum burial age. Using the feldspar portion of MMC, the luminescence signal was generated from unfilled electron traps and is more consistent with a true burial age. In contrast, samples WL-1 and WL-3 have LGM, quartz-based OSL burial ages, albeit in reversed stratigraphic position, consistent with their location at the LGM margin. The electron traps for the quartz in the WL-1 and 3 samples are not full, and there was no need to use the feldspar fraction for an IRSL age determination.

Relative weathering characteristics of the Cheeseman delta (MMC) deposits indicates that the depth of leaching (DOL) and depth of oxidation (DOO) are approximately 10 and 22 m, respectively (D'Urso, 2000). These values are within DOL and DOO values reported for both Illinoian (Titusville; White et al., 1969; White, 1982) and LGM (Kent; Sitler, 1957; Shepps et al., 1959; White et al., 1969; White, 1982) glacial deposits. Given the differences in texture and permeability of deltaic sediments and tills, and poorly-constrained original depths of burial, the DOL and DOO data cannot unambiguously distinguish an LGM or Illinoian age for the delta.

Table 1a. Luminescence Age Information

Sample	USU number	Lat	Long	Elev (m)	Method[1]	Number of aliquots[1]	Dose rate (Gy/kyr)	Fading Rate g_{2days} (%/decade)	Equivalent Dose[2] ±2σ (Gy)	Age[3]±2σ(kyr)
MMC	USU-2981	40.93933	-80.16634	375	IRSL	16(18)	2.85±0.13	2.4±0.3	316.1±44.0	140 ± 23
WL-1	USU-3550	40.99696	-80.08162	382	OSL	20(35)	0.9±0.04	N/A	17.89±7.78	19.94 ± 4.84
WL-3	USU-3551	40.99261	-80.07931	388	OSL	35(53)	0.91±0.04	N/A	23.0±5.66	25.41 ± 4.61

1 = Age analysis using the single-aliquot regenerative-dose procedure of Murray and Wintle (2000) on 1-2 mm small-aliquots of quartz sand.
Number of aliquots used in age calculation and number of aliquots analyzed in parentheses.
2 = Equivalent dose (De) calculated using the minimum age model (MAM) of Galbraith and Roberts (2012).
3 = IRSL age on each aliquot corrected for fading following the method by Auclair et al., (2003) and correction model of Huntley and Lamothe (2001).

Table1b. Dose Rate Information

Sample	USU number	Depth (m)	In-situ H2O (%)[1]	Grain size (μm)	K(%)[2]	Rb (ppm)[2]	Th (ppm)[2]	U(ppm)[2]	Cosmic (Gy/ka)
MMC	USU-2981	5	3.6	125-212	0.87±0.02	37.5±1.5	6.3±0.6	1.6±0.1	0.12±0.01
WL-1	USU-3550	15	3.6	150-250	0.5±0.01	22.1±0.9	3.1±0.3	0.87±0.02	0.047±0.005
WL-3	USU-3551	15	3.4	150-250	0.52±0.01	20.9±0.8	3.0±0.3	0.87±0.02	0.047±0.005

1 = Assumed 5.0±2.0% for samples as moisture content over burial history.
2 = Radioelemental concentrations determined using ICP-MS and ICP-AES techniques; dose rate is derived from concentrations by conversion factors from Guerin et al. (2011).

Table 2a. TCN lab and AMS analysis results

Sample Name	Quartz Mass (g)	Mass of ^{9}Be Added (µg)*	AMS Cathode Number	Uncorrected ^{10}Be/^{9}Be Ratio**	Uncorrected ^{10}Be/^{9}Be Ratio Uncertainty**	Background Corrected ^{10}Be/^{9}Be Ratio	Background Corrected ^{10}Be/^{9}Be Ratio Uncertainty	^{10}Be Concentration (atoms g^{-1})	^{10}Be Concentration Uncertainty (atoms g^{-1})
SRY-MM1	20.0331	250.5	157214	6.124E-14	3.707E-15	5.599E-14	3.834E-15	4.678E+04	3.204E+03
SRY-MM2	20.0948	250.4	157215	1.532E-14	1.370E-15	1.007E-14	1.682E-15	8.384E+03	1.400E+03
SRY-MM4	20.1610	249.9	157216	3.125E-14	1.992E-15	2.600E-14	2.218E-15	2.153E+04	1.837E+03
SRY-GN	20.1343	251.0	157213	1.801E-13	6.533E-15	1.749E-13	6.605E-15	1.456E+05	5.501E+03

*^{9}Be was added through a carrier made at University of Vermont with a concentration of 304 µg mL^{-1}

**Isotopic analysis was conducted at PRIME Laboratory; ratios were normalized against standard 07KNSTD3110 with an assumed ratio of 2850 x 10-15 *(Nishiizumi et al., 2007)*

Table 2b. Modeled TCN ages

Sample Name	Lat	Long	Elev (m)	sample thickness (cm)	sample density (g/cm^{3})	Topographic shielding (no shielding = 1)	Standard model age for no erosion (yrs)	Internal* uncertainty (yrs)	External* uncertainty (yrs)	Steady-state erosion rate (m/Myrs)	Internal* (measure-ment) uncertainty (m/Myrs)	External* (total) uncertainty (m/Myrs)
SRY-MM1	40.95321	-80.16933	335	2	2.5	0.694	**12006**	833	1271	**71**	5	7
SRY-MM2	40.95327	-80.17049	300	2	2.5	0.91	**1684**	282	312	**498**	83	92
SRY-MM3	40.93748	-80.17846	326	2	2.5							
SRY-MM4	40.904	-80.2249	308	2	2.5	0.645	**6044**	519	707	**148**	13	17
SRY-GN	40.98174	-80.17978	325	2	2.5	0.986	**27142**	1055	2445	**29**	1	3

*** Reported as 2σ uncertainties;**

Internal uncertainty includes ^{26}Al and ^{10}Be measurement uncertainties as well as site-specific uncertainties in the thicknesses, densities, ages and estimated erosion units of overburden units. Should be used when comparing ages to each other.

External uncertainty includes production rate and decay constant uncertainties.

Should be used when comparing exposure ages to ages determined by other methods (like OSL).

We find that CRONUS modeling of our ^{10}Be concentrations (Table 2) to be fairly insensitive to sample thickness, density, and erosion rate. We explored a range of rock density, sample thickness, and surface erosion rate values finding that they had little effect on the modeled exposure ages and erosion rates. Using surface erosion rates of zero, the maximum TCN exposure ages in SRG range from ~1.7±0.3 ka for sample MM2 collected at river level at McConnells Mill to 27±2.5 ka collected for sample GN in a mid-gorge position in the SRG reach between McConnells and Kennedy mills. In general, the exposure ages are all LGM in age, young towards the river and young downstream (Figures 5 and 6). The steady-state erosion rates for the four TCN samples is highest at 500±90 m/Myr for sample MM2 and 30±3 m/Myr for sample GN (Table 2). All of the calculated steady-state erosion rates for these exposed bedrock samples are unrealistically high in comparison to others measured in western PA (Pazzaglia et al., 2021) and in the Appalachians (Hancock and Kirwan, 2007; Portenga et al., 2013) which typically report steady-state erosion rates < 5 m/Myr. The young exposure ages and corresponding high steady state erosion rates may have resulted from a sample collection strategy to find and sample fresh, rather than obviously weathered surfaces. Insofar that the fresh surfaces sampled represent a recent process to remove more weathered material, such as rockfalls or slumps, then the TCN ages and erosion rates indicate where these processes are active in the SRG.

SRG Age Model

An age model for Slippery Rock gorge emerges from a projection of the TCN and OSL data to a long profile of Slippery Rock Creek superimposed on a swath profile of the surrounding topography (**Figure 5**). This age model can be used to test the various ideas that have been proposed for the SRG. Not considered here, and only rarely in the earlier literature on the origin of glacially reversed drainages and the carving of glacio-fluvial gorges is glacio-isostatic adjustment (GIA), the resulting transient crustal deformation (Pico et al., 2019), and subsequent determination of topographic and lake-level elevations. Interpretations here follow from a small crustal deformation assumption where the GIA is long-wavelength, short amplitude, and of subordinate consequence to local topographic

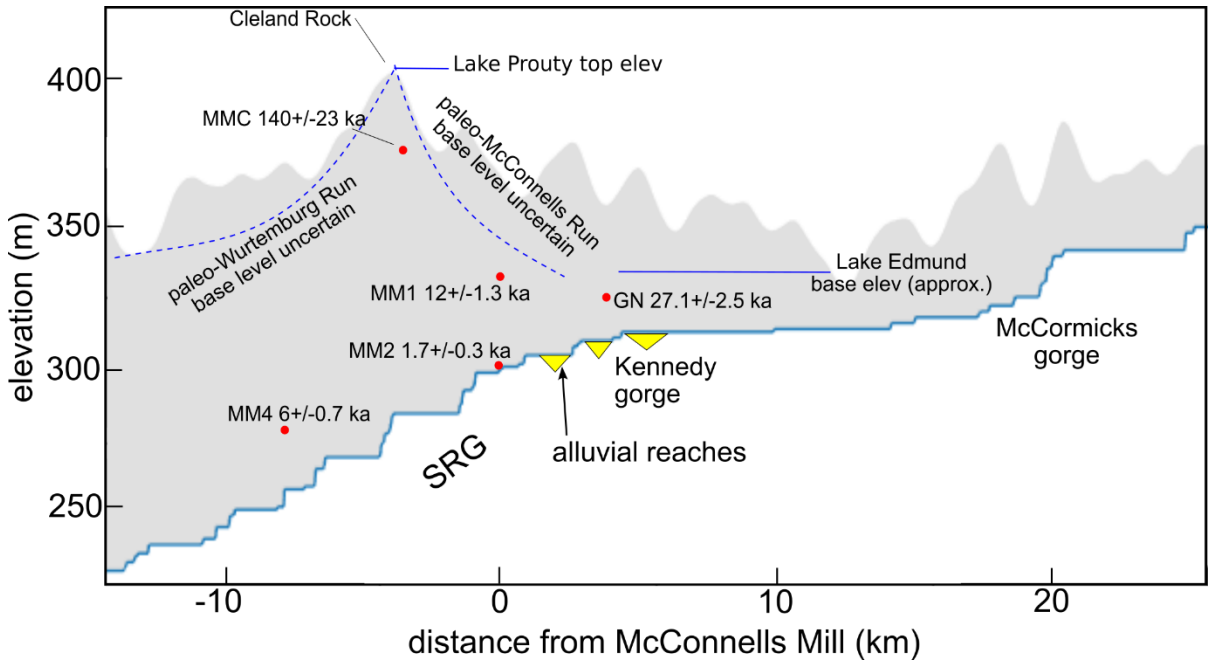

Figure 5. *Projection of numerically dated exposure age (MM1,MM2, MM4, and GN) and IRSL burial age (MMC) on the long profile and hillslope swath profile of Slippery Rock Creek.*

features like the SRG. Further GIA modeling would be required to assess the validity of this assumption.

To recap, the SRG, one idea holds that both the steep inner portion below the Homewood Sandstone and the broader, outer section including the Allegheny Formation was cut rapidly in the LGM (Preston, 1977). If true, all numeric ages should be LGM or younger. As a modification of this idea, the upper, broader valley was initiated by one or more pre-LGM glaciations and subsequently deepened by LGM lake-draining discharges (Fleeger et al., 2011; Braun, 2022). If true, outer gorge ages should be > LGM age whereas the inner gorge should have ≤ LGM ages. If Lake Prouty, *sensu stricto*, played a role in the carving of the inner gorge and/or overall drainage integration of the south-flowing Slippery Rock Creek, the Cheeseman delta IRSL age should indicate the timing of when the Cleland Rock col was breached (or deepened) or when a pre-existing SRG was filled with a tongue of ice to create pro-glacial Lake Prouty. Lastly, if LGM discharges played a role in backfilling, then excavating a pre-LGM SRG (D'Urso, 2000; 2022), the Homewood Sandstone exposure ages at the top of the inner gorge should be pre-LGM, as long as they have not been refreshed by subsequent erosion/rock falls.

Taken at face-value, the OSL age of ~140 ka argues that a pro-glacial lake (Lake Prouty ?) was present and impounded either against the paleo-drainage divide during the Illinoian (Titusville, MIS 6; Figure 3) ice advance or by a lob of Illinoian ice that occupied the SRG at this time. Whether or not the draining of this proglacial lake initiated SRG incision that ultimately led to the full reversal of Slippery Rock Creek is not interpretable from this single date. However, if in fact Lake Prouty formed and breached the paleo-drainage divide at this time, the long-term integrated rate of incision at Cleland Rock has been ~ 0.7 mm/yr (700 m/Myr; Figure 6). This rate is 2-3 times faster than rivers have carved gorges in the American west including the Grand Canyon of the Colorado, and 10 to 20 times faster than most rivers are incising the Appalachian Ohio slope (Pazzaglia et al., 2021; Kurak et al., 2021). If SRG, including the upper, outer, more gentle portion is as young as the Illinoian glaciation, then the very fast integrated rate of incision is an ongoing transient driven by the inherited steep paleo-slope of Wurtemburg Run and the increased discharge of the upstream captured headwaters of Slippery Rock Creek. As the knickpoint through the gorge reach is erased by incision, the expectation is that the incision rate will ultimately slow.

Similarly, taken at face value, the TCN exposure ages would argue that SRG is a very young feature, having been carved in the late Pleistocene-Holocene perhaps in response to the LGM glaciation at rates approaching 1 mm/yr (**Figure 6**). Alternatively, the TCN data can be interpreted as late Pleistocene-Holocene re-freshening of existing gorge walls and valley bottom. The < 2 ka exposure age of sample MM2 is completely consistent with ongoing fluvial incision of the bedrock channel banks of Slippery Rock Creek driven by historic floods with discharges that that have reached ~500 m3/s (D'Urso, 2000). Such floods would have had flow depths of only 1-2 meters at the MM2 sampling site, attesting to ongoing erosion and re-freshening of bedrock surfaces. Our biased sampling of the walls of SRG to only obtain material from fresh, rather than weathered surfaces may have revealed slumping, rockfall, and related slope processes to be more active in the late Pleistocene, coincident with LGM climatic conditions, than they are presently. Considering the TCN exposure ages as minima means that SRG was already present by the late Pleistocene, but that it continued to deepen and widen, perhaps accelerated by LGM climates, related glacio-fluvial discharges (Braun, 2022), and isostatic rebound.

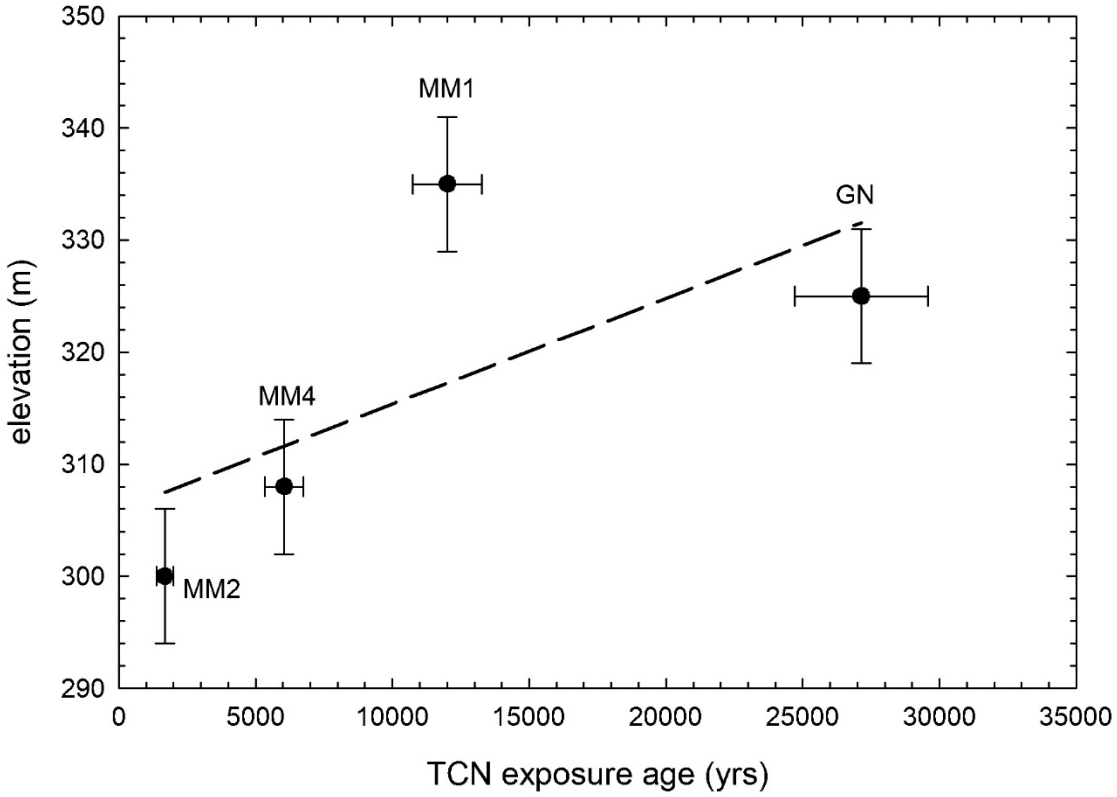

Figure 6. *TCN exposure age-elevation plot of rock surfaces in the SRG reach. The regression line indicates a mean incision rate of ~1 mm/yr (1 km/Myr).*

There are other, plausible explanations for the TCN exposure ages that may have origins in multiple generations of SRG formation, the transient headward propagation and reclining of the SRG knickzone, or complicated exposure histories that include times of SRG burial and re-exhumation. Despite being sampled in the same rock and at the same elevation, sample GN is ~twice as old as sample MM1. This caveat may indicate that there are multiple segments of the gorge, with variably active erosional walls, that have since been integrated into a single through-flowing system. Alternatively, the fact that the TCN ages are progressively younger downstream could be interpreted to mean that the SRG knickzone is deepening, reclining, and propagating upstream in the ~140 ka, or greater time period, since the breaching of the paleo-divide. Lastly, it is possible that the TCN exposure ages hint at complex exposure histories acquired from a gorge that has been alternately carved, backfilled, and exhumed. In this scenario that is supported by the location of alluvial deposits commonly interpreted as paleo-flood levels (c.f. D'Urso, 2000), the deeper parts of the gorge have been buried by one or more post-glacial alluvial fills. These fills would shield the bedrock in the deeper parts of the gorge and there would be no accumulation of 10Be during these times. As a result, SRG would be much older than the LGM or Illinoian glaciation, with the TCN exposure ages simple reflecting these complicated exposure histories, further modified by active, but unsteady hillslope and fluvial processes that periodically refresh rock surfaces.

Conclusion

An age model constructed for SRG composed of one IRSL luminescence age on the Cheeseman delta and four TCN exposure ages in the gorge walls help to constrain several plausible models for the

timing of the formation of the SRG and the reversed drainage of Slippery Rock Creek. The numeric data presented here are silent on the scale of the discharges that may have been responsible for breaching the paleo-divide at Cleland Rock. These data do indicate SRG was most likely already present by the LGM, and that LGM-related fluvial and hillslope processes have served to widen and deepen the gorge in the late Pleistocene and Holocene, re-freshening the sampled and dated rock surfaces in the process. The minimum age model for the MMC IRSL luminescence age of 140±23 ka in the Cheeseman delta would indicate an Illinoian age proglacial lake, possibly the Lake Prouty of Preston (1977), that may have overflowed at this time to breach the paleo-divide at Cleland Rock. If that was the case, the long-term rate of incision at Cleland Rock is ~0.7 mm/yr. The steep knickzone in the SRG reach continues to recline and migrate upstream, resulting in TCN exposure ages becoming older on gorge walls that are wider and less steep near Kennedy Mill in comparison to the reach near McConnells Mill.

Acknowledgements

The authors wish to express their gratitude to the Pennsylvania Geological Survey and Department of Earth and Environmental Sciences at Lehigh University for the funding used for field work and in obtaining the TCN and luminescence numeric ages. External reviewers Duane Braun, Patrick Burkhart, Ty Johnson, Gary D'Urso, and Fred Zelt greatly improved the manuscript with constructive comments, suggestions, and edits.

References

Auclair, M., Lamothe, M., Huot, S., 2003. Measurement of anomalous fading for feldspar IRSL using SAR. Radiation Measurements 37, 487-492.

Balco, G., Stone, J. O., Lifton, N. A., and Dunai, T. J., 2008, A complete and easily accessible means of calculating surface exposure ages or erosion rates from 10Be and 26Al measurements: Quaternary Geochronology, 3, 175-195.

Braun, D. D., and Inners, J. D., 1998, Ricketts Glen State Park, Luzerne, Sullivan, and Columbia Counties - The rocks, the Glens, and the falls (2nd ed.): Pennsylvania Geological Survey, 4th ser., Trail of Geology 16–013.0, 10 p.

Braun, D. D., 2022, Pleistocene evolution of the Slippery Rock Creek gorge, (this volume).

Carll, J. F., 1880, The geology of the oil regions of Warren, Venango, Clarion, and Butler Counties, including surveys of the Garland and Panama Conglomerates in Warren and Crawford, and in Chautauqua Co. N.Y., descriptions of oil well rig and tools, and a discussion of the preglacial and postglacial drainages of the Lake Erie County: Penn. Second Geological Survey Report, Volume III.

Chamberlin, T. C. and Leverett, F., 1894, Further studies of the drainage features of the upper Ohio basin: American Journal of Science, 47, 247-284.

D'Urso, G. J., 2000, Revised glacial margins and Wisconsin meltwater paleoflood hydrology in Slippery Rock Creek basin, central western Pennsylvania [Ph.D. dissertation]: Morgantown, WV, West Virginia University, 174 p.

D'Urso, G. J., 2022, Origin of the Cheeseman kame delta and some thoughts on the origin of Slippery Rock Creek gorge (this volume).

Fleeger, G., Bushnell, K., and Watson, D., 2003, Moraine and McConnells Mill State Parks; Butler and Lawrence Counties; glacial lakes and drainage changes. Harrisburg, PA: Pennsylvania Department of Conservation and Natural Resources, Bureau of Topographic and Geologic Survey, Harrisburg, PA, United States, 18 p.

Fleeger, G., Grote, T., Straffin, E., and Szabo, J., 2011, Quaternary geology of northwestern Pennsylvania, in Ruffolo, R.M., and Ciampaglio, C.N., eds., From the Shield to the Sea: Geological Field Trips from the 2011 Joint Meeting of the GSA Northeastern and North-Central Sections: Geological Society of America, Field Guide 20, p. 87–109, doi:10.1130/2011.0020(05).

Forte, A.M., and Whipple, K.X., 2019, Short commnication: The Topographic Analysis Kit (TAK) for Topotoolbox: Earth Surface Dynamics, v. 7, p. 87–95, https://doi.org/10.5194/esurf-7-87-2019.

Foshay, P. M., 1890, Preglacial drainage and recent geological history of western Pennsylvania: American Journal of Science, 40, 397-404.

Galbraith, R.F., Roberts, R.G., 2012. Statistical aspects of equivalent dose and error calculation and display in OSL dating: An Overview and some recommendations. Quaternary Geochronology 11, 1-27.

Granger, D. E., Lifton, N. A., and Willenbring, J. K., 2013, A cosmic trip: 25 years of cosmogenic nuclides in geology: Geological Society of America Bulletin, 125, 1379-1402, doi:10.1130/B30774.1.

Guérin, G., Mercier, N., Adamiec, G., 2011. Dose-rate conversion factors: update: Ancient TL 29, 5-8.

Hancock, G. and Kirwan, M., 2007, Summit erosion rates deduced from 10Be: Implications for relief production in the central Appalachians: Geology, 35, 89-92, doi: 10.1130/G23147A.1.

Huntley, D.J., Lamothe, M., 2001. Ubiquity of anomalous fading in K-feldspars and the measurement and correction for it in optical dating. Can. J. Earth Sci. 38, 1093–1106.

Kurak, E., Pazzaglia, F. J., Li, C.X., Patching, A., Shaulis, J., Corbett, L., Bierman, P., Nelson, M., and Rittenour, T., 2021, Incision of the Youghiogheny River through the Laurel Highlands determined by a new river terrace stratigraphic age model, Ohiopyle State Park, southwestern Pennsylvania, in Anthony, ed., Geology of Ohippyle State Park and the Laurel Highlands of southwestern Pennsylvania: Field Conference of Pennsylvania Geologists Guidebook 85, 51-73.

Leverett, F., 1902, Glacial formations and drainage features of the Erie and Ohio basins: U. S. Geological Survey Monograph 41, 808 p.

Leverett, F., 1934, Glacial deposits outside the Wisconsin terminal moraine in Pennsylvania: Pennsylvania Geological Survey, 4th series, General Geology Report 7, 123 p.

Murray, A. S., and Wintle, A. G. 2000. Luminescence dating of quartz using an improved single-aliquot regenerative-dose protocol. Radiat. Meas. 32:57–73.

Nishiizumi, K., Imamura, M., Caffee, M.W., Southon, J.R., Finkel, R.C., McAninch, J., 2007, Absolute calibration of 10Be AMS standards: Nucl. Instrum. Methods. Phys. Res. B 258, 403-413.

Pazzaglia, F. J., Kurak, E., and Shaulis, J., 2021, Geology of Ohiopyle State Park and the Laurel Highlands of southwestern Pennsylvania, Stops 3 and 5, in Anthony, ed., Geology of Ohippyle State Park and the Laurel Highlands of southwestern Pennsylvania: Field Conference of Pennsylvania Geologists Guidebook 85, 25-29; 5-40.

Pico, T., Mitrovica, J. X., Perron, J. T., Ferrier, K. L., and Braun, J., 2019, Influence of glacial isostatic adjustment on river evolution along the U. S. mid-Atlantic coast: Earth and Planetary Science Letters, 522, 176-185.

Portenga, E.W., Bierman, P.R., Rizzo, D.M., and Rood, D.H., 2013. Low rates of bedrock outcrop erosion in the central Appalachian Mountains inferred from in situ 10Be. Geological Society of America Bulletin 125. p. 201–215. DOI:10.1130/B30559.1.

Preston, F. W.,1977, Drainage changes in the Late Pleistocene in central western Pennsylvania: Pittsburgh, PA, Carnegie Museum of Natural History, 56 p.

Rittenour, T. M., 2018, Dates and rates of Earth-surface processes revealed using luminescence dating: Elements, 14, 21-26.

Schwanghart, W., Scherler, D., 2014, TopoToolbox 2 – MATLAB-based software for topographic analysis and modeling in Earth surface sciences: Earth Surface Dynamics, 2, 1-7, DOI:10.5194/esurf-2-1-2014.

Shepps, V. C., White, G. W., Droste, J. B., and Sitler, R. F., 1959, Glacial geology of northwestern Pennsylvania: Pennsylvania Geological Survey 4th series, Bulletin G32, 64 p.

Sitler, R. F., 1957, Glacial geology of a part of western Pennsylvania: [Ph.D thesis], Urbana, University of Illinois, 120 p.

White, G.W., 1982, Glacial geology of northeastern Ohio: Ohio Department of Natural Resources Division of Geological Survey, Bulletin 68, 75 p.

White, G.W., Totten, S.M., and Gross, D.L., 1969, Pleistocene stratigraphy of northwestern Pennsylvania: Pennsylvania Geological Survey, 4th series, General Geology Report 55, 88 p.

Wright, G. F., 1890, The glacial boundary in western Pennsylvania, Ohio, Kentucky, Indiana, and Illinois: U.S. Geological Survey Bulletin 58, 112 p.

Wright, J. D., 2000, Global Climate Change in marine stable isotopic records, in Noller, J. S., Sowers, J. M., Lettis, W. R., eds., Quaternary geochronology: methods and applications, American Geophysical Union, Wiley, p. 427-433.

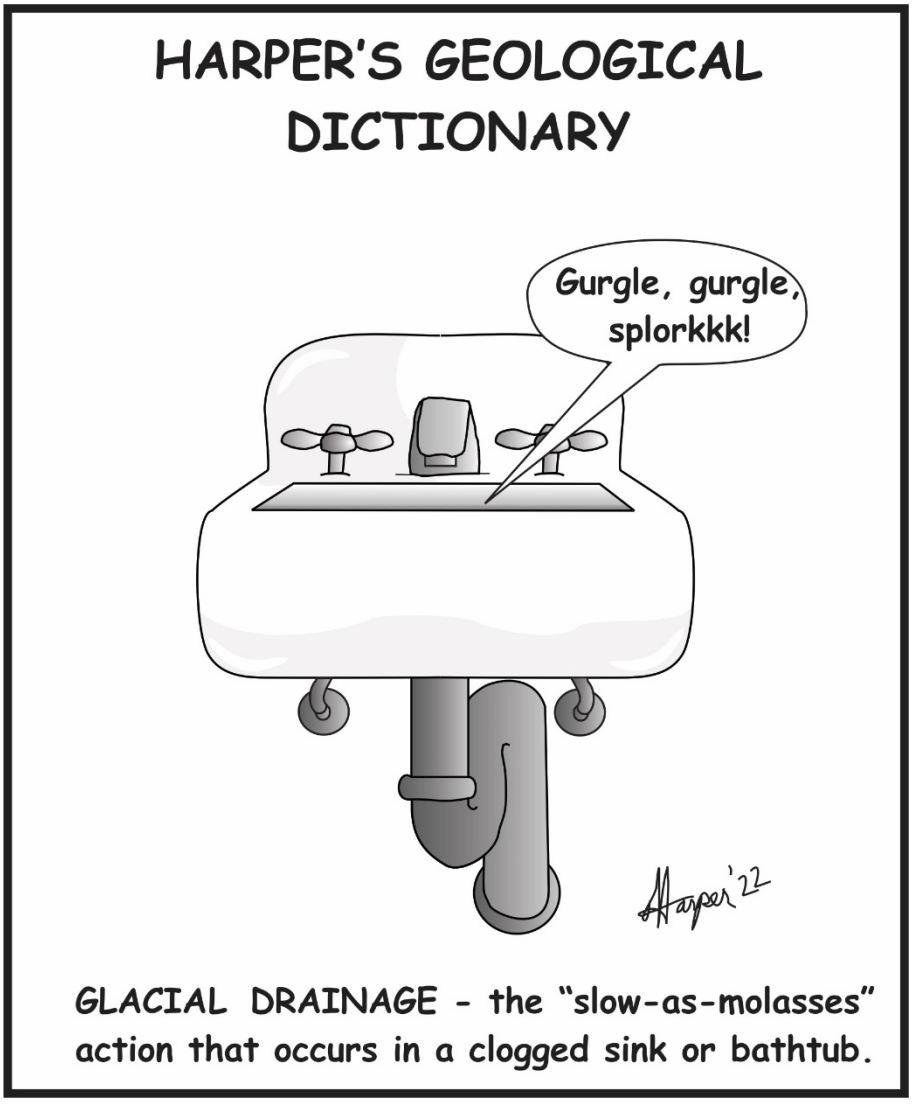

PLEISTOCENE EVOLUTION OF THE SLIPPERY ROCK CREEK GORGE

DUANE BRAUN – PROFESSOR EMERITUS, BLOOMSBURG UNIVERSITY OF PENNSYLVANIA

Overview – Pleistocene glacial advances in Pennsylvania

Background context for the evolution of the Slippery Rock Creek gorge

The near parallel pattern of the glacial borders of the various age glacial advances indicates that each glacier advance flowed in essentially the same direction, to the southeast in western PA and to the southwest in eastern PA (**Figure 1**). Preglacial drainage was to the northwest in western PA and to the northeast in north central PA. In both those regions the advancing glaciers blocked the drainage, diverting it to a southerly direction (Carll, 1880; Chamberlin and Leverett, 1894; Leverett, 1902; Williams, 1902, 1920; Lohman, 1939; Shepps et. al., 1959). Such drainage diversions across preglacial drainage divides produce deep gorges like the Pine Creek gorge in north central PA and the Kinzua gorge on the upper Allegheny River. The Slippery Rock Creek gorge is simply a smaller version of such a divide-crossing glacial drainage diversion.

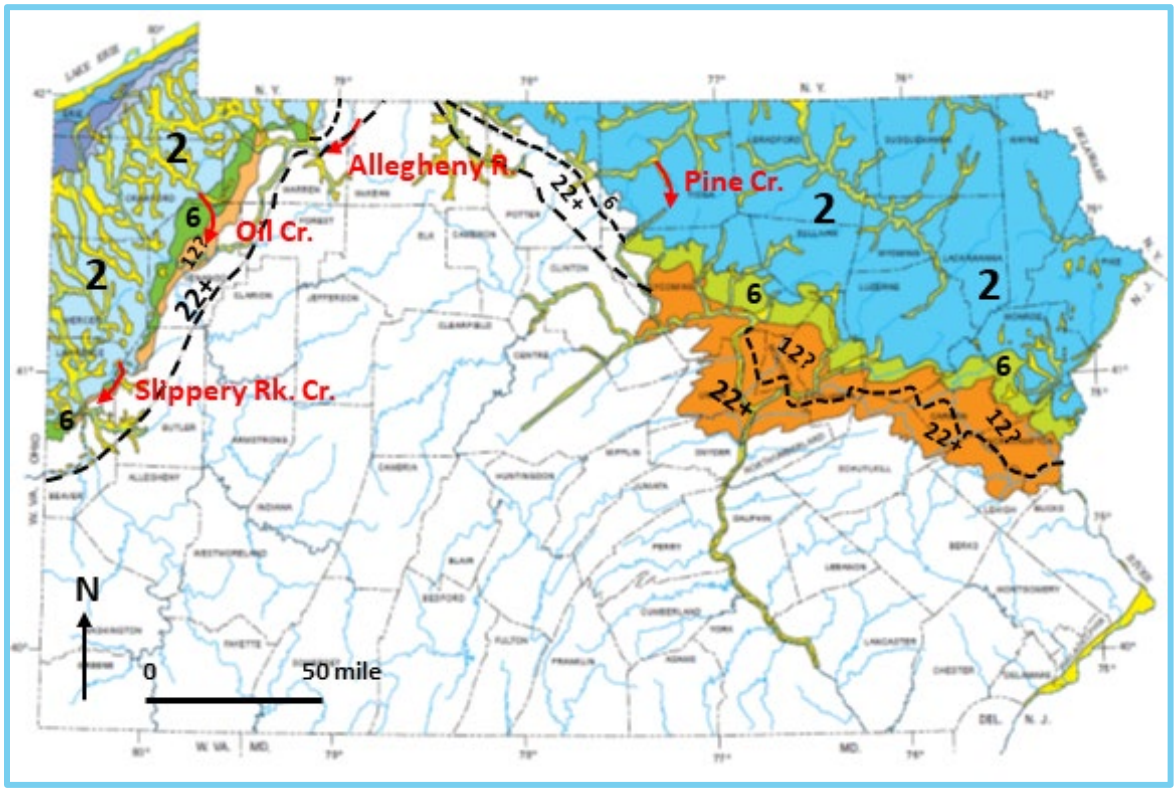

Figure 1. Map of the extent and age of glacial deposits in Pennsylvania. *The numbers are the Marine Isotope Stage ages for the different glacial limits. The older glacial limits have uncertain ages. Narrow strips along stream valleys are glaciofluvial deposits. Red arrows and labels mark major preglacial divide-crossing Pleistocene drainage derangements.*

(modified from Sevon and Braun, 1997 & Braun, 2011)

The first or oldest glacial advance in PA extended farther south than any of the later glacial advances (Figure 1) (Braun, 2011). That glacial advance both in the Susquehanna River basin and in the Ohio River basin left proglacial lake sediments that have a reversed magnetic direction (Jacobson et. al., 1988; Gardner et. al., 1994; Ramage et. al., 1998). That dates the advance to the early Pleistocene prior to 880 ka or Marine Isotope Stage (MIS) 22+. There are very sparse deposits left as

evidence of that advance, best exposed in strip mines in both eastern and western PA. This advance may be represented by the Slippery Rock Till and/or various isolated erratics found beyond the younger mapped glacial borders (White et al, 1969). Other landform evidence of the early Pleistocene advance is a series of notched cols that were proglacial lake outlets mostly in western PA but also in places in north central and eastern PA. That first glaciation left a distinct terminus in eastern PA on the floors of gently sloping strike valleys as much as 45 miles to the southwest of the Late Wisconsinan limit. A somewhat similar advance beyond the Late Wisconsinan limit would be expected in western PA but the relief there leaves limited places for deposits to remain.

There is some evidence of a middle Pleistocene advance approximately mid-way between the earliest advance limit and the Late Wisconsinan limit. That evidence is a series of kames that forms a chain of deposits in the strike valleys of the Susquehanna drainage and what was termed the outer Illinoian in western PA by Shepps et. al. (1959) and named the Mapledale by White et al (1969). From the marine record, likely times for that advance would have been MIS 12 at around 450 ka or MIS 16 at around 650 ka. Also, deposits are more common and thicker within that limit and cols tend to be notched deeper than in the area covered by MIS 22+ advance.

There is abundant evidence for a late middle Pleistocene advance, the late Illinoian or MIS 6 event at about 150 ka. It is marked by a chain of thick kame deposits in both eastern and western PA where it was called the inner Illinoian by Shepps et al (1959) and the Titusville event by White et. al. (1969). The terminus of the Illinoian advance is only a few miles in front of the Late Wisconsinan terminus, in places they are almost on top of each other. On a side note, Braun (2011) had suggested that there was a question as to the age of this margin, whether it was MIS 6 or the older MIS 12. That was due to exceptionally deep weathering of an uneroded kame top at Bloomsburg, PA that soil scientists considered far too deep to be MIS 6. OSL dating at the Cheeseman delta site (Stop 8) just east of the Slippery Rock Creek gorge confirmed a MIS 6 age for that glacial advance in western PA. It is expected that in coming years OSL dating the deposits in eastern PA will confirm a MIS 6 age there also.

The final glacial advance, the Late Wisconsinan or MIS 2 at about 25 ka, named the Kent advance in western PA (White et al, 1969) left a prominent terminal moraine in many places. The deposits in the terminal zone are quite thick though in many places the total thickness of the deposits is a composite of both the Illinoian and Wisconsinan advances

All these glacial advances collectively have produced the drainage derangements or diversions such as the Slippery Rock Creek gorge.

Slippery Rock Creek gorge evolution – sequence of events

Prior to glaciation drainage pattern

The Slippery Rock Creek drained to the northwest towards today's Mercer through a now abandoned buried valley (**Figure 2**). All buried channels discussed below have been identified through the accumulation of well data over the last 50 years or so (Poth, C. W., 1963; Reese, S. O. and Fleeger, G. M., 2022).

Muddy Creek drained westward in a now abandoned buried valley (Figure 2). That valley continues westward towards today's New Castle.

A Muddy Creek tributary, McConnell Run, drained northward from the Cleland Rock divide through the present Mc Connells Mill reach to present Rose Point and then northwest to near today's Princeton Station (Figure 2). That tributary headed in the col or saddle at about 1300 feet and then

sloped rapidly down to the north to about 1200 feet, the elevation at which stream heads on the west side of the valley start dropping rapidly into the present gorge. Then the tributary sloped more gently to less than 1100 feet near Rose Point.

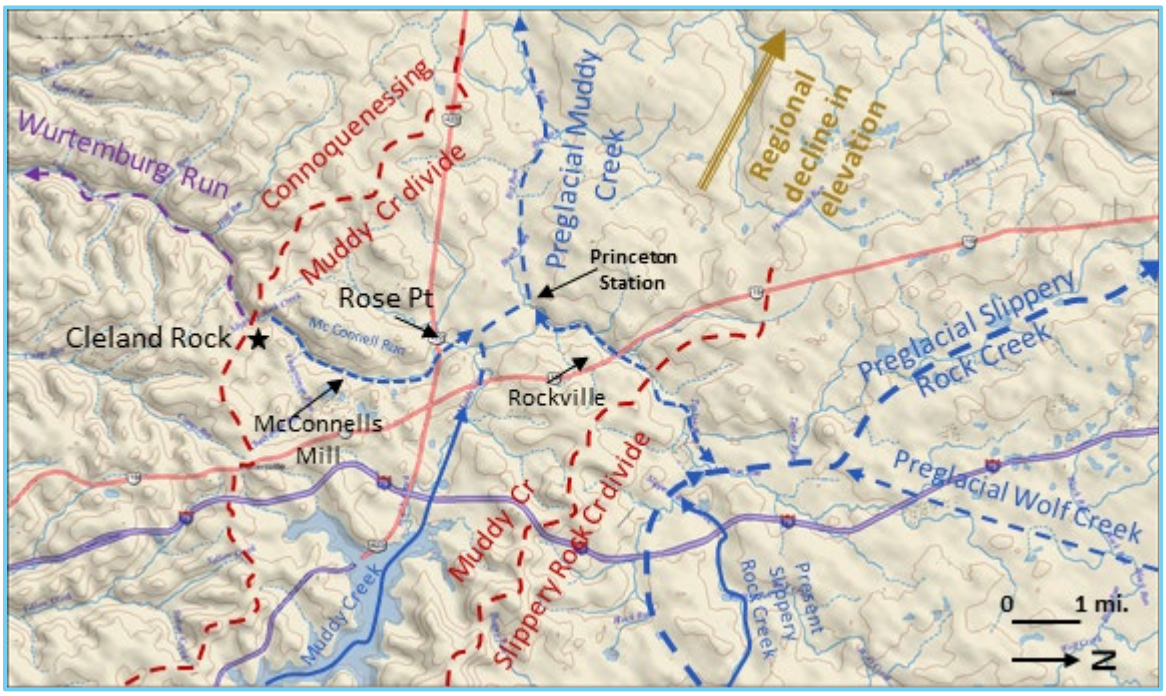

Figure 2. Preglacial drainage*. Preglacial drainage pattern in the Slippery Rock gorge region.*

Early Pleistocene initial blockage and diversion of Slippery Rock Creek to Muddy Creek

The MIS 22+ or >880 ka Slippery Rock event. Ice advance blocks NW trending part of Slippery Rock Creek and diverts it across the Rockville narrows or constricted reach into Muddy Creek valley (Figure 3). Further ice advance dams Muddy Creek valley. Muddy Creek and Slippery Rock Creek are diverted across the 1300 ft or so elevation Cleland Rock col or saddle.

Ice advances across the Cleland Rock col and continues southeast for more than 10 miles. It dams a large proglacial lake in the Connoquenessing drainage basin and a series of notched cols mark where branches of that proglacial lake spilled out to the southwest. Some subglacial meltwater flow may have continued across the Cleland Rock col.

Ice retreats to northwest reopening the Cleland Rock col with some proglacial lake discharge through the col. Incipient gorge through the col may be on the order of 50 ft deep, the typical depth of other notched cols in the area from this first advance.

Ice continues its northwest retreat opening Muddy Creek valley to the west. Slippery Rock Creek remains diverted through the narrows at Rockville and joins Muddy Creek near present day Princeton Station (Figure 3).

A long period of erosion before the next glacier arrives (200 – 400 kyrs) permits considerable incision of the Rockville narrows and Muddy Creek valley to the west. Muddy Creek incises to below the elevation of the present Slippery Rock gorge at their confluence. The Muddy Creek tributary, McConnell Run, from the Cleland Rock divide also incises below present gorge level in the Rose Point area just before that tributary joins Muddy Creek (Figure 3).

Figure 3. Early to middle Pleistocene drainage. *Early through mid-Pleistocene diversion of Slippery Rock Creek into Muddy Creek by first glacial advance. PS = Princeton Station.*

Second glacial advance in middle Pleistocene

The MIS 12 (450 ka) or MIS 16 (650 ka) Mapledale event. Overall repeat performance of the advance and retreat of the first glaciation.

The notch deepens more in the Cleland Rock col (another 50 ft or so down to 1200 ft?) but not enough for the Muddy – Slippery Rock Creek to continue flowing through the shallow gorge. The flow returns to the west out the Muddy – Slippery Rock Creek valley, continuing the incision of that drainage system.

Third glacial advance in late middle Pleistocene

The MIS 6 or Illinoian Titusville event at about 150 ka. As with earlier advances west draining Muddy – Slippery Rock Creek valley is blocked sending flow over the notched Cleland Rock col (starting at 1200 ft elevation at this point?).

This glacier terminates around the Cleland Rock col area and sends clast laden meltwater down the Slippery Rock gorge for a 1000 years or more.

This flow with abundant cutting tools markedly deepens the gorge across the Cleland Rock col (down to 1100 feet or so?). Erosion work needed to deepen the gorge is increasing due to the increasing length of rock being cut.

Upon ice recession, short lived proglacial lake discharges should have done some additional cutting.

Thick deposits in the terminal zone block the west draining part of Muddy – Slippery Rock Creek valley and permanently divert the drainage through the Slippery Rock Creek gorge (**Figure 4**). Similar thick deposits bury a major north side of Slippery Rock Creek tributary, Wolf Creek (Figure 4) (Also discussed at the Wolf Creek Stop).

Muddy – Slippery Rock Creek continues to down-cut the gorge in post glacial times for about 125 kyrs.

Figure 4. Middle Pleistocene to present drainage. *Middle Pleistocene to present drainage pattern with flow through the Slippery Rock Creek gorge. MIS 2 = Late Wisconsinan MIS 6 = Late Illinoian PS = Princeton Station KM = Kennedy Mill. (Braun, 2011, Fleeger, ongoing work)*

Fourth and last glacial advance

The MIS 2 or Late Wisconsinan or Kent advance at about 25 ka essentially completes the cutting of the gorge. Ice advance blocks the drainage again and the glacier terminates just a couple of miles north of the Cleland Rock col (Figure 4) (Fleeger, ongoing work). Again, clast laden meltwater flows down the Slippery Rock gorge for a 1000 years or more.

Ice recession from the abandoned Muddy – Slippery Rock Creek valley leaves thick enough deposits to block the Kennedy Mill-Princeton Station-Rose Point course of Slippery Rock Creek. The creek is diverted to the east across two buried bedrock ridges to either side of the buried Muddy Creek channel. This initiates the two very narrow gorges (Kennedy Mill or "Kame terrace" gorge) to either side of where Muddy Creek joins Slippery Rock Creek today. This gorge may have been started as an ice marginal channel because just north of it at Rockville is an abandoned side hill channel at a 1220-1240 elevation directed towards the present gorge. A 27 Ka Be-10 date (Simoneau et al, 2022) from the top of the Kennedy Mill gorge suggests that it may have been initiated during late Illinoian (Titusville) recession or Late Wisconsinan (Kent) advance. Another gorge of similar form and age occurs just upstream of the Slippery Rock – Wolf Creek confluence, the McCormicks gorge.

Post glacial latest Pleistocene – Holocene

Continued down-cutting of the gorge. Deepening and some widening of the main gorge and the two gorges upstream where Muddy Creek comes in. Continued active erosion confirmed by "youthful" rock surface age Be-10 dating (Simoneau et al, 2022) in the 2,000 to 30,000 yrs range.

Continued upstream knick point migration along the main gorge and in tributary valleys such as at Grindstone, Hell Hollow, and Skunk Run Falls.

References

Braun, D.D., 2011, The Glaciation of Pennsylvania, USA. In J. Ehlers, P.L. Gibbard and P.D. Hughes, editors: Developments in Quaternary Science, Vol. 15, Amsterdam, The Netherlands, 2011, p.521-529.

Carll, J. F., 1880, The geology of the oil regions of Warren, Venango, Clarion, and Butler Counties, including surveys of the Garland and Panama Conglomerates in Warren and Crawford, and in Chautauqua Co. N.Y.; descriptions of oil well rig and tools, and a discussion of the preglacial and postglacial drainages of the Lake Erie County: Penn. Second Geological Survey Report, Volume III, 482 p.

Chamberlin, T. C. and Leverett, F., 1894, Further studies of the drainage features of the upper Ohio basin: Am. Jou. Sci., 47, p.247-284.

Gardner, T.W., Sasowsky, I.D., Schmidt, V.A., 1994,Reversed polarity glacial sediments, West Branch Susquehanna River Valley, Central Pennsylvania. Quaternary Research, 42, p.131–135.

Jacobson, R.B., Elston, D.P., Heaton, J.W., 1988, Stratigraphy and magnetic polarity of the high terrace remnants in the upper Ohio and Monongahela Rivers in West Virginia, Pennsylvania, and Ohio. Quatern. Res. 29, p.216–232.

Leverett, F., 1902, Glacial formations and drainage features of the Erie and Ohio Basins. U.S. Geologic Survey Monograph, 41, 802 p.

Leverett, F., 1934, Glacial deposits outside the Wisconsin terminal moraine in Pennsylvania. Pennsylvania Geological Survey, 4th ser., General Geology Report, 7, 123 p.

Lohman, S.W., 1939, Ground water in North-Central Pennsylvania, with analyses by E.W. Lohr. Pennsylvania Geological Survey, 4th ser., Bulletin, W6, 219 p.

Poth, C. W., 1963, Geology and hydrology of the Mercer quadrangle, Mercer, Lawrence, and Butler Counties, Pennsylvania: Pennsylvania Geological Survey, 4th ser., Water Resource Report 16, 149p.

Ramage, J.M., Gardner, T.W., Sasowasky, I.D., 1998, Early Pleistocene Glacial Lake Lesley, West branch Susquehanna River valley, central Pennsylvania. Geomorphology, 22, p.19–37.

Reese, S. O. and Fleeger, G. M., 2022, Bedrock-Topography and Drift-Thickness Maps of the Edinburg, Harlansburg, New Castle North, and Slippery Rock 7.5-Minute Quadrangles, and Pennsylvania part of the Campbell 7.5-Minute Quadrangle, Butler, Lawrence, and Mercer Counties, Pennsylvania. Open-File Surficial Geologic Map 22–01.0, 7 p. and four figures.

Sasowsky, I.D., 1994, Paleomagnetism of glacial sediments from three locations in eastern Pennsylvania. *In:* Braun, D.D. (Ed.), Late Wisconsinan to Pre-Illinoian (G?) Glacial and Periglacial Events in Eastern Pennsylvania, Guidebook for the 57th Field Conference, Friends of the Pleistocene, p. 21–24. U.S. Geologic Survey Open File Report 94-434.

Sevon, W.D., Braun, D.D., 1997, Glacial deposits of Pennsylvania, second ed. Pennsylvania Geological Survey, 4th ser., Map 59, scale 1:2,000,000.

Shepps, V.C., White, G.W., Droste, J.B., Sitler, R.F., 1959, Glacial geology of Northwestern Pennsylvania. Pennsylvania Geological Survey, 4th ser., General Geology Report 32, 59 p.

Simoneau, M., F.J. Pazzaglia, and G.M. Fleeger, 2022, Pleistocene drainage reversals and gorge cutting at the Laurentide ice margin in northwestern Pennsylvania interpreted from new cosmogenic exposure and luminescence ages, *in* Dating in the Pleistocene, Guidebook 86th Annual Field Conference of PA Geologists, in prep.

White, G.W., 1969, Pleistocene deposits of the north-western Allegheny Plateau, USA. Quarterly Jour. Geo. Soc. London, 124, p. 131–151.

White, G.W., Totten, S.M., Gross, D.L., 1969, Pleistocene stratigraphy of Northwestern Pennsylvania. Pennsylvania Geological Survey, 4th ser., General Geology Report, 55, 88 p.

White, I.C., 1896, Origin of the high terrace deposits of the Monongahela River. Am. Geol. 18, p.368–379.

Williams, E.H., Jr., 1902, Kansan glaciation and its effects on the river systems of northern Pennsylvania. Proc. Wyo. Hist. Geol. Soc. 7, p.21–28.

Williams, E. H., 1920, The Deep Kansan Pondings in Pennsylvania and the Deposits Therein. Am. Phil. Soc. Proc. 59, p.49-84.

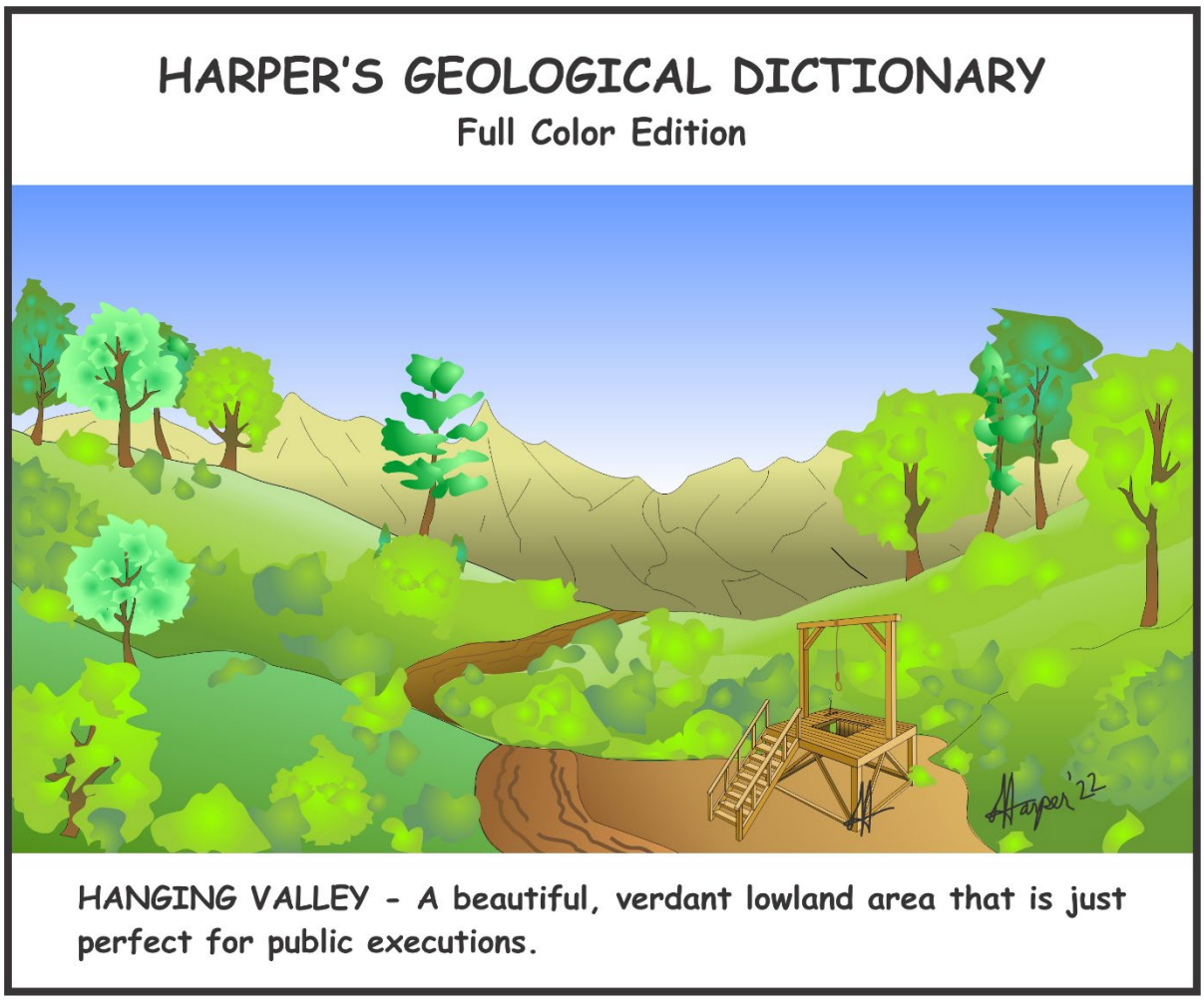

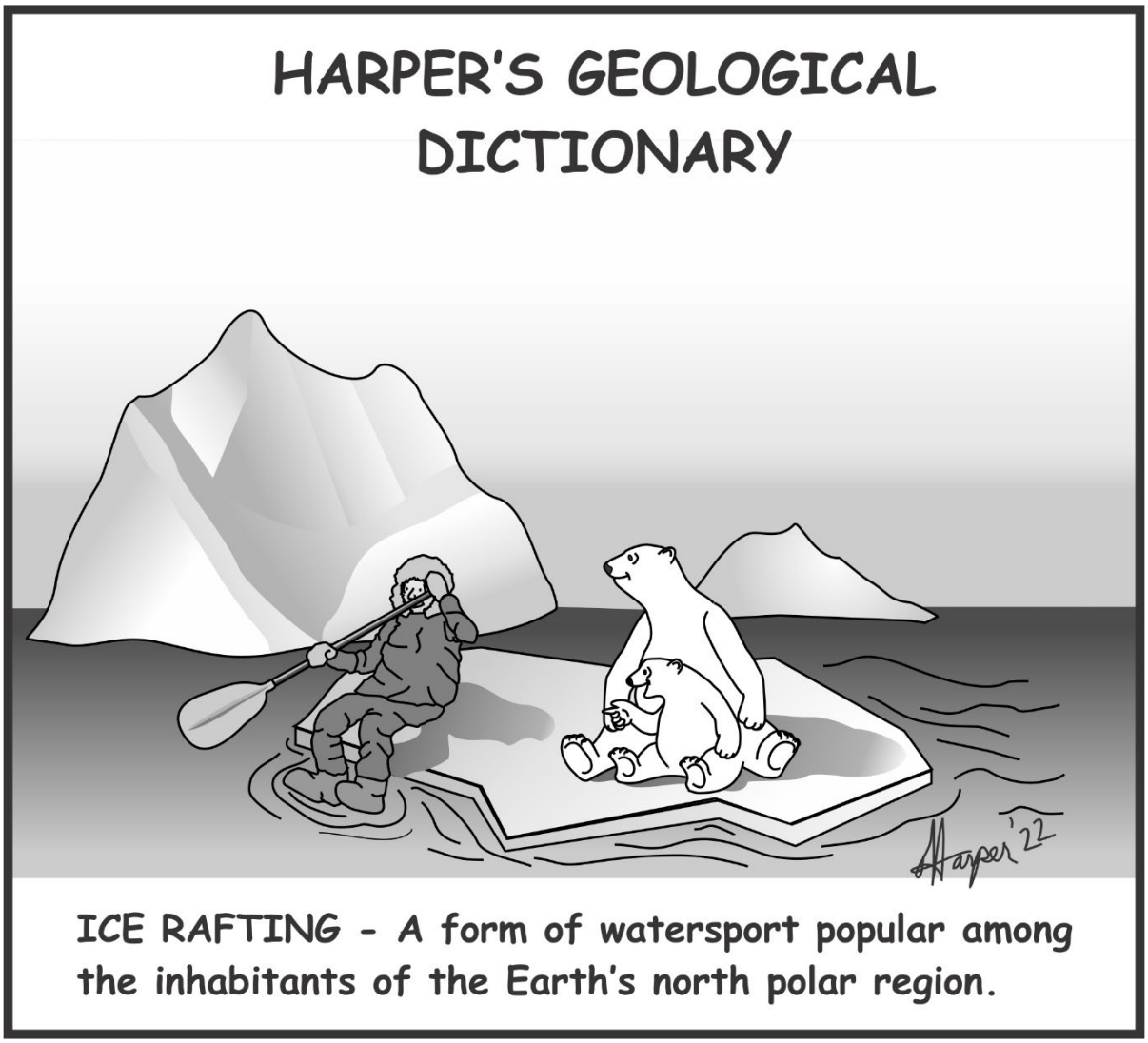
HARPER'S GEOLOGICAL DICTIONARY
Harper '22
ICE RAFTING - A form of watersport popular among the inhabitants of the Earth's north polar region.

ORIGIN OF STRAY CARBON DIOXIDE GAS
WASHINGTON TOWNSHIP, LAWRENCE COUNTY PENNSYLVANIA[1]

LAUGHREY, C. D.[2] AND BALDASSARE, F. J.[3]

Introduction

In August 2000, former Pennsylvania State Representative Frank LaGrotto filed a complaint with the United States Office of Surface Mining Reclamation and Enforcement concerning carbon dioxide (CO_2) accumulations in three residential homes occupied by members of his constituency. Office of Surface Mining (OSM) personnel installed gas meters in the homes and drilled a total of 10 groundwater monitoring wells around the buildings (Figure 1). The gas meters installed in the three homes (Drager MultiWarn II monitors) measured oxygen (O_2), CO_2, carbon monoxide (CO), and methane (CH_4). These instruments continuously recorded the levels of the gases at 10-minute intervals for 28 days at a time (Figure 2).

The OSM routinely downloaded the data from the meters and continued monitoring the homes for more than one year while investigating the source of the CO_2. Carbon dioxide concentrations as high as 25% and corresponding O_2 levels as low as 10% occurred in the homes during periods of low barometric pressure. Carbon dioxide levels in the atmosphere directly above the water table in some of the monitoring wells exceeded 25% at these times and corresponding O_2 levels dropped to 3% (**Figure 3**). Trace quantities of CO and CH_4 were sometimes noted during the monitoring period. The OSM assisted the families residing in the homes with constructing temporary remediation systems so they could safely occupy the buildings during the site investigation. If the stray CO_2 contamination was related to an abandoned mine, then federal funding from OSM would be available to construct a permanent abatement system.

In recent years, the acceleration of remote working and retirement of the baby boomer generation has led to increased development in rural settings, including areas of reclaimed surface mining. This uptick in development has led to increased risk of dangerous concentrations of CO_2 inside residences and commercial buildings.

---

[1] This review is adapted from Laughrey, C.D. and F.J. Baldassare (2003), Some applications of isotope geochemistry for determining sources of stray carbon dioxide gas, Environmental Geosciences, v. 10, p. 107 – 122.

[2] Stratum Reservoir; Pennsylvania Geological Survey, *retired*

[3] Echelon Geochemistry; Pennsylvania Department of Environmental Protection, *retired*

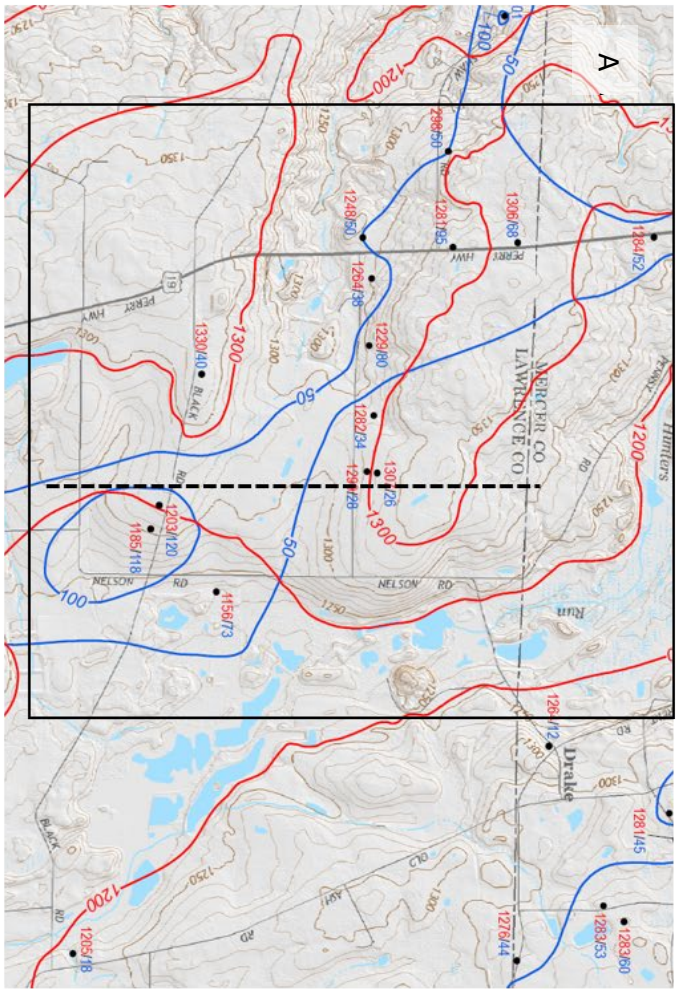

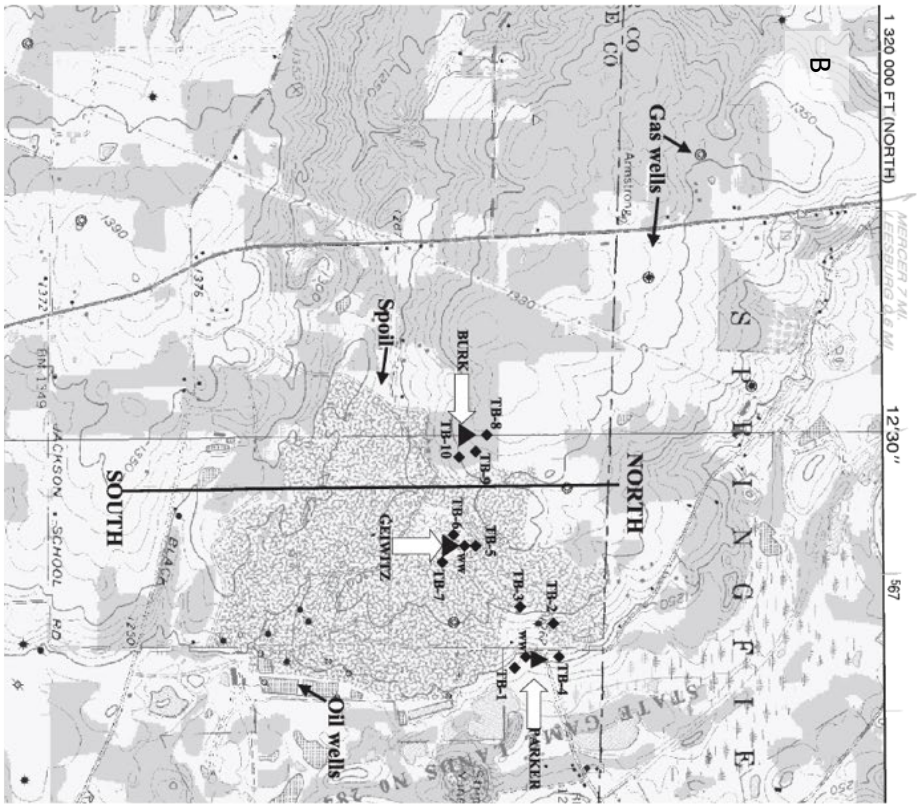

Figure 1. A. *Portion of the most recently published Harlansburg 7.5-minute quadrangle showing bedrock topography and glacial drift-thickness (from Reese et al., 2022). Bedrock topographic contours are red. Drift-thickness contours are blue. Black dots represent water wells that intersect bedrock. Open circles represent water wells that did not reach bedrock. The study area for this investigation is outlined in black. The dashed black line is the north-south line of cross section shown in B and in Figure 5B.* ***B.*** *Study area for this report shown on the 2002 Pennsylvania Geological Survey Oil and Gas Well Base Map. USGS topographic map is the 1961 version updated in 1990. Reclaimed strip mine spoil is indicated by the stippled patten. Note that the Geiwitz home sits on the reclaimed spoil. The gas wells produced from Lower Silurian Medina Group reservoirs at the time of the stray gas investigation. The oil wells produced from shallow Upper Devonian sandstone reservoirs. Compare with Figure 4D.*

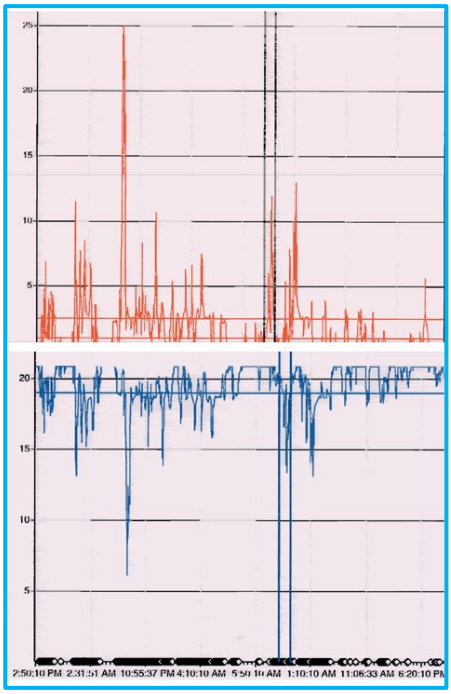

Figure 2. *The photographs above show set-up of laptop and real-time gas meter monitoring of CO_2, O_2, CO, and CH_4 levels in the Geiwitz basement in 2002. Screen shots of the laptop plots of %CO_2 (upper right) and %O_2 (lower right) reveal variations in gas concentrations in the basement atmosphere over a six-and-a-half-hour period on that particular day.*

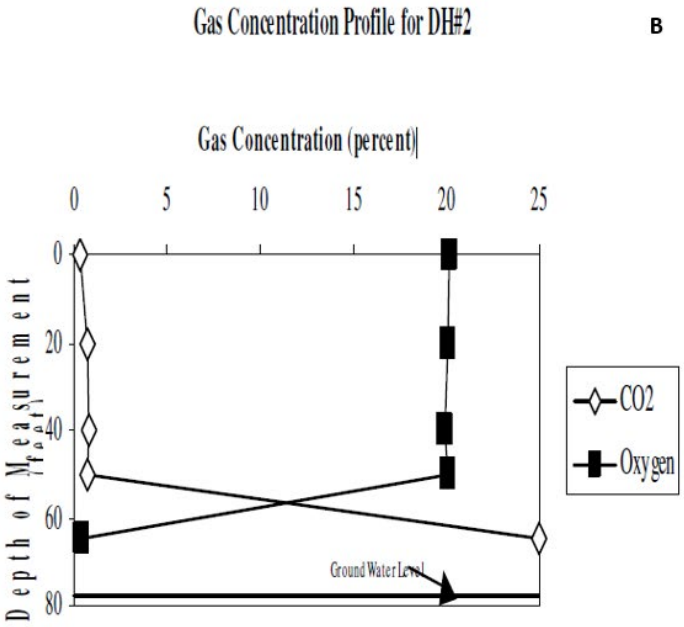

Figure 3. A. *Geologists Bill Ehler (left) and Fred Baldassare (right) at groundwater monitoring well DH#2 (labeled TB-2 on Figure 1B).* ***B.*** *CO_2 and O_2 concentrations measured in monitoring well DH#2 on the same afternoon the Geiwitz basement gas samples were collected while monitoring gas composition as shown in Figure 2.*

Potential Gas Sources

There were many possible sources of stray CO_2 at the Lawrence County site (**Figure 4**). The site is in the Glaciated Pittsburgh Plateau Section of the Appalachians Plateau Province. The homes were built on glacial drift and are directly adjacent to spoil in a large, reclaimed surface mine (Figures 1 and 4). Carbon dioxide and CH_4 are common constituents in natural gases generated by bacterial decomposition of organic material in glacial drift sediments (Coleman and others, 1988; Coleman, 2020). And CO_2 emissions from reclaimed mine soils are well documented at many locations in the eastern United States (Cravotta and others, 1994; Ehler, 2002; United States Environmental Protection Agency, 2005; Shrestha and Lal, 2006; Robinson, 2010a and 2010b). Additional potential source of CO_2 included subsurface acid mine drainage (AMD) reactions with the lower Pennsylvanian Vanport Limestone (**Figures 4 and 5**), gas migration from caves in the Vanport Limestone (Fawley and Long, 1997), swamp gas from wetlands adjacent to the site, active gas wells in the area, and an abandoned oil field (see Figures 1, 4, and 5). An additional possible source of the CO_2 was an abandoned deep mine in the lower Pennsylvanian Brookville coal. Entries to this abandoned mine were encountered during surface mining activities in the late 1980s. However, we quickly eliminated blackdamp from this mine as a CO_2 source because the mine is located up dip of the contaminated homes, is completely flooded, and discharged AMD at volumes as high as 2.83 m^3/s into a large mine pool (Figure 4c). The water drains south into a wetland up dip of both spoil from the reclaimed surface mine and glacial drift deposits.

We suspected either organic matter buried in spoil at the reclaimed surface mine or in situ AMD reactions with carbonate in the spoil. Organic matter in the spoil was a potential source of microbially mediated CO_2 (Whiticar and others, 1986; Whiticar, 1994; Hoefs, 2018). Calcium carbonate indigenous to and/or added to the spoil to help increase the alkalinity (i.e., bicarbonate (HCO_3^-) concentration) of acidic groundwater in the material was a potential inorganic source of CO_2 (Brady and others, 1998; Smith and Brady, 1988; Awuah-Offei and others, 2016). AMD discharging from the abandoned deep mine entry also could react with carbonate material in the spoil and generate CO_2 through a series of reactions involving several carbonate species, including carbonate (CO_3^{2-}), HCO_3^-, and carbonic acid (H_2CO_3). Bedrock in the study area consists of Allegheny Formation units (Figures 4 and 5). Although the Vanport Limestone is cut out by Kittanning channel sandstones in parts of the study area (Figure 5), the bedrock is highly fractured which affects groundwater levels and gas migration directions. AMD reactions with the Vanport Limestone was a plausible, though less likely, source for the stray CO_2 (Laughrey and Baldassare, 2003).

Stray Gas Isotope Analysis

We utilized isotope geochemical analyses to determine if the stray CO_2 was of organic or inorganic origin (Laughrey and Baldassare, 2003). These results, in combination with published geologic reports and ground-water data, facilitated our determination of the source of the CO_2 gas accumulations in the private homes.

Carbon has three naturally occurring isotopes, stable ^{12}C which accounts for 98.93% of carbon in nature and ^{13}C which accounts for 1.07% (Hoefs, 2018). In addition, radioactive ^{14}C occurs on Earth due to due to its formation in the upper atmosphere by cosmic rays whose protons engender secondary neutrons. These neutrons react with stable ^{14}N which is the target nucleus, *n* (neutron) is the projectile, and *p* (proton) is the particle ejected (Allégre, 2008). ^{14}C is the radioactive isotope produced by this reaction.

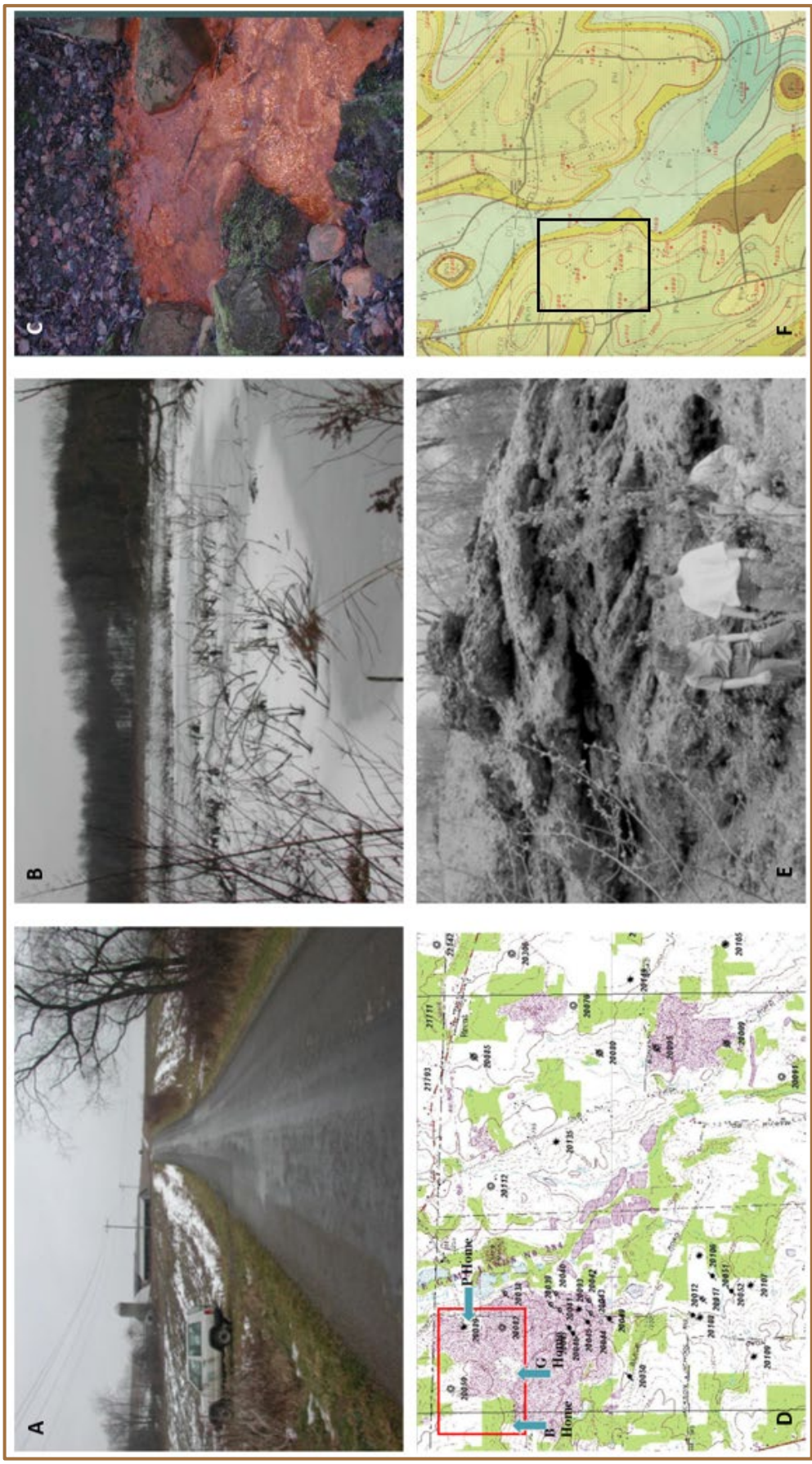

Figure 4. *Potential source of stray CO_2 at the Washington Township, Lawrence County, Pennsylvania site discussed in this review (Figure 1).* ***A.*** *View looking east-southeast at undulating topography associated with late Wisconsinan Kent till glacial deposits.* ***B.*** *Wetland located east-northeast of monitoring wells TB-1 and TB-4 and the Parker residence (Figure 1).* ***C.*** *AMD discharge from abandoned deep Brookville coal mine encountered during surface mining activities in the 1980s.* ***D.*** *2002 oil and gas well base map with the study area enclosed by the red rectangle.* ***E.*** *Vanport Limestone outcrop with Pennsylvania Geological Survey interns for scale.* ***F.*** *Portion of Poth's (1963) bedrock geology map showing Kittanning Formation bedrock in the study area (black rectangle). Vanport Limestone (brown) is mapped south of the study area.*

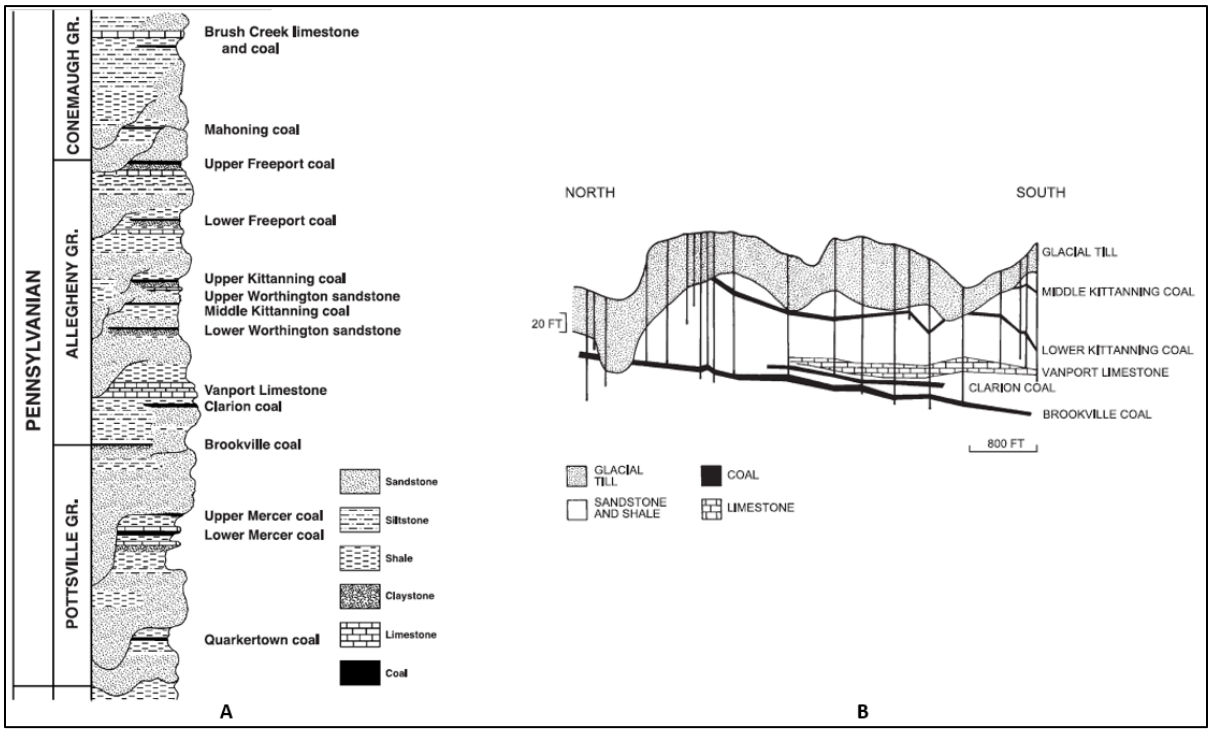

Figure 5. A. *Stratigraphic column for the Pottsville Formation, Allegheny Formation, and a portion of the Conemaugh Group in western Pennsylvania (from Laughrey and Baldassare, 2003). Note that the Pottsville and Allegheny Group status shown in the stratigraphic column has changed since publication of our paper.* ***B.*** *North-south geologic cross section for the stray CO_2 gas investigation site (see Figure 1 for line of section). Note that the Vanport Limestone is cut out (by Kittanning channel sandstones) south of the area where gas samples were collected. from Laughrey and Baldassare (2003)*

The ratio of stable $^{13}C/^{12}C$ isotopes in the stray CO_2 samples (**Table 1**) is reported as the difference between the ratios of the two isotopes of interest in the sample and the ratio in a primary reference standard (see Hoefs, 2018). That is,

$$X_{sample} = [(R_{sample} - R_{standard})/ R_{standard}] \times 1000,$$

where X represents the isotope of interest, in this case ^{13}C, and R represents the ratio of $^{13}C/^{12}C$. The value (δ) is expressed in terms of per mil (‰), or parts per thousand.

Table 1 provides the chemical and isotopic data collected from the basement of the Geiwitz home and from four of the monitoring wells installed near the home (Figure 1b). The CO_2 concentration in the Geiwitz basement at the time of sampling was 8.96% and the O_2 concentration was 13.05%. The N_2/Ar ratio of the basement atmosphere was 84.7 (air ~ 83.9). Methane and higher hydrocarbon gases were not detected.

Table 1. Stray gas composition and isotope data for the Geiwitz home and monitoring wells, Washington Township, Lawrence County, Pennsylvania CO_2 contamination site.

Sample Name	CO_2 %	O_2 %	N_2 %	Ar %	He %	CH_4 %	C_{2+} %	N_2/Ar	N_2/O_2	$\delta^{13}CO_2$ ‰	$^{14}CO_2$
Geiwitz Basement	8.96	13.05	77.08	0.91	0.004	nd	nd	84.703	5.906	-3.99	15
TB-2	2.19	18.73	78.15	0.92	0.0052	nd	nd	84.945	4.172	2.86	21.2
TB-5	15.58	9.08	74.45	0.88	0.0047	0.0097	nd	84.602	8.2	-4.02	13.2
TB-7	17.46	7.83	73.82	0.88	0.0062	0.0015	nd	83.886	9.427	-2.64	7.8
TB-10	10.86	7.87	80.31	0.96	0.0028	nd	nd	83.656	10.204	-7.01	24.5

nd – not detected

The $\delta^{13}CO_2$ of the samples at the Lawrence County stray gas contamination site ranged from -7.01‰ to 2.86‰ (Table 1). CO_2 in the basement of the Geiwitz home had a $\delta^{13}C$ of -3.99‰. All of the other CO_2 samples are from atmosphere directly above the water table in the monitoring wells. All of the CO_2 samples listed in Table 1 are relatively depleted in ^{12}C. We interpreted the CO_2 in our sample set as having an inorganic carbonate source (**Figure 6**), specifically $CaCO_3$ associated with glacial drift materials used as fill during surface mine reclamation (Brady and others, 1998; Smith and Brady, 1998; Ehler, 2002). Glacial till in the vicinity contains 4 to 8% $CaCO_3$ so was utilized as fill because of its high acid neutralization potential (Smith and Brady, 1998; Ehler, 2002). Variations in the $\delta^{13}CO_2$ of the samples (differences of as much as 9.87‰) are most likely due to heterogeneity in the source carbonate material. We considered mixing of CO_2 generated from carbonate in the subsurface at the site with bacterially mediated gas in the local aquifer as another plausible cause of the variations observed in $\delta^{13}CO_2$ of the samples (see Chapelle and Knobel, 1985), but our measurements of $^{14}CO_2$ activity in the samples precludes that possibility (discussed below).

As described above, radioactive ^{14}C is produced in the Earth's atmosphere by nuclear reactions based on interactions of cosmic-ray produced neutrons with stable ^{14}N. As soon as it has formed, ^{14}C combines with oxygen to give CO_2 which mixes rapidly throughout the atmosphere and the hydrosphere and attains constant levels of concentration representing a steady-state equilibrium (Allégre, 2008). This equilibrium concentration is maintained by the production of ^{14}C in the atmosphere and its continuous decay (^{14}C disintegrated by β^- radioactivity to give ^{14}N). Molecules of $^{14}CO_2$ enter plant tissue as a consequence of photosynthesis and by absorption through the roots. The concentration of ^{14}C in living green plants is maintained at a constant level by its continuous absorption from the atmosphere and its continuous decay. Animals that feed on the plants or absorb carbon-bearing ions or molecules from the biosphere also acquire a constant level of radioactivity due to ^{14}C. When the plant or animal dies, the absorption of ^{14}C from the atmosphere ceases and its activity

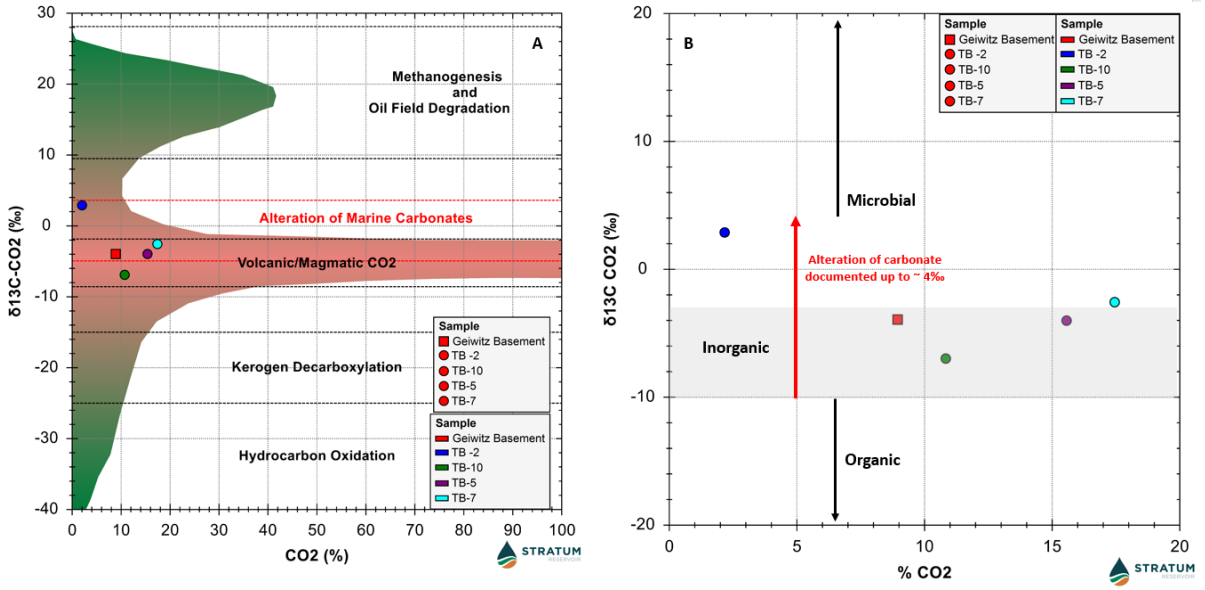

Figure 6. ***A.*** *Plot of molecular percentage of CO_2 versus $\delta^{13}CO_2$ for the Geiwitz home and monitoring wells showing interpretive genetic fields for carbon dioxide origins (modified from Golding and others, 2013). Natural gases with elevated CO_2 contents and $\delta^{13}CO_2$ between -3 and -10‰ are derived from inorganic sources, either carbonate mineral degradation or magmatic, i.e., mantle, sources based on association with ^4He or ^3He ratios. Magmatic sources are readily dismissed for the stray CO_2 discussed herein based on geologic setting. Note that alteration of carbonate is documented to result in $\delta^{13}CO_2$ values as high as 4‰. Microbial communities that degrade organic material to methane both produce and consume CO_2 with significant enrichment in $^{13}CO_2$. $^{13}CO_2$ depletion characterizes gas generated by thermal degradation of sedimentary organic matter and petroleum.* ***B.*** *Enlargement of the plot shown in A.*

due to ^{14}C declines as a result of radioactive decay. If the activity of ^{14}C in living tissue is known, the activity of ^{14}C in dead plant tissue can be used to calculate the time elapsed since death. This is the well-known ^{14}C date or age of a sample.

Atmospheric testing of nuclear devices in the 1950's and 1960's produced substantial amounts of ^{14}C-enriched CO_2. All plant or animal material that has grown since approximately 1955 has ^{14}C concentrations above natural equilibrium levels (Coleman and others, 1990). This ^{14}C concentration can be utilized as a tracer for recently generated microbial gas. ^{14}C activity is typically expressed as percent modern (pMC) where 100% modern is defined as the normal ^{14}C activity (or concentration) of atmospheric CO_2 in the year 1950. Organic materials that grew before 1950 would have ^{14}C activity <100 pMC. Organic materials that grew after ~1955 have ^{14}C activities >100 pMC due to the enhanced concentration of ^{14}C in the atmosphere caused by the testing of nuclear bombs. The five gas samples collected for this investigation have $^{14}CO_2$ activities between 7.8 and 24.6 pMC (Table 1 and **Figure 7**) indicating mixing of CO_2 generated from carbonate in the reclaimed mine spoil with atmospheric CO_2 and/or glacial drift gas (Coleman, 1994; Laughrey and Baldassare, 2003).

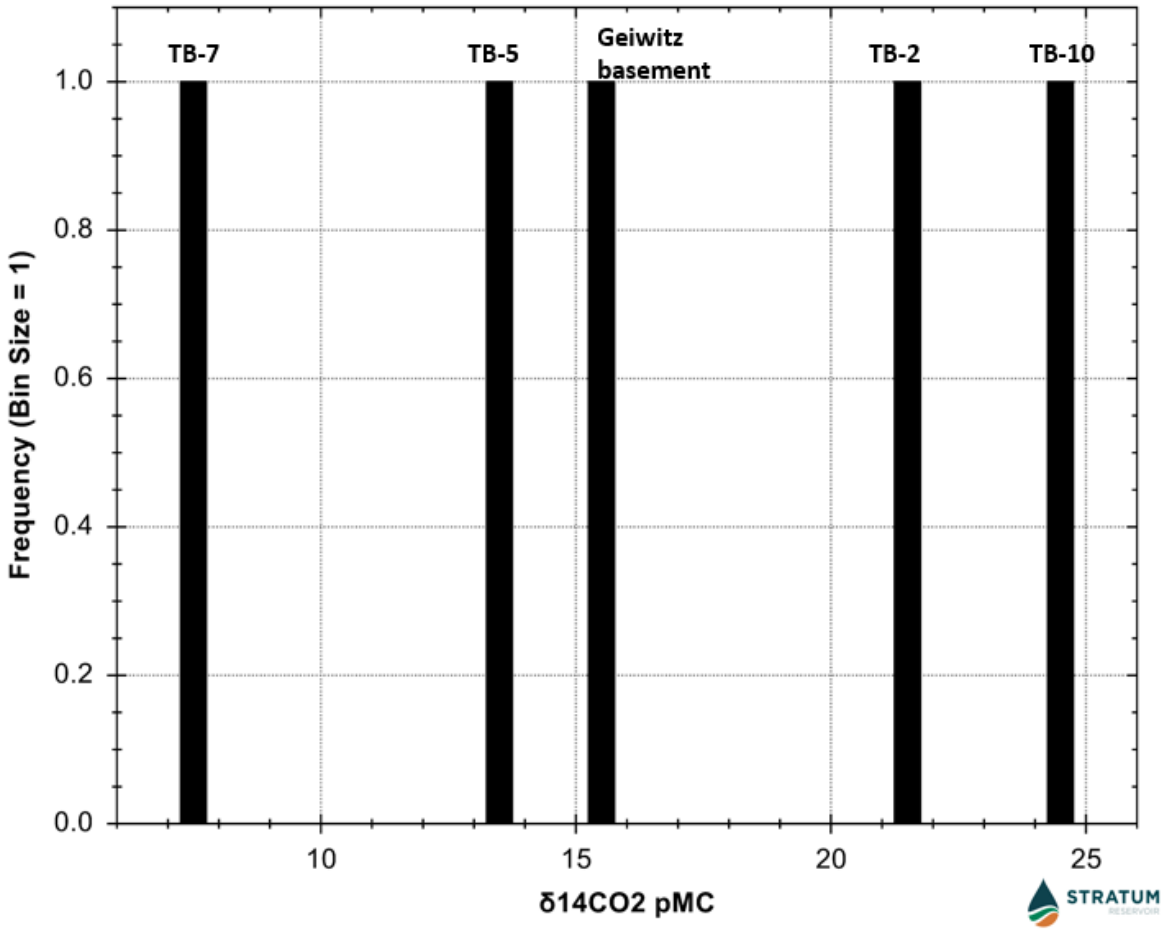

Figure 7. *Histogram showing the ^{14}C activity of the five gas samples collected from the Geiwitz home basement and monitoring wells listed in Table 1. pMC is percent modern carbon. 100 pMC is defined as natural (equilibrium) pre-bomb, i.e., pre-atmospheric nuclear weapons testing, ^{14}C concentration of atmospheric CO_2. All plant or animal material that has grown since approximately 1955 has ^{14}C pMC above 100. The low pMC values of these CO_2 samples support our interpretation of a carbonate source for the stray gas at the Lawrence County site.*

Geologic and Groundwater Data

The geochemistry of ground water collected from the deep mine drain and from the various monitoring wells at the site supported our interpretation of the gas isotope geochemistry (**Table 2**). The partial pressure of CO_2 in the collected water samples was 0.01 to 0.2 atm. Although alkalinity was moderately elevated (31.36 to 136.84 mg/l) and pH was slightly low (5.82 to 6.55), the water was undersaturated with respect to calcite, dolomite, and siderite (Table 2). During reclamation, no one anticipated the high water discharge from the abandoned deep mine, nor that such high volumes of CO_2 could form and exsolve in the spoil and move so efficiently as a free phase through permeable earth materials to nearby structures. See Ehler (2003) for a discussion of the CO_2 migration on the site.

Table 2. Groundwater and AMD discharge chemistry for the stray CO_2 gas site (from Ehler, 2002).

Sample	pH	Alkalinity mg/L	pCO_2 (atm)	SI (CO_2)	SI (calcite)	SI (dolomite)	SI (siderite)
Mine Drain	6.31	113.64	0.0544503	-1.264	-1.3352	-3.0419	-0.4581
TB-1	6.36	110.7	0.0489779	-1.31	-1.37	-3,17	-0.06
TB-2	6.2	337.1	0.2009555	-0.6969	-0.838	-2.0382	-0.1099
TB-3	6.2	136.84	0.0888383	-1.0514	-1.4216	-3.2502	-1.4181
TB-4	5.97	71.6	0.0786502	-1.1043	-2.0199	-4.2497	-2.0108
TB-7	5.82	31.36	0.0284315	-1.5462	-2.3601	-4.8631	-0.4786
TB-8	6.55	43.98	0.0125516	-1.9013	-2.0002	-4.4499	-3.0787

***p*CO_2 = partial pressure of CO_2; SI = saturation index**

Remediation

The geochemical data and interpretations presented above indicated that the CO_2 contamination of the homes and groundwater at the Lawrence County site was related to past surface mining activity. This conclusion allowed OSM to provide funds for remediation. The remediation process consisted of several steps:

- Concrete foundation blocks were filled with a special grout mix to decrease the permeability of the basement to gas (Figure 8A);
- Vapor barriers were installed to help make basement subfloors impermeable to gas (Figure 8B);
- Vents were installed; and
- Fan systems designed to create positive pressure beneath the homes were installed to maintain a meter-scale buffer zone between migrating CO_2 and the basements (Figure 8C).

Continuous basement atmosphere monitoring after remediation, as depicted in Figure 2, showed complete resolution of the stray CO_2 problem in the Geiwitz home. The remediation procedure described above succeeded in reducing CO_2 levels in all three of the homes to normal atmospheric levels (0.03%), including during periods of low atmospheric pressure.

Figure 8. *Stray CO_2 remediation, Geiwitz residence basement.* ***A.*** *Concrete foundations blocks were filled with a special grout mix to decrease permeability of the basement to gas.* ***B.*** *Vapor barriers installed to make subfloor impermeable to migrating gas.* ***C.*** *Vents were installed as was a fan system designed to create positive pressure beneath the home that maintains a meter-scale buffer zone between migrating CO_2 and the basement.*

Summary

The Washington Township, Lawrence County stray CO_2 problem was one of several such cases we investigated in western Pennsylvania between 1996 and 2003 (Laughrey and Baldassare, 2003). Elevated volumes of CO_2 and depressed concentrations of O_2 in building spaces appeared to be emerging as a serious environmental hazard in some areas of the Appalachian coalfields. We documented CO_2 concentrations in private residences in excess of 25% and O_2 levels less than 10% at many of these locations. CO_2 concentrations this high are dangerous and potentially lethal (information pertaining to CO_2 toxicity is available at http://www.osha.gov/). Humans lose consciousness in only a few minutes when exposed to air containing 10% or greater CO_2 and respiratory paralysis and death may follow. Lower CO_2 concentrations can lead to high pulse rates and hyperventilation, as well as clumsiness, severe headaches, and dizziness. Humans suffer hypoxia at O_2 concentrations less than 16% and unconsciousness when oxygen drops to 10% or less.

During these investigations, we found that CO_2 in the spoil of reclaimed surface mines may be of organic or inorganic origin (Laughrey and Baldassare, 2003). Organic CO_2 in spoil forms through aerobic respiration of plant roots and organisms. Inorganic CO_2 forms in spoil treated with alkaline addition by neutralization of acid from pyrite oxidation through reactions with carbonate minerals. Even near-neutral AMD waters can be undersaturated with respect to carbonate and react with calcite and dolomite in reclaimed mine spoil to produce CO_2 under certain conditions.

Active and reclaimed surface mines historically were located in rural regions isolated from homes and commercial real estate. However, contemporary urban expansion, suburban sprawl, and Brownfield development now juxtapose surface mining and building spaces in many parts of the Appalachian basin. This problem occurs in other North American coalfields as well (Awuah-Offei and others, 2016). Ironically, the practice of alkaline addition to surface mines has saved hundreds of kilometers of streams in western Pennsylvania from degradation caused by AMD. Fortunately, the unintended consequence of CO_2 off gassing caused by this practice can be mitigated by using recommended building construction techniques. Abatement of stray CO_2 and other gases in new building construction is accomplished by using existing building code requirements for radon-resistant construction with the recommendation that the ventilation system is reversed to create a positive pressure system.

Correct identification of the source of stray CO_2 is the most important step in the mitigation process. Gas composition and ground water chemistry data by themselves are ambiguous in defining a mechanism for CO_2 generation and a specific source. Isotope geochemistry is the most powerful tool available for discriminating CO_2 from different sources. Accurate recognition of a CO_2 source

facilitates the assignment of liability, the procurement of appropriate remediation funds, and the design of adequate abatement protocols in stray gas migration cases.

Subsurface sequestration of anthropogenic CO_2 is a significant and necessary emerging technology for helping to curtail the detrimental accumulation of greenhouse gases in the Earth's atmosphere:

https://netl.doe.gov/coal/carbon-storage/atlas/mrcsp#:~:text=The%20MRCSP%20monitoring%20period%20between,approximately%20320%2C000%20cars%20from%20roads

Subsurface CO_2 sequestration has been accomplished using various types of carbon storage reservoirs: from depleting/depleted petroleum reservoirs to unminable coal seams to deep saline formations. Assuring the environmental safety of subsurface CO_2 storage is critical and can be accomplished using best-practice monitoring, verification, and accounting methods, as developed through the U.S. Department of Energy's Carbon Sequestration Partnership Program. If a carbon storage project is not carefully planned and implemented, sequestered CO_2 may migrate and contaminate potable groundwater or accumulate as free gas in buildings with consequences similar to those described in this review. It is also important to recognize that there are several possible sources of CO_2 in the oil and gas fields and coalfields of the Appalachian basin before storing anthropogenic CO_2 there.

References

Allégre, C.J. (2008), Isotope geology, Second edition, Cambridge University Press, 512 p.

Awuah-Offei, K., M. Mathiba, and F.J. Baldassare (2016), Identifying the presence of AMD-derived soil CO_2 in field investigations using isotope ratios, Minerals, v. 6, 18, doi: 10.3390/min6010018.

Brady, K.B.C., R.J. Hornberger, and G. Fleeger (1998), Influence of geology on postmining water quality: Northern Appalachian basin in K.B.C. Brady, M.W. Smith, and J. Schueck, eds., Coal mine drainage prediction and pollution prevention in Pennsylvania, Chapter 8, p. 8-1 – 8-92.

Chapelle, F.H. and L.L. Knobel (1985), Stable carbon isotopes of HCO_3^- in the Aquia Aquifer, Maryland: Evidence for an isotopically heavy source of CO_2, GroundWater, v. 23, p. 592-599.

Coleman, D.D., C.-L. Liu, and K.M. Riley (1988), Microbial methane in the shallow Paleozoic sediments and glacial deposits of Illinois, U.S.A., Chemical Geology, v. 71, p. 23 – 40.

Coleman, D.D, L.J. Benson, and P.J. Hutchinson (1990), The use of isotope analysis for identification of landfill gas in the subsurface, in Proceedings of the GRCDA 13th Annual Landfill Gas Symposium, Silver Spring, MD, Government Refuse Collection and Disposal Association, Silver Spring, MD.

Coleman, D.D. (1994), Advances in the use of geochemical fingerprinting for gas identification. Paper presented at the American Gas Association Operations Conference, San Francisco, California, May 9 – 11, 9 p.

Coleman, D.D. (2020), 6. The origin of drift-gas deposits as determined by radiocarbon dating of methane, in R. Berger and H E. Suess (eds.), Radiocarbon dating: Proceedings of the Ninth International Conference Los Angeles and La Jolla, 1976, Berkeley: University of California Press, p. 365 – 387. http://doi.org/101525/9780520312876-036.

Cravotta, C.A., III, D.L. Dugas, K.B.C. Brady, and T.E. Kovalchuk (1994), Effects of selective handling of pyritic, acid-forming materials on the chemistry of pore gas and groundwater at a reclaimed

surface coal mine, Clarion County, PA, USA, in Proceedings of the International Land Reclamation and Mine Drainage Conference and the 3rd International Conference on the Abatement of Acid Drainage, Pittsburgh, PA, USA, 24 – 29 April 1994, p. 365 – 374.

Ehler, W.C. (2002), Dangerous atmosphere created by strip mine spoil, in Proceedings of the 24th National Association of Abandoned Mine Lands Programs, Park City, Utah, USA, p. 1 – 16.

Fawley, J.P. and K.M. Long (1997), Harlansburg Cave: The longest cave in Pennsylvania, Journal of Cave and Karst Studies, v. 59, p. 106 – 111.

Hoefs, J. (2018), Stable isotope geochemistry, Eighth Edition, Springer, 437 p.

Laughrey, C.D. and F.J. Baldassare (2003), Some applications of isotope geochemistry for determining sources of stray carbon dioxide gas, Environmental Geosciences, v. 10, p. 107 – 122.

Mathiba, M., K. Awuah-Offei, and F.J. Baldassare (2014), Influence of elevation, soil temperature, and soil moisture content on reclaimed mine land soil CO_2 fluxes, Environmental Earth Science, DOI 10.1007/s12665-014-3839-0

Poth, C.W. (1963), Geology and hydrology of the Mercer quadrangle, Mercer, Lawrence, and Butler Counties, Pennsylvania, Pennsylvania Geological Survey Ground Water Report W 16, 4th Series, 149 p.

Reese, S.O., G.M. Fleeger, and Z.C. Schagrin (2022), Bedrock-topography and drift-thickness maps of the Edinburg, Harlansburg, New Castle North, and Slippery Rock 7.5-minute quadrangles, and Pennsylvania part of the Campbell 7.5-minute quadrangle, Butler, Lawrence, and Mercer Counties, Pennsylvania, Pennsylvania Geological Survey, 4th ser., Open-File Report OFSM 22-01.0, 7 p., 4 pls., scale 1:24,000, geodatabase. Available online.

Robinson, B.A. (2010a), The occurrence and attempted mitigation of carbon dioxide in a home constructed on reclaimed coal mine spoil, Pike County, Indiana, U.S. Geological Survey Scientific Investigations Report 2010-5157, 30 p.

Robinson, B.A. (2010b), The occurrence and mitigation of carbon dioxide in homes built on reclaimed coal mines, U.S. Geological Survey, Reston, VA, USA.

Shrestha, R.K. and R. Lal (2006), Carbon dioxide emissions from reclaimed mine soils in eastern Ohio, Conference Paper, ASA-CSSA-SSSA International Annual Meetings, November 12- 16, 2006, Indianapolis, USA.

Smith, M.W. and K.B. Brady (1988), Chapter 13: Alkaline addition, in K.B. Brady, M.W. Smith, and J. Schueck, eds., Coal mine drainage prediction and pollution prevention in Pennsylvania, Pennsylvania Department of Environmental Protection, p. 13-1-13-22.

United States Environmental Protection Agency (2005), U.S. Surface mines emissions assessment, https://www.epa.gov/sites/default/files/2016-03/documents/us_surface_coal_mines_markets-update_feb2015.pdf.

Whiticar, M.J., E. Faber, and M. Schoell (1986), Biogenic methane formation in marine and freshwater environments: CO2 reduction vs. acetate fermentation – isotope evidence, Geochimica et Cosmochimica Acta, v. 50, p. 693 – 709.

Whiticar, M.J. (1994), Correlation of natural gases with their sources, in L.B. Magoon and W.G. Dow (eds.), The petroleum system – from source to trap, AAPG Memoir 60, p. 261 – 283.

STOP 1: ACA SAND AND GRAVEL

LEADERS: ERIC STRAFFIN – PENNWEST UNIVERSITY, EDINBORO CAMPUS
TODD GROTE – INDIANA UNIVERSITY SOUTHEAST

41.898848 / -79.7035226

Introduction

Very little is known about the age of glacial ice advance and retreat in northwestern Pennsylvania, with most of our knowledge about the timing of events coming from outside the state (e.g. Dalton et al., 2020). Recent advances in imaging landforms (LiDAR) and dating techniques (in particular OSL, or Optically Stimulated Luminescence) permit a better understanding of the region. However, these techniques also make clear that we have much to learn regarding the geologic details of the late Quaternary Epoch in northwestern Pennsylvania, and how multiple glaciations of the elevated Appalachian Plateau correlate with adjacent areas in Ohio and New York. Details regarding ice margin position are much more complicated than previously understood, and the data presented here provide some preliminary results.

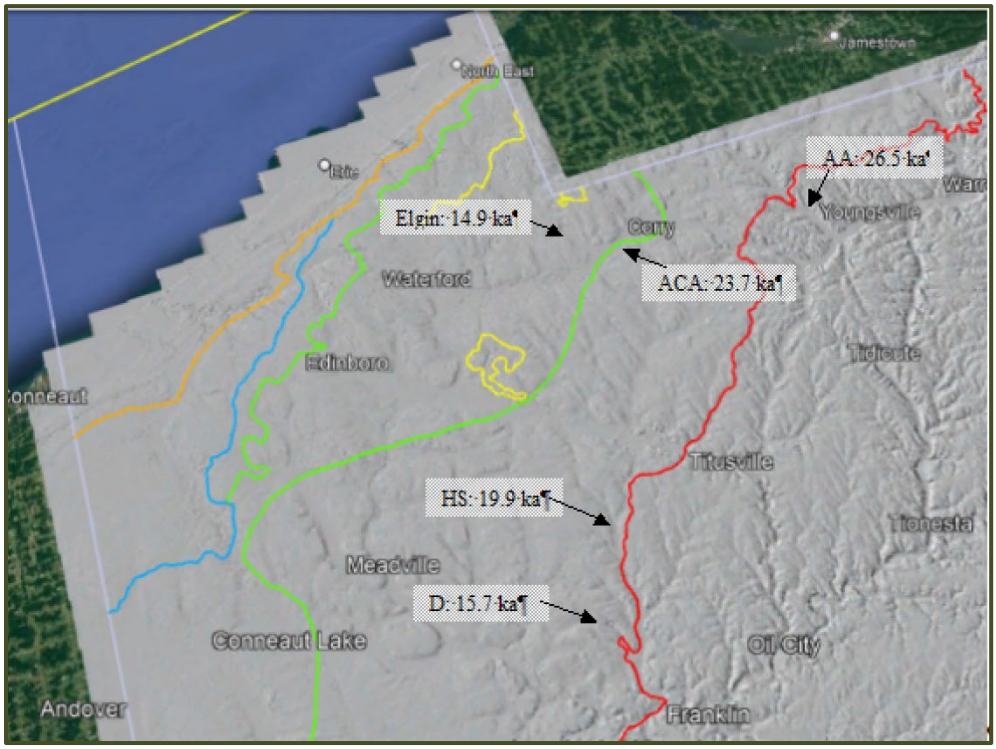

Figure 1.1. *Oblique view of northwestern Pennsylvania with overlain DTM model showing location of OSL ages discussed in this article. Moraine fronts and glacial borders (Shepps et al, 1969) are Ashtabula (orange), Hiram (Defiance Moraine-blue), Lavery Moraine and extended Lavery of White et al (1969) (green), Kent (red), Clymer and Findley Lake recessional moraines (yellow). See also Figure 1.2. From Google Earth and PASDA.*

Mapping across the region by Shepps et al (1959) and others (e.g. White et al, 1969) provides an excellent foundation upon which to build more detailed surficial geologic maps, using geomorphic mapping on LiDAR hillshade digital terrain models (DTM's; **Figure 1.1**). Landforms and associated sediments can then be used to guide site selection for potential dating (Straffin and Grote, 2010; Grote and Straffin, 2019). In particular, subtle moraines marking past ice

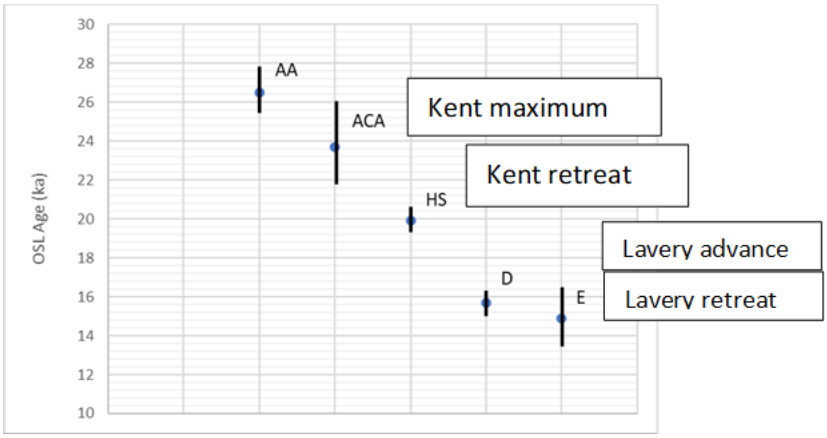

AA	Allegheny Aggregate	Little Brokenstraw Creek
ACA	ACA Sand and Gravel	East Branch French Creek
HS	Hillside Stone	Sugar Creek
D	Deckard pit	Deckard Run
E	Elgin pit	Beaver Run

Figure 1.2. *OSL ages plotted by age with error bars for locations discussed in the text and Figure 1.*

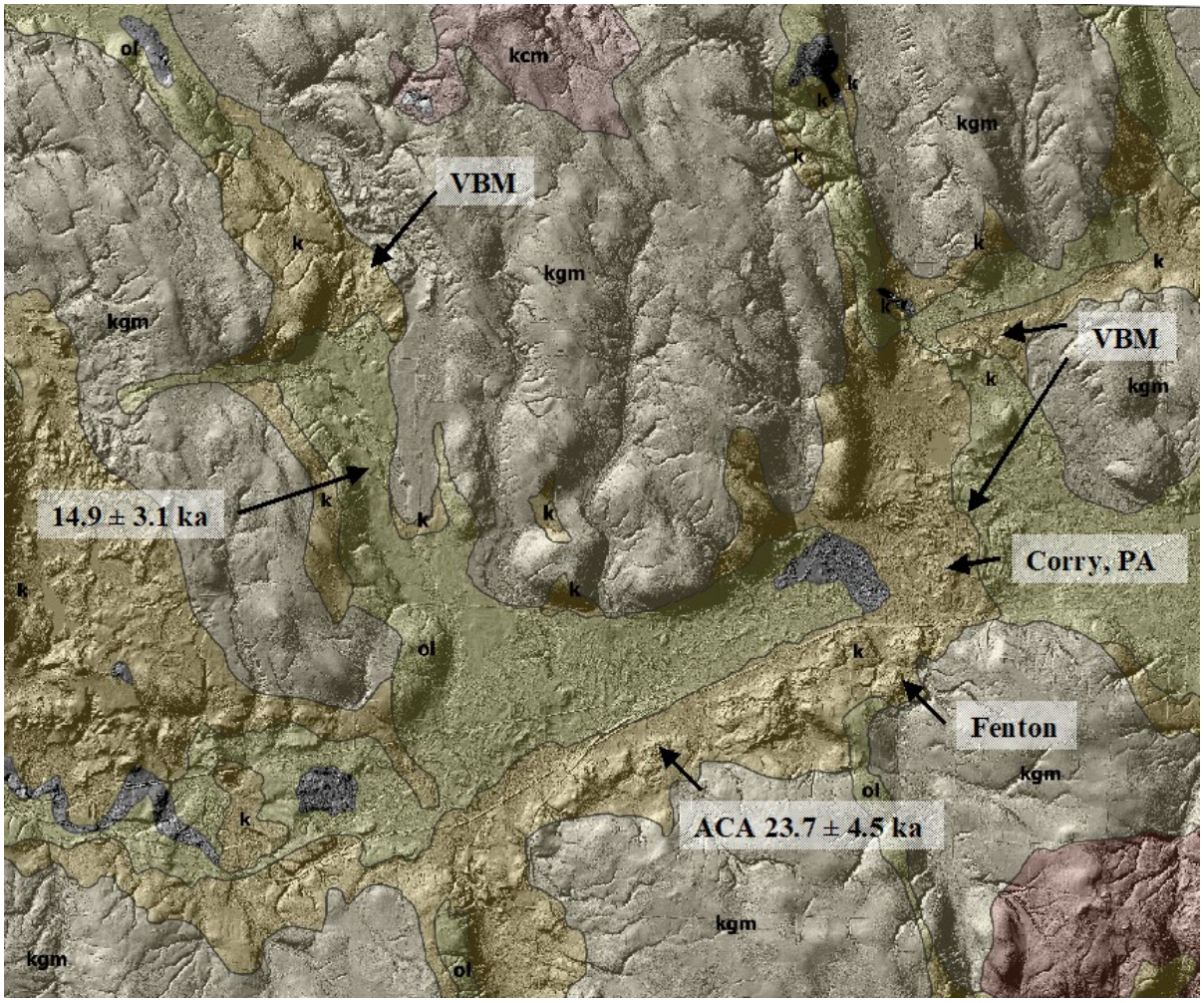

Figure 1.3. *OSL ages plotted by age with error bars for locations discussed in the text and Figure 1.1.*

margins can be traced across uplands that were previously unmapped and/or uncorrelated across the region. These same subtle, upland terminal moraines can also be traced and correlated to adjacent valleys with distinctive hummocky topography, forming valley blocking moraines (VBM). VBM's were previously mapped in many valleys as kames (**Figure 1.3**) and are analogous to the valley choker moraines of MacClintock and Apfel (1944). Meltwater from glaciers produced outwash surfaces that dip away from many of the VBM's (**Figure 1.4**). Sand in outwash is potentially dateable with OSL (Fuchs and Owen, 2008; Huot et al., 2018) which can provide ages on the timing of ice advance and retreat.

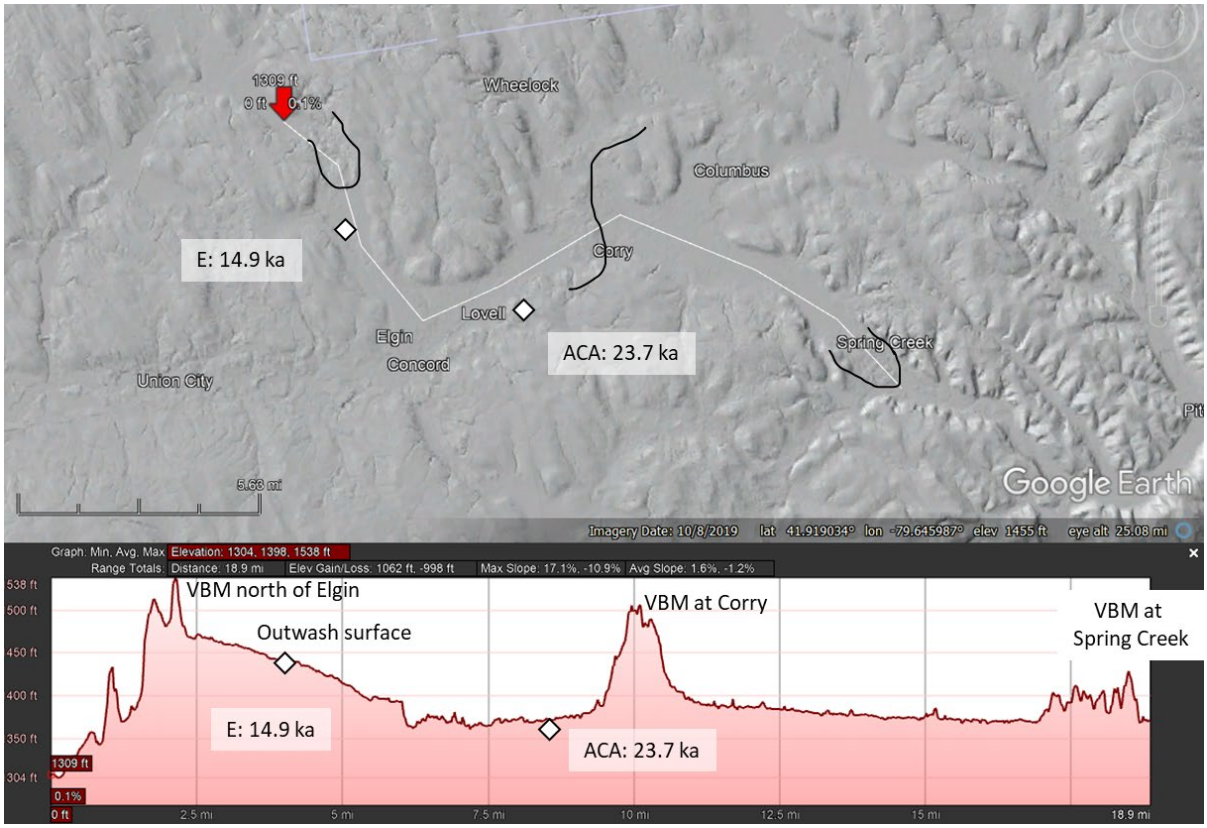

Figure 1.4. *Top: DTM with a section line down the valley axis through the study area, with terminus of valley blocking moraines (VBM) marked by black lines. Below: Topographic profile of section line illustrating geometry of valley profile.*

Stop #1: ACA Sand and Gravel

The ACA Sand and Gravel company is situated within hummocky topography associated with a lobe of ice that extended to the city of Corry, Pennsylvania (Figure **1.1**, **1.3** and **1.4**). The pit exposed several distinct, stacked packages of cross bedded sand and gravel, interpreted to be aggrading braided channel deposits (outwash; **Figure 1.5**). Wide, shallow channel fills fine upward from dark coarse sand to lighter, finer sands and silt. An OSL sample was recovered from cross bedded sand with an age of 23.7 ± 4.5 ka (Figures 5 and 6) which roughly corresponds with the regional late Wisconsinan ice maximum position. Cross beds indicate eastward transport, which is opposite of the post glacial drainage direction. Deposition of a subsequent VBM (situated at the town of Corry) resulted in drainage diversion (**Figure 1.4**). Sediments overlying outwash were not well exposed at the ACA pit, having been removed as overburden. However, correlable sediments exposed in a nearby quarry (C.B. Fenton Gravel) were well exposed, but too coarse for OSL dating. The overlying sediments were poorly sorted kame deposits (gravelly till and silty

Figure 1.5. *Bedsets of cross bedded sand (light) and gravel (dark). Beds generally fine upward. OSL sample location center of photo. See Figure 3 for a close up. Photo Eric Straffin.*

Figure 1.6. *Close up of fining-upward, cross bedded sand with OSL sample. Top is to the right. Photo Eric Straffin.*

kettle fills, **Figure 1.7**) associated with the hummocky topography of the ice margin and valley blocking moraine. The OSL age thus marks a date prior to the advance of the ice lobe that advanced to what is now the town of Corry. An OSL date of 26.5 ka from very coarse outwash just beyond the mapped Kent moraine margin to the east of Corry (AA, **Figure 1.1**) falls within the error range of the ACA date, further defining the timing of ice advance in the region.

Up-valley from ACA Sand and Gravel is a younger outwash surface that can be mapped to a younger valley blocking moraine (**Figure 1.1**), which can be correlated with what Shepps et al (1959) mapped as the Clymer recessional moraine. A small quarry north of Elgin exposed weakly

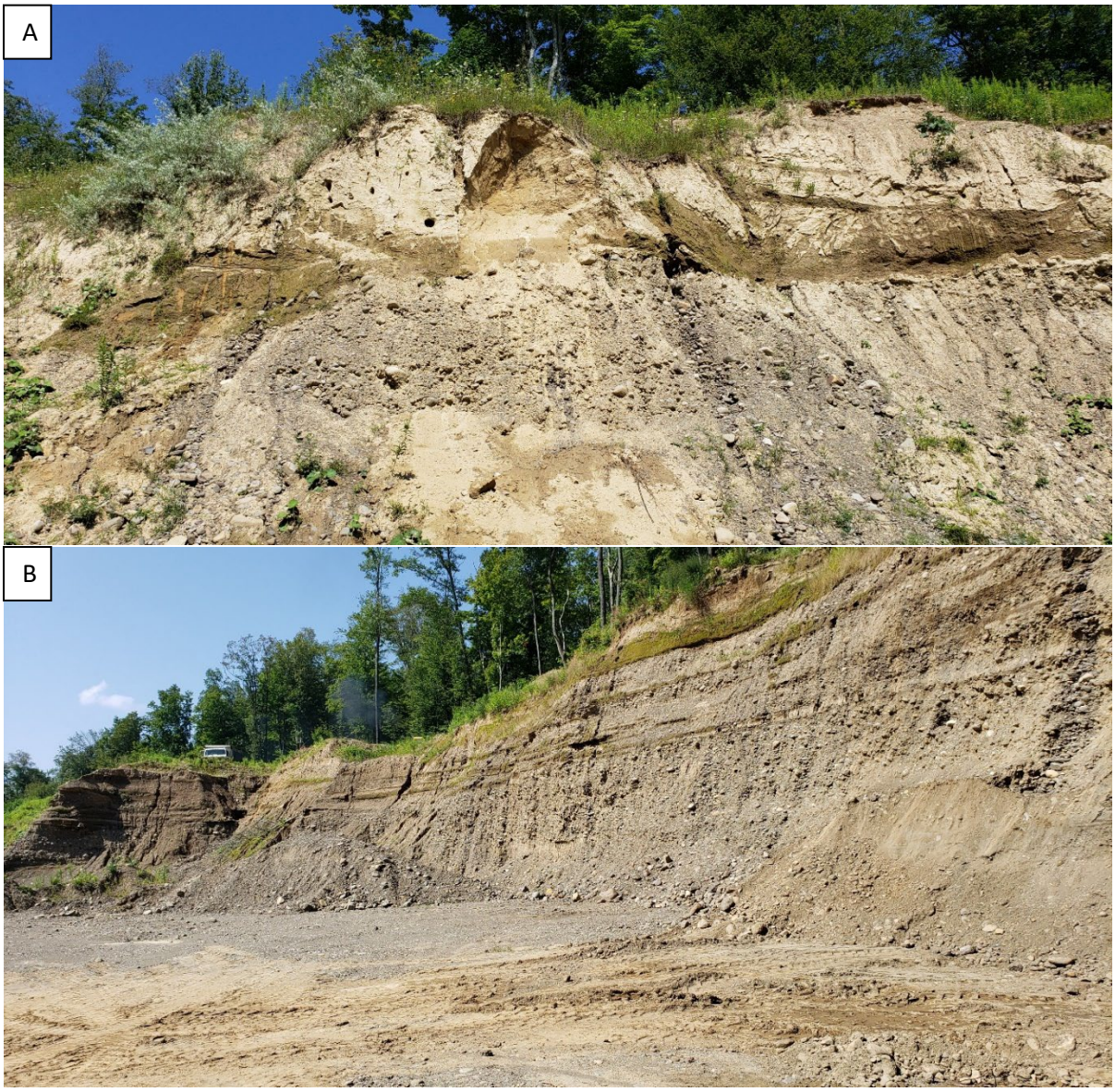

Figure 1.7. *Fenton pit. A) Upper section with laminated very fine sand and silt filling small channels or kettles, overlying coarse, poorly sorted, clast supported gravel (outwash). B) Exposure of lower portion of pit, with same lower gravel fining upward to cross bedded sand and gravel. Photo by Eric Straffin.*

imbricated, very poorly sorted, cross bedded gravels typical of braided stream channels. Cross bedded coarse to fine sand lenses were interbedded with the gravel and sampled for OSL (**Figure 1.8**). An age of 14.9 +/- 3.1 ka was obtained, which provides a minimum age on the "Clymer" moraine. This date may be significantly younger than the moraine itself, as braided stream deposition may have continued for some time after iced retreat. This age is similar to an OSL age on braided stream deposits associated with a VBM near Deckard, PA (**Figure 1.1**). **Figure 1.4** illustrates the cross sectional topography of the VBM and outwash surfaces within the valley, and helps to demonstrate that more northerly VBM's are related to more recent advances of ice than southerly VBM's. Another OSL age of 19.9 ka from outwash traceable to the Kent end moraine (**Figure 1.1**) constrains the timing of the end of deposition of that distinctive landform.

Figure 1.8. *Exposure of cross bedded sand lens within clast supported gravels. OSL sample location illustrated to right of notebook, located in outwash traceable to valley blocking moraine near Elgin, PA. See Figure 1.1 for location. Photo by Eric Straffin.*

References

Dalton, A. S., Margold, M., Stokes, C. R., Tarasov, L., Dyke, A. S., Adams, R. S., Allard, S., Arends, H. E., Atkinson, N., Attig, J. W., Barnett, P. J., Barnett, R. L., Batterson, M., Bernatchez, P., Borns, H. W., Breckenridge, A., Briner, J. P., Brouard, E., Campbell, J. E., ... Wright, H. E. (2020). An updated radiocarbon-based ice margin chronology for the last deglaciation of the North American Ice Sheet Complex. Quaternary Science Reviews, 234, [106223]. https://doi.org/10.1016/j.quascirev.2020.106223

Wright, H. E. (2020). An updated radiocarbon-based ice margin chronology for the last deglaciation of the North American Ice Sheet Complex. Quaternary Science Reviews, 234, [106223]. https://doi.org/10.1016/j.quascirev.2020.106223

Fuchs, M. & Owen, L. A. (2008) Luminescence dating of glacial and associated sediments: review, re-commendations and future directions. Boreas, Vol. 37, pp. 636–659.

Grote, T. and Straffin, E.C. (2019) Analysis of Late Wisconsinan Ice-Marginal Environments in Northwestern Pennsylvania, The Pennsylvania Geographer, V. 57, No.1.

Huot, S., Caron, O. J., & Curry, B. B. (2018). Applying luminescence dating on fluvioglacial outwash deposited after the LGM near Chicago (USA). Paper No.19-11. Paper presented at GSA North-Central 2018 Annual Meeting, Ames, Iowa, United States. https://doi.org/10.1130/abs/2018NC-313240

MacClintock, P. & Apfel, E.T. (1944). Correlation of the drifts of the Salamanca re-entrant, New York. Geological Society of America Bulletin, 55, 1143-1164.

Shepps, V. C., G. W. White, J. B. Droste and R. F. Sitler. 1959. The glacial geology of northwestern Pennsylvania. Pennsylvania Geologic Survey, 4th Series, General Geology Report 32, 59 p.

Straffin, E. C., and Grote, T. (2010) Surficial geology of the Sugar Lake 7.5-minute quadrangle, Crawford and Venango Counties, Pennsylvania: Pennsylvania Geological Survey, 4th ser., Open-File Report OFSM 10–05.0, 23 p.

White, G. W., S. M. Totten, and D. L. Gross. 1969. Pleistocene Stratigraphy of northwestern Pennsylvania. Pennsylvania Geological Survey, 4th ser. General Geology Report 55, 88p.

POI Figure Source: *Daderot, 2015, Wangjianglou Park – Chengdu, Sichuan, China, https://commons.wikimedia.org/wiki/File:Bamboo_-_Wangjianglou_Park_-_Chengdu,_China_-_DSC05737.jpg.*

Point of Interest: The 1859 Drake Well in Titusville is not the world's first oil well! As early as 347 C.E., the Chinese used bamboo poles to construct oil wells that went as deep as 800 feet (PBS, 2004). That means the Chinese constructed oil wells over 1,500 years before the Drake Well and that their wells went over 700 feet deeper (Drake Oil Well Museum, 1979).

POI Sources:

PBS, Thirteen/WNET Net York, 2004, Extreme Oil, accessed from https://www.thirteen.org/wnet/extremeoil/history/prehistory.html.

Pees, S. T., 2004, Oil History: Drake's Well, accessed from http://www.petroleumhistory.org/OilHistory/pages/drake/drakewell.html.

STOP 2: GEOLOGY OF ERIE BLUFFS STATE PARK

ERIC STRAFFIN – PENNWEST UNIVERSITY, EDINBORO CAMPUS
TAMARA MISNER – ALLEGHENY COLLEGE

42.01516 / -80.37666

Introduction

Erie Bluffs State Park encompasses 587 acres along the southern shore of Lake Erie, in Erie County, Pennsylvania (**Figure 2.1**). The park includes the largest stretch of undeveloped bluffs overlooking Lake Erie in Pennsylvania, providing beautiful wilderness views of the lake 90 feet below. Erie Bluffs State Park was established in 2004 as Pennsylvania's 117th state park. At that time, a (predominantly) biological survey was conducted that documented diverse flora, fauna, and landforms. That work was used in part to inform and develop the Master Plan for Erie Bluffs State Park, 2008. The vision for the Park includes protection of the integrity of its glacial landscapes and natural communities, to provide recreational, interpretive and educational opportunities for the public, and to contribute to the quality of life and economy of northwestern Pennsylvania (Master Plan, 2008).

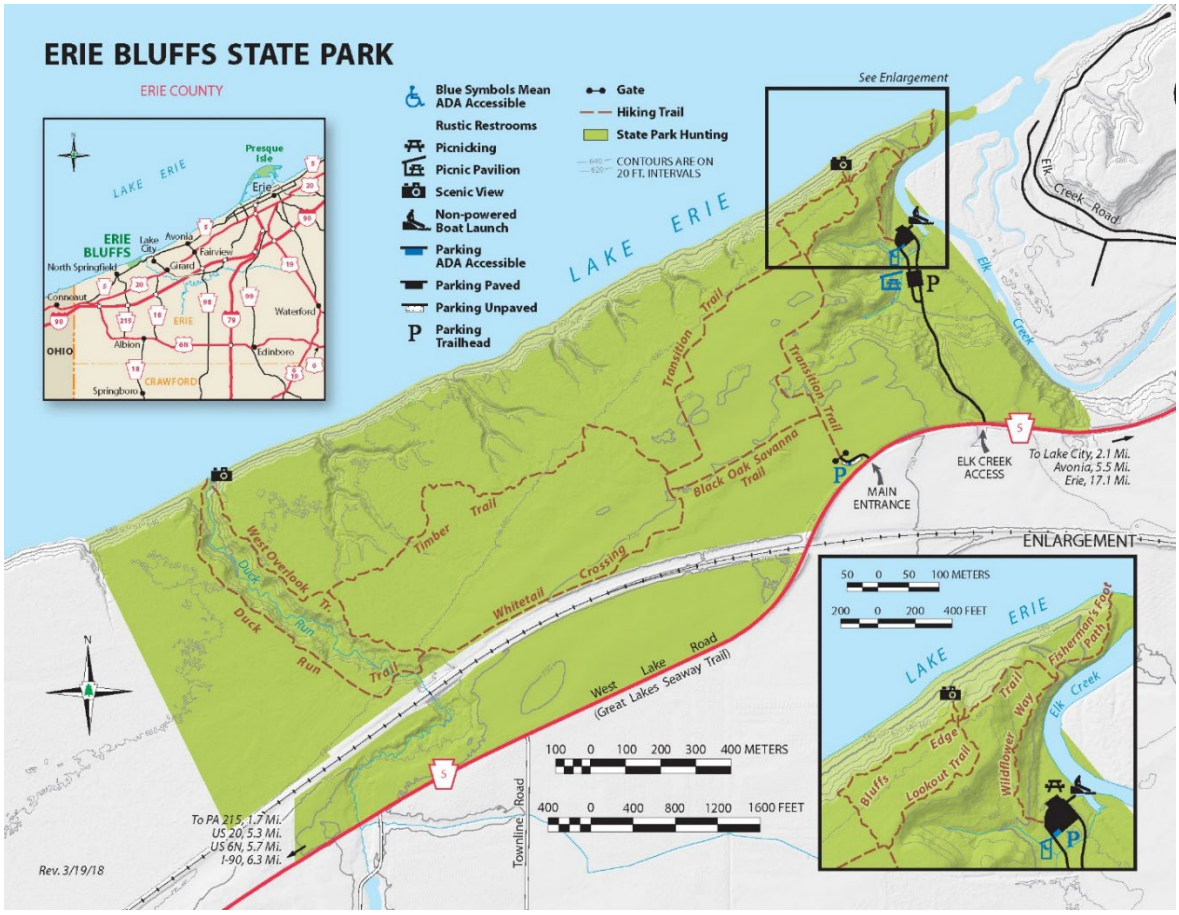

Figure 2.1. *Erie Bluffs State Park. DCNR, 2018.*

It is the late-glacial landscape that is the focus of this article. While generally documented (see **Figure 2.2**), few details regarding the geology of Erie Bluffs State Park have been published. Presented here-in is a description of sediments exposed along the bluffs, related to landforms (**Figure 2.3**). These observations add to the known geologic history of the Erie region, and have

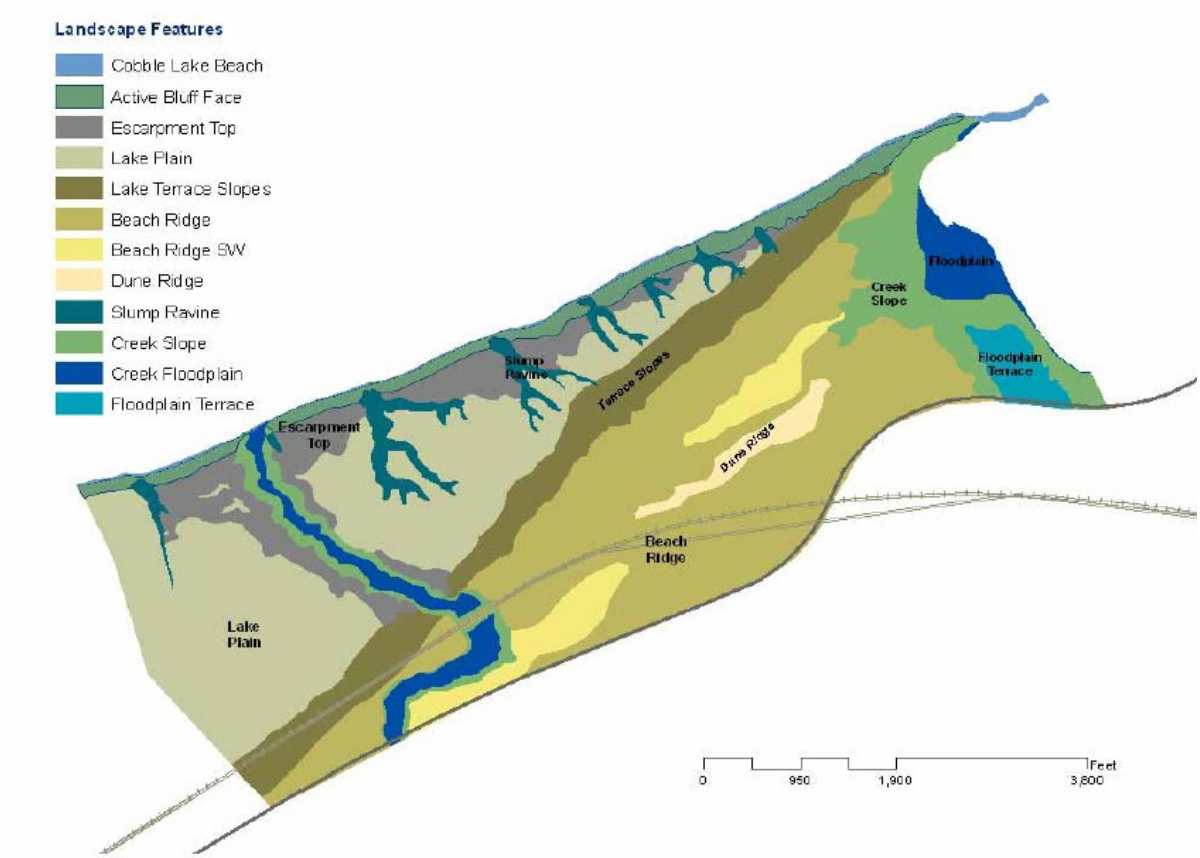

Figure 2.2. *Landscape features map (Master Plan, 2008).*

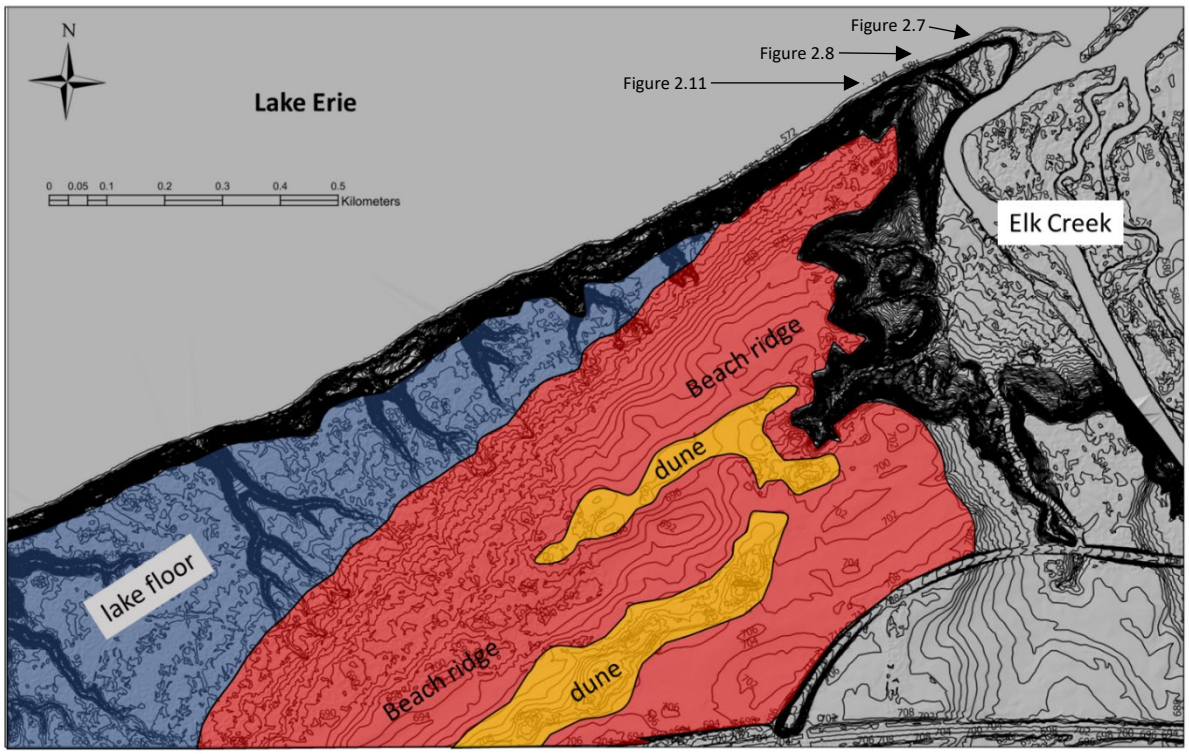

Figure 2.3. *Map of a portion of Erie Bluffs State Park. Gullies and erosional bluffs not mapped. Lake floor = blue, beach ridges and associated shoreline = red, dunes =yellow, gray = not mapped. Contour interval 1 foot plotted on DTM.*

implications for a range of important issues, including bluff erosion, sediment production and down-drift sediment supply to the beaches of Presque Isle.

Landforms

Paleo-shorelines of ancestral Lake Erie are clearly visible on hillshade models of Erie County. These features include erosional scarps as well as constructional shorelines that can be regressive and/or progradational in nature. At Erie Bluffs State Park, the most prominent paleo-shoreline feature has been previously mapped as the Warren I shoreline (Schooler, 1974; Totten, 1985) with a crest elevation of ~212 m (694 ft) a.s.l. The prominent northwest facing slope along the beach ridge dips down to 206 m (675 ft) where it transitions to a less steep lake bottom. Eolian sand dunes can be found as two ridges that cap the beach deposits, oriented roughly parallel to one another, in a northeast-southwest direction (**Figure 2.3**). These landforms developed along the margin of Lake Warren (**Figure 2.4**), a proglacial lake that formed during major drainage reorganization during Late Wisconsinan glacial fluctuations (**Figure 2.5**).

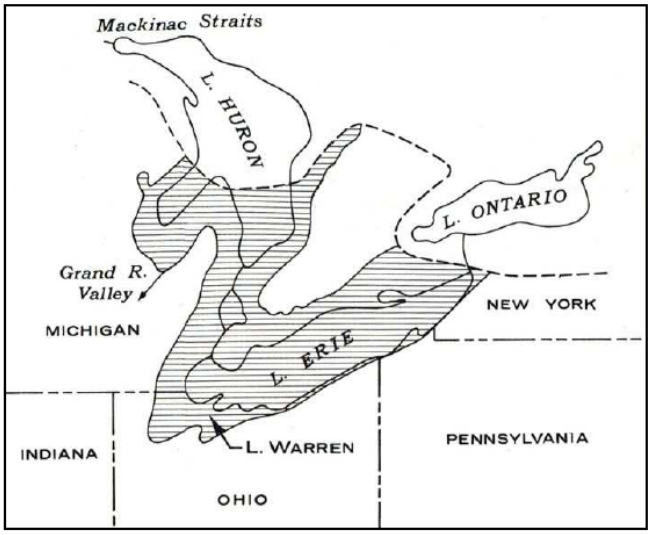

Figure 2.4. *Map of proglacial Lake Warren and approximate location of glaciers blocking lake outlets. Modified from Schooler, 1974 and McCoy, 2010).*

Stratigraphy

Exposures of the bluffs occur as waves erode the base, oversteepening the bluffs, leading to slumping and removal of slumped sediment by ongoing wave action (**Figure 2.6**). Bluff exposures permitted intermittent but detailed examination of sediments exposed for ~ 1 mile from the mouth of Elk Creek, southwest along the modern shoreline. **Figure 2.7** shows a described and interpreted section exposed at the east side of the State Park, near the mouth of Elk Creek. The exposed Elk Creek deposits were from a time when the stream was graded to a lake level higher than that of today. At that site, Devonian bedrock was observed at lake level, overlain by till (12 ft), overlain by convoluted, laminated lacustrine silt/sand (8 ft), capped by alluvium (2 ft) from Elk Creek. Further to the southwest, bluff height increases as it transitions from an intersection of the Elk Creek valley to paleo-shoreline sediments (**Figure 2.8**). The general profile is similar at the base, with the exception of increasing thicknesses of deposits, and a cap of shoreline sand and gravel from ancestral Lake Erie (Warren shoreline). Of note are laterally continuous lacustrine sand/silt couplets (**Figure 2.9**). In places these rhythmically laminated sediments are contorted, features consistent with rapid sediment deposition and loading of underlying soft sediment. Asymmetrical climbing ripples in lacustrine sediments clearly show paleocurrents to the northeast throughout the section, and further support episodic, rapid sedimentation. Occasionally, rounded cobbles and gravel can be found as isolated dropstones (**Figure 2.10**),

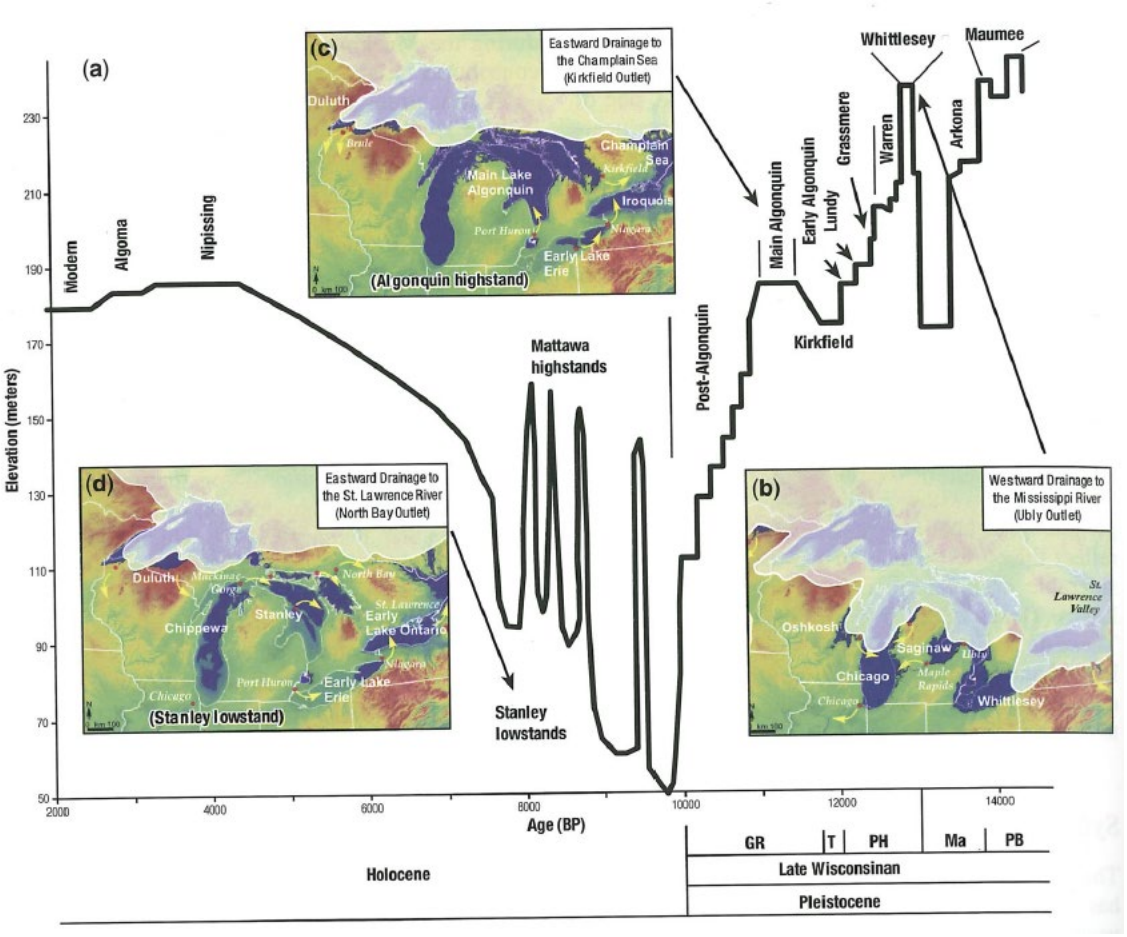

Figure 2.5. *Lake Level history during the time of beach ridge formation at Erie Bluffs State Park. From Johnston et al., 2014.*

Figure 2.6. *Typical exposure of east side of Erie Bluffs State Park, with a recent slump in the background, depositing material directly into Lake Erie. Photo by Eric Straffin.*

Figure 2.7. *Oblique view of exposure of Erie Bluffs near the mouth of Elk Creek. Lower till (t) is contorted by over-riding till, with shearing direction to the southwest (right). Pebbly, dense gray till (t) overlies contorted till. Convoluted, ripple laminated lacustrine silt and sand (ls) is capped by oxidized terrace alluvium (fsg) from Elk Creek, which is ~ 2 ft thick. Scale varies across photo, taken by Eric Straffin.*

disrupting and convoluting laminated lake bottom sediments. Dropstones clearly indicate ice rafted debris.

There are also very large, convoluted sands that occur near the top of the section (**Figures 2.11 and 2.12**). These features are fairly consistent along the length of the bluffs where the lower sandy shoreline sediments intersect the bluffs. Convoluted sand units often have ball and pillow structures at the base of the bed, where heavier sand was deposited on soft lake silts, permitting the sand to sag. Flame structures at the contact between silt and overlying sand demonstrate en-masse movement of sand to the northeast.

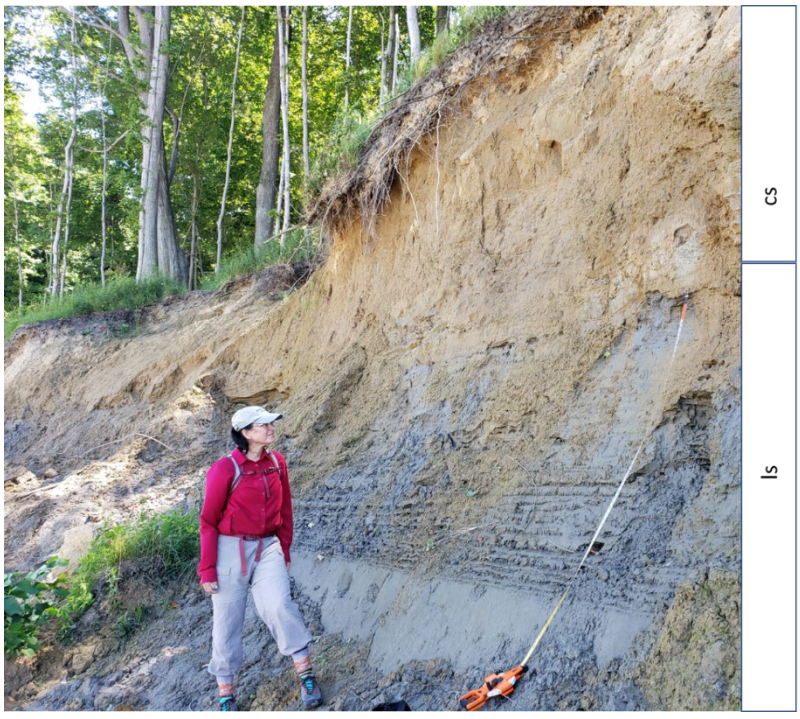

Figure 2.8. *Photograph of bluff exposure with gray massive lake silt (ls) overlain by rhythmically laminated, rippled sand/silt couplets. Differential weathering of sand and silt makes these easily visible. Convoluted, oxidized sandy lacustrine sediments (cs) at top. Photo by Eric Straffin.*

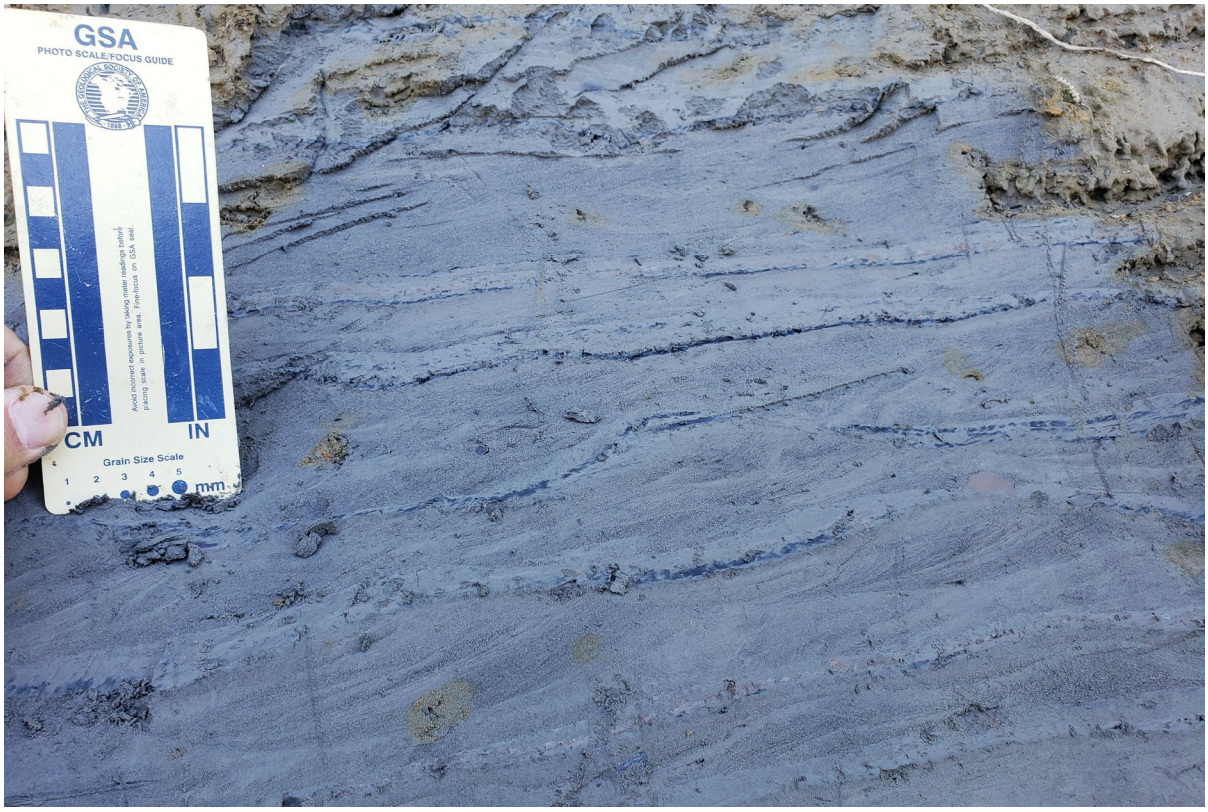

Figure 2.9. *Close up photograph of rippled sand/silt couplets scraped off with a trowel. Asymmetrical, climbing rippled sand is draped by silt/clay, averaging 1-2 inches thick. Photo by Eric Straffin.*

Figure 2.10. *Dropstones (from ice rafted debris) occur occasionally within the contorted section of lacustrine silt/sands. Large gravel clast shown here deform laminations. Photo by Eric Straffin.*

Figure 2.11. *Highly contorted, oxidized, laminated sands (cs) overlying gray lacustrine silt (ls). Rapid loading of sand onto underlying silt resulted in soft sediment deformation. Flow indicators (e.g. flame structures) show that contorted sand moved from southwest to northeast (right to left on photo). Photo by Eric Straffin.*

The relatively coarse sand grain size, and abundance of sedimentary structures common in the nearshore environment, suggest that the cause of the widespread convoluted sands is likely related to bank or bar collapse, and rapid, local sedimentation into proglacial ancestral Lake Erie (see **Figure 2.13**). The broad beach profile preserved at Erie Bluffs State Park is interpreted to be a regressive shoreline, related to strong longshore currents (features of rapid sedimentation) and dropping lake level (broad slope of shoreface deposits and progressively lower beach crest) at the time of deposition. Large gravel pit exposures of the correlative Warren shoreline in northeastern Erie County clearly depict lake-ward dipping gravel/sand shoreline facies suggested in the cross section of **Figure 2.13**, illustrating a lake-ward progradation of the shoreline. At Erie Bluffs SP, this relationship is not well exposed, but coarse shoreline facies clearly grade to and overlie sandy/silty lake bottom facies.

Geology, water, and the environment at Erie Bluffs State Park

There are many interesting features to see throughout the park, that are controlled by the underlying geology. For example, if one walks along Timber Trail (and side trails out to the bluffs;

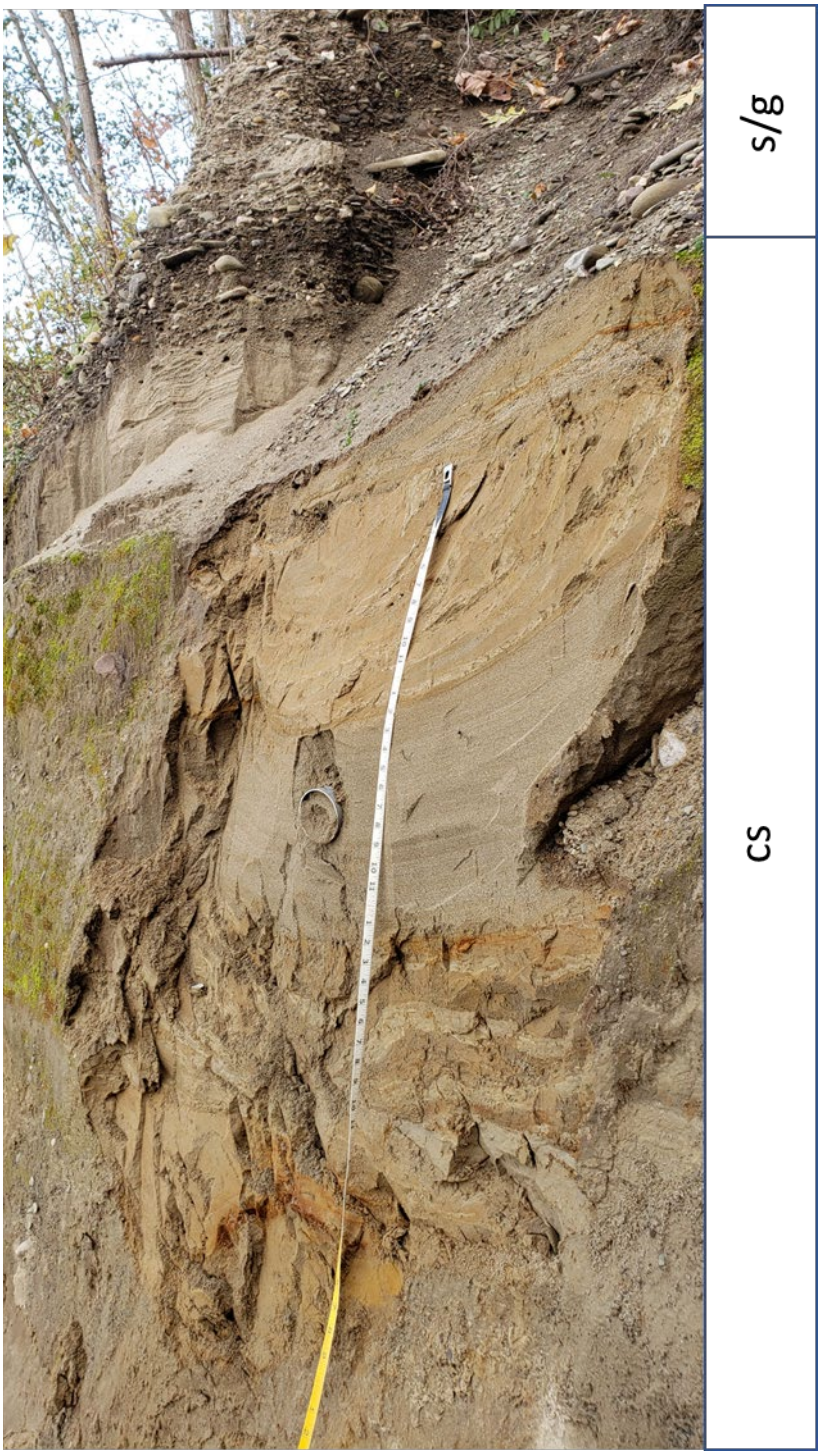

Figure 2.12. *Pillow structure in laminated lacustrine sand (cs) overlain by cross bedded beach sand and gravel (s/g). Photo by Eric Straffin.*

Figure 2.1) they will note that the gullies have flowing springs and interesting riparian vegetation that is very different from the surrounding relatively dry forest floor. The springs/gullies begin abruptly at a small but distinct break in slope, which is the contact of sandier nearshore/beach ridge sediments that overlie finer lacustrine silt and fine sand of the lake floor (**Figures 2.3 and 2.13**). Infiltrating water percolates rapidly through coarse shore-zone sand and gravel, then slows to create a perched water table atop the less permeable, silty lake bottom facies. Groundwater then migrates down-dip (lake-ward) where springs emerge at the base of the shore-zone sediments in sufficient quantity to cause surface erosion and gully

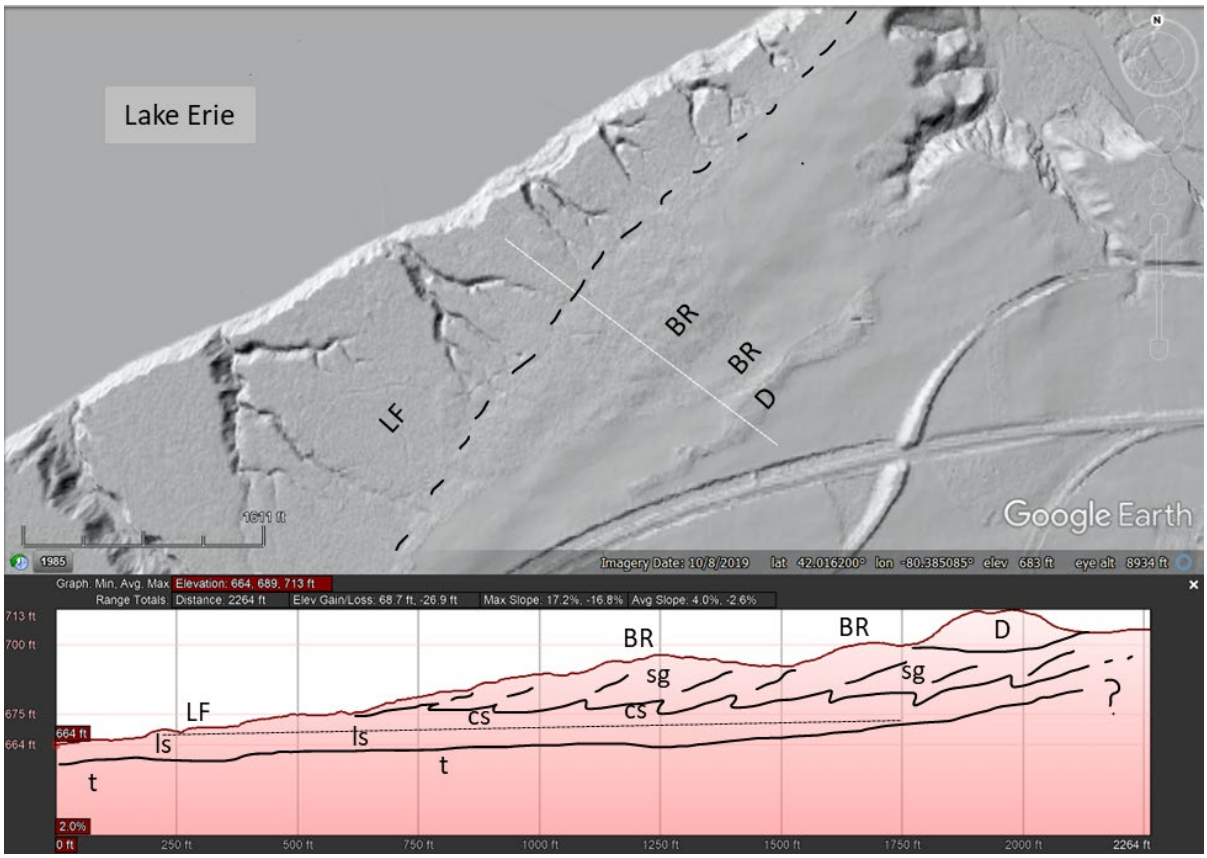

Figure 2.13. *Hillshade model, topographic profile, and interpreted cross section of paleo shoreline features at Erie Bluffs State Park. Landforms: LF = lake floor, BR = beach ridge, D = dune. Sediments: t=till, ls = lake silt/sand, cs= convoluted silt/sand, sg = sand/gravel. Dune sand is well sorted fine sand. Dashed line on hillshade marks boundary of lake floor-beach ridge transition, white line marks section line. Sinuous curves at southeast corner of image are roads and railways. Elk Creek valley wall visible in northeast corner of image.*

formation. The head of gullies leading uphill from the Lake Erie shoreline thus terminate near this boundary (**Figures 2.3 and 2.13**) at approximately 206 m (675 ft) a.s.l.

Landslides and bluff erosion are both a hazard and a benefit to people utilizing the modern Lake Erie shoreline. Bluff erosion rates along Erie Bluffs State Park are relatively high, ranging between ~ 0.2 m/yr and 0.8 m/yr (0.656 ft/yr and 2.64 ft/yr) but with local rates as high as 1 m/yr (3.28 ft/yr) (Hapke et al., 2009). Bluff retreat occurs as waves erode and steepen the base of the bluffs, which over-steepens slopes leading to landslides that then deliver material downslope into the surf zone. Waves then remove that material, which is carried with the prevailing longshore current to the east. Water that infiltrates the upper portion of the bluffs also facilitates slope failures, especially at the contact between sandy lacustrine sediments that overlie silty lake bottom or till sediments.

While bluff retreat threatens bluff-top homes around Lake Erie, it also provides sediment necessary for the development of beaches along Presque Isle State Park, down-current. Landslides contribute significant sediment to the long shore current system. In fact, the bluffs are not primarily composed of silty till, but rather are predominantly sandy near-shore sediments of ancestral Lake Erie. Diminished bluff erosion will reduce the amount of sand that makes it into the longshore current resulting in less available sand for beaches on the most visited state park in Pennsylvania, Presque Isle.

References Cited

Barnett, P.J. (1979) Glacial Lake Whittlesey: The probable ice frontal position in the eastern end of the Erie Basin: Canadian Journal of Earth Sciences, 16: 568–574.

Calkin, P.E., and Feenstra, B.H. (1985) Evolution of the Erie-Basin Great Lakes: GAC Special Paper 30.

Fisher, T.G; Blockland, J.D; Anderson, B., Krantz, D.E; Stierman, D.J., Goble, R. (2015) Evidence of sequence and age of ancestral Lake Erie lake-levels, northwest Ohio. The Ohio Journal of Science, V. 115, no. 2, p. 62-78.

Hapke, C. J., Malone, S., and Kratzmann, M., 2009, National assessment of historical shoreline change: A pilot study of historical coastal bluff retreat in the Great Lakes, Erie, Pennsylvania: U.S. Geological Survey Open-File Report 2009-1042, 25 p.

Johnston, J. W., Thompson, T. A., & Wilcox, D. A. (2014). Palaeohydrographic reconstructions from strandplains of beach ridges in the Laurentian Great Lakes. Geological Society, London, Special Publications, 388(1), 213-228.

Master plan for Erie Bluffs State Park, 2008, Girard and Springfield Townships, Erie County, Pennsylvania. Bureau of State Parks, PA DCNR, 56p.

McCoy, C. (2010) Using slope to map Pleistocene beach ridges along the Pennsylvania portion of Lake Erie. Undergraduate Thesis, Mercyhurst University, Erie, PA, 26 p.

Schooler, E.E. (1974) Pleistocene beach ridges of northwestern Pennsylvania: Pennsylvania Geological Society, General Geology Report 64: 38.

Totten, S.M. 1985 Chronology and nature of the Pleistocene beaches and wave-cut cliffs and terraces, NE Ohio: GAC Special Paper 30.

Point of Interest: In 1913, the Battle of Lake Erie (sometimes called the Battle of Put-in-Bay) was fought during the War of 1812. The US Navy coordinated the capture of six British Royal Navy vessels, which resulted in American control of Lake Erie for the remainder of the war.

POI Figure Source: *Powell, W. H., 1865, Battle of Lake Erie, U.S. Senate Art Collection, U.S. Capitol, Washington, D.C., https://commons.wikimedia.org/w/index.php?curid=251007.*

STOP 3: LUNCH – EDINBORO LAKE

BRIAN ZIMMERMAN AND ERIC STRAFFIN – PENN WESTERN UNIVERSITY, EDINBORO

41.8778739 / -80.133665979

Introduction

Edinboro Lake is a kettle lake, one of 8 small glacial lakes in northwestern Pennsylvania (**Figure 3.1**) (Grund and Bissell, 2004). A dam on the lake's outlet raises the lake level approximately 9 feet (2.7 m) above the level of the original kettle lake. The maximum lake depth is 29.3 feet (8.9 m) with an average depth of 9.4 feet (2.9 m) (**Figure 3.2**). The Edinboro Lake Fen (an alkaline wetland) is located along the northern shore of the lake and is a natural wetland community of global significance (WPC, 2000; Grund and Bissell, 2004). The shrub fen bordering Edinboro Lake is unique due the abundance of calcite in the glacial deposits surrounding the lake which maintains a high pH in the local groundwater. This provides habitat for a variety of rare and endangered plants which require alkaline conditions. Twenty-three plant species of special concern, eleven of which are listed as endangered in Pennsylvania occur within the watershed (WPC, 2000; Grund and Bissell, 2004).

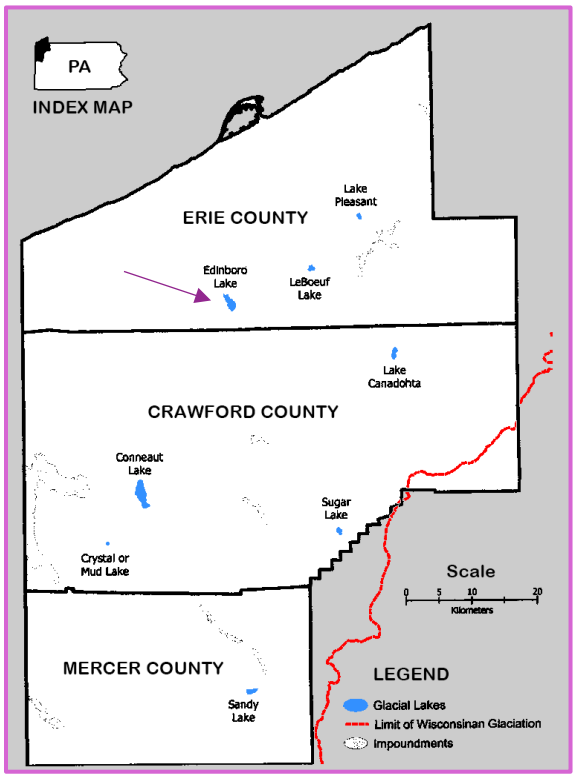

Figure 3.1. *(left) Location of glacial lakes in northwest Pennsylvania. Arrow points to Edinboro Lake. Other glacial lakes are Lake Pleasant, LeBoeuf Lake, Lake Canadohta, Conneaut Lake, Sugar Lake, Crystal/Mud Lake, and Sandy Lake. (Grund and Bissell, 2004).*

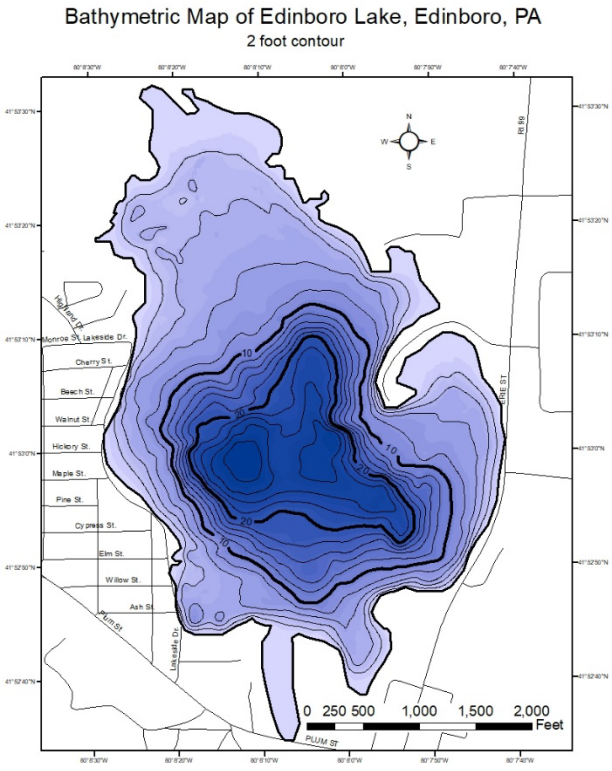

Figure 3.2. *(right) Bathymetric map of Edinboro Lake (Byars and Zimmerman, 2000).*

Edinboro Lake formed after the time of a Lavery advance, when two lobes of ice approached Edinboro from the north. One lobe of ice moved south down the Shenango Creek valley and a larger lobe moved from McLane into the Conneauttee Creek valley (Shepps et al., 1959). At the southern end of these ice lobes a morainal kame was deposited. The morainal kame forms the low gravel hills that surround Edinboro Lake to the southeast including the locations of the Edinboro Cemetery and Edinboro Mall. **Figure 3.3** illustrates several moraines in the Edinboro area.

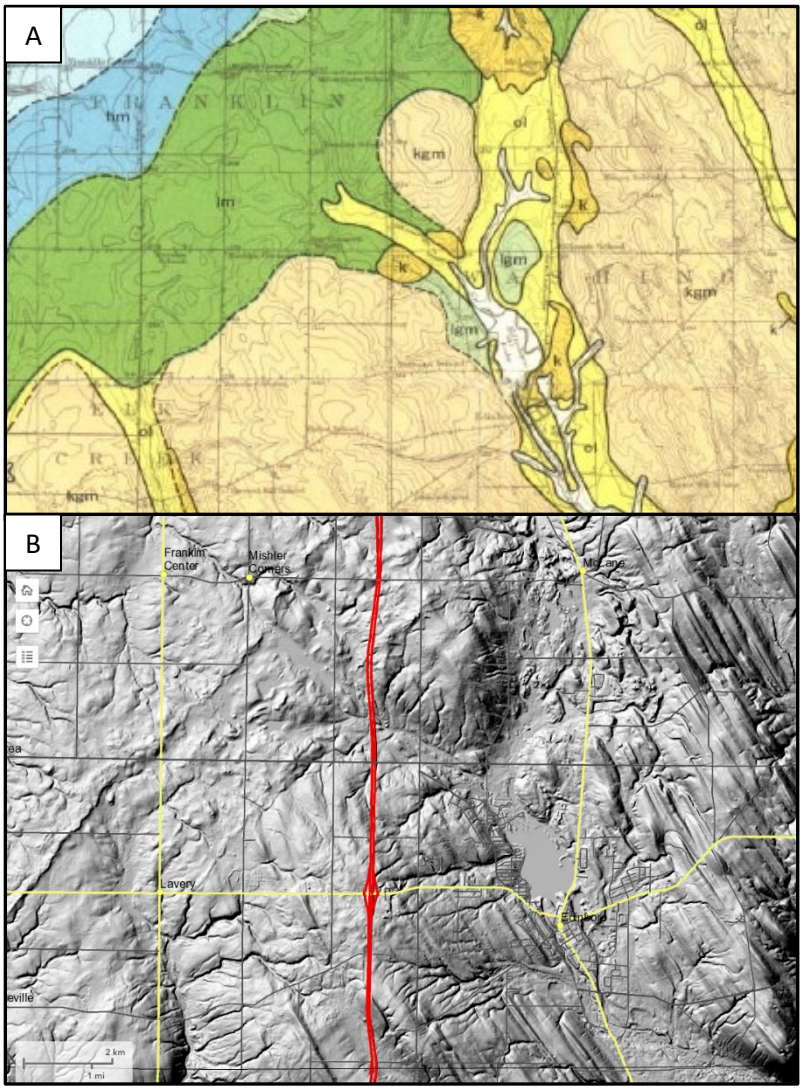

Figure 3.3. *A) Clip of glacial geologic map by Shepps et. al. (1959), B) Lidar hillshade model of area around Edinboro Lake (in blue). Morainal topography is are clearly visible in b. Drumlins occur on hilltops and are composed of thin Kent ground moraine over Devonian bedrock.*

The ecologically important habitats around Edinboro Lake, as well as a wide range of environmental issues related to sedimentation rates and water quality, have spurred many studies in and around the lake. For example, rapid sedimentation in the shallow margins of the lake have been an ongoing issue and led to two major dredging operations within the lake basin. In order to more precisely measure the rate of sedimentation in the deepest part of Edinboro Lake a 1.4-meter sediment core was collected in 2007 by Edinboro University students (Szall et al., 2016). The sediment core was divided into 4 cm sections which were dated using 210-lead (210-Pb) radiometric dating techniques. The results of this study are shown in a graph of mass sedimentation rate versus depth in the sediment core (**Figure 3.4**).

These data indicate that 96 cm (3.1 ft) of sediment has accumulated in the deepest part of Edinboro Lake since 1772. The data indicate a gradual increase in sedimentation rate from 14.8 mg/cm2/yr in 1772, prior to construction of the first dam and land-clearing in the watershed, to 286 mg/cm2/yr today. This is most likely caused by the gradual increase in population and accompanying development within the watershed. The rate of increase in sedimentation is less today than it was in the period prior to 1972. Significant short-term increases in the sedimentation rate ca. 1953-1955 and 1987-1992 correlate with periods of intensive dredging within the lake. Disturbance during dredging caused redistribution of sediment from the shallower to deeper parts of the lake.

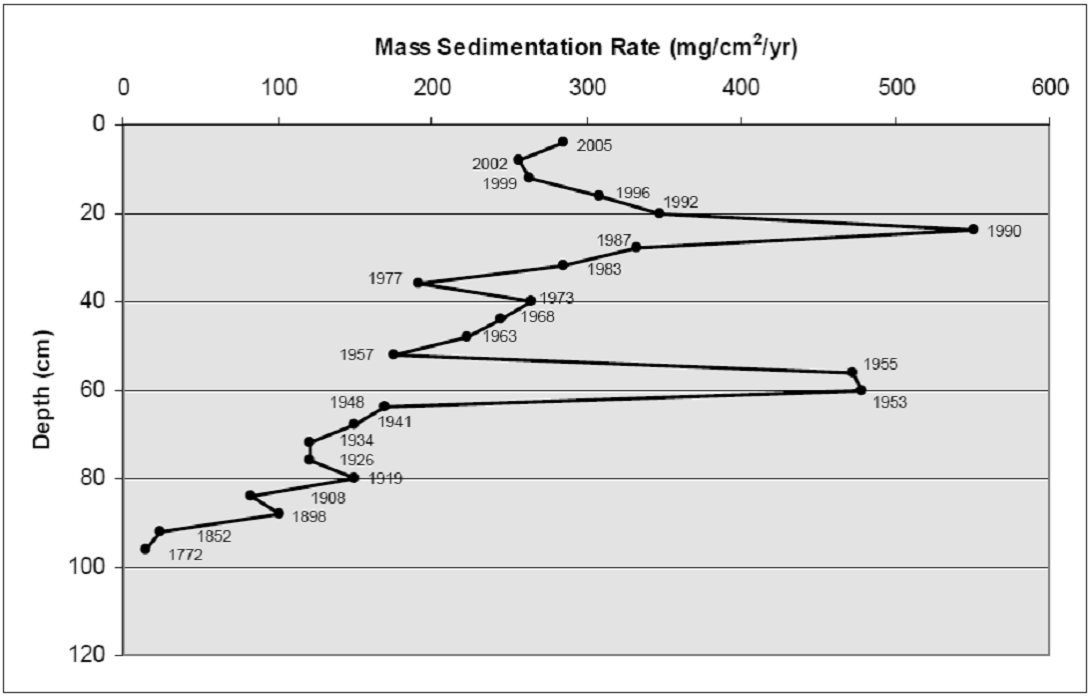

Figure 3.4. *Sedimentation rate in Edinboro Lake (Szall et al., 2016).*

As is typical of lakes in the region, Edinboro Lake is dimictic and currently eutrophic to hypereutrophic. Diatom analysis of sediment samples from the 2007 core (Bradley, 2009) show that the lake was mesotrophic prior to European settlement and very rapidly transitioned to eutrophic conditions following construction of the dam and land-clearing within the watershed. Eutrophic conditions due to high Nitrogen and Phosphorous levels in the lake promote algal growth, and diminish water quality for activities such as swimming and boating.

In 2003 a 5.52 m sediment core was extracted from the deepest part of the lake by students and faculty of Edinboro University. Radiocarbon dates of 3,315, 6,430, and 9,575 years BP (calibrated) were obtained at depths of 1.90, 4.00 and 5.52 meters, respectively yielding an average sedimentation rate of only 0.56 mm/yr (Winger et al., 2004; Zimmerman and Straffin, 2006). The sample dated at 9,575 years BP was taken from just above the contact between deposits of underlying varved/inorganic silt and overlying non-varved organic rich lacustrine sediments, indicating that this transition occurred well after the Lavery ice advance. The authigenic phosphorous mineral vivianite occurs in the core below 220 cm indicating that a significant change in the trophic state of the lake occurred at approximately 4,000 years B.P. Prior to this time there was sufficient oxygen in the hypolimnion to allow phosphorous to be retained in the sediments as vivianite. After this time, the lake bottom become more anoxic,

which decreased biological activity at the bottom of the lake, and also promoted the accumulation of organic mud.

References Cited

Bradley, C.P. (2009) Reconstructing the Historical Trophic Status of Edinboro Lake, Pennsylvania Using Diatom Analysis, Unpublished MS Thesis, Department of Biology and Health Services, Edinboro University of Pennsylvania.

Byars, R. and Zimmerman, B.S. (2000) Unpublished bathymetric map. Department of Geosciences, Edinboro University of Pennsylvania.

Grund, S. and Bissell, J. (2004) Laying the Groundwork for Community Based Conservation Planning for Western Pennsylvania's Glacial Lakes: Documenting The Native and Introduced Flora Associated with Glacial Lakes in Northwest Pennsylvania with Emphases on Rare Species and Invasive Alien Species. Western Pennsylvania Conservancy, Pittsburgh, PA.

Shepps, V., White, G., Droste, J. and Sitler. R. (1959) The Glacial Geology of Northwestern Pennsylvania: Pennsylvania Geological Survey, 4th ser., General Geology Report G 32, 59 p.

Szall, J., Straffin, E.C., and Zimmerman, B. (2016) A historic sediment record of landscape disturbance around Edinboro Lake, northwestern Pennsylvania. Geological Society of America Abstracts with Programs, Vol. 48, No. 2.

Western Pennsylvania Conservancy (WPC). (2000) Summary report; health and management of the Edinboro Lake ecosystem. Report to Edinboro Regional Community Services, Inc.

Winger, A., Straffin, E.C. and Zimmerman, B.S. (2004) Determining Sedimentation Rates

and Patterns of Edinboro Lake, Geol. Soc. Amer. Abs. with Programs, Northeastern – Southestern Section Joint Meeting, March 25-27.

Zimmerman, B.S. and Straffin, E.C. (2006) Sedimentation and Trophic History of Edinboro Lake, Erie County, Pennsylvania. Geological Society of America Abstracts with Programs Vol. 38, No. 4.

Point of Interest: Because Lake Erie is the shallowest of the Great Lakes, it has the warmest temperatures. In 1999 this became problematic for two nuclear power plants that relied on the Erie waters to maintain safe reactor temperatures. That year Lake Erie's temperature rose dangerously close to the upper limit set by the Nuclear Regulatory Commission. The company that owned both power plants responded by asking that the NRC raise the upper temperature limit for nuclear reactors.

POI Figure Source: *Davis Bess Power Plant, n.d., https://commons.wikimedia.org/wiki/File:Davis_besse_power_plant-CN.jpg.*

POI Source: Los Angeles Times, 1999, Lake Erie Heat Wave Threatens Nuclear Plants' Cooling Systems, https://www.latimes.com/archives/la-xpm-1999-aug-10-mn-64303-story.html.

STOP 4: CONNEAUT LAKE-MARSH SYSTEM

ICE TONGUES, KAME MORAINES AND PALEOENVIRONMENTAL RECONSTRUCTION

TODD GROTE – INDIANA UNIVERSITY SOUTHEAST
ERIC STRAFFIN –PENNWEST UNIVERSITY, EDINBORO CAMPUS
LARA HOMSEY-MESSER – INDIANA UNIVERSITY SOUTHEAST
ANDY MYERS – ALLEGHENY ARCHAEOLOGY RESEARCH, LLC

41.605662 / -80.30263946

Introduction

The purpose of this stop is two-fold: (1) Discuss newly mapped, but formerly recognized (e.g. Shepps et al., 1959), post-Kent (the Late Wisconsin terminal moraine) ice margins and ice tongues of the Laurentide Ice Sheet (LIS) throughout northwestern Pennsylvania (NWPA); (2) Provide a preliminary paleoenvironmental reconstruction of the Conneaut Lake-Marsh system using LiDAR-based surficial geologic mapping, water well data, radiocarbon assays and time-diagnostic artifacts. Purpose 2 demonstrate the valuable synergy between the geoscience and archaeology communities.

A brief overview of the late- and de-glacial history of NWPA is as follows. The Grand River sub-lobe of the Erie Lobe of the LIS advanced into NWPA at least 8 times during the Quaternary, with 4 advances occurring during the Late Wisconsin (~ 36,000-11,700 cal yrs BP) (**Figure 4.1**; Shepps et al., 1959; White et al., 1969; Braun, 2004; Fleeger et al., 2011). The Kent End Moraine marks the maximum position of the LIS, which is regionally thought to have occurred around 28,000-25,000 cal yrs BP (Karrow et al., 2000; Young et al., 2021). It is likely that permafrost extended tens to hundreds of kilometers south of the LIS terminal moraine (Merritts and Rahnis, 2022). Post-Kent LIS advances into NWPA are recorded by the Lavery, Hiram and Ashtabula moraines (from oldest to youngest respectively), with the proglacial permafrost zone waxing and waning with ice margin positions. These tills represent more limited advances of the Erie Lobe onto the Allegheny Plateau. In addition, the end moraines that mark the edge of these later advances are much more narrow and lack the diversity of landforms that are characteristic of the Kent End Moraine (Straffin and Grote, 2010). It is thought that NWPA was ice free around 16 cal yrs BP based on the estimated age of the Ashtabula-correlative Valley Heads/Lake Escarpment Moraine in New York (Young et al., 2021) and revised ice margin maps of Dalton et al. (2020) (**Figure 4.2**). The timing of final ice retreat from NWPA is still open for debate. Interestingly in western New York, it has recently been proposed that a possible ice re-advance into the state occurred during the late Bolling-Allerod/early Younger Dryas (~13,300-13,000 cal yrs BP) (**Figure 4.2D**), which post-dates the Ashtabula Moraine system that demarcates the final ice advance into NWPA by about 3,000 years or so (Young et al., 2021). This proposed ice advance is coincident with the continued expansion and eventual demise of Glacial Lake Iroquois, cool and wet climate conditions, and a well-established boreal forest as suggested by proxies throughout the Erie-Ontario Lowlands and Appalachian Plateau of New York possibly as early as 14,200 cal yrs BP (Griggs et al., 2022). As you will see at this stop, the landscape surrounding Conneaut Lake

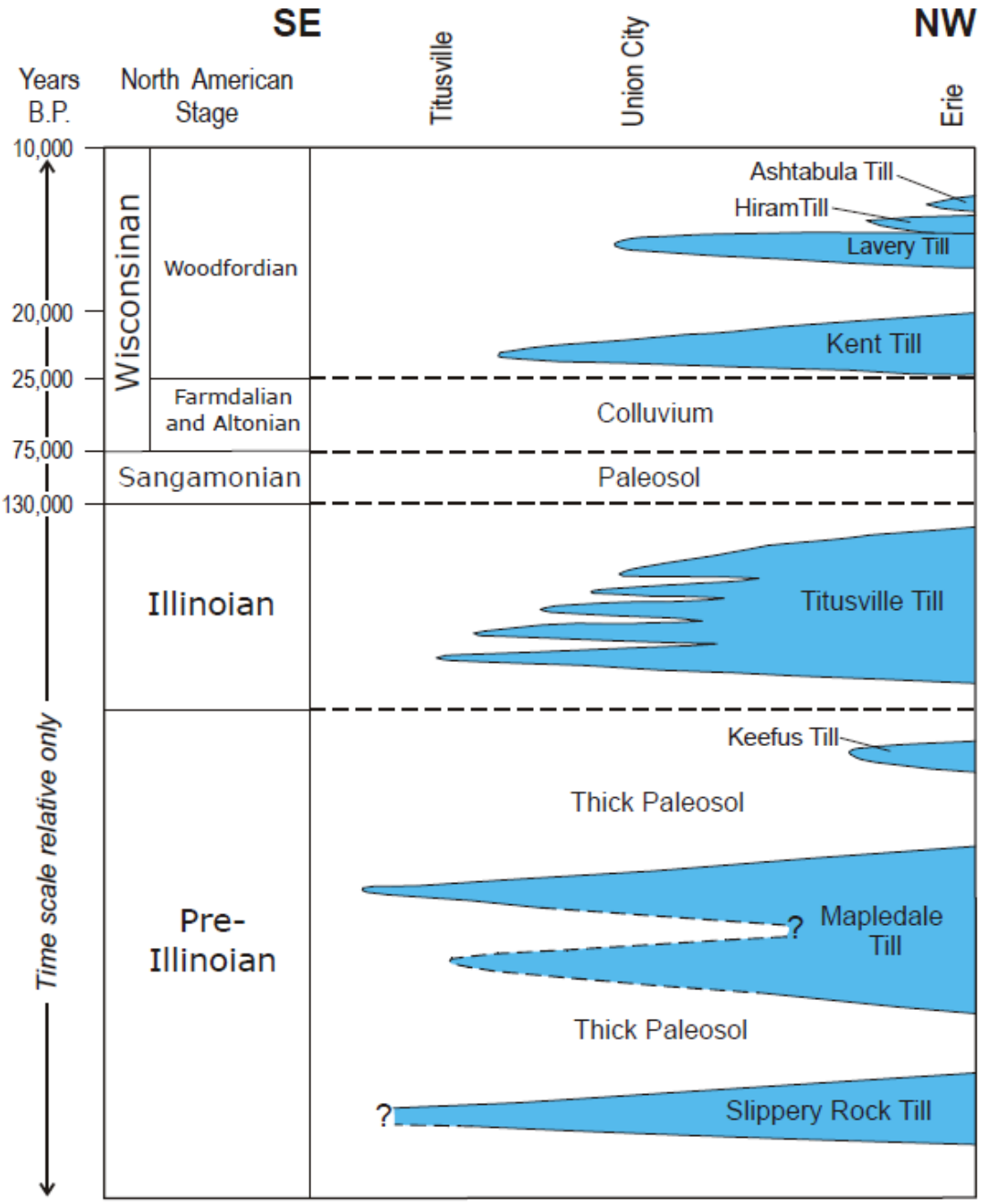

Figure 4.1. *Time-distance diagram for northwestern Pennsylvania. The last glacial maximum is represented by the Kent End Moraine. Although the age of the Ashtabula Moraine is poorly constrained, it is though that the region was ice-free by ~ 16,000 cal yrs BP. Figure modified from Shepps et al. (1959) and White et al., (1969).*

was ice-free and inhabited by Woolly Mammoth (*Mammuthus primigenius*) and other megafauna by ~14,000 cal yrs BP during the Bolling Allerod.

Regional paleoenvironmental information suggest that the early deglacial landscape, possibly, but questionably, as early as ~20,000 cal yrs BP (during or possibly slightly predating the Erie Interstade which occurred ~ 19,800-18,200 cal yrs BP) for the lower Conneaut Lake-Marsh valley (**Figure 4.2A**; Grote et al., 2022), consisted first of tundra and then a Boreal-like

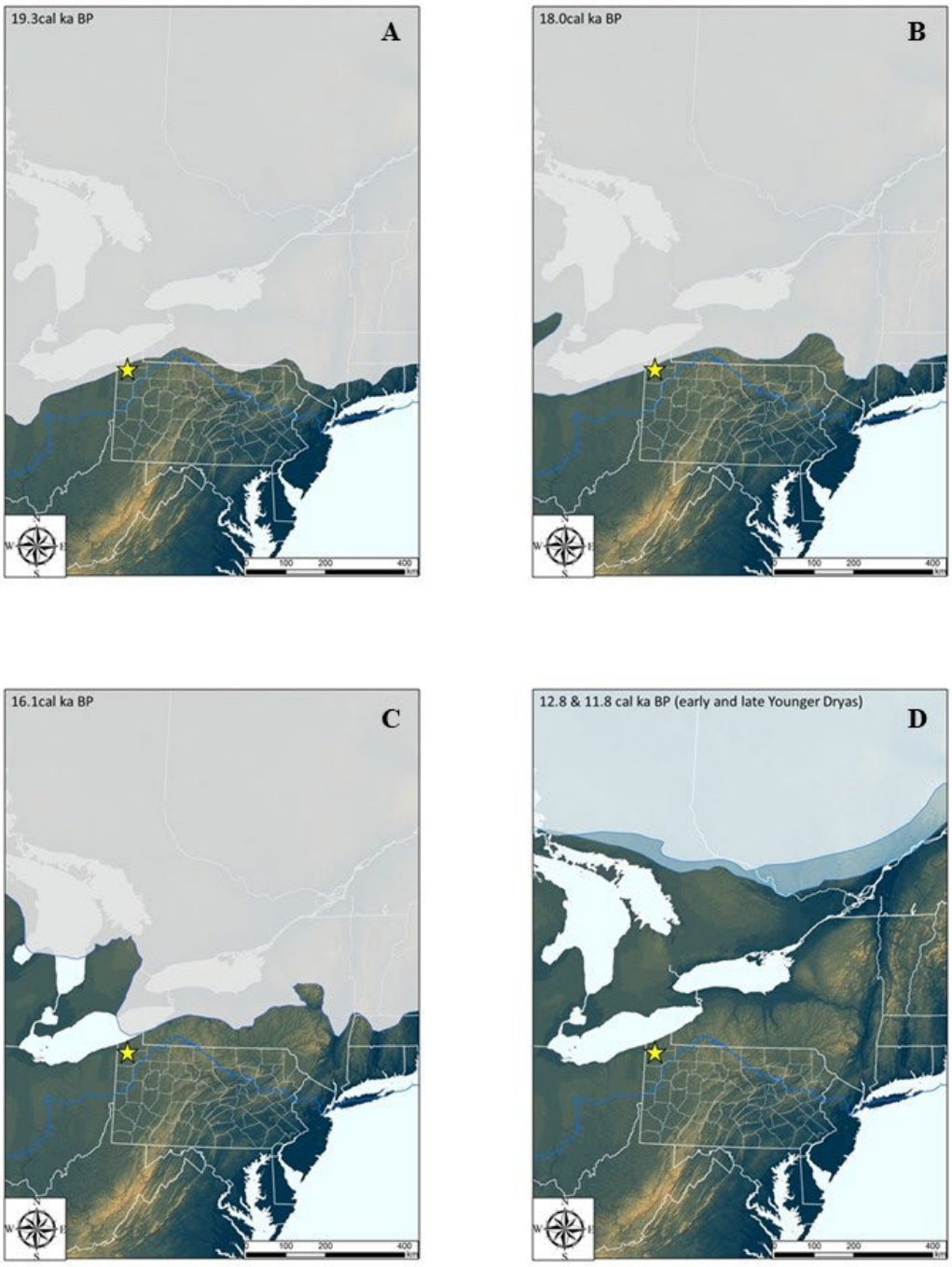

Figure 4.2. *Reconstructed post-glacial maximum ice marginal positions. A) 19.3 cal ka BP during the Erie Interstade. B) 18.0 cal ka BP. C) 16.1 cal yrs BP when northwestern Pennsylvania was ice-free. D) The 12.8 cal yrs BP (medium blue, early Younger Dryas) and 11.8 cal yrs BP (light blue, late Younger Dryas). Yellow star is approximate location of this study. Blue line is the position of the last glacial maximum, locally the Kent End Moraine. Ice margins from Dalton et al., 2020.*

parkland/forest consisting of spruce, pine, fir and tamarack trees, shrubs and wet meadow being present by the Bolling-Allerod (Watts et al., 1979; Shuman et al., 2002 & 2004; Webb III et al., 2003; Miller and Futyma, 2003; Gajewski et al., 2006; Griggs et al., 2017; Griggs et al., 2022) (**Figures 4.3 & 4.4** and **Table 4.1**). In the Erie-Ontario Lowlands and Glaciated Appalachian Plateau of western and central New York, boreal-like climate and forest conditions were well established by the Bolling-Allerod (~14,700-12,900 cal yrs BP) and persisted through the

Younger Dryas (~12,900-11,700 cal yrs BP; YD) and into the early Holocene (**Figures 4.2D & 4.3** and **Table 4.1**; Lothrop et al., 2016; Griggs et al., 2022). As noted above, Woolly Mammoth and other megafauna such as mastodon (*Mammut americanum*) and woodland musk ox (*Ovibos moschatus*) among others lived within the landscape of NWPA by ~14,000 cal yrs BP, during the relative warmth of the BA (Burkett, 1981; Carr and Adovasio, 2020; Vento et al., 2020 and references therein). Watts (1979) suggested that the Mid-Atlantic region during the BA was a patchwork of boreal forest dominated by spruce, fir and pine, a variety of shurbs and wet meadow/marsh in areas that lacked permafrost.

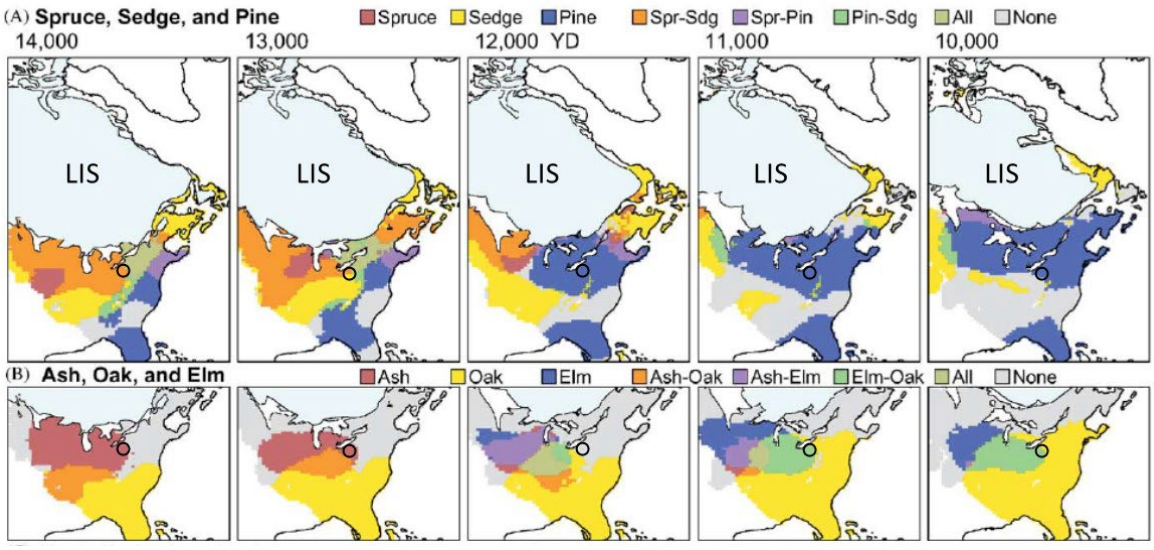

Figure 4.3. *Reconstructed forest types for eastern North America during the late glacial and Early Holocene. LIS = Laurentide Ice Sheet. Black circle shows approximate location of this study. Modified from Shuman et al. (2002).*

Like elsewhere in the Northern Hemisphere, the Younger Dryas in the eastern United States is marked by a rapid return to cold climatic conditions, and ecological and cultural changes (**Figure 4.3 & 4.4** and **Table 4.1**; Shuman et al., 2002, Webb III et al., 2003; Newby et al., 2005; Munoz et al., 2010; Ellis et al., 2011; Lothrop et al., 2016; Griggs et al., 2017; Swisher and Peck, 2020; Vento et al., 2020; Griggs et al., 2022). Throughout the eastern Great Lakes region and northeastern North America in general, colder climate conditions were experienced, but paleoclimate proxy records (e.g. pollen, macrofossils, stable isotopes) show variable ecological responses. In the eastern Great Lakes region, pollen and plant macrofossils record forests dominated by pine, spruce, tamarack/larch and fir (**Figures 4.3** and **Table 4.1**; Shuman et al., 2002; Webb III et al., 2003; Lothrop et al., 2016; Griggs et al., 2017; Swisher and Peck, 2020; Griggs et al., 2022) throughout the Younger Dryas. Warming and drying beginning in the late Younger Dryas allowed pine to persist at the expense of spruce, fir and tamarack and for the introduction of more cool-temperate species (e.g. hemlock, oak, beech) in the early Holocene (Munoz et al., 2010; Panyushkina et al., 2015; Griggs et al., 2017; Swisher and Peck, 2020; Griggs et al., 2022). Ecological changes during the Holocene are much more subtle than that experienced during the Pleistocene-Holocene transition, but do generally track the long-term warming trend as well as shorter intervals of climate variability (e.g. warm and dry, cool and wet) (e.g. Shuman et al., 2002 & 2004; Munoz et al., 2010). The Early Holocene landscape of the region remained a pine-spruce-fir-dominant, but with continued warming and drying, cold tolerant boreal species were gradually replaced by cool temperate species. By the Middle Holocene (~ 8200-5400 cal yrs BP), hemlock/oak/hickory/beech ecology (inferred warm and wet paleoclimate) was

Climate Event	Middle Ohio Valley Paleoenvironments	Mid-Atlantic Paleoenvironments	Eastern Great Lakes Paleoenvironments	Cultural Period	Time-Diagnostic Paleoindian Point Types	Time-Diagnostic Early Archaic Point Types
Early Holocene 11.7-8.2 cal yrs BP (10.1-9.0 ^{14}C yrs BP) Warm-Dry	Pine-oak forest	Oak deciduous forest	Pine-Oak forest	Late Paleoindian 11.7-10.0 cal yrs BP / Early Archaic 11.7-8.2 cal yrs BP	Agate Basin/Hell Gap Quad/Beaver Lake/Dalton/Carson Lanceolate? Hi-Lo Eden-like	Charleston Palmer Kirk Corner- and Side-Notched St. Charles Kanawha
Younger Dryas 12.9-11.7 cal yrs BP (11.0-10.1 ^{14}C yrs BP) Cool-Wet/Dry	Spruce-pine-oak forest	Mixed boreal and deciduous forest	Spruce parkland to pine forest	Middle Paleoindian 12.2-11.6 cal yrs BP Early Paleoindian 12.9-12.2 cal yrs BP	Holcombe Crowfield Barnes/Cumberland Eastern Clovis Gainey	
Bolling-Allerod 14.6-12.9 cal yrs BP (14.0-10.9 ^{14}C yrs BP) Warming-moist	Deciduous woodland	Mixed boreal and deciduous forest	Spruce-tamarack-pine-oak forest	Pre-Clovis?	Non-diagnostic	

Table 4.1. *Summary of late Pleistocene and Early Holocene climate events, regional paleoenvironmental conditions, and eastern Great Lakes archaeology. Data compiled from Lothrop et al. (2016).*

established, and ultimately transitioned to the markedly different pine/hickory/beech dominant forests (inferred cool and wet paleoclimate) of the latest Holocene, ~ 3 ka to present (e.g. Shuman et al., 2004; Gajewski et al., 2006; Munoz et al., 2010; Vento et, 2020). A key recent concept suggests that the rapid and dramatic changes in climate and regional vegetation during the Late Pleistocene-Holocene transition has been linked to cultural change and transformations in the archaeological record (e.g. Newby et al., 2005; Munoz et al., 2010; Ellis et al., 2011). Additionally, Munoz et al. (2010) note three other times during the Holocene where "synchronous" climate, vegetation and cultural changes occurred at 8200 cal yrs BP with the final collapse of the LIS, and increase in regional moisture availability and expansion of hemlock and beech that coincides with the Early-Middle Archaic transition, at 5400 cal yrs BP with the regional hemlock decline and the Middle-Late Archaic transition. Finally, at 3000 cal yrs BP with a change from prevailing warm and dry conditions to cool and wet conditions, and regionally recognized Native American population declines (Munoz et al., 2010 and references therein).

An understanding of the Paleoindian and Early Archaic cultural history (**Table 4.1** and **Figure 4.4**) of the Pleistocene-Holocene transition (~Bolling-Allerod warming-Younger Dryas cooling-early Holocene warming), and the impact of changing paleoenvironmental conditions on human activity, in the glaciated region of NWPA is virtually nonexistent when compared to other portions of the Eastern Great Lakes region and northeastern North America in general (e.g. Laub, 2003; Newby et al., 2005; Munoz et al., 2010; Ellis et al., 2011; Lothrop et al., 2016; Lothrop et al., 2017). The chronology of the Paleoindian Period in North America is still debated, so the chronology outlined by Lothrop et al. (2016) will be used in this guide and integrated with regional paleoenvironmental information (**Figures 4.3 & 4.4** and **Table 4.1**). Although numerous Paleoindian and Early Archaic sites on, or adjacent to, the Glaciated Appalachian Plateau in NWPA have been documented by professional and avocational archaeologists (e.g. Mayer-Oakes, 1955; Burkett, 1981; Lantz, 1984), only a few select sites have undergone detailed site excavations (e.g. McConaughy et al., 1977; Koetje, 1998; Myers and Myers, 2007). As part of this stop, we will explore the potential of utilizing time-diagnostic artifacts from the scant Paleoindian and Early Archaic archaeological record for the benefit of some age control to reconstruct the post-glacial evolution of Conneaut Lake. We may also have time to discussed in terms of archaeological site locations and potential site functions in part 2 of this stop.

Part 1: Field and LiDAR-based mapping of post-GM (Kent End Moraine) ice margins and ice tongues

With the widespread availability and use of light detection and ranging (LiDAR) digital terrain models (DTMs) our understanding of the glaciation of northwestern Pennsylvania and adjacent regions has been greatly advanced. Recent analyses of the new high-resolution (1 m) LiDAR DTMs provides an opportunity for re-examination, and in some cases revision, of the currently accepted glacial history of the region (**Figure 4.1**) as it reveals topographic detail not available to earlier workers. The recognition of previously unmapped landscape elements using LiDAR DTMs and the continued development of a sound Late Quaternary chronostratigraphic framework are of great importance for understanding landscape evolution, paleoenvironmental changes, and cultural resource (archaeological) potential across NWPA.

High-resolution LiDAR DTMs in conjunction with field mapping of surficial deposits and landforms are defining previously unmapped, but previously recognized (e.g. White 1881; Leverett, 1902; Shepps, 1959; Shepps et al., 1959) Late Wisconsin ice tongues of the Erie Lobe, locally the Grand River Sub-lobe, of the LIS (**Figure 4.5**). The sediment/landforms discussed here include: a) coarse, chaotic to stratified valley (kame) moraines, b) silty, moraine-dammed lakes, c) coarse, stratified heads of outwash, and d) coarse, stratified lacustrine deltas. At this stop, you

Figure 4.4. *Examples of Paleoindian projectile points recovered from northwestern Pennsylvania. A) Barnes point (Middle Paleoindian) made from Onondaga Chert, Andy Myers photo. B) Half of a Crowfield point made from Upper Mercer Chert, Gary Fogelman photo. C) Eastern Clovis point made from chalcedony, Gary Fogelman photo. D) Eastern Clovis point made from Onondaga Chert, Carl Burkett photo.*

can see the chaotic internal stratigraphic architecture of a valley-blocking "kame moraine" (**Figure 4.6**) that has also been observed in numerous other sand-and-gravel pits in NWPA (e.g. Straffin and Grote, 2010; Grote and Straffin, 2019).

As ice retreated away from the LGM position (marked by the Kent End Moraine on **Figures 4.1, 4.2 & 4.5**) a series of thin, discontinuous recessional moraines were deposited on uplands, which can be traced to distinctive 'kame' moraine/heads-of-outwash within numerous valleys. These newly mapped, valley ice tongues are often linked to valley kame moraines/heads-of-outwash and demonstrate the highly digitate and dynamic nature of an irregular ice front during

deglaciation (**Figure 4.5**). This is in sharp contrast to the relatively smooth ice margins illustrated on established maps of glacial deposits in NWPA (**Figure 4.1**). Shepps et al. (1959) recognized the occurrence of numerous ice tongues within valleys behind the Kent End Moraine and attributed them to Lavery and Hiram ice advances. However, they did not map their positions and extents, but instead listed valleys in which evidence of ice tongues, primarily through the presence of "kame moraine" and "morainal kames" (using the terminology of Shepps et al. (1959)). Extensive ice tongues advanced through all or nearly all ice-parallel valleys during Lavery time producing prominent valley-crossing "morainal kames". Ice tongues and "morainal kames" were also associated with Hiram ice, which Shepps et al. (1959) believed to be responsible for damming the valley and producing Conneaut Lake (**Figures 4.1, 4.5, 4.6 & 4.7**). White et al (1969), however, believed that an ice tongue associated with the Lavery advance formed Conneaut Creek valley. Hartley (2009) supports the original interpretation of Hiram ice in the Conneaut Lake valley. Lidar DTMs suggest that in fact the previously mapped Hiram and Lavery Moraines in NWPA may in fact be part of the same recessional group of landforms, with the Hiram simply being the final vestiges of that retreat, rather than a separate, later advance.

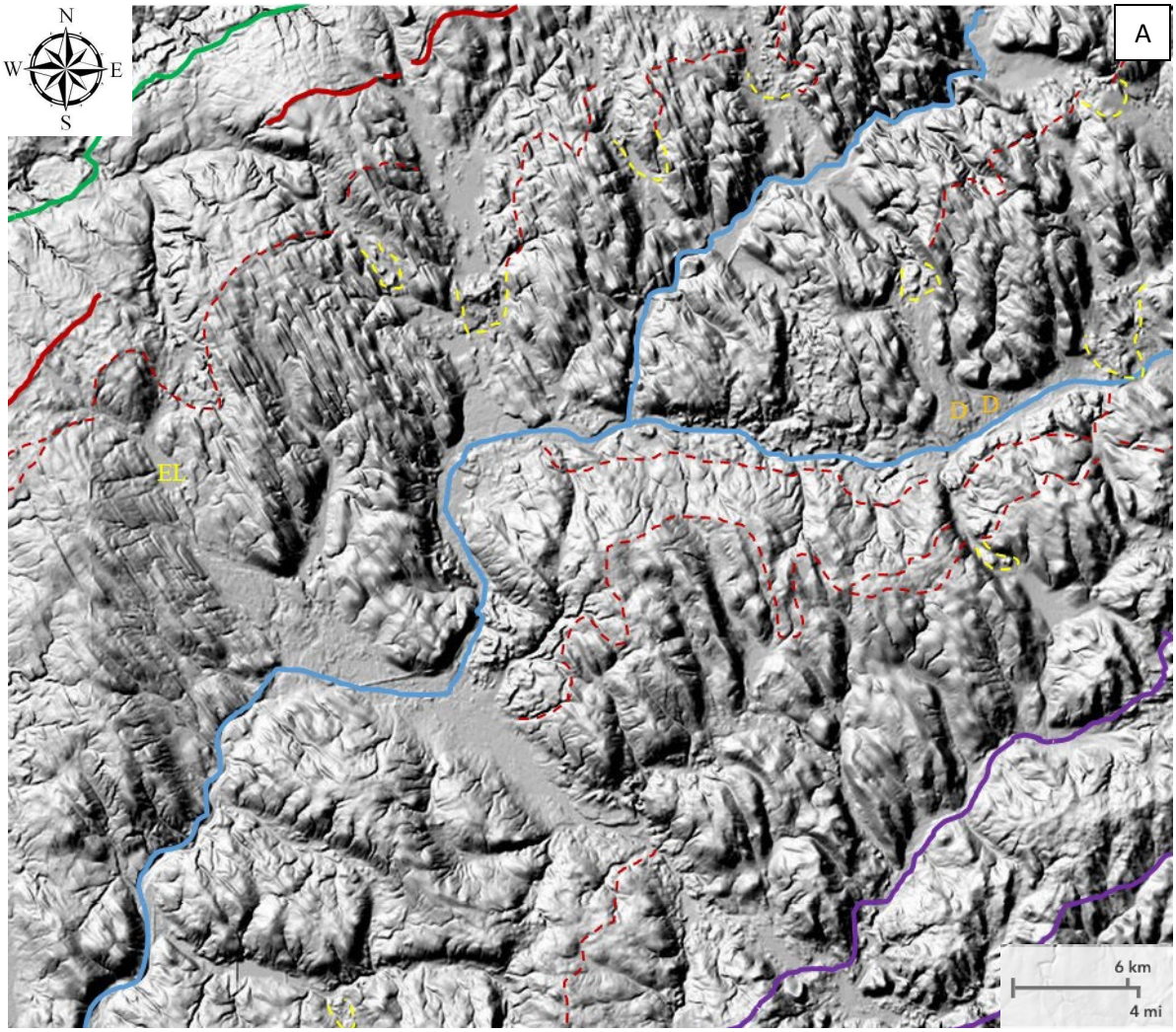

Figure 4.5. *A) LiDAR digital terrain model showing the drumlinized landscape of portions of Erie and Crawford counties, Pennsylvania. Green solid line is the Ashtabula moraine margin, Maroon solid line is the "Lavery" margin, Purple solid lines are the Kent End Moraine complex. Light Blue lines represent French Creek. Dashed maroon lines show previously unmapped ice-marginal positions on uplands. Dashed yellow lines denote valley-blocking kame moraines/heads-of-outwash. Note how the upland margins can be linked to valley kame moraines. EL – Edinboro Lake. D – glaciolacustrine delta.*

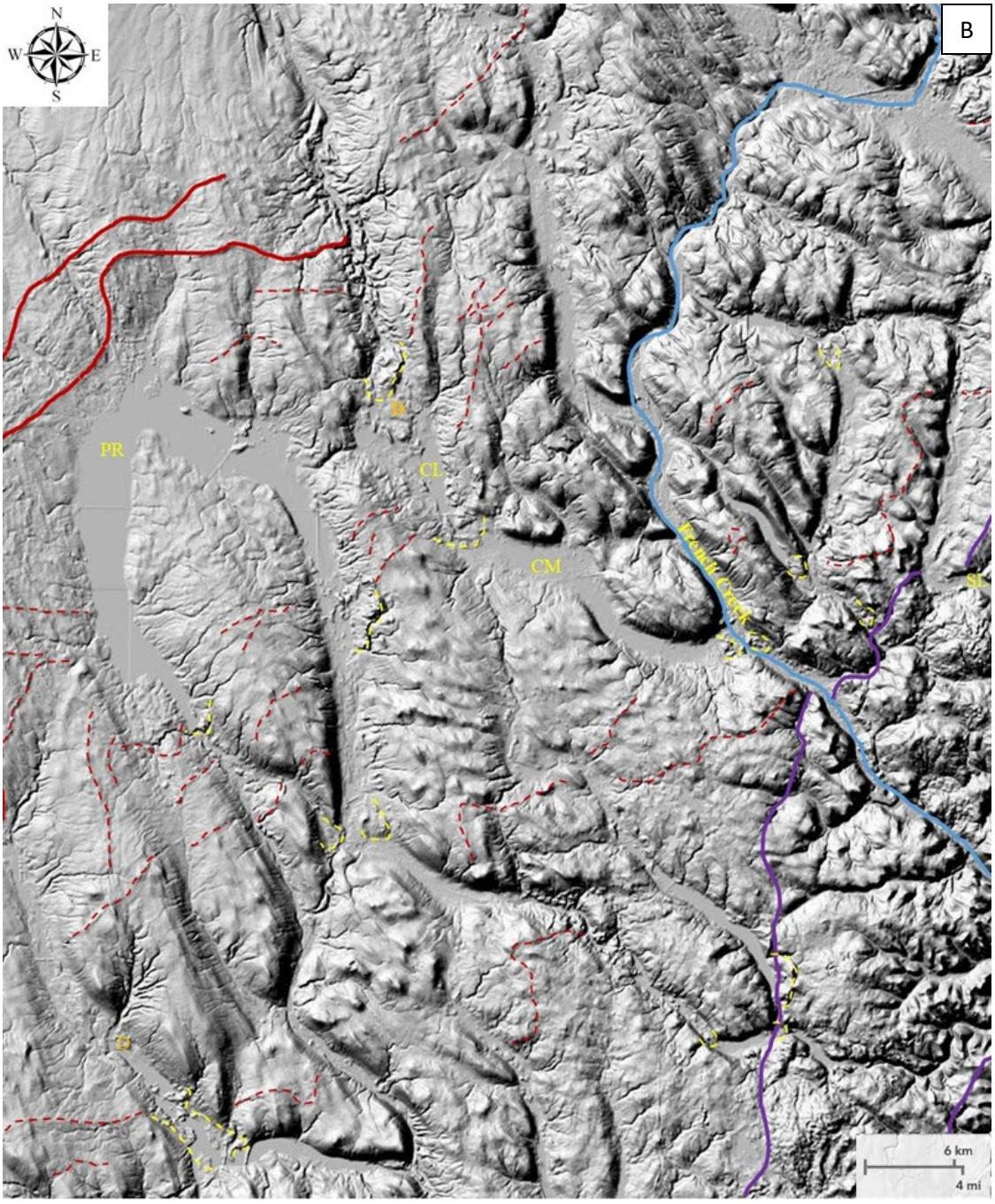

Figure 4.5. (con't) *B) LiDAR digital terrain model showing Conneaut Lake (CM), Conneaut Marsh (CM) and surrounding landscape. Maroon solid line is the mapped "Hiram" margin, Purple solid lines are the Kent End Moraine complex. Light Blue lines represent French Creek. Dashed maroon lines show previously unmapped ice-marginal positions on uplands. Dashed yellow lines denote valley-blocking kame moraines/heads-of-outwash. Note how the upland margins can be linked to valley kame moraines. SL – Sugar Lake. PR – Pymatuning Reservoir. D – glaciolacustrine delta.*

Today, major 'glacial' lakes still exist, including Pleasant Lake, Conneaut, Edinboro, Canadohta, LeBeouf, and Sugar Lakes. Many of these have been described as "kettle" lakes, when in fact they were formed as a result of damming of glacial valleys by valley-blocking end and/or kame moraines. Many drainage divides across NWPA are in fact created by these features.

Figure 4.6. *Conneaut Sand and Gravel quarry depicting silty sediments contained within a kettle (steeply dipping gravel). Photo by Eric Straffin.*

Recent LiDAR interpretations of the Conneaut Creek valley and surrounding landscape, soil survey information (SSURGO), field-examination of sediments and soils, archaeological information, and numerical ages are used to reconstruct the late- and post-glacial history of the Conneaut Lake-Marsh system is the focus of part 2 of this stop.

Part 2: Preliminary reconstruction of the Conneaut Lake-Marsh system

Field and LiDAR-based geomorphic mapping as discussed in Part 1 of this stop, SSURGO soil parent material information and water well data were used to reconstruct Glacial Lake Conneaut as part of an undergraduate senior project by Jeremy Barnett at Indiana University Southeast (Barnett, 2019), and recently updated by Grote et al. (2022) with the addition of geochronological and archaeological information. The "Harmonsburg Moraine" lies just to the north of modern Conneaut Lake and creates the local drainage divide between the Ohio River Basin and Lake Erie. During the late Pleistocene, the "Harmonsburg Moraine" was the marginal position of an ice-tongue within the valley and the source of meltwater and sediment flowing into the moraine-dammed Glacial Lake Conneaut, which is dammed on the southern end by another kame moraine. Abutting the "Harmonsburg Moraine" to the south is a delta/fan-delta that would have fed into Glacial Lake Conneaut (**Figures 4.5 & 4.7**). The kame moraine at the south end of Conneaut Lake can be physically traced to equivalent landforms within both arms of Pymatuning Reservoir, the former Shenango River and Crooked Creek valleys, and to minor moraines on the intervening uplands (**Figures 4.5 & 4.7**). These cross-valley kame moraines in each of the valleys allowed for ice-dammed glacial lakes to exist and can be confirmed by the presence of glaciolacustrine sediments within the valleys (Shepps, 1959; Shepps et al., 1959; Fleeger et al., 2011). The only

local palynological record for the area (Walker and Hartman, 1960) was extracted from Hartstown Bog within kame moraine in the Crooked Creek arm of modern Pymatuning Reservoir, but the pollen record's utility is limited due to a lack of age control (green triangle on **Figure 4.7A**).

In terms of paleolake reconstructions, at an elevation of 342 m (1122 ft), nearly all of the valley-blocking kame moraine at the south end of the lake would have been submerged and is considered an unlikely high-water level. Therefore, it was decided to base the reconstructions on an estimated a high-water level that approached the highest elevations of the kame moraine, but did not breach the top, and presence of a delta/fan-delta (almost entirely submerged at 340 m; 1116 ft) immediately in front of the "Harmonsburg Moraine" (**Figure 4.7B**). A question to ask is – was the delta subaqueous or subaerial? All Paleoindian archaeological sites near the lake would have been submerged at the 340 m water level suggesting that this reconstructed time-slice pre-dates the late BA and YD. At a lower water level of approximately 335 m (1101 ft), what appears to be a steep erosional scarp at the front of the delta/fan-delta emerges (335 m; 1101 ft). The fact that this contour line largely aligns with the base of the kettle, and sediments and soils appear to suggest a stable lake level for some period of time (**Figure 4.7C**). At the 335 m water level elevation, portions of the delta are now sub-aerially exposed. Two Paleoindian sites occur along the eastern margin of the delta suggesting that this landform was possibly habitable by the late BA or YD, but neither of the sites contain time-diagnostic artifacts to help constrain the timing of paleolake reconstruction. Another reduction in water level to 328 m (1077 ft), roughly 2 m above the modern lake level, exposes most of the area where peat occurs within the kettle, the entire proglacial delta and all of the Paleoindian sites surrounding the reconstructed lake footprint (**Figure 4.7D**). Let us now attempt to place these lake level reconstructions into chronological and paleoenvironmental context.

Based on the approximate location of where the radiocarbon-dated mammoth vertebra was discovered within Conneaut Lake, the reported locations of other megafauna remains extracted from peat and nearshore lacustrine sediments within the lake (Burkett, 1981) and the distribution of Paleoindian archaeological sites surrounding the lake (**Figure 4.7**), it is estimated that water levels fell rather rapidly in Glacial Lake Conneaut to within a few meters of modern by the time megafauna and early humans entered the formerly glaciated portion of NWPA. That being said, regional geochronological evidence suggest that ice retreated from NWPA, and surrounding area, by ~16,000 cal yrs BP (**Figure 4.2D**). Within the Conneaut Lake-Marsh valley, deglaciation of the lower valley is recorded by charcoal-bearing sediments recovered from a sediment core on a kame terrace, and adjacent from the multicomponent Smock-Biguziak archaeological site (36CW248), overlooking Conneaut Marsh by ~ 20,246 cal yrs BP (16,740 +/- 70 14C yrs BP), indicating an ice-free, and habitable, landscape just prior to or during the very early Erie Interstate (**Figures 4.2, 4.7A, & 4.8**). The age of an ice-free and vegetated lower Conneaut Valley during the Erie Interstate however maybe questionable but plausible given other paleoenvironmental records for the region. Re-advance and retreat of Lavery (older) and/or Hiram (younger) ice into the Conneaut Lake-Marsh valley led to the formation of valley-crossing kame moraines which ponded water within the valley, thus forming Glacial Lake Conneaut (**Figures 4.5B, 4.6 & and 4.7**). The topography within the Conneaut Creek valley north of the Harmonsburg Moraine (**Figure 4.5B & 4.7**) suggest collapse of the ice-tongue during deglaciation, and an assortment of what are interpreted as ice-contact sediments, including glaciolacustrine varves, suggests impounded water behind the Harmonsburg Moraine as the ice-tongue disintegrated (Shepps, 1959; Shepps et al., 1959; Fleeger et al., 2011; Grote et al., 2022).

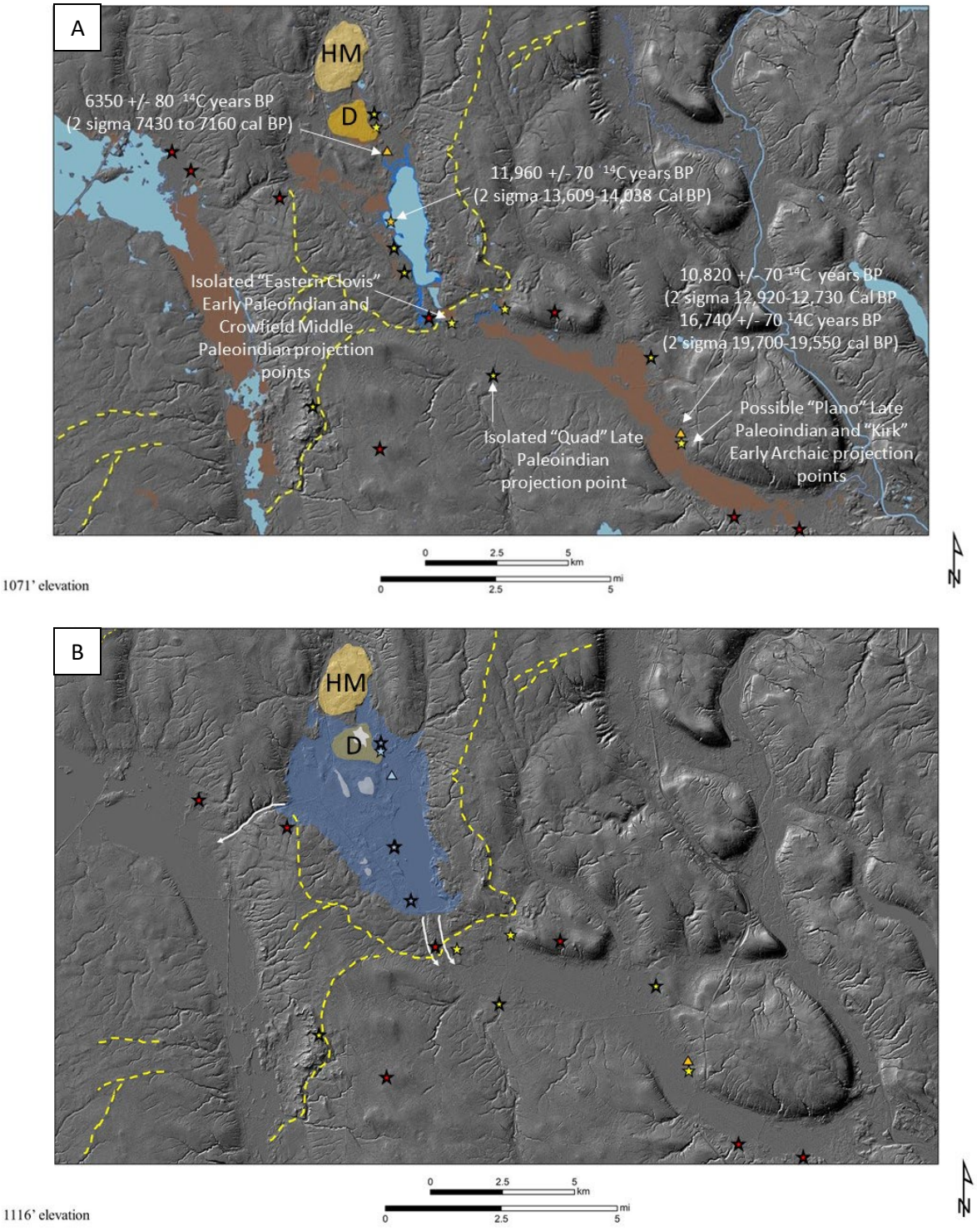

Figure 4.7. *A) Modern level of Conneaut Lake (326-327 m; 1071-1073 ft) and the down-valley Conneaut Marsh. Brown solid shading denotes peat, light blue shading denotes water. Dashed yellow lines are reconstructed ice marginal positions. Medium orange shading denotes the location of a delta/fan-delta associated with the Harmonsburg Moraine (light orange). Yellow stars denote Paleoindian sites, red stars denote Early Archaic sites and the orange star is the approximate location of the 14C-dated mammoth bone discovery by divers. Orange triangles denote locations of 14C assays. Modified from Barnett (2019). B) The 340 m (1116 ft) elevation contour is the highest water level considered likely based on topographic features within the valley. Ice-marginal features shown in dashed yellow. Possible spillways shown in solid white. Modified from Barnett (2019).*

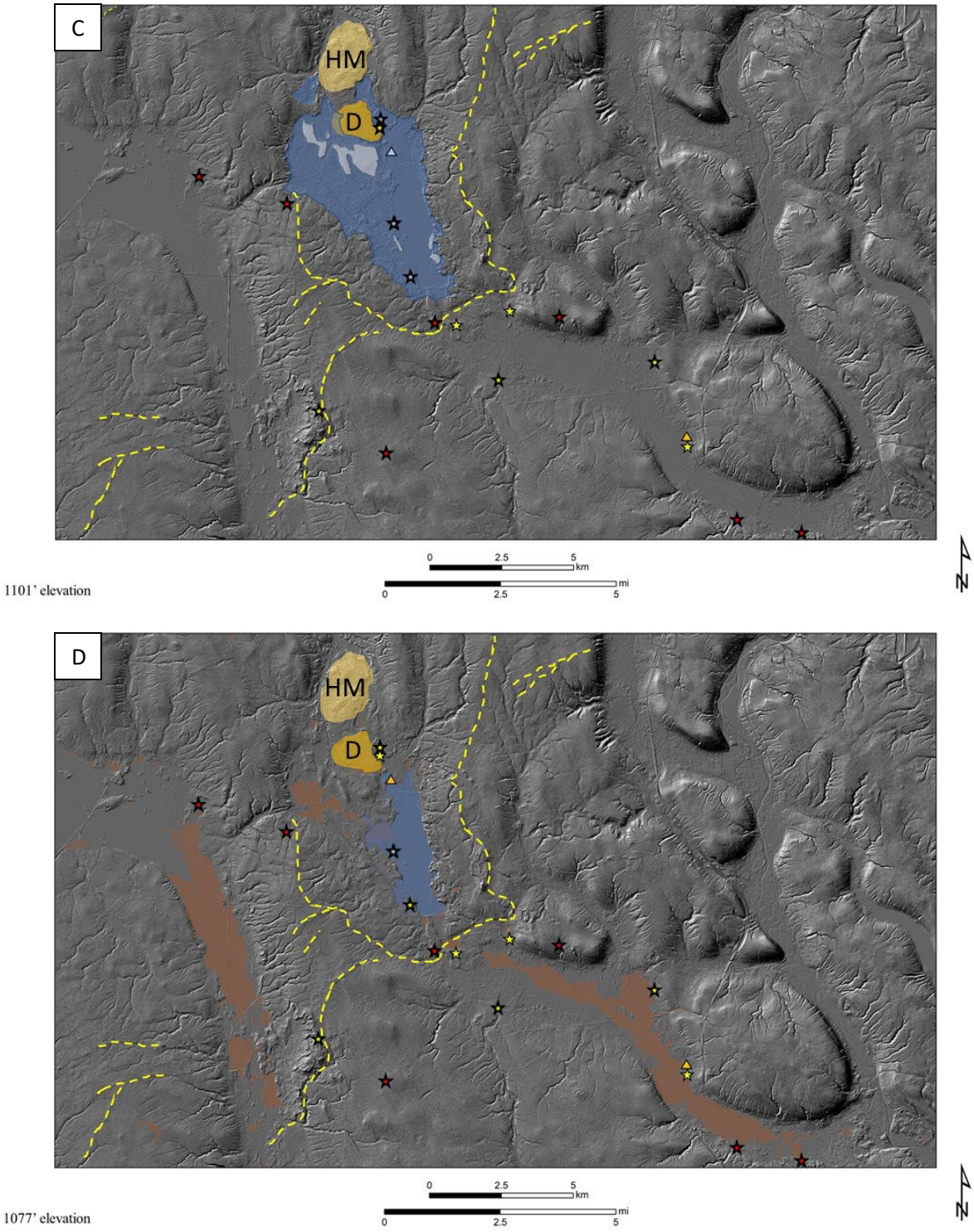

Figure 4.7. *C) The 335 m (1101 ft) in elevation contour lies at and near the base of delta/fan-delta. At this elevation, the reconstructed lake level appears to align with several erosional features within the valley. Drainage through the northern outlet would have ceased near this lake level. Dashed yellow lines show ice-marginal features. Modified from Barnett (2019). D) The 328 m (1077 ft) elevation contour is approaching the modern lake level of 326-327 m (1071-1073 ft). At this elevation, much of the former kettle hole is water-free and peat has developed in numerous poorly drained depressions and in areas of high groundwater. Dashed yellow lines show ice-marginal features.*

Little is known about the lake level history of Glacial Lake Conneaut from the time of Lavery and/or Hiram ice stagnation and collapse within the valley, and the formation of Glacial Lake Conneaut until megafauna are known to be present in the area during the Bolling-Allerod (e.g. Vento et al., 2020). A radiocarbon assay from a woolly mammoth vertebra recovered from within Conneaut Lake (**Figure 4.7A**) yielded a median age of 13,857 cal yrs BP (11,960 +/- 70 14C yrs BP; mid Bolling-Allerod), consistent with other regional findings (e.g. Lothrop et al., 2016; Lothrop et al., 2017; Carr and Adovasio, 2020; Vento et al., 2020). Regional paleoenvironmental reconstructions for the Bolling-Allerod suggest a warming climate at that time and a habitable landscape likely dominated by spruce-pine-tamarack-oak forest (**Figure 4.3** and **Table 4.1**; Webb III et al., 2003; Lothrop et al., 2016; Swisher and Peck, 2020; Vento et al., 2020; Griggs et al., 2022). No Pre-Clovis archaeological sites are known to exist within the glaciated portion of NWPA. The few time-diagnostic artifacts found in the vicinity of the Conneaut Lake-Marsh system indicate Early and Middle Paleoindian Period occupations during the late Bolling-Allerod and Younger Dryas, and Late Paleoindian Period occupations during the Early Holocene, possibly co-eval with Early Archaic bands as discussed in Lothrop et al. (2016) (**Table 4.1** and **Figures 4.4 & 4.7**). These sites nearly exclusively occur on kames or outwash terraces overlooking the lake-marsh system (**Figure 4.7**), consistent with the model of Paleoindian settlement patterns in NWPA suggested by Lantz (1984) and elsewhere in the formerly glaciated eastern Great Lakes region and northeastern North America (Ellis et al., 2011; Lothrop et al., 2016; Lothrop et al., 2017). This means that early Native Americans were living close to perceived resources near water bodies, often not on higher elevation uplands during the Pleistocene-Holocene Transition. What does this mean for the long-held idea that Paleoindian bands were "big game" hunters? Caution is warranted in making cultural interpretations of settlement and subsistence because none of these sites have undergone formal intensive excavations and due to the sometimes-sketchy nature of information in the PASS files entered into PA-SHARE.

Figure 4.8. *Wetland core extracted adjacent to the multi-component Smock-Biguziak (36CW248, also sometimes called Peterson 5) archaeological site. The site was partially excavated by Gerald Lang who recovered Archaic Kirk projectile points and a possible Late Paleoindian "Plano" point, as well as an assortment of younger cultural materials. The oldest radiocarbon date from the core suggest an ice-free landscape immediately prior to or at the beginning of the Erie Interstade. The upper, younger radiocarbon date is from a paleosol within the core and suggest a drop in water level within Conneaut marsh, and presumably lake, during the Younger Dryas. The 2 sigma calibrated ages are shown on this image. See guidebook text for the median calibrated ages.*

Water levels in the lake-marsh system apparently fell ~12,768 cal yrs BP (10,820 +/- 70 ^{14}C years BP) based on the presence of an oxidized, charcoal-bearing buried soil on the adjacent kame terrace (**Figures 4.7 & 4.8**). The presumed drop in water level occurs during early Younger Dryas, and when paleoenvironmental conditions were rapidly changing from warming to cooling, and initial Early and early Middle Paleoindian bands were populating formerly glaciated portions of the region (**Table 4.1** and **Figure 4.4**; Newby et al., 2005; Ellis et al., 2011; Lothrop et al., 2016; Lothrop et al., 2017; Carr and Adovasio, 2020; Vento et al., 2020; Grote et al., 2022). At Silver Lake, located ~ 120 km (75 mi) southwest of Conneaut Lake in Summit County, Ohio, the Younger

Dryas is also well expressed sedimentologically and within the pollen spectrum (Swisher and Peck, 2020). The Silver Lake pollen spectrum indicates that during the early YD (~12,910 cal yrs BP) spruce, fir and oak dominate the pollen spectra, which is consisted with numerous other regional paleobotanical studies in the Midwest and northeastern North America. At about 12,130 cal yrs BP, during the middle Younger Dryas, organic matter dramatically increases accompanied by a rapid increase in pine pollen, and decreasing concentrations of spruce and oak, and to a lesser extent fir, at Silver Lake, and other nearly sites on the Appalachian Plateau in Ohio (Swisher and Peck, 2020). They suggest that in the middle Younger Dryas there is a hydroclimate change from cool-wet to cool-dry in eastern Ohio. Several lakes and bogs located ~ 200-250 km (~124-155 mi) northeast of Conneaut Lake in western New York paint a similar picture as Silver Lake, Ohio (e.g. Webb et al., 2003) and are in general agreement with the reconstructions of Shuman et al. (2002) for the eastern United States (**Figure 4.3** and **Table 4.1**). Although the pollen record at Hartstown Bog (see **Figure 4.7** for location) is poorly constrained (only a single accepted radiocarbon assay), five changes in reconstructed vegetation have been identified and when compared to the "nearby" Ohio and New York pollen diagrams they appear reasonably similar. Additional evidence of landscape instability during the Younger Dryas in NWPA is found at Sugar Lake, located to the east of the Conneaut Lake-Marsh system (see **Figure 4.5B** for location). A Sediment core extracted from Sugar Lake (see **Figure 4.5B** for location) records and influx of clastic sediment presumably occurring during the Younger Dryas suggesting increased hillslope erosion, reflecting a loss of vegetation (Straffin et al., 2010). No pollen analysis has been performed on this core to date.

Rapid warming at the end of the Younger Dryas signals the end of the Pleistocene glacial period and the ushering in of the Holocene Interglacial (**Table 4.1** and **Figures 4.3 & 4.4**). The end of the Younger Dryas also witnessed the abandonment of fluted technology and a shift in land utilization practices such as the abandonment of less productive land in favor of lake shores and the periphery of wetlands (Newby et al., 2005; Munoz et al., 2010; Ellis et al., 2011; Lothrop et al., 2016). It is assumed that water levels in the Conneaut lake-marsh system (**Figure 4.7**) were near modern levels at that point and Early Archaic archaeological sites in the vicinity likely suggest a continued use of the lake and marsh. The Early Holocene climate is interpreted to have been cool, but warming, and dry which allowed for the rise of closed forests of pine, oak and birch (**Figures 4.3** and **Table 4.1**; Watts, 1979; Webb III et al., 2003; Shuman et al., 2004; Munoz et al., 2010; Vento et al., 2020). The dominance of pine ends during the late Early Holocene (10,900-8200 cal yrs BP) in many regional pollen spectra and is replaced by oak and hickory (Shuman et al., 2004; Munoz et al., 2010; Lothrop et al., 2016). Regionally, 8200 cal yrs BP marks another major climate-ecosystem-human transition with a shift from cool and dry to warm and wet, and the end of the Early Holocene and Early Archaic cultural period (**Table 4.1** and **Figure 4.4**; Munoz et al., 2010). The shift in climate at 8200 cal yrs BP is related to the final collapse of the LIS. During the Middle Archaic cultural period the regional climate remained warm and wet with forests consisting of hemlock, beech and hickory (Shuman et al., 2004; Munoz et al., 2010). Marshland was present within the northern portions of the kettle around the lake inlet by ~ 7273 cal yrs BP (6350 +/- 80 14C yrs BP) as water levels stabilized at or very near (maybe 1 m or so from modern) the modern elevation of ~327 m (~1071-1073 ft) above mean sea level (**Figures 7A & 7D**). Sometime afterwards, overbank sedimentation produced a clastic-dominated floodplain in the lowest portions of the Conneaut Lake inlet valley while marshland persisted within the outlet valley and at higher elevations within the kettle.

References

Barnett, J., 2019. GIS-based investigation of the glacial history of the Conneaut Valley, northwestern Pennsylvania. Unpublished undergraduate senior project, Indiana University Southeast.

Braun, D. D. 2004. The glaciation of Pennsylvania, USA. In: Quaternary Glaciations Extent and Chronology, Part II: North America, J. Ehlers and P. L. Gibbard, 237-242. Amsterdam, Netherlands: Elsevier.

Burkett Jr., C., 1981. The analysis and distribution of paleoindian artifacts in western Crawford County, Pennsylvania. Manuscript on file with the Anthropology Department of the Carnegie Museum of Natural History.

Carr, K.W. and J.M. Adovasio, 2020. Chapter 2: The Paleoindian Period in Pennsylvania. In: The Archaeology of Native Americans in Pennsylvania, K.W. Carr, C. Bergman, C.B. Rieth, B.K. Means and W. Roger. Philadelphia, Pennsylvania, University of Pennsylvania Press.

Dalton, A.S., M. Margold, C.R. Stokes and 68 others, 2020. An updated radiocarbon-based ice margin chronology for the last deglaciation of the North American Ice Sheet Complex. Quaternary Science Reviews, v. 234, 106223, doi.org/10.1016/j.quascirev.2020.106223.

Ellis C.J., D.H. Carr and T.J. Loebel, 2011. The Younger Dryas and Late Pleistocene people of the Great Lakes region. Quaternary International, v. 242(2), p. 534-545, doi.org/10.1016/j.quaint.2011.02.038.

Fleeger, G. M., T. Grote, E. Straffin and J. P. Szabo. 2011. Quaternary geology of northwestern Pennsylvania. In: From the shield to the sea: Geological Field Trips from the 2011 Joint Meeting of the GSA Northeastern and North-Central Sections, R. M. Ruffolo and C. N. Ciampaglio (eds), 87-109. Geological Society of America Field Guide 20. Denver, Colorado, Geological Society of America.

Gajewski, K., Viau, A., Sawada, M., Atkinson, D., and Fines, P., 2006, Synchronicity in Climate and Vegetation Transitions Between Europe and North America During the Holocene. Climatic Change, v. 78, p. 341–361, doi.org/10.1007/s10584-006-9048-z.

Griggs, C.B., D. Peteet, B. Kromer, T. Grote and J. Southon, 2017. A tree-ring and paleoclimate record for the Younger Dryas-Early Holocene transition from northeastern North America. Journal of Quaternary Science, v.32, p. 341-346, doi.org/10.1002/jqs.2940.

Griggs, C.B., C.F.M. Lewis and D.A. Kristovich, 2022. A late-glacial lake-effect climate regime and abundant tamarack in the Great Lakes region, North America. Quaternary Research, doi.org/10.1017/qua.2021.76.

Grote, T. and E. Straffin, 2019. An analysis of Late Wisconsinan ice-marginal environments in northwestern Pennsylvania. Pennsylvania Geographer, v. 57, p. 17-33.

Grote, T. E. Straffin, J. Barnett, L. S. Buth, Homsey-Messer and A. Myers, 2022. Mapping previously unrecognized ice margin positions and their relationship to the Conneaut lake-marsh system, northwestern Pennsylvania. Biannual meeting of the American Quaternary Association program with abstracts.

Hartley, K.A., 2009, Stratigraphic analysis of areal discontinuities of Late Wisconsinan till sheets near Conneaut Lake, northwestern Pennsylvania. Unpublished M.S. thesis, University of Akron.

Karrow, P.F., A. Dreimanis and P.J. Barnett, 2000. A proposed diachronic revision of Late Quaternary time-stratigraphic classification in the eastern and northern Great Lakes area. Quaternary Research, v. 54, p. 1-12, doi.org/10.1006/qres.2000.2144.

Koetje, T., 1998. The Archaic in northwestern Pennsylvania. In: The Archaic Period in Pennsylvania: Hunter-Gathers of the Early and Middle Holocene Period, P.A. Raber, P.E. Miller and S.M. Neusius (eds). Recent Research in Pennsylvania Archaeology No. 1, Pennsylvania Historical and Museum Commission, p. 29-44.

Laub, R.S. (ed.), 2003. The Hiscock Site: Late Pleistocene and Holocene paleoecology and archaeology of western New York state. Bulletin of the Buffalo Society of Natural Sciences, v. 37, 327 p.

Lantz, S.W., 1984. Distribution of Paleoindian projectile points and tools from western Pennsylvania: Implications for regional differences. Archaeology of Eastern North America, v. 12, p. 210-230.

Leverett, F., 1902 Glacial formations and drainage features of the Erie and Ohio basins, US Geological Survey, Monograph XLI, 802 p.

Lewis, C.F.M. and T.W. Anderson, 2020. A younger glacial Lake Iroquois in the Lake Ontario basin, Ontario and New York: Re-examination of pollen stratigraphy and radiocarbon dating. Canadian Journal of Earth Sciences, v. 57, 453-463, doi.org/10.1139/cjes-2019-0076.

Lothrop, J.C., D.L. Lowery, A.E. Spiess and C.J. Ellis, 2016. Early human settlement of northeastern North America. Paleoamerica, v. 2, p. 192-251, doi.org/10.1080/20555563.2016.1212178.

Lothrop, J.C., M.L. Beardsley, M.L. Clymer, J.E. Diamond, P.C. LaPorta, M.H. Younge and S. Winchell-Sweeny, 2017. Paleoindian landscape in southeastern and central New York. Paleoamerica, v. 3, p. 351-363, doi.org/10.1080/20555563.2017.1383086.

Mayer-Oaks, W.J., 1955. Prehistory of the Upper Ohio Valley: An introductory archaeological study. Anthropology Series number 2, Annals of the Carnegie Museum, 296 p.

McConaughy, M.A., J.D. Applegarth and D.J. Faingnaert, 1977. Fluted points from Slippery Rock, Pennsylvania. Pennsylvania Archaeologist, v. 47, p. 30-36.

Merritts, D.J. and M.A. Rahnis, 2022. Pleistocene periglacial processes and landforms, Mid-Atlantic region, eastern United States. Annual Review of Earth and Planetary Sciences, v. 50, p. 541-592, doi.org/10.1146/annurev-earth-032320-102849.

Miller, N.G. and R.P. Futyma, 2003. Extending the paleobotanical record at the Hiscock Site, New York: Correlations among stratigraphic pollen assemblages from nearby lake and wetland basins. In: The Hiscock Site: Late Pleistocene and Holocene paleoecology and archaeology of western New York state, R.S. (ed). Bulletin of the Buffalo Society of Natural Sciences, v. 37, p. 43-62.

Munoz, S.E., K. Gajewski and M.C. Peros, 2010. Synchronous environmental and cultural change in the prehistory of the northeastern United States. Proceedings of the National Academy of Sciences, v. 107, p. 22008-22013, doi.org/10.1073/pnas.1005764107

Myers, A.J. and M. Moses Myers, 2007. A preliminary report of the Paleoindian assemblage from Indian Camp Run no. 1 (36FO65). Pennsylvania Archaeologist, v. 77, p. 1-33.

Newby, P., J. Bradley, A. Spiess, B. Schuman and P. Leduc, 2005. A Paleoindian response to Younger Dryas climate change. Quaternary Science Reviews, v. 24, p. 141-154, doi.org/10.1016/j.quascirev.2004.04.010.

Panushkina, I.P., S.W. Leavitt, E.W. Domack and A.C. Wiedenhoeft, 2015. Tree-ring investigation of Holocene flood-deposited wood from the Oneida Lake Watershed, New York state. Tree-Ring Research, v. 71, p. 83-94, doi.org/10.3959/1536-1098-71.2.83.

Shepps, V.C., 1959, Field Trip 5: Glacial geology of northwestern Pennsylvania, in, Guidebook for field trips, Pittsburgh meeting, 1959, National GSA Guidebook.

Shepps, V.C., White, G.W., Droste, J.B., and Sitler, R.F., 1959, Glacial geology of northwestern Pennsylvania: Pennsylvania Geological Survey General Geology Report G 32, 59 p.

Shuman, B., T. Webb III, P. Bartlein, J.W. Williams, 2002. The anatomy of a climate oscillation: Vegetation change in eastern North America during the Younger Dryas chronozone. Quaternary Science Reviews, v. 21, p. 1777-1791, doi.org/10.1016/S0277-3791(02)00030-6.

Shuman, B., Newby, P., Huang, Y., and Webb, T., 2004, Evidence for the close climatic control of New England vegetation history: Ecology, v. 85, p. 1297–1310, doi.org/10.1890/02-0286.

Straffin, E.C., and Grote, T., 2010, Surficial geology of the Sugar Lake 7.5-minute quadrangle, Crawford and Venango Counties, Pennsylvania: Pennsylvania Geological Survey, 4th ser., Open-File Report OFSM 10-05.0, 23 p., Portable Document Format (PDF).

Straffin, E., T. Grote, K. Jones, Z. Robinson, B. Zimmerman, 2010. Late and post-glacial sediment history and landscape change from Sugar Lake, Pennsylvania. Joint Northeast-Southeast Sections of the Geological Society of America Annual Meeting Program with Abstracts.

Swisher, S.E. and J.A. Peck, 2020. Vegetation changes associated with the Younger Dryas from the sediments of Silver Lake, Summit County, Ohio, USA. The Ohio Journal of Science, v. 120, p. 30-38, doi.org/10.18061/ojs.v120i2.7095.

Vento, F.J., A. Vega and H. Rollins, 2020. Chapter 1: Genetic stratigraphy: Late Pleistocene through the Holocene paleoclimates and paleoenvironments of Pennsylvania. In: The Archaeology of Native Americans in Pennsylvania, K.W. Carr, C. Bergman, C.B. Rieth, B.K. Means and W. Roger. Philadelphia, Pennsylvania, University of Pennsylvania Press.

Walker, P.C., and Hartman, R.T., 1960, The forest sequence of the Hartstown Bog area in western Pennsylvania: Ecology, v. 41, p. 461–474, doi:10.2307/1933321.

Webb III, T., B. Shuman, P. Leduc, P. Newby and N. Miller, 2003. Late Quaternary climate history of western New York state. In: The Hiscock Site: Late Pleistocene and Holocene paleoecology and archaeology of western New York state, R.S. (ed). Bulletin of the Buffalo Society of Natural Sciences, v. 37, p. 11-17.

White, G.W., Totten, S.M., and Gross, D.L., 1969, Pleistocene stratigraphy of northwestern Pennsylvania, Pennsylvania Geological Survey, 4th series, general Geology Report 55, 88 p.

White, I.C., 1881. Geology of Crawford and Erie Counties, Pennsylvania. Pennsylvania Geological Survey 2nd Series. QQQQ.

Watts, W. A., 1979. Late Quaternary vegetation of central Appalachia and the New Jersey coastal plain, Ecological Monographs, 49:427-469.

Young, R.A., L.M. Gordon, L.A. Owen, S. Huot and T.D. Zerfas, 2021. Evidence for a late glacial advance near the beginning of the Younger Dryas in western New York state: An event postdating the record fro local Laurentide Ice Sheet recession. Geosphere, v. 17, p. 271-305, doi.org/10.1130/GES02257.1.

Point of Interest: Titusville was the home of Ida Tarbell, one of the most influential muckrakers of the Gilded Age. In 1900, she wrote a series of investigative articles (later compiled into the book The History of the Standard Oil Company) that highlighted the illegal practices being used by J. D. Rockefeller to stamp out smaller competing oil companies. She was able to prove that Standard Oil had a history of strong-arm tactics, espionage, and collusion going back over thirty years. Her exposé is generally thought to be the inciting incident for the U.S. Supreme Court case in 1911, in which Standard Oil was found guilty of violating the Sherman Antitrust Act. As a result, Standard Oil was fractured into a series of smaller companies, the descendants of which include ExxonMobil and Chevron.

POI Source: *King, G., 2012, The Woman Who Took on the Tycoon, Smithsonian Magazine, https://www.smithsonianmag.com/history/the-woman-who-took-on-the-tycoon-651396/?no-ist.*

POI Figure Source: *Purdy, J. E., Public Domain, 1904, "Ida M. Tarbell (1857-1944), head-and-shoulders portrait, facing front," http://www.commons.wikimedia.org/w/index.php?curid=9091982.*

Point of Interest: Titusville was also the birthplace of John Heisman, for whom the Heisman Trophy is named. Among other things, Heisman's impact on football includes:

- Legalizing the forward pass
- Invented the hidden ball play
- Originated the "hike" or "hep" shouted by the quarterback to start each play
- Led the effort to cut the game from halves to quarters
- Listing downs and yardage on the scoreboard

POI Source: *National Football Foundation & College Hall of Fame, Inc., 2022, Hall of Fame: John Heisman, https://footballfoundation.org/hof_search.aspx?hof=1297.*

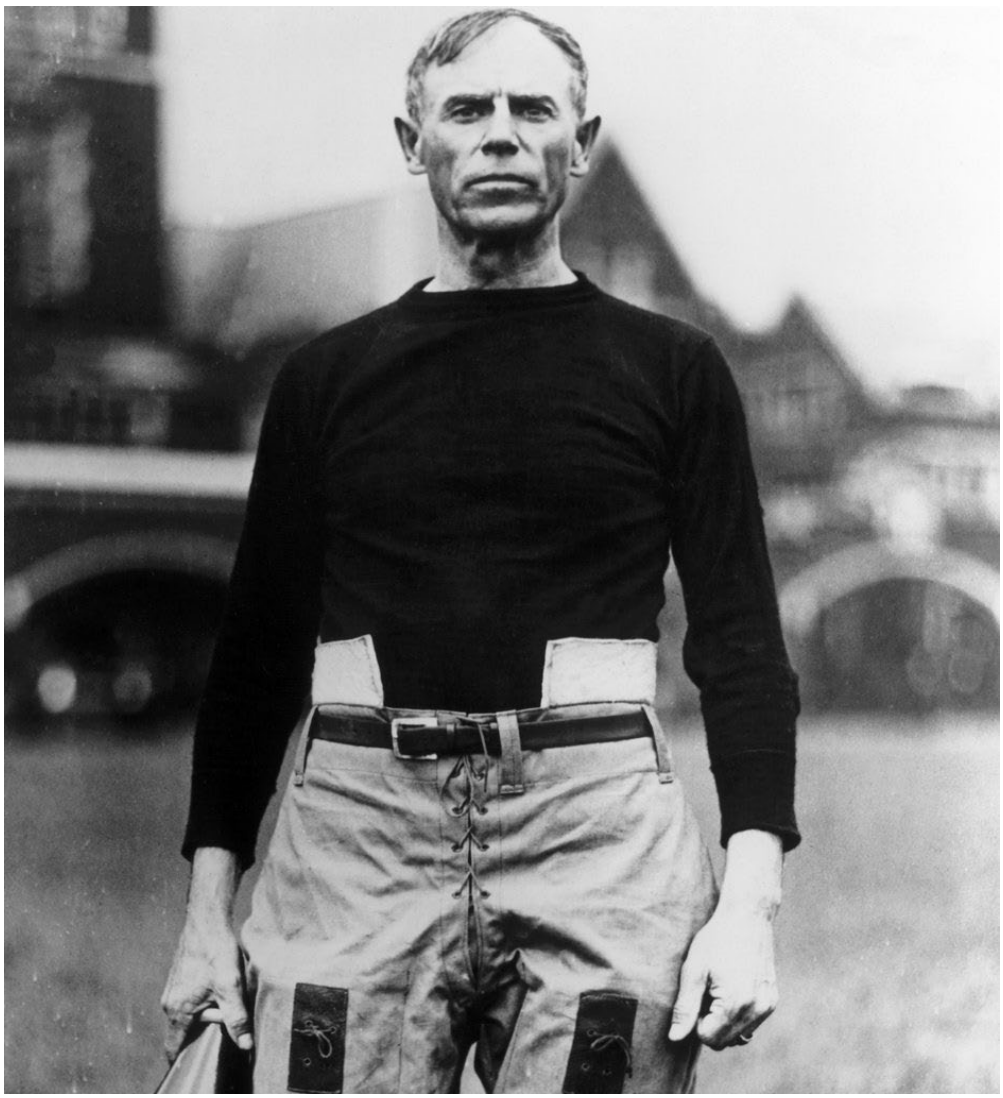

POI Figure Source: *Georgia Tech Archives & Records Management, 1917, John Heisman standing on Bowman Field, in front of Tillman Hall, on the Clemson University Campus, https://commons.wikimedia.org/wiki/File:John_Heisman.jpg.*

STOP 5: VINCENT SAND AND GRAVEL PIT

ERIC STRAFFIN – PENNWEST UNIVERSITY, EDINBORO CAMPUS
GARY M. FLEEGER – PENNSYLVANIA GEOLOGICAL SURVEY *(RETIRED)*

41.421266 / -79.845179

Location

The Vincent Excavating and Gravel pit has been in operation since 1953 by the Vincent family. It is located along Patchel Run, a tributary to French Creek downstream from the confluence of Sugar and French Creeks, and northwest of Franklin, Pennsylvania (**Figures 5.1 and 5.2**).

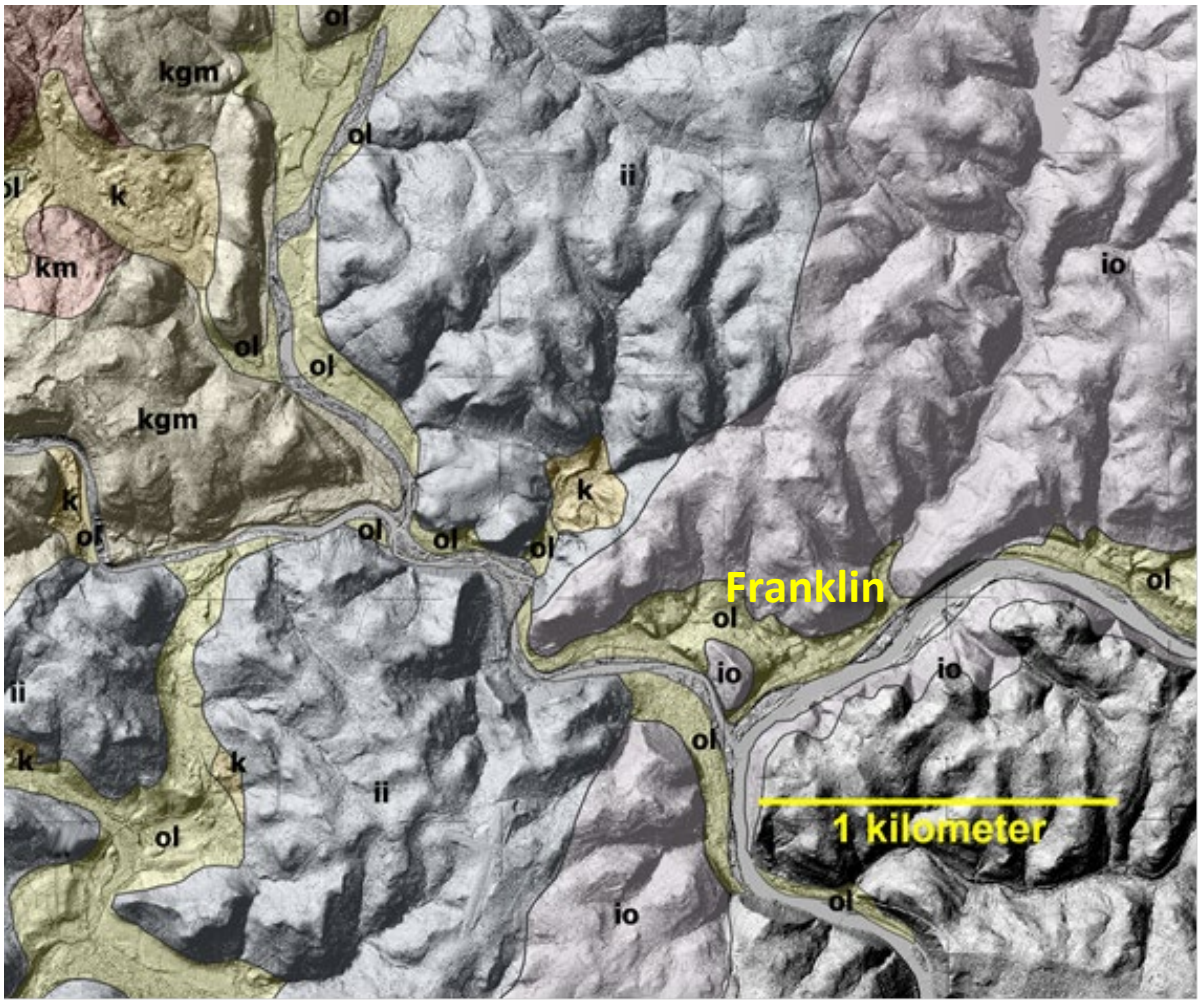

Figure 5.1. *The Vincent and Cooperstown pits are located in the kame deposit (k) in the center of the map. The ii is the mapped extent of Titusville Till. io is Mapledale Till. km and kgm are Kent Moraine and ground moraine, respectively. Outwash is labeled ol. Geology from Shepps et al (1959), Plate 1 overlain on 10x lidar hillshade.*

Geology

White et al (1969) interpreted this deposit, exposed in the Vincent pit and nearby Cooperstown S&G pit, ¼ mile to the west across Patchel Run, as a Mapledale kame deposit (**Figure 5.1**). It is right at the mapped Titusville till border, just beyond the well-defined Kent end moraine (**Figure 5. 1**; Shepps et al, 1959). White et al (1969) interpreted less weathered Titusville till and gravel over Mapledale gravel in the Cooperstown pit. These kame deposits are

Figure 5.2. *Location of the Vincent (southeast of Patchel Run) and Cooperstown (northwest of Patchel Run) pits. Cooperstown appears to be a flat-topped terrace. Vincent deposit is partly covered to the east by hillslope (colluvial) deposits. Locations of the 2 OSL samples (Figures 5.3 and 5.4) are noted. From the USGS Franklin 7.5' quadrangle map.*

along the Patchel Run valley walls (**Figure 5.2**). Previous work (White et al, 1969) suggests that pre-Illinoian tills could be present at depth.

We chose this stop because we sampled it for OSL dating, to confirm or revise the White et al (1969) age interpretation; however, we did not receive the dates from the lab in time to include them in the guidebook.

Figure 5.3. *Aerial view of the Vincent and Cooperstown pits, and locations of the OSL samples. Aerial photo from Google Earth, dated 10/9/2019. The pit had expanded in the 2 years between the photo and the sampling date.*

The Vincent pit exposes deposits from several different depositional environments, including glacial, fluvial, lacustrine, and colluvial settings. The southeastern edge of the pit (**Figures 5.3 and 5.4**) bisects the westward sloping original hillslope (**Figure 5.4**), and from the top down (**Figures 5.4 and Figure 5.5**): a) colluviated till, with numerous horizontal platy sandstone clasts, b) weathered till, tentatively identified at the Mapledale(?) Till, with an eluvial horizon at the top (**Figure 5.6**), c) weathered coarse sand and gravel, with some imbrication, cemented with iron and manganese, d) unweathered, light, cross

bedded, rippled sand and fine gravel. The stratified sand and gravel below the iron cemented unit were sampled for OSL (Sample 11-19-21-1; **Figures 5.5 and 5.7**) and provide a maximum age on the timing of that deposit.

The white clay eluvial horizon (**Figure 5.6**) is intensely weathered and has had most of the iron and manganese removed, which has leached into the underlying weathered coarse sand and gravel. Much of the contact at the top of the coarse sand and gravel has an accumulation of manganese (**Figure 5.8**), and the pattern of iron and manganese accumulation suggest preferred groundwater flow paths (**Figure 5.9**).

The southwestern edge and western wall of the Vincent pit exposed till overlain by cross bedded sandy fluvial and silty, horizontally laminated sediments, likely of lacustrine origin. Cross bedded sands from fluvial units were sampled for OSL (Sample 11-19-21-2, **Figure 5.10**) in order to provide age estimates of outwash, and a minimum age for the underlying till.

Considerable complexity in geometry and thickness of units were observed in the different walls of the pit. Cross bedded sand with coal coarsened upward to weathered coarse sand and gravel in the southeastern end of the pit, overlain by till, while a boulder to cobble rich till was present at the base of the west wall of the pit, overlain by laminated silt and sand (**Figure 5.4**). It was difficult to trace the till from the south to the west wall through a covered interval (**Figure**

Figure 5.4. *South (distant) and west (right side) walls of Vincent Pit. OSL samples taken in the unweathered sand below dark weathered sand and gravel (maximum age of overlying till) in the southeast corner, and in sand above till (minimum age) in the west wall.*

Figure 5.5. *Southeastern pit wall, Vincent Pit. Cross bedded sand and gravel lenses at base of pit, overlain by dark, cemented sand and gravel, and till. Colluviated till at top. See Figure 5.7 for a close up view of lower sand.*

5.4), to determine if the same till is exposed above sand and gravel in the SW corner, and below sand and silt in the west wall.

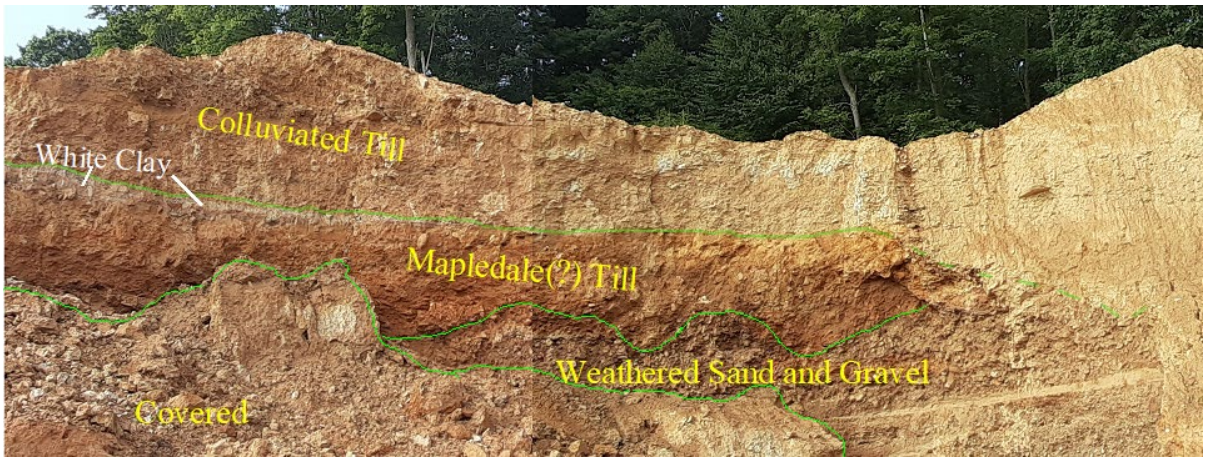

Figure 5.6. *Detail of the southeastern wall of the Vincent Pit. The white clay of the eluvial horizon is shown in this view. The horizontal platy sandstone pieces are obvious in the colluviated till.*

Figure 5.7. *Close up of location of OSL sample 11-19-21-1 in asymmetrical ripple cross laminated sand. Coal is dark material that accentuates ripple laminations. Scale is 1.7 meters.*

Just to the northwest of the Vincent pit is another exposure of correlatable deposits, in the Cooperstown pit. In 2021, it exposed cross bedded coal rich sand with climbing ripples at the base. The rippled and cross bedded sand covered sandy contorted beds, became pebbly upward, and had small normal faults throughout (**Figure 5.11**). Rapid sedimentation produced climbing ripples, and likely caused soft sediment deformation of sandy beds below. Normal faults occurred later from thawing ice, creating collapse structures that were later filled by outwash. Higher in the section, repeating packages of steeply dipping, cross bedded sand and interbedded gravel most likely represent rapid filling of ice thaw/collapse structures (**Figure 5.12**). Cross bedded sand was sampled for OSL but awaits funding.

The Cooperstown pit was visited by the 1976 Field Conference of PA Geologists (Chapman and Craft, 1976). At that time of the 1976 Field Conference, it had spectacular collapse structures cause by the melting of a buried ice block (**Figure 5.13**).

A. Colluviated Till

B. Mapledale (?) Till

C. Weathered coarse sand and gravel.

D. Unweathered fine sand and gravel (OSL sample)

Figure 5.8. *Manganese accumulation in coarse, weathered sand and gravel at the contact with the overlying weathered Mapledale(?) Till.*

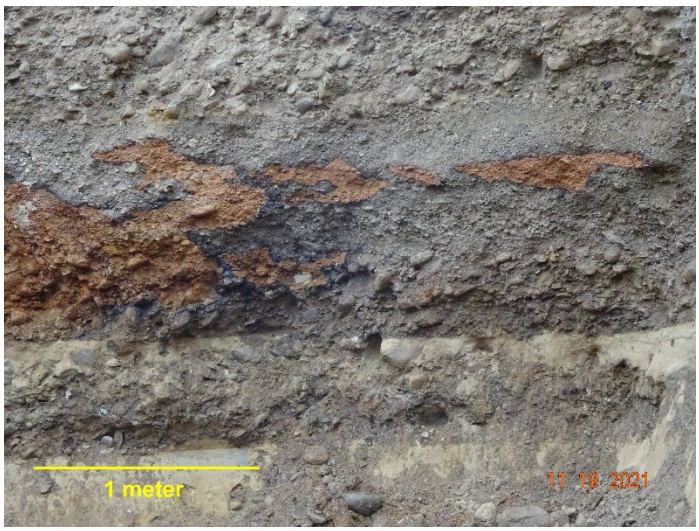

Figure 5.9. *(Left) Pattern of manganese and iron accumulation in the weathered coarse sand and gravel, suggesting accumulation along preferred groundwater flow paths. The contact with lighter, unweathered, finer sand and gravel is just below the center of the photo, below the iron and manganese accumulation.*

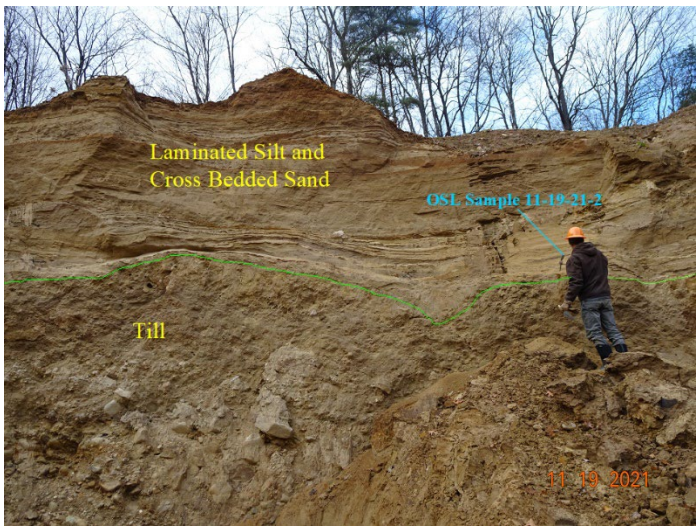

Figure 5.10. *(Left) Vincent Pit, west wall illustrating till at base, overlain by cross bedded sand and topped by silty laminated sediment. OSL sample 11-19-21-2 was taken just above till within sand.*

Figure 5.11. *(Left) Near the base of the Cooperstown pit exposure, planar laminated sand, offset by small scale normal faults. Faults are eroded at top and covered by asymmetrical climbing ripples and ripple laminations. Iron staining darkens boundaries with large changes in grain size.*

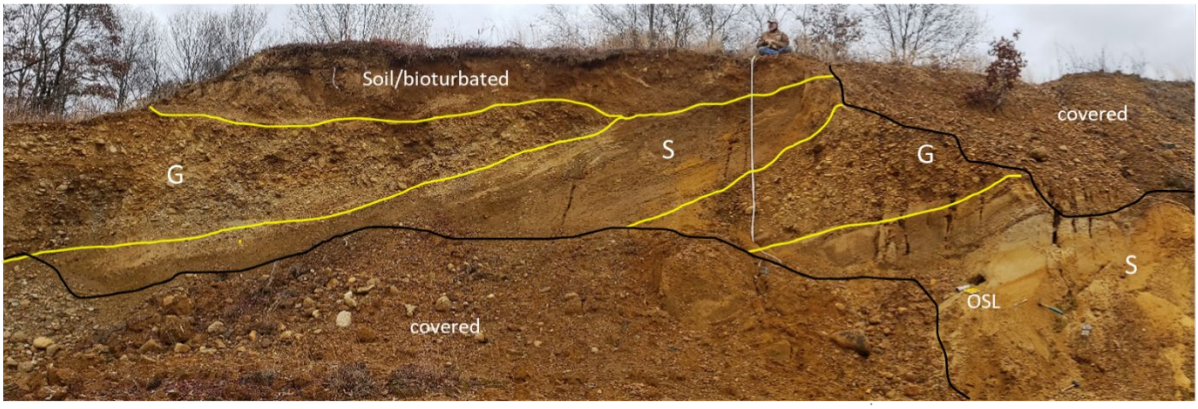

Figure 5.12. *Cooperstown pit. The upper portion of the section is covered, disturbed, and/or modified by soil forming processes. Below the soil are steeply dipping (down to left, or northwest) cross bedded sand (S) interbedded with poorly sorted, clast-supported gravels (G). OSL sample at bottom right, 5.5 m below the top. Gary Fleeger atop the outcrop, for scale.*

Figure 5.13. *(Left) High-angle reverse faults created by normal faulting and rotation from the melting of a buried ice block in the Cooperstown pit, as exposed at the 1976 Field Conference. Donald M. Hoskins in foreground for scale. Photo from Field Conference files.*

References

Chapman, W.F. and J.L. Craft (1976) Stop XI- Four Corners gravel pit, in, Bedrock and glacial geology of northwestern Pennsylvania in Crawford, Forest, and Venango Counties, 41st Annual Field Conference of Pennsylvania Geologists, Titusville, PA, pp. 58-59.

Shepps, V.C, G.W. White, J.B. Droste, and R.F. Sitler (1959) Glacial geology of northwestern Pennsylvania, Pennsylvania Geological Survey, 4th series, General Geology Report 32, 59 p.

White, G.W., S.M. Totten, and D.L. Gross (1969) Pleistocene stratigraphy of northwestern Pennsylvania, Pennsylvania Geological Survey, 4th series, General Geology Report 32, 85 p.

POI Figure Source: *Azovtsev, D., 2005, North American River Otters, Lontra canadensis, https://commons.wikimedia.org/wiki/File:LutraCanadensis_fullres.jpg.*

Point of Interest:
Venango County got its name from a variation on the Native American word for the region: *Onenge*. English settlers butchered the pronunciation of this term into the present-day equivalent. So what does *onenge* mean in the original Iroquois? It is the Iroquois word for "otter!"

HARPER'S GEOLOGICAL DICTIONARY

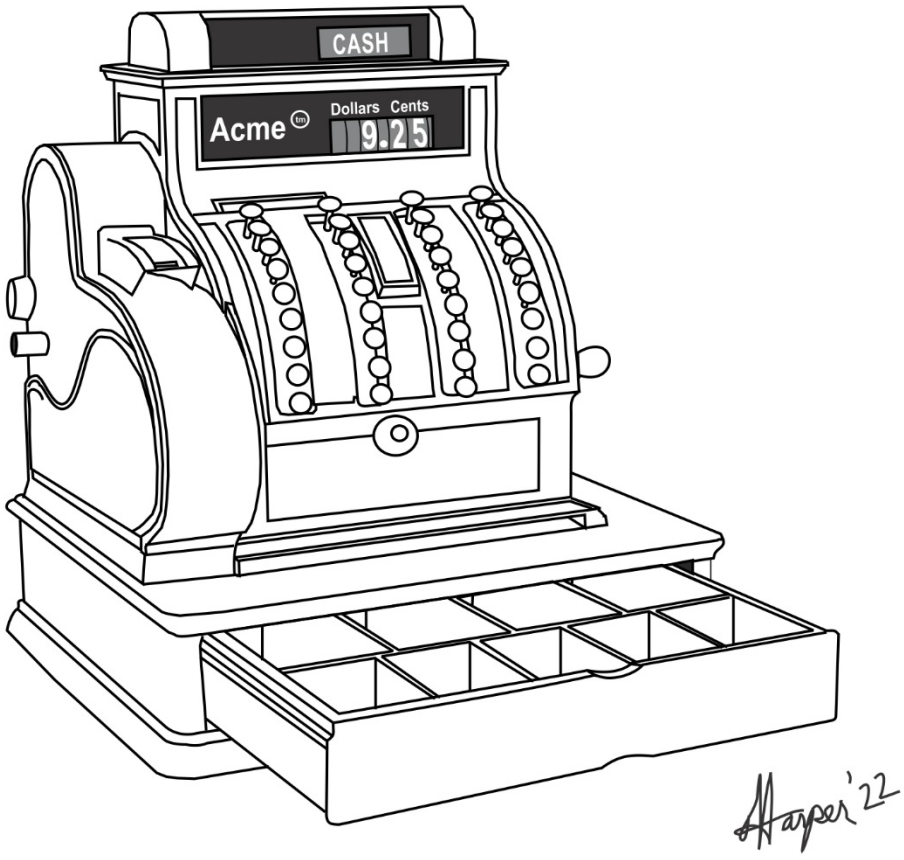

TILL - An antique machine used to store and change money at retail establishments prior to the computer age.

STOP 6: McCLYMONDS SAND & GRAVEL PIT

3 RIVERS AGGREGATE COMPANY QUARRY, PLAIN GROVE, PA

AARON D. BIERLY & GARY M. FLEEGER *(RETIRED)* – PENNSYLVANIA GEOLOGICAL SURVEY
CONTRIBUTORS:
ALLAN C. ASHWORTH – NORTH DAKOTA STATE UNIVERSITY
DOROTHY M. PETEET – COLUMBIA UNIVERSITY
MARGARET A. DAVIS AND BRENDAN J. CULLETON – PENN STATE UNIVERSITY

41.049 / -80.1485

Stop 2 is the site of a core hole drilled by the Pennsylvania Geological Survey in 2020. It is located on the western side of a buried bedrock valley, up to 200 feet deep, near Plain Grove (Figure 6.1).

Regional Setting

The buried bedrock valley is very obvious on the geologic and bedrock topographic map of the Mercer 15' quadrangle (**Figure 6.1**).

The buried valley is unusual for several reasons:

1. Much of it is very linear (**Figures 6.1 and 6.2**).
2. The gradient in the bedrock valley is south-southwest, approximately perpendicular to general northwest direction of pre-glacial drainage.
3. There are four well-developed partially-buried bedrock valleys extending northwest from the buried valley (**Figures 6.1 and 6.2**).
4. There are only a few, short tributary valleys on the east side of the buried valley.

The southernmost of the four partially-buried NW valleys, which today contains Schollard and Taylor Runs, is likely the pre-glacial course of Slippery Rock Creek (**Figure 6.3**). It flowed north in the buried valley from Elliotts Mill and northwest, probably to Lackawannock Creek and the Erie basin.

Each of the northwest-trending buried bedrock valleys has a bedrock divide in it (**Figure 6.2**). Each valley is currently occupied by a pair of streams flowing from a divide in the valley that does not coincide with the divide in the bedrock valley (**Figure 6.4**).

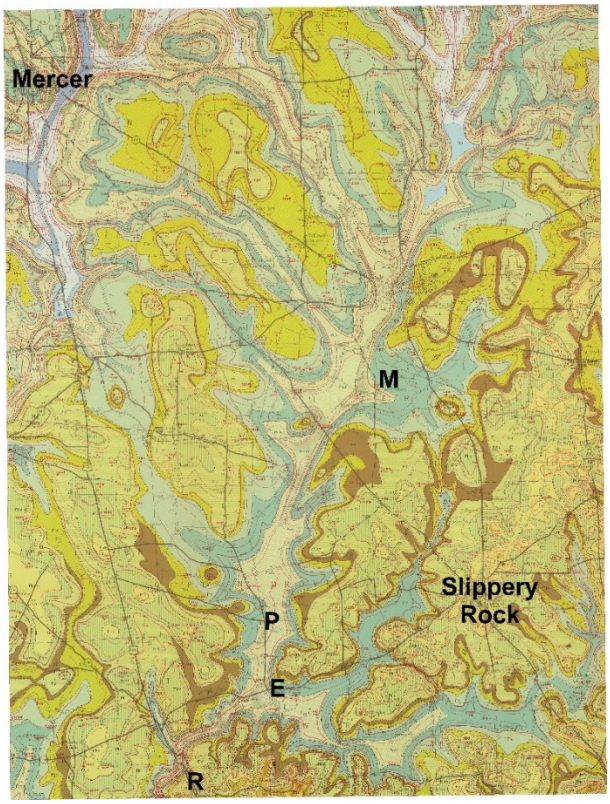

Figure 6.1. *(Right) Geologic and bedrock topographic map of the Mercer 15' quadrangle. Modified from Plate 2 from Poth (1963).*
M = McCoys Corners
E = Elliotts Mill
R = Rockville
P = Plain Grove

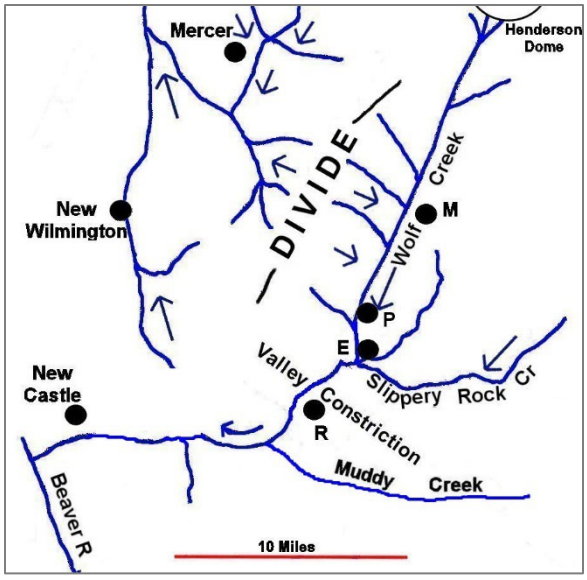

Figure 6.2. *(Left) Map of original Wolf Creek, Slippery Rock Creek, and 4 northwest-southeast bedrock valleys, as they are configured today. Most of these valleys are now partly or mostly buried with glacial sediment.*

M = McCoys Corners
E = Elliotts Mill
R = Rockville
P = Plain Grove

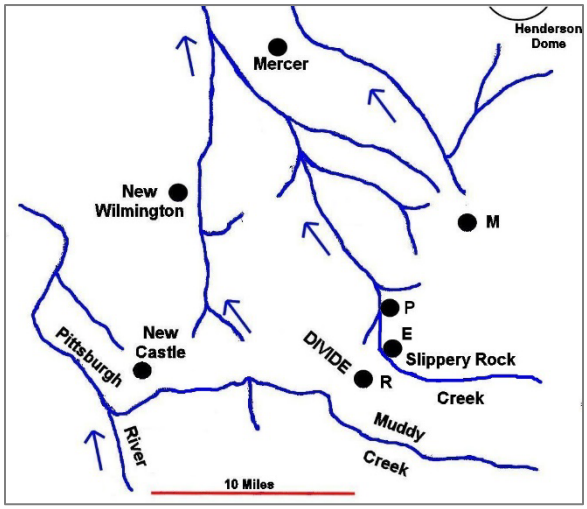

Figure 6.3. *(Left) Map of interpreted pre-Wolf Creek drainage to northwest through the 4 northwest-southeast valleys.*

M = McCoys Corners
E = Elliotts Mill
R = Rockville
P = Plain Grove

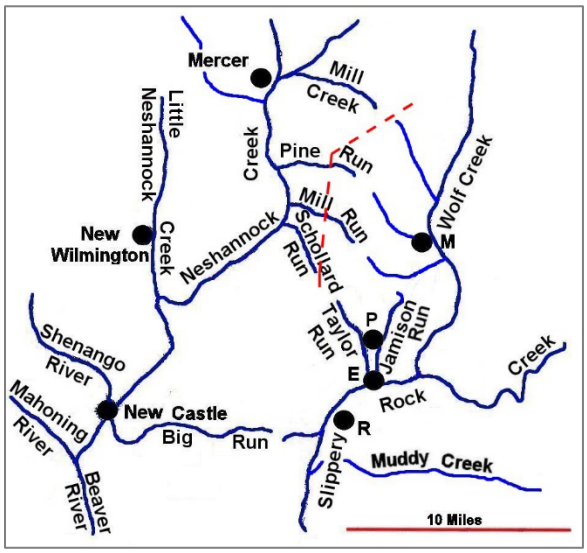

Figure 6.4. *(Left) Map of modern stream configuration. All drainage today is ultimately to the south. Red dashed line indicates current location of the bedrock divide in the four NW valleys.*

M = McCoys Corners
E = Elliotts Mill
R = Rockville
P = Plain Grove

Modern day Wolf Creek (**Figure 6.4**) roughly coincides with the course of the large NE-SW buried valley from near its origin to McCoys Corners, where it diverges to the east. From there, the buried valley continues to the south-southwest, along approximately the same course taken by modern Jamison Run. The linear portion of the buried valley extends to the intersection with the southern of the four partly buried NW valleys, where joined the pre-glacial Slippery Rock Creek near Plain Grove, and flowed to the northwest.

The linear southwest-trending buried valley was the original course of Wolf Creek (**Figure 6.2**), flowing to its confluence with the NW-flowing pre-glacial Slippery Rock Creek (**Figures 6.2 and 6.3**). The SW orientation of the buried Wolf Creek valley was likely structurally controlled, because it is so linear and heads at the Henderson Dome, a diapiric intrusion of Reedsville Shale (Fettke, 1950, 1954, Kuminecz and Gorham, 1993) or a magmatic intrusion (Pees and Palmquist, 1985).

Because it has four well-developed bedrock valleys extending from the northwest side of original Wolf Creek, and none on the southeast side, I would interpret the four NW trending valleys to predate the original Wolf Creek valley, and were part of the pre-glacial drainage to the northwest. The original Wolf Creek valley was probably short-lived, because it was not in existence long enough for tributaries of any significant size to develop to the east side. Original Wolf Creek probably developed by stream piracy at the heads of the four NW-trending streams because of the relative ease of erosion of the structurally weakened rock. Whether that stream piracy occurred pre-glacially or as a result of glacier damming and glacial lake overflow is unknown.

The entire pre-glacial Slippery Rock system, including the original Wolf Creek, eventually diverted through a col near Rockville, which is now a significant narrowing of the Slippery Rock Creek valley (Valley Constriction on **Figure 6.2**), by glacier damming and lake overflow. This diverted the Slippery Rock drainage into the adjacent Muddy Creek drainage in the adjacent basin to the south, and then west toward New Castle and the Beaver River

After diversion of the Slippery Rock Creek through the Rockville col, Slippery Rock and original Wolf Creeks downcut enough that they captured part of the flow through the four NW-trending valleys. As it captured more of the flow, a divide in the bedrock between NW drainage and SE drainage into Wolf Creek developed in each valley, and migrated to the NW. Eventually, glacial deposition filled or partially filled the 4 NW valleys and the original Wolf Creek valley, terminating the bedrock erosion in the original Wolf Creek and tributary valleys. Since glacial retreat Slippery Rock Creek has continued to deepen its valley, and smaller streams have developed in the abandoned, buried bedrock valleys (**Figure 6.4**), developing divides on the glacial sediments at different locations than the underlying bedrock divides.

Proposed Sequence of Events

1. The original pre-glacial drainage was to the NW through the 4 valleys. The southern one was Slippery Rock Creek (**Figure 6.3**).
2. An advancing glacier dammed Slippery Rock Creek. Lake overflow at the Rockville col (Valley Constriction on **Figure 6.2**) diverted Slippery Rock Creek through the col into the Muddy Creek valley and west to New Castle (**Figure 6.2**).
3. Slippery Rock Creek continued to erode deeper. Stream piracy of the headwaters of the other three NW streams by headward migration along lineament formed the original Wolf Creek bedrock valley (**Figure 6.2**). Erosion of the Wolf Creek bedrock valley along the lineament could have occurred partly or completely pre-glacially, but likely after the Rockville col eroded and Slippery Rock Creek was diverted through it.

4. As the combined Slippery Rock-Wolf Creeks downcut, the four west side tributaries eroded along the pre-glacial bedrock valleys by headward migration, capturing part of the flow of the four NW streams, and creating cols in those bedrock valleys (**Figure 6.2**). Some of the headward migration could have occurred by glacial damming of the four NW streams, and lake overflow into the Wolf Creek valley, which now had an outlet to Slippery Rock Creek through the Rockville col.
5. Glaciation partly filled Wolf Creek and the four NW valleys, terminating the erosion in those bedrock valleys. Modern post-glacial streams developed in those valleys at higher levels (**Figure 6.4**).

While the relative sequence of events can be interpreted, we have insufficient data to determine when these events occurred. Radiocarbon dates of about 40,000 years from organic material in the upper 40 feet this core hole in the buried valley suggest that the valley was largely filled prior to the late Wisconsin glacial episode. But when the earlier events took place is unknown. The diversion through the Rockville col was likely during one of the earliest Pleistocene glaciations (MIS 22+, Braun, this volume).

Core Hole and Quarry

Key Points

- The quarry is located within a buried valley with glacial sourced sediments between 100 and 170 feet thick in the immediate area
- Sediment at 32 feet below ground surface at the quarry date between 41,000 BC and 46,000 BC
- The insect and pollen samples from 32 feet below land surface (bls) indicates a wetland environment in a spruce-dominant forest similar to those found currently in central Canada.
- The insect and pollen samples from 39 feet bls indicates a tundra environment similar to that of the North Slope of Alaska and the Canadian Arctic.
- The faunal and floral changes indicate climatic warming from the lower ft bls to 32 feet bls. The mean July temperature at 39.2 feet bls is estimated to be 11-12°C and at 32.0 ft bls 15-17°C compared to 21°C at Slippery Rock today. Representing deposition during a warming period (interstade)

The quarry at Reese Road is excavating Wisconsinan-aged, sand and gravel from till and glaciofluvial deposits. Drilling records from water wells indicate the sand and gravel operation is located on the western side of a buried valley (**Figure 6.5**). Northeast of the quarry the valley locally deepens preserving up to 170 feet of glacial drift.

In July 2020, the Pennsylvania Geological survey drilled a single sonic core that captured the entire glacial profile with depth of bedrock 118.5 feet bls (**Figure 6.6**). The core showed four intervals of sand, gravel, and till separated by three packages of silt and clay **(Figure 6.7)**. At 32 feet below land surface the quarry intersected a thin peat horizon. The peat contained sparse and disarticulated insect fragments including *Patrobus*, *Cytilus*, *Acidota*, and either *Enochrus* or *Cymbiodyta* (**Figure 6.7 and 6.8**). Along with the beetle remains, wood, moss, charcoal, fungal sclerotia, *Picea* (spruce) needles, *Salix* (willow) buds, *Carex* (sedge) achenes, and a *Viola* (violet) seed were recovered (**Table 6.1**). Pollen (n=664) and spores (n=14) compiled from two samples showed additional flora (**Table 6.2**). Comparing the pollen to modern day assemblages (Farley-Gill, 1980 and Lichti-Federovich, 1968), the biota from this peat indicates a wetland environment

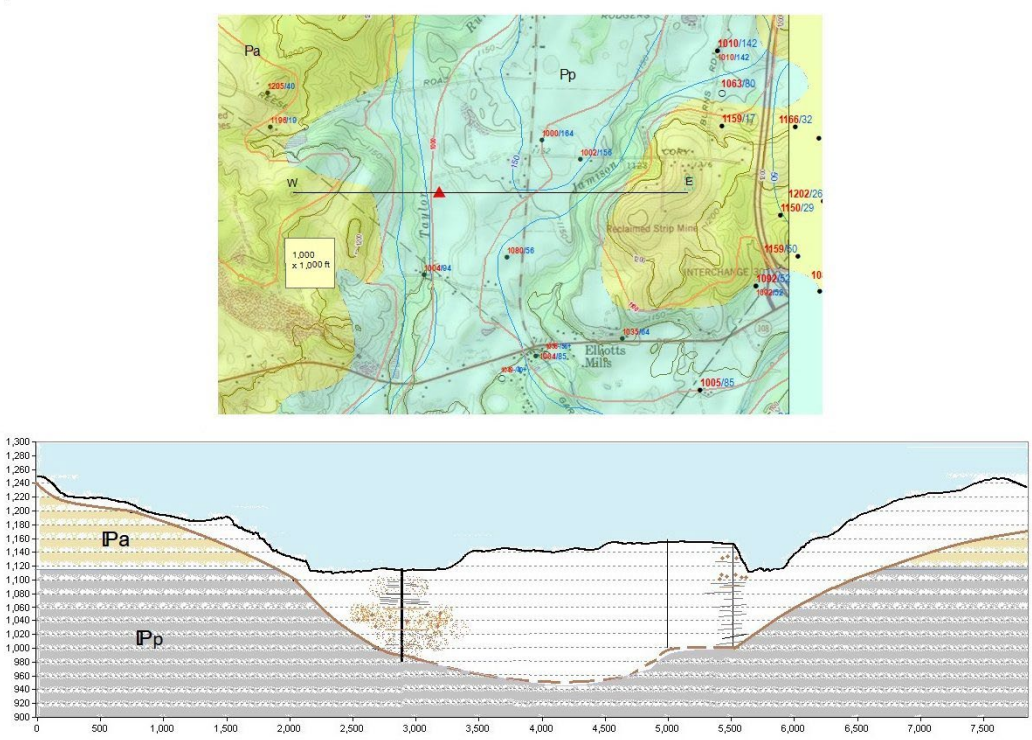

Figure 6.5. *Top - Geologic, bedrock topography, and drift-thickness map of the area of the core hole, LAW073_2360, Blue drift-thickness and red bedrock elevation contours from Reese et al (2022). Wells in the area noted with the bedrock elevation labeled in red and the drift thickness labeled in blue. Bedrock geology from Berg et al (1980). Pa = Allegheny Formation. Pp = Pottsville Formation. Bottom - Cross section showing location of core hole within the buried valley.*

(bog, fen, or lake shore) in a spruce-dominant forest similar to those found currently in central Canada. Two radiocarbon samples from this horizon have ages of 42,110±1280 BP (41,006 cal BC to 45,833 cal BC) and 42,190±1290 BP (41,029 cal BC to 45,938 cal BC) (Bierly et al, 2022).

At 39.2 ft bls, a ground beetle, *Blethisa catenaria*, was discovered in the core (**Figure 6.9**). Pollen from the interval was similar to that of the pollen assemblages at 32 feet. This biota assemblage suggests the sediment was deposited in a tundra-spruce environment similar to that today on the North Slope of Alaska and the Canadian Arctic (**Figure 6.10**). The only other record of this beetle was also found approximately 45 miles northeast of this quarry near Titusville, Pennsylvania (Cong et al, 1996). Radiocarbon dates from this site show similar ages to those found here at the quarry.

The faunal and floral changes indicate climatic warming from the strata at 39 ft (the interval containing *Blethisa catenaria*) to the strata at 32 ft (the peat zone). The mean July temperature at 39.2 ft bls is estimated to be 11-12°C and at 32.0 ft bls 15-17°C compared to 21°C at Slippery Rock today. These sediments represent deposition during the MIS 3 interstade.

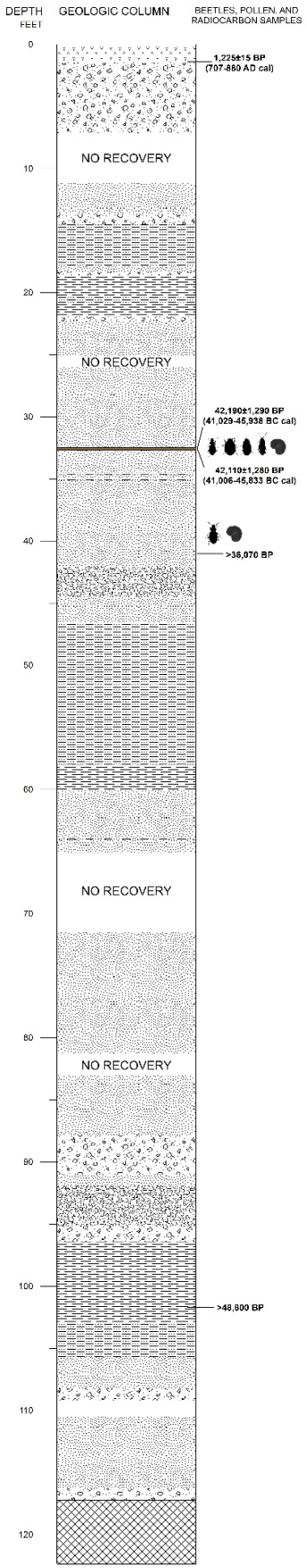

Figure 6.6. *(Left) Geologic Column. Geologic column of the entire glacial section constructed by nearby excavations (Figure 6.7) and sonic core (Archived at Pennsylvania Geological Survey, LAW073_2360). Column displays lithologies and stratigraphic position of beetle fossils, palynology analysis, and radiocarbon sampling. Calibrated radiocarbon dates used IntCal20: Northern Hemisphere (Reimer et al. 2020) with the OxCal 4.4 program.*

Photo A) Sample of peat excavated at 32 ft bls in sand and gravel mine. Radiocarbon dating reinforces that the excavated material and the core sample are from the same horizon with near identical dates. The peat horizon could not be seen at the base of the excavation as it submerged (below water table).

Photo B) Wing case of the beetle Patrobus *observed still in the matrix under microscope.*

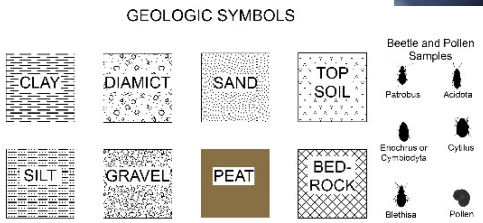

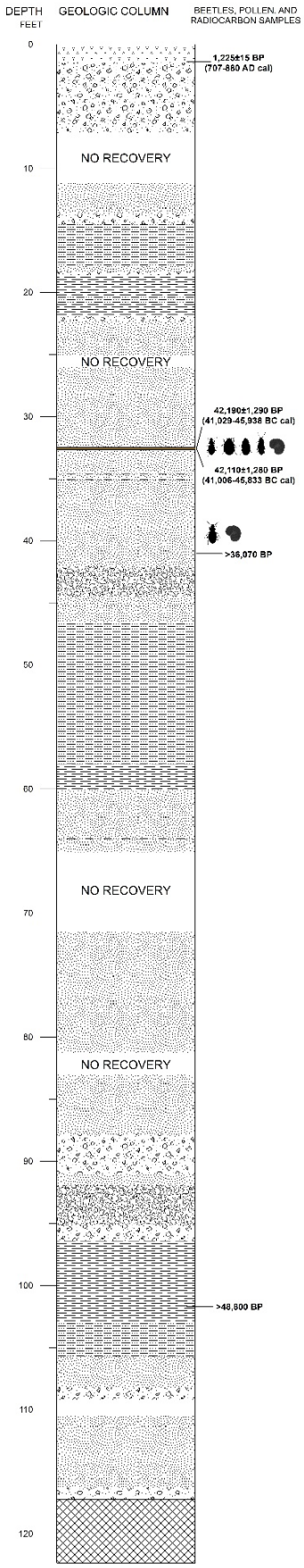

Figure 6.7. *Same geologic column as Figure 6.6 showing nearby outcrop deposits overlying the beetle-bearing deposits in the quarry. A) The approximate top 6 feet including the thick topsoil horizon (rock hammer rests on layer). A radiocarbon sample from the base of this soil dated 1225±15 BP. Underlying the soil is a till. B) The contact between glaciofluvial sand and gravel (above) and glaciolacustrine clay (below). The thickness of the exposed sand and gravel is between 6 and 8 feet. Yellow dashed lines marks contact between lithologies.*

Figure 6.8. *(Description continued on next page.)*

Patrobus

Beetle Size: 13 millimeters

A

B

Enochrus or Cymbiodyta

Beetle Size: ~5 millimeters

C

Black Scale Bars = 1 millimeter

(Fossil specimens only)

Acidota

Beetle Size: 4.7 millimeters

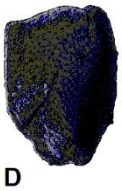

D

E

Cytilus

Beetle Size: ~5 millimeters

F

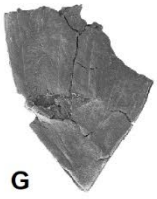

G

H

Figure 6.8. *(Continued from previous page) Scanning electron microscope images (in grayscale) of the fossil beetles from the silty peat interval at 32 feet bls with examples of modern-day specimens (in color) of each genus (may not be the same species as fossil specimens). All specimens from the 32 ft bls horizon were taken from peats samples from the spoil pile of the sand and gravel quarry. A. Left elytron of the groundbeetle,* Patrobus *(*Carabidae*). B. Right elytron of* Patrobus *C. Right elytron of the waterbeetle,* Enochrus *or* Cymbiodyta *(*Hydrohilidae*). D. Left elytron of a rove beetle (*Staphylinidae*), probably a small* Philonthinae*. E. Right elytron of a rove beetle* Acidota *(*Staphylinidae*). F. Fragment of a pronotum, probably the pill beetle* Cytilus *(*Byrrhidae*). G. Elytra fragment of* Cytilus*. H. Left elytron of* Cytilus*. Modern-day beetle images modified from photographs taken by Chris Rorabaugh (*Patrobus*), Alain Hogue (*Enochrus*), Tom Murray (*Acidota*), and Brandon Woo. SEM images of fossil beetles taken by Adam Ianno, Pennsylvania Geological Survey. All identifiable specimens listed above were found in excavated material (Not found in core).*

All of the identified genera are consistent with a well-vegetated lake margin. Generally, the assemblage is non-descript in terms of climate. The Acidota *elytron E is most similar to the species* Acidota subcarinata Erichson, *which is an eastern North American endemic with a range from the boreal forest on the Gaspé Peninsula in southern Canada to the Eastern Deciduous Forest in the Appalachians in Georgia. It has also been recorded from the alpine zone on Mt. Washington, New Hampshire.*

Beetle specimens are archived at the State Museum of Pennsylvania, Harrisburg, PA.

Table 6.1. Macrofossils from Core LAW073_2360.

Sample Depth (feet below ground surface)	*Picea* needle (Spruce)	*Salix* bud (Willow)	*Carex* achene (Sedge)	*Viola* seed (Violet)	Bud Genera Unknown	Wood	Moss	Charcoal	Fungal Sclerotia	Beetle remains
31.85-31.89	1	3	3	-	1	many pieces	several	several	10	-
32.03	1	1	-	1	-	many pieces	2	many pieces	17	1
32.4	-	1	-	-	-	many pieces	-	-	2	1

Macrofossils from Core LAW073_2360. Macrofossils observed in and near the peat horizon. Note the addition of two plant species not observed in the palynology as well as fungi. Also, evidence of fire occurring during deposition of peat based on the abundance of charcoal fragments.

Table 6.2. Pollen and Spore Count from LAW073_2360.

Sample Depth (feet below ground surface)	*Picea* (Spruces)	*Pinus* (Pines)	Poaceae (Grasses)	Cyperaceae (Sedges)	Asteroideae (Flowering Plants)	Cichoroideae (Flowering Plants)	*Huperzia selago* (Northern Firmoss)	*Selaginella selaginoides* (Northern Spikemoss)	Polypodiaceae (Ferns)
31.85-31.89	156	142	-	-	1	-	-	-	13
32.03	205	118	2	12	3	1	-	1	-
39.2	182	102	-	22	-	1	3	5	-

Pollen and Spore Count from LAW073_2360. Pollen and spore counts taken at the peat horizon (31.85-31.89 feet), directly below the peat horizon (32.03 feet), and at the interval where Blethisa catenaria *was discovered (39.2 feet). Unlike the modern-day eastern temperate forest of today, the peat horizon has a diversity of plant species common of that of a boreal wetland such as a treed fen. The 39.2 ft interval suggests a similar environment but the presence of* Blethisa catenaria *constrains the horizon's environment/climate to tundra or the tree line edge of the Taiga.*

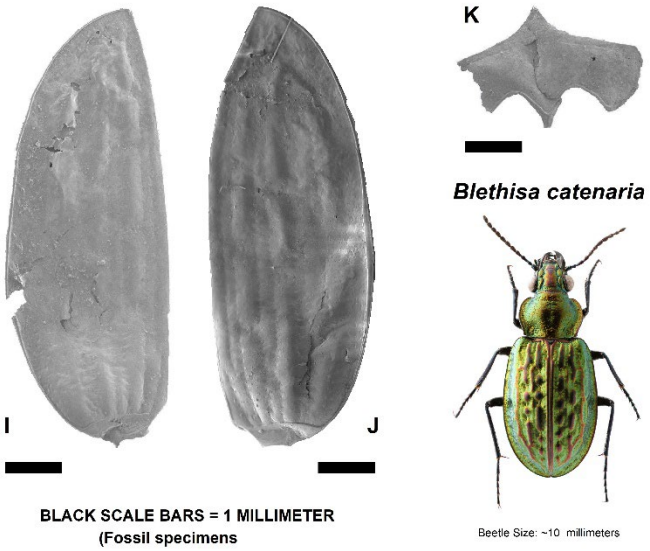

Figure 6.9. *(Left) Scanning electron microscope images of a single specimen of the fossil beetle,* Blethisa catenaria *Brown, from the sand interval at 39.2 feet bls with example of a modern-day specimen. I. Left elytron. J. Right elytron. K. Unidentified fragment. Modern-day beetle images modified from photograph taken by Dr. Henri Goulet. SEM images of fossil specimen taken by Adam Ianno, Pennsylvania Geological Survey. This specimen was found in the core.*
Blethisa catenaria *occurs in bog habitats. It is rarely collected probably because it appears to spend most of its time in saturated vegetation. It has a restricted arctic distribution occurring from the north slope of Alaska to Hudson Bay always occurring in tundra habitats. The mostly northwestern American range indicates this species was more widely distributed before the last glacial maximum.*

Beetle specimen is archived at the State Museum of Pennsylvania, Harrisburg, PA.

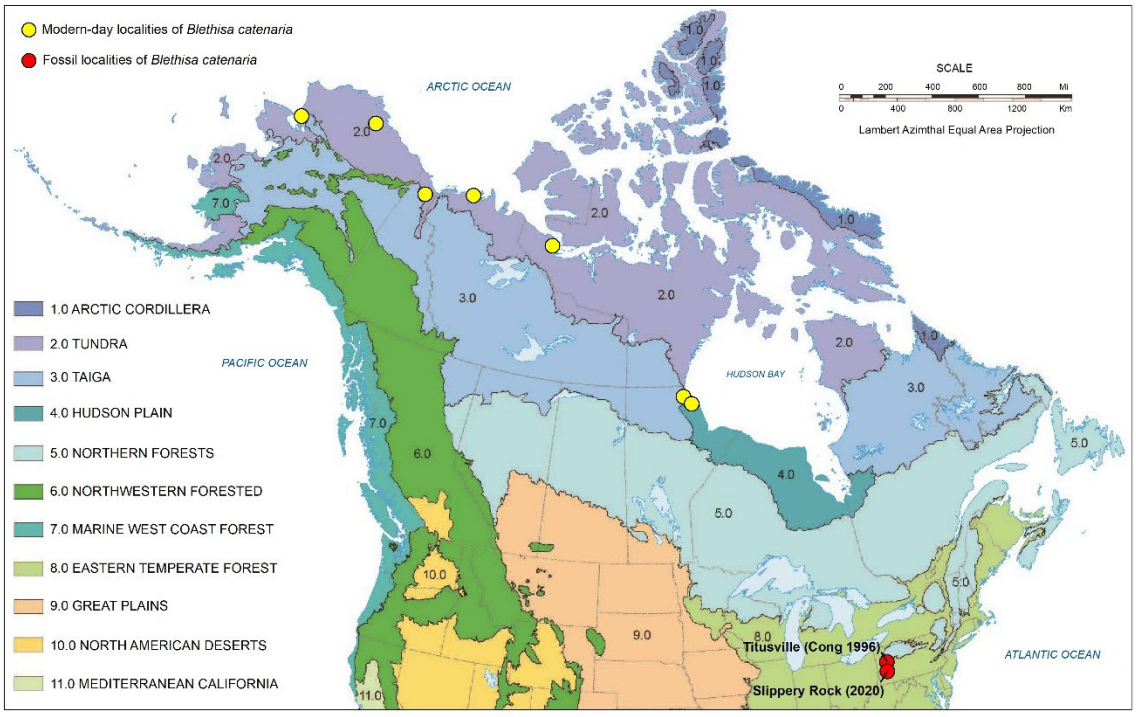

Figure 6.10. Blethsia *Range Map. Modified map of the ecological regions of North America (CEC 2007) displaying recorded observations of* Blethisa catenaria *with modern-day observations in yellow and fossil observations in red. Interestingly, the only other fossil locality this species is known from in North America is Titusville, PA (Cong et al, 1996). This makes the observation of* Blethisa catenaria *at the Three Rivers Aggregate Quarry near Slippery Rock currently the most southerly reported fossil observation of the species.*

References

Berg, T. M., Edmunds, W. E., Geyer, A. R., and others, compilers, 1980, Geologic map of Pennsylvania (2nd ed.): Pennsylvania Geological Survey, 4th ser., Map 1, 3 sheets, scale 1:250,000. [Available online.]

Bierly, A.D., Ashworth, A.C., Peteet, D.M., Davis, M.A., Culleton, B.J., 2022, Pleistocene beetles and plants from near Slippery Rock, Pennsylvania, from the Titusville Interstade (MIS 3): Northeastern Section Geological Society of America Abstracts with Programs, 2 plates, https://gsa.confex.com/gsa/2022NE/webprogram/Paper374435.html

Braun, Duane, 2022, Pleistocene Evolution of the Slippery Rock Creek Gorge, in, Dating in the Pleistocene, Field Conference of Pennsylvania Geologists, Titusville, PA, pp. ____.

CEC, 2007, Ecological regions of North America, Level 1, Commission of Environmental Cooperation, 1 plate, https://www.epa.gov/eco-research/ecoregions-north-america

Cong, S., Ashworth, A. C., Schwert, D. P., Totten, S. M., 1996, Fossil Beetle Evidence for a Short Warm Interval near 40,000 yr B.P. at Titusville, Pennsylvania, Quaternary Research: vol. 45, p. 216-225

Farley-Gill, L.D., 1980, Contemporary pollen spectra in the James Bay Lowland, Canada, and comparison with other forest-tundra assemblages, Géographie physique et Quaternaire, vol. 34, no. 3, p. 321-334.

Fettke, C. R. (1954), Structure-contour maps of the plateau region of north-central and western Pennsylvania, Pennsylvania Geol. Survey, 4th ser., Bull. G-27, 27 p.

Fettke, CR (1950) Henderson dome, a unique structure in northwestern Pennsylvania [abs], Geological Society of America Bulletin, v. 61, no. 12, pt. 2, p. 1458

Iowa State University Department of Entomology, [2022], BugGuide.Net, [Accessed March 9, 2022], https://bugguide.net/node/view/15740

Kuminecz, C.P. and Gorham, S.B., 1993, Henderson Dome: A hydrocarbon producing, basement-involved structural anomaly of the Coshocton zone, Mercer County, western Pennsylvania, in Catacosinos, P. and others, conveners, Basement and basins of eastern North America: American Association of Petroleum Geologists Hedberg Reasearch Conference Proceedings [Ann Arbor, MI, Nov. 10-13,1993], 2 p.

Lichti-Federovich S. and Ritchie, J.C., 1968, Recent pollen assemblages from the western interior of Canada, Review of Palaeobotany and Palynology, vol. 7, no. 4, p. 297-345

Pees, S.T. and J.C. Palmquist, (1985) Lineaments, geophysical and subsurface anomalies, resurgent basement block, and oil and gas in Mercer Co, NW Pennsylvania, GSA Abstracts with Programs, v. 14?, no. 1?, p. 58.

Poth, CW (1963) Geology and hydrology of the Mercer quadrangle, Pennsylvania, Pennsylvania Geological Survey, 4th series, Water Resource Report 16

Reese, S. O., Fleeger, G. M., and Schagrin, Z. C., 2022, Bedrock-topography and drift-thickness maps of the Edinburg, Harlansburg, New Castle North, and Slippery Rock 7.5-minute quadrangles, and Pennsylvania part of the Campbell 7.5-minute quadrangle, Butler, Lawrence, and Mercer Counties, Pennsylvania: Pennsylvania Geological Survey, 4th ser., Open-File Report OFSM 22–01.0, 7 p., 4 pls., scale 1:24,000, geodatabase. [Available online.]

Reimer, P., Austin, W., Bard, E., Bayliss, A., Blackwell, P., Bronk Ramsey, C., Butzin, M., Cheng, H., Edwards, R., Friedrich, M., Grootes, P., Guilderson, T., Hajdas, I., Heaton, T., Hogg, A., Hughen,

K., Kromer, B., Manning, S., Muscheler, R., Palmer, J., Pearson, C., van der Plicht, J., Reimer, R., Richards, D., Scott, E., Southon, J., Turney, C., Wacker, L., Adolphi, F., Büntgen, U., Capano, M., Fahrni, S., Fogtmann-Schulz, A., Friedrich, R., Köhler, P., Kudsk, S., Miyake, F., Olsen, J., Reinig, F., Sakamoto, M., Sookdeo, A., & Talamo, S. (2020). The IntCal20 Northern Hemisphere radiocarbon age calibration curve (0–55 cal kBP). Radiocarbon, 62.

Point of Interest: There is disagreement on how Slippery Rock Creek was named, but most stories agree that this name was taken from the Seneca Native Americans. Slippery Rock, or *Wechachapohka* in Iroquoian, was likely named for a natural oil seep that resulted in particularly slippery rocks.

POI Sources:

Slippery Rock Heritage Association, Inc., 2016, The Story Behind the Name, https://srheritage.org/the-story-behind-thename/.

Pennsylvania Department of Conservation and Natural Resources, n.d., History of McConnells Mill State Park, https://www.dcnr.pa.gov/StateParks/FindAPark/McConnellsMillStatePark/Pages/History.aspx.

POI Figure Source:

Merrilove, 2016, McConnel's Mills covered bridge over Slippery Rock Creek, https://commons.wikimedia.org/wiki/File:McConnel%27s_Mills_covered_bridge_over_Slippery_Rock_Creek.jpg.

STOP 7: MCCONNELLS MILL
AND THE SLIPPERY ROCK GORGE

GARY M FLEEGER – PENNSYLVANIA GEOLOGICAL SURVEY (RETIRED)

DUANE D. BRAUN – PROFESSOR EMERITUS, BLOOMSBURG UNIVERSITY OF PENNSYLVANIA

MICHAEL SIMONEAU – VERINA CONSULTING GROUP, LLC AND LEHIGH UNIVERSITY

FRANK J. PAZZAGLIA – LEHIGH UNIVERSITY

GARY J. D'URSO

40.95167 / -80.168279

Introduction

This stop will discuss the origin of the Slippery Rock Gorge and the cosmogenic ages obtained from various parts of the gorge. **Figure 7.1** identifies various features mentioned in the discussion.

The geology and glacial origin of the Slippery Rock Gorge has been discussed in numerous publications for more than 100 years (Leverett, 1902; Preston, 1950; Shepps and others, 1959; Peck and Deere, 1964; Preston, 1977; Fleeger, 1984; D'Urso, 2000; Fleeger et al, 2003; D'Urso, 2004; Fleeger et al, 2011; Braun, 2022). The reader is referred to these reports for details.

We saw at **Stop 6** how Slippery Rock Creek was diverted into the Muddy Creek watershed between the divides at Rockville and Cleland Rock. Now we will further evaluate how the Slippery Rock Gorge was created, diverting Slippery Rock Creek into the Connoquenessing watershed, south of the Cleland Rock divide.

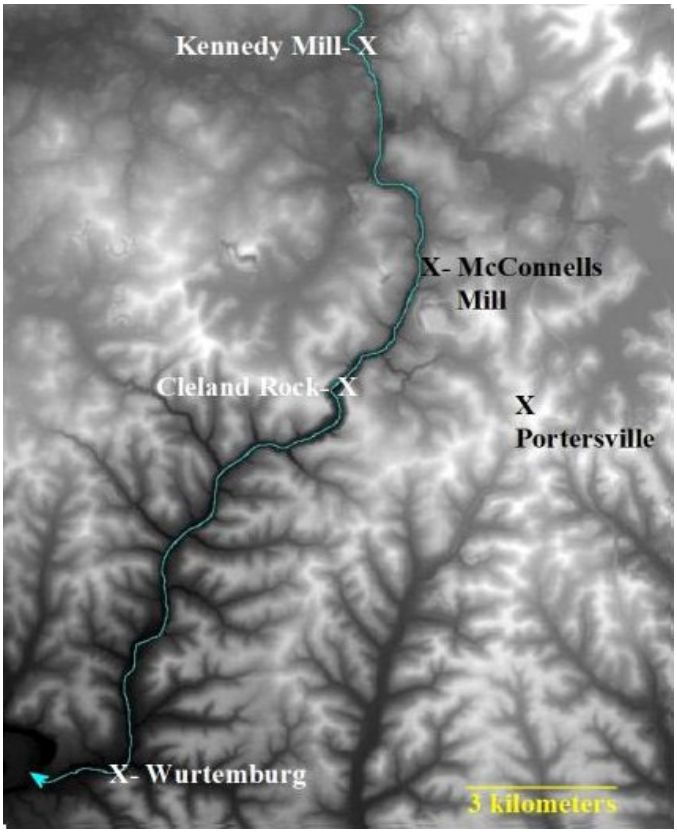

Figure 7.1. *Lidar DEM of Slippery Rock Gorge area*

Slippery Rock Gorge – the topographic setting

The Slippery Rock Gorge is about 12 miles long, extending from Kennedy Mill to Wurtemburg, where it enters Connoquenessing Creek (**Figure 7.1**). Slippery Rock Creek at Kennedy Mill turns its course southward into the gorge (**Figures 7.2 and 7.3**) from its broad northeast- southwest valley (**Figure 7.4**). The upstream part of the bedrock gorge, the Kennedy gorge, is bracketed by non-bedrock reaches and is broken into two parts by a 1000 ft. long non-bedrock reach at the Muddy Creek confluence (**Figure 7.2**). A 1500-ft long non-bedrock reach at Rose Point separates the lower Kennedy gorge from the rest of the Slippery Rock Gorge that continues past McConnells Mill (**Figure 7.2**).

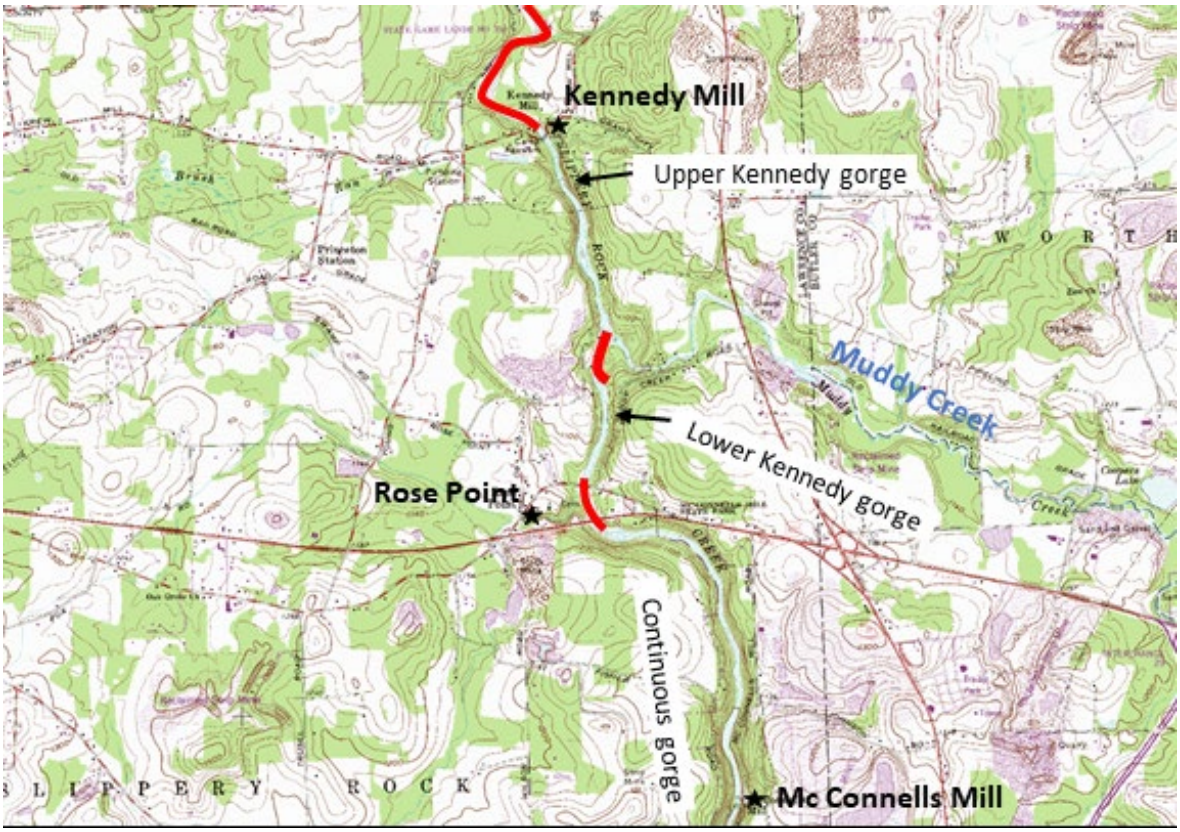

Figure 7.2. *The upper segmented Slippery Rock Creek gorge from Kennedy Mill to Mc Connells Mill. Segments with no bedrock in red.*

Figure 7.3. *Photo of Slippery Rock Creek looking downstream into the Kennedy gorge at the head of the Slippery Rock Gorge. Photos in Figures 7.3 and 7.4 were taken from the same spot.*

Figure 7.4. *Photo of Slippery Rock Creek looking upstream at the head of the Slippery Rock Gorge. Photos in Figures 7.3 and 7.4 were taken from the same spot. This view marks the location of the upper non-bedrock reach shown in Figure 7.2.*

The main continuous part of Slippery Rock Gorge deepens from Rose Point, past McConnells Mill, to a maximum depth of 400 ft at Cleland Rock (**Figure 7.5**). What is deepening is an inner narrow very steep sided gorge with a wider less steeply sloping valley form rising above the inner gorge (**Figure 7.6**). At Cleland Rock there is only a narrow steep-sided gorge. South or downstream from Cleland Rock the inner gorge becomes progressively less deep towards Wurtemburg. Tributary valleys to either side of the main gorge themselves have inner gorges that abruptly shallow upstream above knickpoints that are often waterfalls. The last few miles to Wurtemburg, the less steeply sloped valley sides above the inner gorge widen markedly with

broad strath terraces on one or both sides of the inner gorge. The average stream gradient through the gorge is about 20 ft/mile, with the steepest section from McConnells Mill to Cheeseman Run, having a 40 ft/mile gradient.

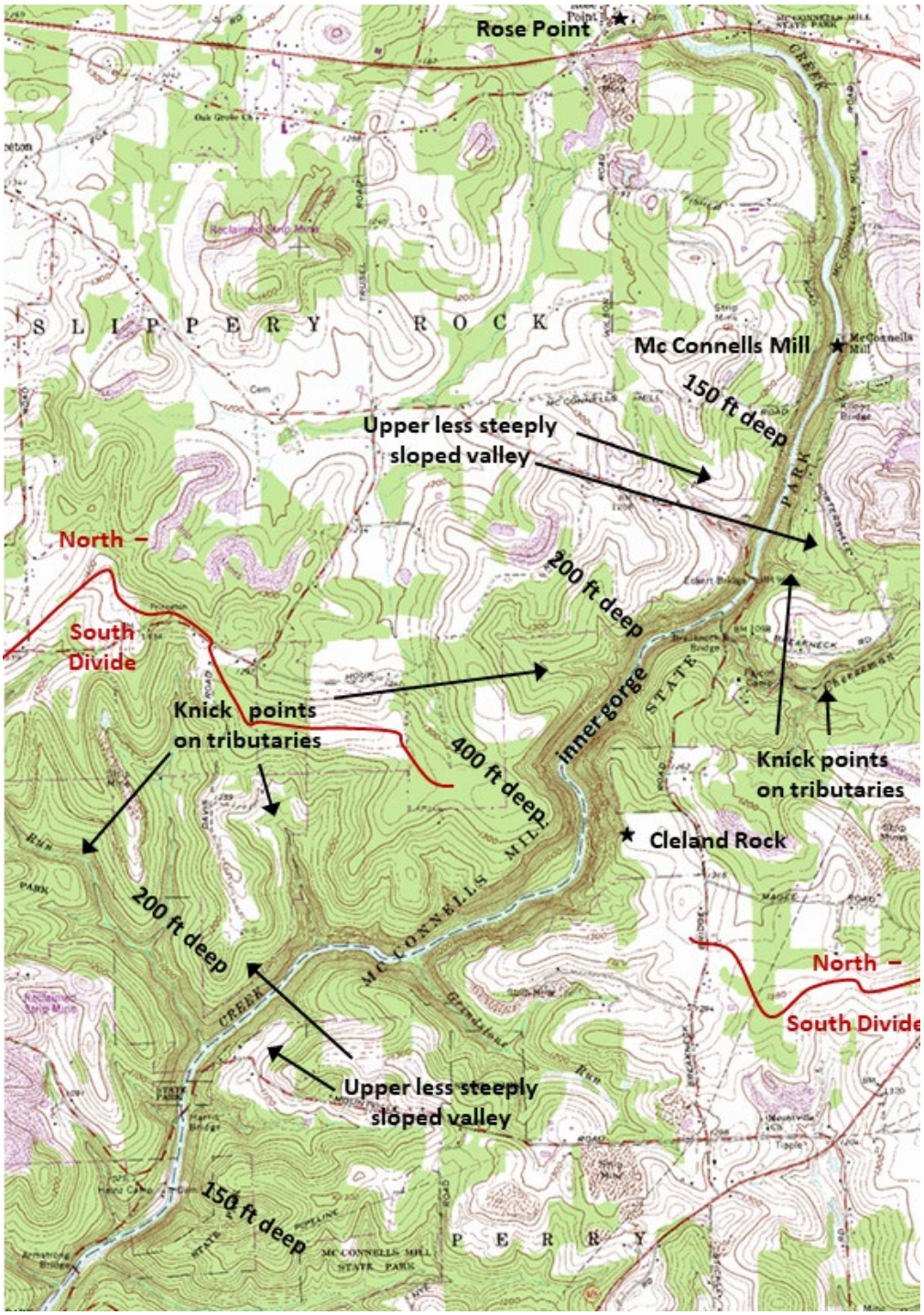

Figure 7.5. *Slippery Rock Gorge, a narrow steep sided inner gorge with a wider less steeply sloped valley above. Deepest at Cleland Rock and becoming less so to either side of that.*

Evidence of Glacial Drainage Diversion – The landform of the Slippery Rock Gorge

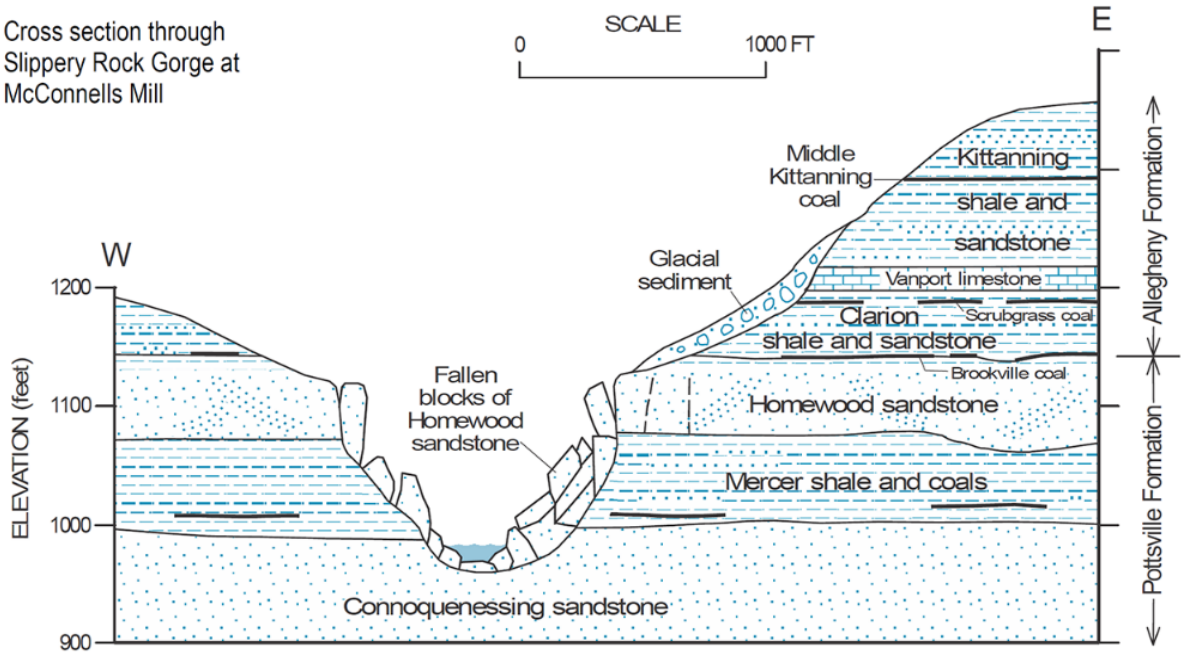

Figure 7.6. *Cross section of the Slippery Rock Gorge at McConnell's Mill showing major rock units. The steep inner gorge at the mill is in the Homewood Sandstone, the Mercer Shale, and the Connoquenessing Sandstone. The outer gorge here is in the Allegheny Formation. From Fleeger et al (2003).*

As noted above, the Slippery Rock Gorge has an inner narrow steep gorge with upper less steeply sloped sides (**Figures 7.5 and 7.6**). The inner gorge deepens downstream to a point that is a regional north-south divide on streams adjacent to Slippery Rock Creek. Then the inner gorge declines in deepness continuing downstream to its confluence with Connoquenessing Creek. This maximum deepness at a regional divide is the topographic signature of a breached divide. It is the same topographic form that is seen at the other major divide breaches on Oil Creek, upper Allegheny River, Pine Creek, and other such sites in Pennsylvania. At all these sites, a northwest or northeast drainage system is blocked by an advancing glacier. First proglacial lake drainage starts notching a preexisting col in a divide, then the glacier approaches and sends sediment laden meltwater over the col, and then on retreat a final proglacial lake drains across the col to finish that glacial advance's cutting. The four glacial advances (Braun, 2011) have a record of having collectively cut down the divide to where it is today.

Valleys Cut Below the Level of the Upper Segmented Slippery Rock Gorge (Kennedy Gorge)

The key to identifying the Slippery Rock Gorge being a glacial diversion centers on the northern segmented part of the gorge, the Kennedy Gorge. The three non-bedrock reaches of the gorge (**Figure 7.2**) mark where the drainage was cut below the level of the present gorge. Well data (Fleeger, ongoing work) shows that those three reaches form a west draining system of buried channels that are eroded below the gorge level (**Figure 7.7**). Those channels must predate the cutting of the shallower present bedrock Slippery Rock Gorge and confirm Mc Connell Run drained north from the Cleland Rock divide.

The segment of the gorge from the sharp bend near Rose Point upstream to Kennedy Mill (Kennedy gorge; Preston, 1977; **Figure 7.7**) does not follow the course of pre-glacial McConnell Run. Rather, it is an ice-marginal channel eroded between the glacier to the west and the bedrock

hill to the east (**Figure 7.8**), probably during the outburst flood draining of Lake Edmund during glacier retreat. The Kennedy gorge joins the preglacial course of McConnell Run at Rose Point. In the middle of the Kennedy gorge, Muddy Creek enters the gorge from the east over a waterfall in a hanging valley. This was the location of the final drainage of glacial Lake Watts (Preston, 1977). The final drainage of Lake Edmund also passed through this gorge, eroding the Kennedy gorge and leaving Muddy Creek hanging.

Pre-glacial Muddy Creek crossed this location at the middle non-bedrock reach (**Figure 7.2**) of Kennedy gorge, and continued west, being joined by McConnell Run, and then by the early Pleistocene course of Slippery Rock Creek to form the Muddy – Slippery Rock Creek (Braun, this guidebook, **Figure 7.5**). That westward course is now partially buried and occupied by Brush and Big Runs. Sandstone ledges exist north and south of the confluence of modern Muddy and Slippery Rock Creeks. TCN sample GN was taken from the ledge north of Muddy Creek (**Figure 7.7**). Kennedy gorge bisects the buried, pre-glacial Muddy Creek valley, so Muddy Creek was eroded and buried prior to the erosion of the Kennedy gorge. Where the buried Muddy Creek valley crosses the gorge today, the bedrock ledges end, the gorge widens, and glacial sand and gravel exist to about 1010 feet elevation, about 20 feet below the bottom of the present gorge (**Figure 7.7**).

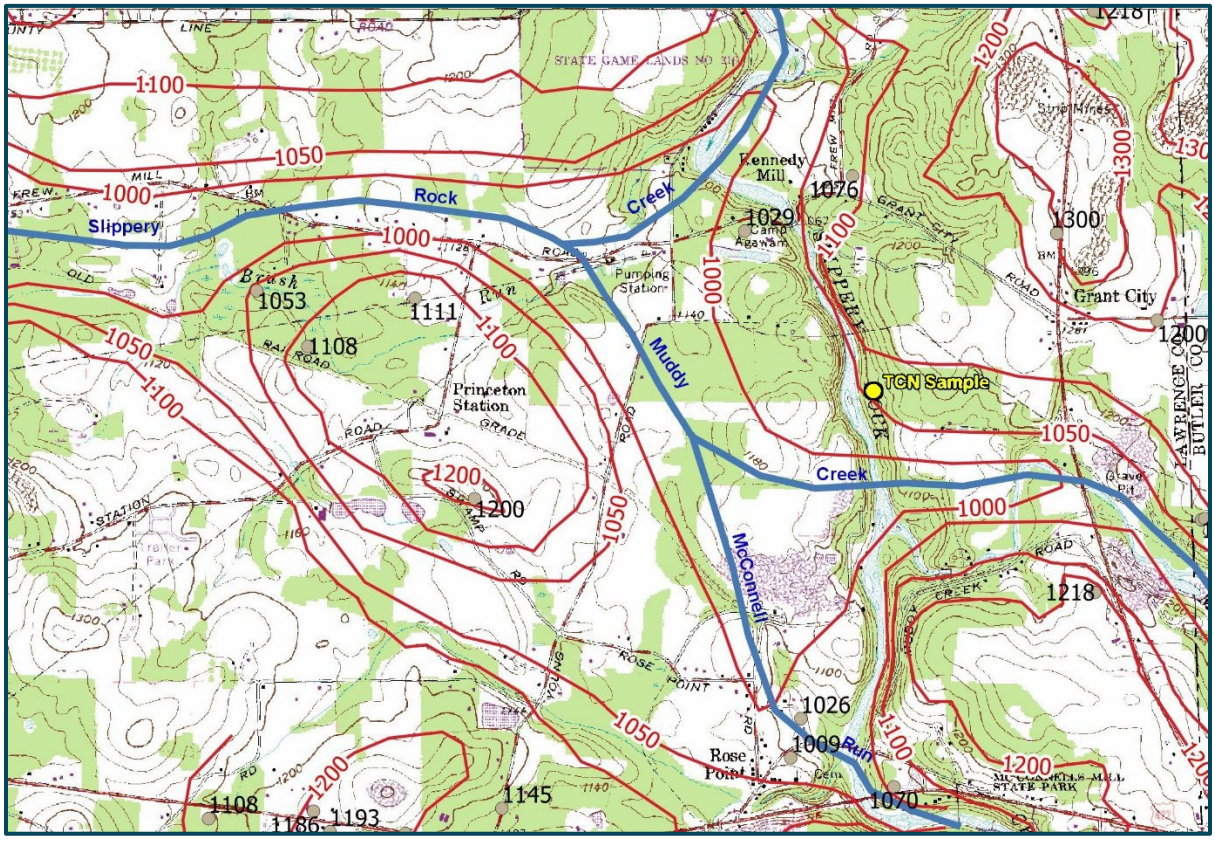

Figure 7.7. *Bedrock topo map of Kennedy gorge, buried Muddy Creek, McConnell Run, and early Pleistocene Slippery Rock Creek. Location of the TCN sample (27,142 ± 1055 years) noted. Each of the 3 places where a bedrock valley crosses current Slippery Rock Creek coincides with the 3 non-bedrock reaches in Figure 7.2.*

Because the Kennedy gorge does not follow the course of McConnell Run, it did not form by the upstream migration of the Cleland Rock col (whether by lake overflow or by stream piracy). The col currently exists near Rose Point from which the buried lower McConnell Run valley descends to the northwest from the southern non-bedrock reach (**Figure 7.2**) of the gorge, and

the current Slippery Rock Creek flows south through the former upper McConnell Run valley (**Figure 7.7**). Kennedy gorge need not have been eroded at the same time as the rest of the Slippery Rock Gorge. But it had to be the last part of the Slippery Rock Gorge to form, because there had to be an outlet to the south. The Muddy - Slippery Rock Creek outlet to the northwest was filled prior to the Kennedy gorge erosion. It could have occurred during different glaciations, or during the same glaciation (filling the Muddy Creek valley during the advance, and eroding the Kennedy gorge during the retreat). The 10Be-derived date from the top of the Kennedy gorge (27,142 ± 1055) is older than the Kent glaciation terminus (about 20 - 25 ka at the West Liberty delta, Stop 9). So this gorge was initiated either upon the retreat of the Illinoian glacier or was initiated as Kent ice advanced toward its terminus. The Kennedy gorge is similar in appearance to the rest of the inner Slippery Rock Gorge through the Cleland Rock divide, suggesting that they both have their near final form carved during late Illinoian (Titusville) to late Wisconsinan (Kent) time.

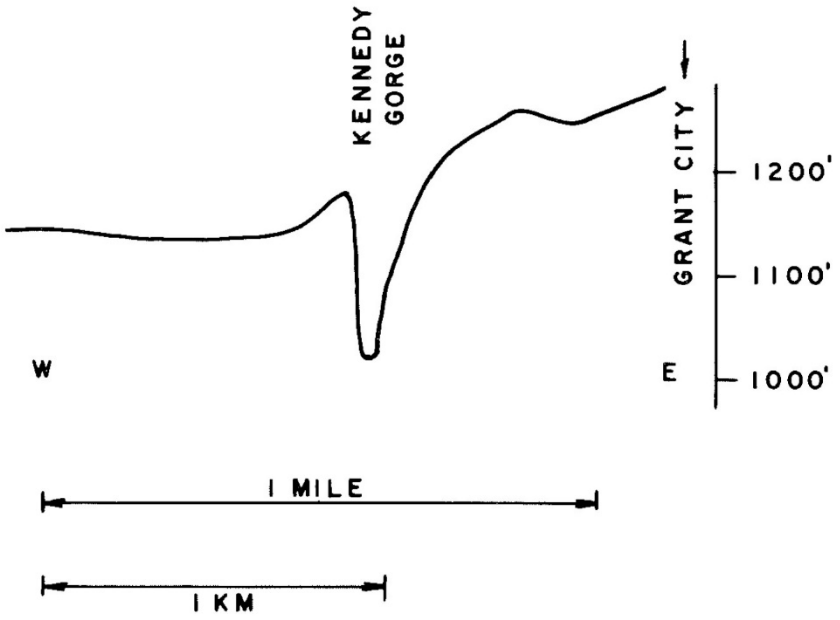

Figure 7.8. *Topographic section of the Kennedy gorge, looking north. From (Preston, 1977).*

The overall preglacial – early Pleistocene drainage pattern in the area of the present Slippery Rock Gorge is marked in blue on **Figure 7.9**. The LiDAR image vividly shows the preglacial dendritic pattern to either side of the Cleland Rock divide. The col or saddle at Cleland Rock must have been slightly lower than other adjacent cols along the divide and that permitted the proglacial lake in the Muddy Creek valley to first spill over there and initiate the Slippery Rock Gorge.

Terrestrial Cosmogenic Nuclide (TCN) dating in the gorge.

We attempted to use TCN to better constrain the age of the Slippery Rock Gorge. Simmoneau et al (2022) discuss the TCN dating technique used in the gorge. Five TCN samples were collected from the walls of SRG to generate an age and erosion rate model of the gorge. When collecting the TCN samples, areas were chosen to represent the top, middle and bottom of the gorge at different locations along the long profile (**Figures 7.10 and 7.11**). Four of these samples, MM1-MM4 were collected in October, 2018. The first two samples, MM1 (**Figure 7.12**) and MM2 were taken very near McConnell's Mill near the top lip of the inner gorge on Homewood sandstone, while MM2 (**Figure 7.13**) was taken about 10 – 15 feet above the present streambed at the right abutment of the mill dam on a bed of the Connoquenessing sandstone. The third sample, MM3 was collected from the proposed Lake Prouty outlet slot canyon beneath Breakneck Bridge, whereas the fourth sample, MM4 was taken at a mid-canyon level along the west bank, near Armstrong Bridge, in the downstream part of the gorge. A fifth sample, GN, was taken at a mid-canyon level in the Homewood sandstone in the Kennedy gorge in Nov, 2018.

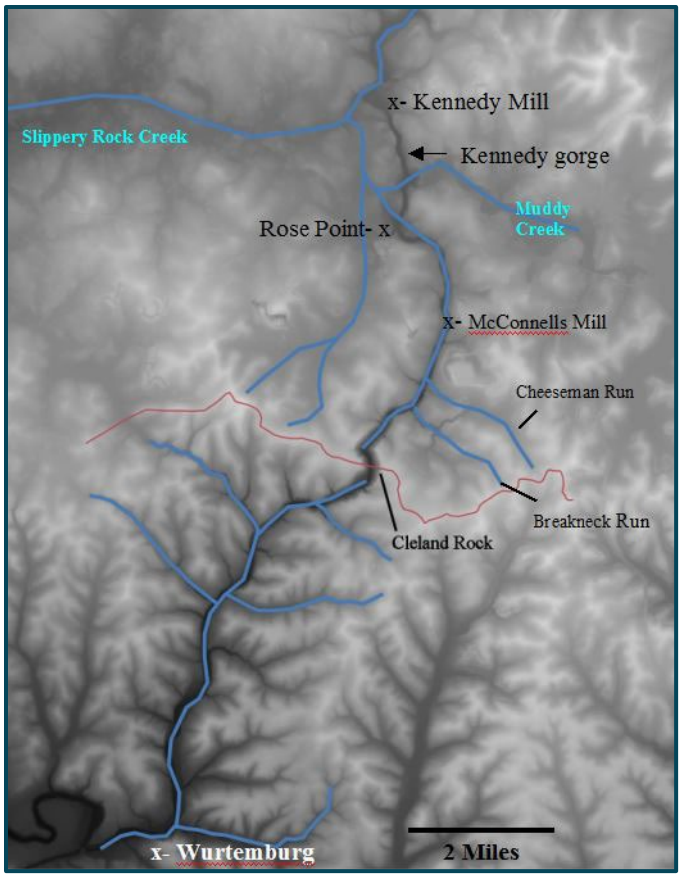

Figure 7.9. *Lidar DEM of Slippery Rock Gorge area. The red line indicates the pre-diversion divide at Cleland Rock. The Blue lines show the preglacial stream pattern with the course of McConnell Run flowing north past McConnells Mill, and Wurtemburg Run flowing south past Wurtemburg from the divide. McConnell Run diverged from the current course of Slippery Rock Creek at Rose Point to join Muddy Creek. Kennedy gorge, between Kennedy Mill and Rose Point, crosses the now-buried Muddy Creek valley.*

Using surface erosion rates of zero, the maximum TCN exposure ages in SRG range from ~1.7±0.3 ka for sample MM2 collected at river level at McConnells Mill to 27±2.5 ka collected for sample GN in a mid-gorge position in the Kennedy gorge. In general, the exposure ages are all LGM in age, young towards the river and young downstream (**Fig. 7.11**). The steady-state erosion rates for the four TCN samples is highest at 500±90 m/Myr for sample MM2 and 30±3 m/Myr for sample GN (See **Table 7.1,** Simoneau, Pazzaglia and Fleeger article on Pleistocene Drainage Reversals, this guidebook). All of the calculated steady-state erosion rates for these exposed bedrock samples are unrealistically high in comparison to others measured in western PA (Pazzaglia et al., 2021) and in the Appalachians (Hancock and Kirwan, 2007; Portenga et al., 2013), which typically report steady-state erosion rates < 5 m/Myr. The young exposure ages and corresponding high steady state erosion rates may have resulted from a sample collection strategy to find and sample fresh, rather than obviously weathered surfaces. Insofar that the fresh surfaces sampled represent a recent process to remove more weathered material, such as

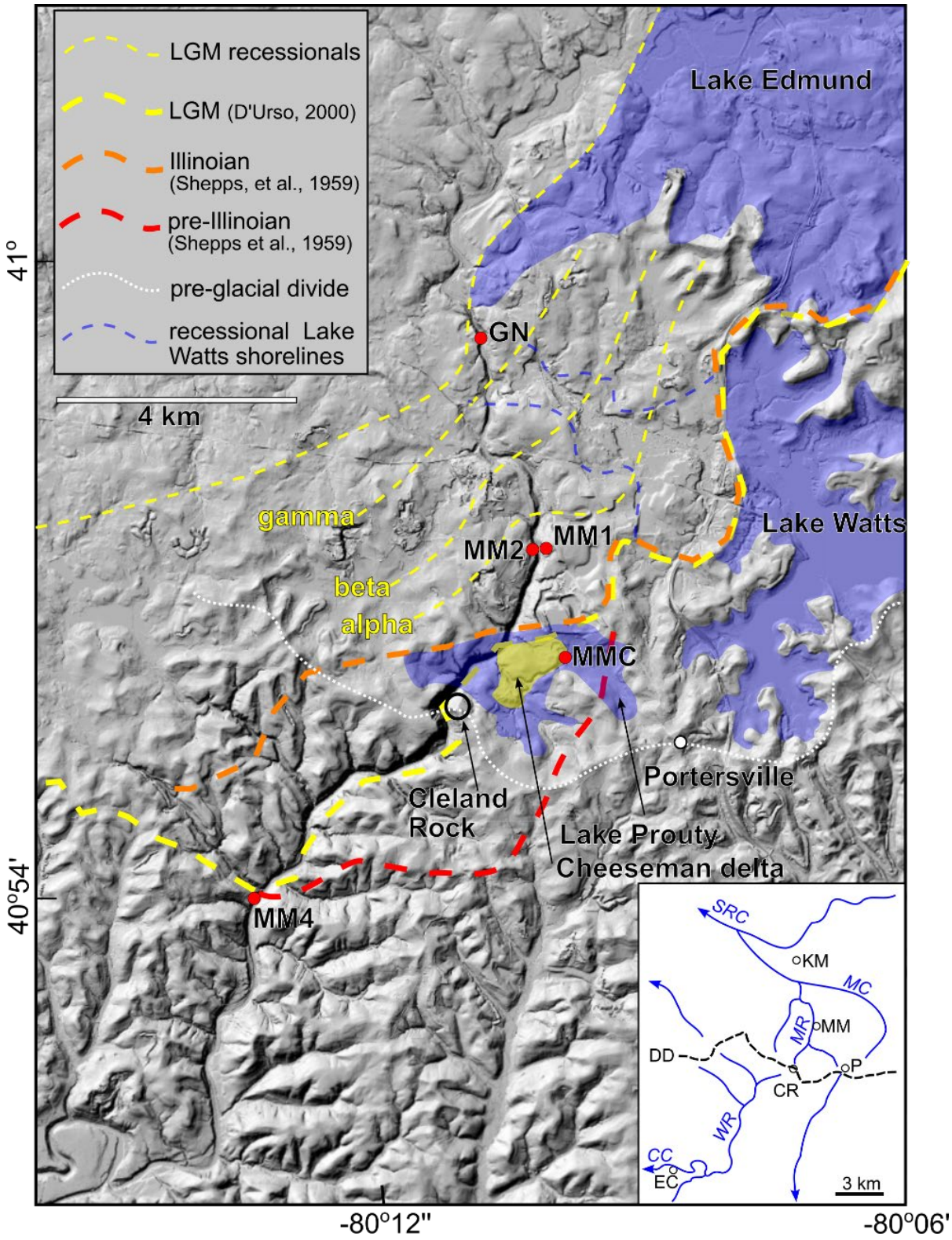

Figure 7.10. *. Shaded relief topographic map showing major geomorphic features of the SRG region, and the locations of the one luminescence (MMC) and four cosmogenic sample locations (MM1, MM2, MM4, and GN). Inset map showing the general, pre-SRG drainage (From Fleeger et al., 2003).*

rockfalls or slumps, then the TCN ages and erosion rates indicate where these processes are active in the SRG.

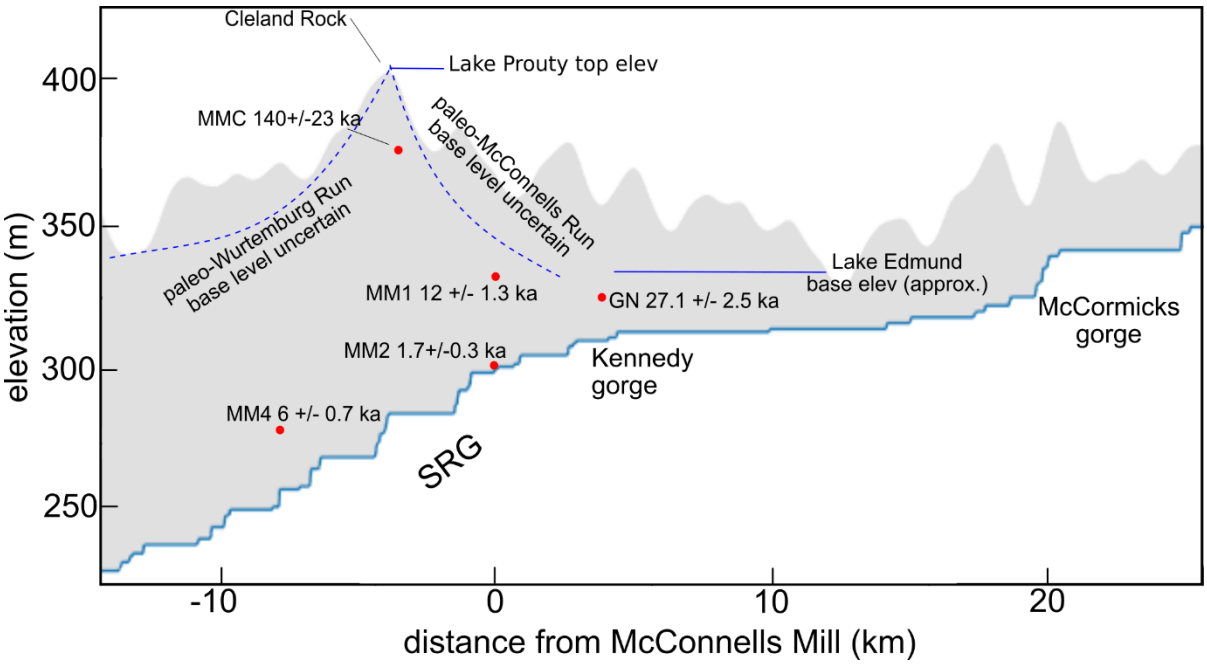

Figure 7.11. *Projection of numerically dated exposure age (MM1,MM2, MM4, and GN) and burial age (MMC) on the long profile and hillslope swath profile of the Slippery Rock Gorge reach.*

Taken at face value, the TCN exposure ages would argue that SRG is a very young feature, having been carved in the late Pleistocene-Holocene perhaps in response to the LGM glaciation. Alternatively, the TCN data can be interpreted as late Pleistocene-Holocene re-freshening of older existing gorge walls and valley bottom. There are other, plausible explanations for the TCN exposure ages that may have origins in multiple generations of SRG formation, the transient laying back of the SRG knickzone, or complicated exposure histories that include times of SRG burial and re-exhumation. SRG could be much older than the LGM or Illinoian glaciation, with the TCN exposure ages simple reflecting these complicated exposure histories, further modified by active, but unsteady hillslope and fluvial processes that periodically refresh rock surfaces. The TCN data also do not help in determining the scale of the Pleistocene glacial and/or interglacial discharges that have cut SRG.

IRSL luminescence age of 140±23 ka in the 1240 ft elevation Cheeseman delta would indicate an Illinoian age proglacial lake, presumably the Lake Prouty of Preston (1977), was able to flow south across the Cleland Rock divide at that time. The Cheeseman delta though is separated from the Cleland Rock divide first by a bedrock gorge and then other glacial-fluvial deposits before it reaches SRG itself. The Cleland Rock divide may have already been cut well below the 1250 ft elevation of the Cheeseman delta and post Illinoian knickpoint recession up the Cheeseman channel from SRG has carved the present gorge of Cheeseman Run. At minimum, the Cheeseman delta indicates significant breaching of the Cleland rock divide and development of SRG by late Illinoian time.

Figure 7.12. *Photo of Homewood sandstone sampled at MM1.*

Figure 7.13. *Photo of sandstone sampled at MM2, illustrating the depth of sampling and the surface characteristics of the sandstone.*

Table 7.1. A) TCN lab and AMS analysis results. B) Modeled TCN ages.

A

Sample Name	Quartz Mass (g)	Mass of ^{9}Be Added (µg)*	AMS Cathode Number	Uncorrected 10Be/9Be Ratio**	Uncorrected 10Be/9Be Ratio Uncertainty**	Background-Corrected 10Be/9Be Ratio	Background-Corrected 10Be/9Be Ratio Uncertainty	10Be Concentration (atoms g-1)	10Be Concentration Uncertainty (atoms g-1)
SRY-MM1	20.0331	250.5	157214	6.124E-14	3.707E-15	5.599E-14	3.834E-15	4.678E+04	3.204E+03
SRY-MM2	20.0948	250.4	157215	1.532E-14	1.370E-15	1.007E-14	1.682E-15	8.384E+03	1.400E+03
SRY-MM4	20.1610	249.9	157216	3.125E-14	1.992E-15	2.600E-14	2.218E-15	2.153E+04	1.837E+03
SRY-GN	20.1343	251.0	157213	1.801E-13	6.533E-15	1.749E-13	6.605E-15	1.456E+05	5.501E+03

*9Be was added through a carrier made at University of Vermont with a concentration of 304 µg mL-1.

**Isotopic analysis was conducted at PRIME Laboratory; ratios were normalized against standard 07KNSTD3110 with an assumed ratio of 2850 x 10-15 (Nishiizumi et al., 2007).

B

Sample Name	Lat	Long	Elev (m)	sample thickness (cm)	sample density (g/cm^3)	Topographic shielding (no shielding = 1)	Standard model age for no erosion (yrs)	Internal* uncertainty (yrs)	External* uncertainty (yrs)	Steady-state erosion rate (m/Myrs)	Internal* (measurement) uncertainty (m/Myrs)	External* (total) uncertainty (m/Myrs)
SRY-MM1	40.95321	-80.16933	335	2	2.5	0.694	**12006**	833	1271	**71**	5	7
SRY-MM2	40.95327	-80.17049	300	2	2.5	0.91	**1684**	282	312	**498**	83	92
SRY-MM3	40.93748	-80.17846	326	2	2.5							
SRY-MM4	40.90395	-80.22487	274	2	2.5	0.645	**6044**	519	707	**148**	13	17
SRY-GN	40.98541	-80.18093	325	2	2.5	0.986	**27142**	1055	2445	**29**	1	3

* Reported as 2σ uncertainties

References

Braun, D.D., 2011, The Glaciation of Pennsylvania, USA. In J. Ehlers, P.L. Gibbard and P.D. Hughes, editors: Developments in Quaternary Science, Vol. 15, Amsterdam, The Netherlands, 2011, pp. 521-529.

Braun, D. D., 2022, Pleistocene Evolution of the Slippery Rock Creek Gorge. in, Dating in the Pleistocene, guidebook, 86th Annual Field Conference of Pennsylvania Geologists, Titusville, PA, this volume.

D'Urso, Gary J., 2000, Revised glacial margins and Wisconsin meltwater paleoflood hydrology in Slippery Rock Creek basin, central western Pennsylvania, unpublished PhD dissertation, West Virginia University, 174 p.

Fleeger, G. M., Bushnell, K. O., and Watson, D. W., 2003, Moraine and McConnells Mill State Parks, Butler and Lawrence Counties—Glacial lakes and drainage changes, with an addendum on Muddy Creek oil field by Carter, K. M., and Sager, Kelly (2010): Pennsylvania Geological Survey, 4th ser., Trail of Geology 16–004.0, 18 p. [Available online.]

Fleeger, Gary M., 1984, Dating the formation of the Slippery Rock Gorge, Pennsylvania Geology, v. 15, no. 3, pp. 8 – 11.

Hancock, G. and Kirwan, M., 2007, Summit erosion rates deduced from 10Be: Implications for relief production in the central Appalachians: Geology, 35, 89-92, doi: 10.1130/G23147A.1.

Leverett,, Frank, 1902, Glacial formations and drainage features of the Erie and Ohio basins, US Geological Survey, Monograph 41, 802 p.

Pazzaglia, F. J., Kurak, E., and Shaulis, J., 2021, Geology of Ohiopyle State Park and the Laurel Highlands of southwestern Pennsylvania, Stops 3 and 5, in Anthony, ed., Geology of Ohippyle State Park and the Laurel Highlands of southwestern Pennsylvania: Field Conference of Pennsylvania Geologists Guidebook 85, 25-29; 5-40.

Peck, Ralph B and Don U. Deere, 1964, Report of proposed Muddy Creek reservoir, Butler County, Pennsylvania, unpublished report, accessed from the Peck Library, Norwegian Geotechnical Institute, File J779, 34 p.

Portenga, E.W., Bierman, P.R., Rizzo, D.M., and Rood, D.H., 2013. Low rates of bedrock outcrop erosion in the central Appalachian Mountains inferred from in situ 10Be. Geological Society of America Bulletin 125. p. 201–215. DOI:10.1130/B30559.1.

Preston, Frank W., 1950, Tour II- Glacial foreland of northwest Pennsylvania, Field Conference of Pennsylvania Geologists, 16th annual meeting, Pittsburgh, PA, pp. 11 - 36.

Preston, Frank W., 1977, Drainage changes in the late Pleistocene in central western Pennsylvania, Carnegie Museum of Natural History, Pittsburgh, PA, 56 p.

Shepps, V. C., White, G. W., Droste, J. B., and Sitler, R. F., 1959, Glacial geology of northwestern Pennsylvania: Pennsylvania Geological Survey, 4th ser., General Geology Report 32, 59 p. [Available online.]

Simoneau, M., F.J. Pazzaglia, and G.M. Fleeger, 2022, Pleistocene drainage reversals and gorge cutting at the Laurentide ice margin in northwestern Pennsylvania interpreted from new cosmogenic exposure and luminescence ages, in, Dating in the Pleistocene, guidebook, 86th Annual Field Conference of Pennsylvania Geologists, Titusville, PA, this volume.

Wagner, W. R., Craft, J. L., Heyman, L., and Harper, J. A., compilers, 1975, Greater Pittsburgh region geologic map and cross sections: Pennsylvania Geological Survey, 4th ser., Map 42, 4 sheets, scale 1:125,000. [Available online.]

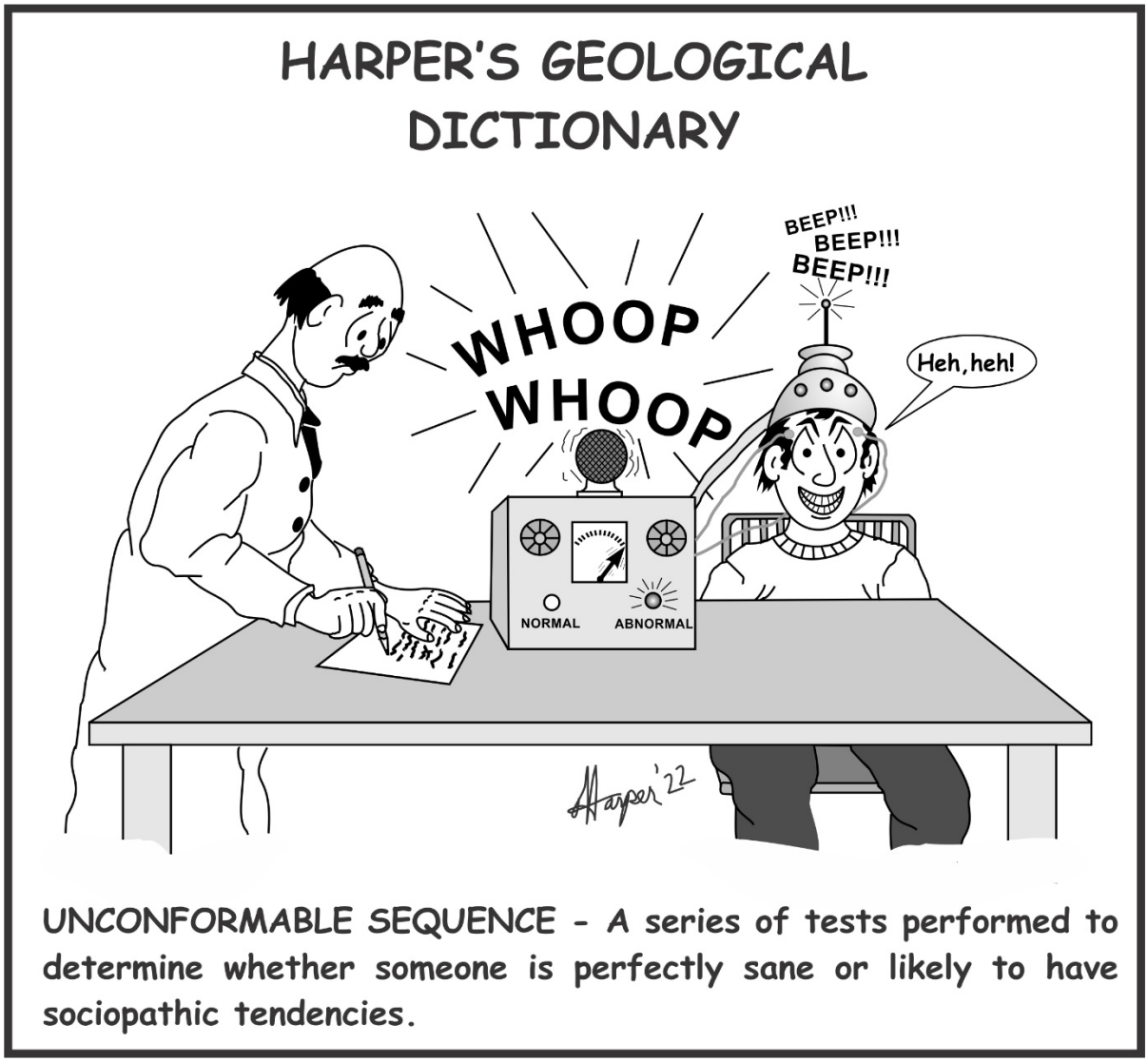

Point of Interest: There is significant disagreement on the origins of Lawrence County's name. Even the county government and their board of tourism disagree! The main consensus is that Lawrence County was either named for Captain James Lawrence, a hero in the war of 1812, or the USS Lawrence, a 493-ton ship named for the captain. Captain Lawrence is well-known for his last words, "Don't give up the ship!" This saying is still a popular battle cry in the US navy and was the motto and flag inscription of the USS Lawrence.

POI Sources:

Lawrence County, 2022, The History of Lawrence County, Pennsylvania, https://lawrencecountypa.gov/history-lawrence_county/.

Visit Lawrence County, n.d., Visit Lawrence County, Pennsylvania – Simply Beautiful!, https://www.visitlawrencecounty.com/about-lawrence-county/history-of-lawrence-county/.

Gannett, H., 1905, The Origin of Certain Place Names in the United States, U.S. Government Printing Office, https://books.google.com/books?id=9V1IAAAAMAAJ&pg=PA182#v=onepage&q&f=false.

POI Figure Source:

Stuart, G., 1812, Oil on wood, 28.5 x 23.5, Painting in the U.S. Naval Academy Museum Collection, https://commons.wikimedia.org/w/index.php?curid=110019164.

CHEESEMAN SAND & GRAVEL PIT – STOP 8

GARY M FLEEGER – PENNSYLVANIA GEOLOGICAL SURVEY (RETIRED)
MICHAEL SIMONEAU – VERINA CONSULTING GROUP, LLC AND LEHIGH UNIVERSITY
FRANK J. PAZZAGLIA – LEHIGH UNIVERSITY
GARY J. D'URSO

40.938534 / -80.167146

Introduction

This sand and gravel pit has been studied for many decades. Richardson (1936) mapped this deposit as terminal moraine. Dr. Frank W. Preston identified it as terminal moraine (1950) and as a delta (1977). Preston led a stop in the 1950 Field Conference of Pennsylvania Geologists at this pit. This deposit is part of a larger complex of features that are critical to the interpretation of the glacial and drainage history (**Figure 8.1**).

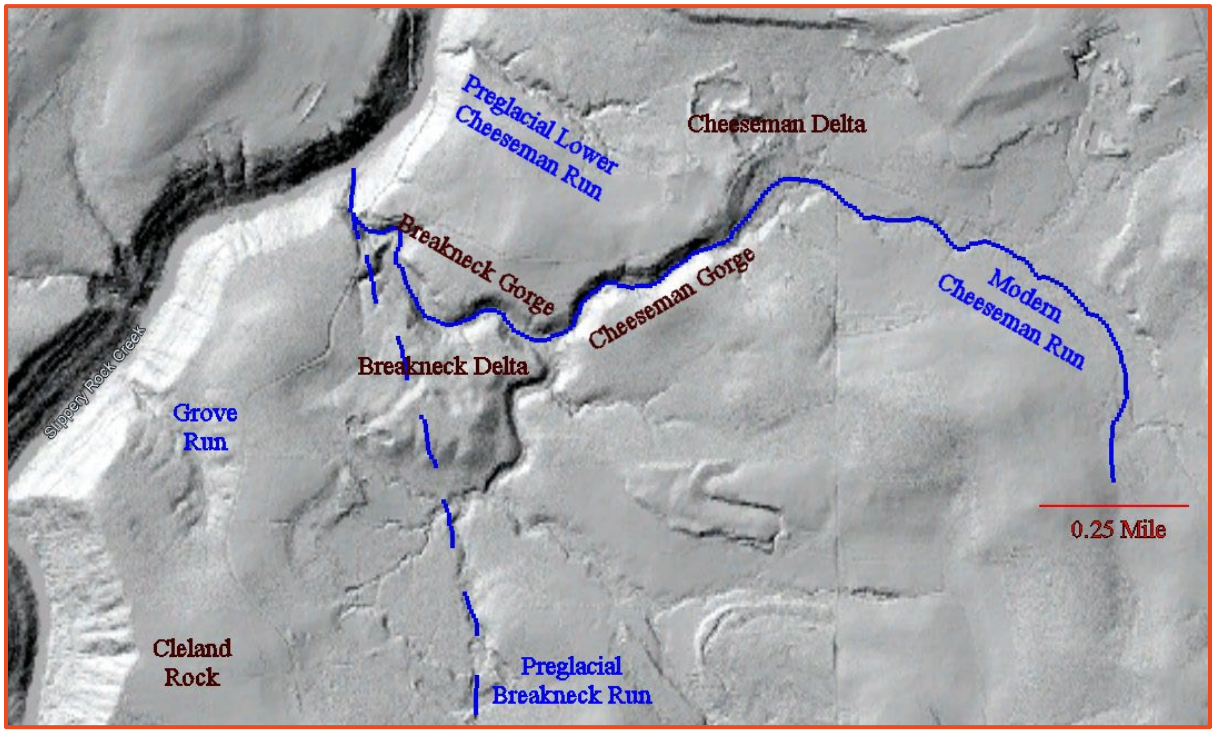

Figure 8.1 *Site location for Stop 8, with names used in text. Base map is the hillshade image derived from LiDAR.*

Description

This pit is in what I (Fleeger) am calling the Cheeseman delta. The top of the delta is at about elevation 1250 feet. Based on projecting the gradient of preglacial Cheeseman Run, I estimate the thickness of the deposit to be up to 80 feet.

A half mile to the southwest is another sand and gravel deposit that I refer to as Breakneck delta. The top of Breakneck delta is 1260 feet, 10 feet higher than that of Cheeseman delta. It has a couple of long-abandoned sand and gravel pits (one appeared to be active in the 1939 aerial photography) that are now completely overgrown with a mature forest. Based on projecting the gradient of preglacial Breakneck Run, this deposit is estimated to be up to 100 feet thick.

Fleeger interprets the Cheeseman and Breakneck deltas as having prograded from the Titusville glacier front just to the north into a proglacial lake, designated by Preston (1977) as Lake Prouty.

Lake Prouty is one of the pro-glacial lakes that Preston (1977) identified in this area (**Figure 8.2**). Lake Edmund occupied the upper Slippery Rock basin, Lake Watts the Muddy Creek basin, and Lake Prouty, the Cheeseman and Breakneck Runs basins.

Sitler (1957) mapped the glacial border adjacent to this site, and Shepps et al (1959) identified that border as Inner Illinoian, now named Titusville (White et al, 1969). It is a Gilbert-type delta with well developed foreset (**Figure 8.3**) and topset beds. The topset bed here is till-like, very coarse, poorly sorted, and contains numerous cobbles (**Figure 8.4**), suggesting that we are likely within the glacier margin, and the Titusville glacier overrode the Cheeseman delta.

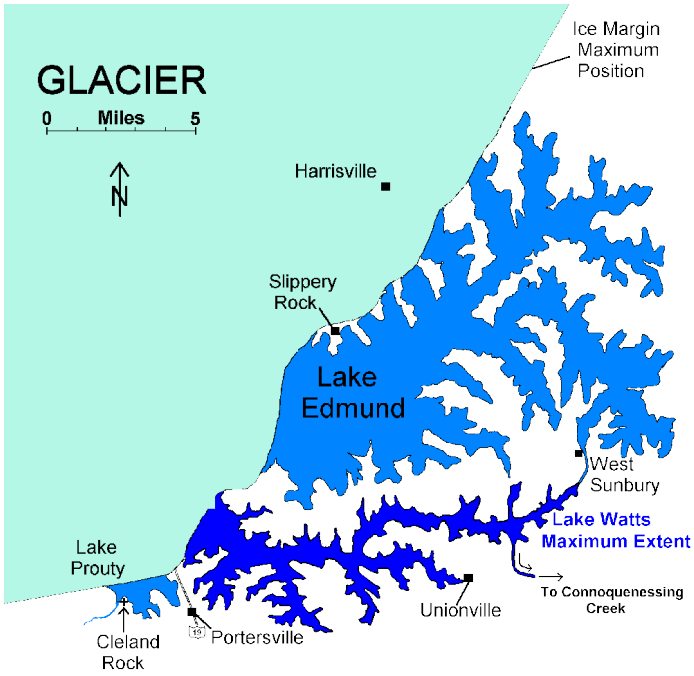

Figure 8.2. *Distribution of glacial Lakes Watts and Edmund at the maximum advance of the damming glacier. Modified from Preston (1977).*

The pits in the Breakneck Delta are totally overgrown. The park manager has recently agreed to bring in their backhoe to expose a section for description and sampling for OSL age determination, but we were unable to get that information in time for inclusion in the guidebook. As best as could be determined in the 1980s, it is mostly sand and fine gravel, although cobbles, many erratic, litter the ground in the abandoned pits. The deposit has several depressions in the surface that have been described as kettles (Preston, 1977). By the 1950 aerial photography, both pits in the Breakneck delta were abandoned, and the Cheeseman pit was active. The owners of the Cheeseman pit have used it periodically since.

Figure 8.3. *Foreset sand and gravel beds in the Cheeseman delta. View is to the west. Hammer for scale. A sample for OSL dating was taken in 2018 to the left of this view.*

Figure 8.4. *Coarse, unsorted topset beds in Cheeseman delta on the north side of the Cheeseman pit, appear to be Titusville Till deposited after overriding the delta.*

Conclusions regarding the origin of these deposits, and their significance to the origin of the Slippery Rock Gorge are preliminary, since we have not yet been able to study the Breakneck delta.

Preston (1977) considered the two sand and gravel deposits to have been originally parts of the same delta, with the intervening area eroded by modern Cheeseman Run; however, some characteristics of the two sand bodies suggest that they may not be the same deposit.

- The elevation of the surface of the two deposits is different, suggesting different lake levels when the two deltas were deposited, and therefore, they formed at different times- either different glaciations or different phases of the same glaciation. Alternatively, because the top sediment in the Cheeseman delta appears to be till (**Figure 8.3**), perhaps here has been erosion of 10 feet of the deltaic sediments by overriding ice, and the two deltas were originally the same elevation.
- The Cheeseman and Breakneck deltas are in adjacent valleys, with a divide between them. The divide between them ranges today between 1256 and 1238, partly lower than the top of Cheeseman delta and completely lower than the top of Breakneck delta. The divide was breached when Cheeseman Run was diverted into the Breakneck Run valley by the Cheeseman delta, creating the Cheeseman gorge, so it is post Cheeseman delta. Its age relative to Breakneck delta is unknown.
- There appears to maybe be a difference in dissection of the two deposits. A significant portion of the Cheeseman deposit has been eroded by Cheeseman Run (at the diversion into Cheeseman gorge) and a small tributary. The Breakneck deposit shows less apparent dissection.
- Breakneck delta blocks the pre-glacial Breakneck Run, diverting it into Breakneck gorge around the east and north sides of the Breakneck delta.

Age of Deltas

Because of its association with the mapped Titusville Till border, Fleeger (1984) interpreted the age of the Cheeseman delta as Titusville in age. The Titusville age had been estimated as 145,000 ± 25,000 years (late Illinoian), based on thermoluminescene dates of the correlative Millbrook Till in the Scioto sublobe at a site in north-central Ohio (Totten and Szabo, 1987, Fleeger, 2022); however, Preston (1977), D'Urso (2000), and D'Urso et al (2004) interpreted this deposit as Late Wisconsinan in age. Preston's interpretation is based on the youthful appearance of the Slippery Rock Gorge, and D'Urso's is based on depth of oxidation and leaching in the deposit, and the degree of weathering of the granitic clasts. In 2018, we took a sand sample from this pit for IRSL (infra-red stimulated luminescence) dating (**Figure 8.5;** see **Table 8.1**, Simoneau, Pazzaglia and Fleeger, Pleistocene Drainage Reversals article, this guidebook). The IRSL date is 140,000 ± 23,000 years (Simoneau, 2022), confirming the 1987 thermoluminescence date. Lake Prouty therefore existed as an ice marginal lake during the maximum advance of the Illinoian Titusville glacier.

Figure 8.5. *IRSL sample location on the west wall of the Cheeseman pit.*

Table 8.1. *OSL age and dose rate information.*

Sample	USU number	Lat	Long	Elev (m)	Method[1]	Number of aliquots[1]	Dose rate (Gy/kyr)	Fading Rate g_{2days} (%/decade)	Equivalent Dose[2] ±2σ (Gy)	Age[3]±2σ(kyr)
MMC	USU-2981	40.93933	-80.16634	375	IRSL	16(18)	2.85±0.13	2.4±0.3	316.1±44.0	140±23
WL-1	USU-3550	40.99696	-80.08162	382	OSL	20(35)	0.9±0.04	N/A	17.89±7.78	19.94±4.84
WL-3	USU-3551	40.99261	-80.07931	388	OSL	35(53)	0.91±0.04	N/A	23.0±5.66	25.41±4.61

1 = Age analysis using the single-aliquot regenerative-dose procedure of Murray and White (2000) on 1-2 mm small-aliquots of quartz sand. Number of aliquots used in age calculation and number of aliquots analyzed in parentheses.

2 = Equivalent dose (De) calculated using the minimum age model (MAM) of Galbraith and Roberts (2012).

3 = IRSL age on each aliquot corrected for fading following the method by Auclair et al., (2003) and correction model of Huntley and Lamothe (2001).

Sample	USU number	Depth (m)	In-situ H2O (%)[1]	Grain size (μm)	K(%)[2]	Rb (ppm)[2]	Th (ppm)[2]	U(ppm)[2]	Cosmic (Gy/ka)
MMC	USU-2981	5	3.6	125-212	0.87±0.02	37.5±1.5	6.3±0.6	1.6±0.1	0.12±0.01
WL-1	USU-3550	15	3.6	150-250	0.5±0.01	22.1±0.9	3.1±0.3	0.87±0.02	0.047±0.005
WL-3	USU-3551	15	3.4	150-250	0.52±0.01	20.9±0.8	3.0±0.3	0.87±0.02	0.047±0.005

1 = Assumed 5.0±2.0% for samples as moisture content over burial history.

2= Radioelemental concentrations determined using ICP-MS and ICP-AES techniques; dose rate is derived from concentrations by conversion factors from Guerin et al. (2011)

Breakneck gorge

The Breakneck gorge between the two deltas is unique for tributaries to the Slippery Rock Gorge. Within the Breakneck gorge, modern Cheeseman Run and a tributary have four characteristics that are different from other similar-sized streams flowing into the Slippery Rock Gorge.

1. While most streams essentially fill a narrow valley bottom, lower Cheeseman Run and tributary in Breakneck gorge meander across a valley bottom up to five times the stream width (**Figure 8.6**).

Figure 8.6. *Cobble bedload in alluvial bars in the Breakneck gorge. Note that the valley bottom is several times the width of the stream, and boulders are rare.*

2. Most streams have a series of small waterfalls where they cross resistant beds and many boulders in the bottom of the valleys. Breakneck gorge has one, very small waterfall, just upstream from the mouth of the Cheeseman gorge, which may be a knickpoint migrating upstream from the mouth of Cheeseman gorge. There are no others until it reaches the top of the Homewood Sandstone several hundred yards above Breakneck Falls.
3. The bottom of the Breakneck gorge is eroded below the delta deposits into bedrock and is largely free of large boulders and has a cobble bedload (**Figure 8.6**) in most places. In contrast, most tributaries to the Slippery Rock Gorge are boulder-choked.
4. Other streams flowing into the Slippery Rock Gorge enter the gorge over waterfalls at or near the top of the Homewood Sandstone (e.g. Alpha Falls, Kildoo Falls (**Figure 8.7**). Modern Cheeseman Run has eroded 30+ ft of the Homewood Sandstone (**Figure 8.8**) before entering the Slippery Rock Gorge at Breakneck Falls at elevation 1,048 ft.

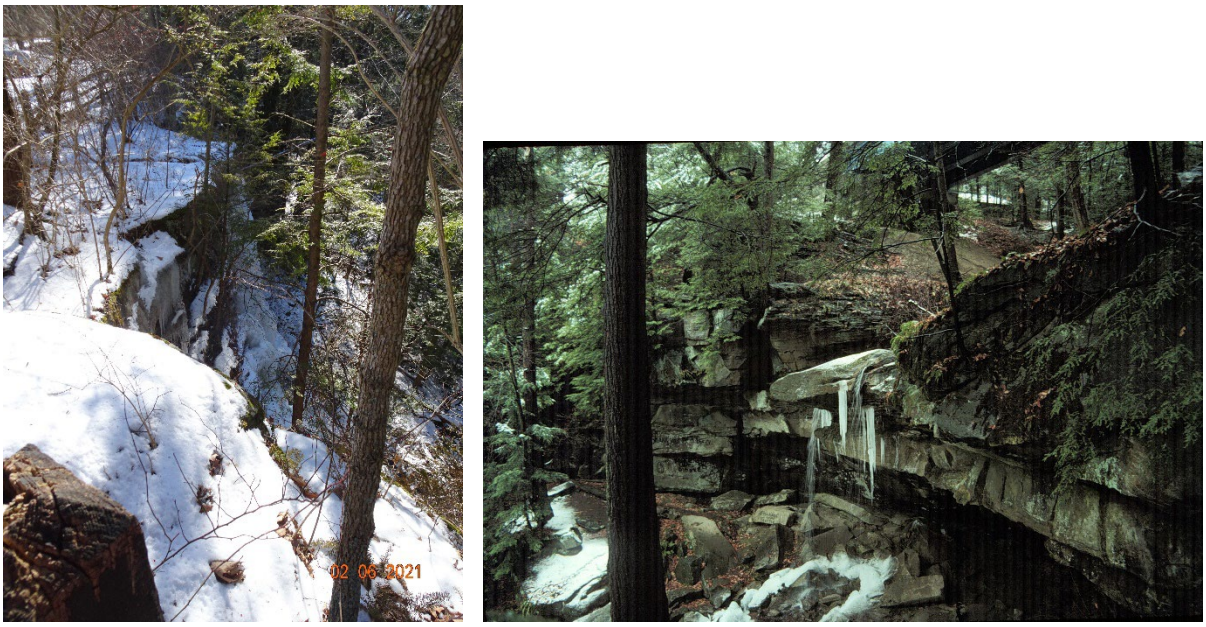

Figure 8.7. *Minimal erosion of the Homewood sandstone at Alpha Falls (left) and Kildoo Falls (right).*

Figure 8.8. *30+ feet of erosion of Homewood sandstone at Breakneck Falls.*

These characteristics suggest that the valley once had a much larger flow than the other tributaries to the Slippery Rock Gorge and/or maintained large flows for a longer period of time than other tributaries (Alpha Pass, Beta Pass, Muddy Creek). Such a flow would be consistent

with an ice marginal channel that had a clear outlet to the south down the Slippery Rock Gorge (**Figure 8.9**).

Significance of Lake Prouty

Preston (1977) hypothesized that Lake Prouty formed by glacier damming of McConnell Run, and that the lake level was controlled by lake overflow through the col at Cleland Rock (**Figure 8.10**). He interpreted that the lake overflow eroded the col downward and headward, creating the incipient Slippery Rock Gorge. The gorge was further extended northward and deepened by glacial lake breakout floods from Lakes Watts and Edmund as successively lower drainage passes were uncovered during glacier retreat.

We have not been able to determine if the dam creating Lake Prouty was as described by Preston (1977) or if the gorge had been eroded earlier (earlier glaciation or pre-glacial). We would expect the Cleland Rock col to have eroded to lower than 1250 feet during two or more earlier glaciations, which would also have created lakes in the McConnells Run valley and drained through the col. Lake Prouty could also have formed by the damming of Cheeseman and Breakneck Runs by a small lobe of the Titusville glacier extending down the Slippery Rock valley. The interpretation of Breakneck gorge as an ice-marginal channel requires only that when the lake drained, that there was an open outlet to the south in the Slippery Rock valley. Perhaps future study of the Breakneck delta will provide additional evidence to help resolve this issue.

Does this tell us anything about the origin of the Slippery Rock Gorge?

Scenario 1

The Slippery Rock Gorge is pre-Titusville (or pre-glacial), and Breakneck and Cheeseman Runs were dammed by a lobe of ice extending down the Slippery Rock Gorge. Lake Prouty overflow is through the Grove Run valley and into Slippery Rock Creek.

- The elevation of the Grove Run col is about 18 feet higher than the top of the Cheeseman delta, suggesting that it did not control the level of the lake in which Cheeseman delta was deposited. It is only 8 feet higher than Breakneck delta, and might have been able to control the elevation of the lake that deposited Breakneck delta.
- When the glacier lobe retreats enough to drain Lake Prouty, the ice-marginal Breakneck Gorge can be eroded.
- If the ice is retreating, the ice margin would likely not be stable long enough to remain in that position for very long, and an ice-marginal Breakneck gorge is less likely to be eroded.

Scenario 2

The Slippery Rock Gorge does not yet exist, and the col is at 1250 or 1260 feet. Lake Prouty forms by a glacier dam across the McConnell Run valley to the north. Lake Prouty overflow is through the Cleland Rock col into Wurtemburg Run (**Figure 8.10**).

- Overflow through the Cleland Rock col erodes the col downward and headward (north), extending Wurtemburg Run and reducing McConnell Run, creating the incipient Slippery Rock Gorge.
- Once the col migration is far enough to reach the mouth of Breakneck Run, Lake Prouty drains into the south-flowing Wurtemburg Run.
- No glacial retreat is required to drain Lake Prouty, and a stable ice front can erode the ice-marginal Breakneck gorge.

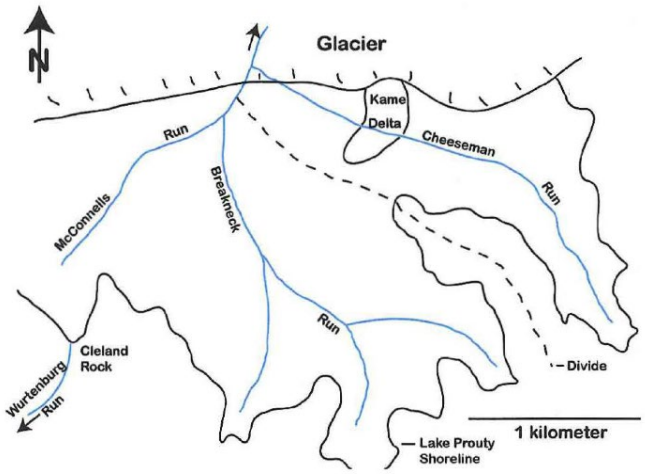

Figure 8.9. A) Pre-glacial drainage. Lake Prouty is formed ahead of the advancing glacier. Lake Prouty's spillway is at the Cleland Rock col into Wurtemburg Run. Alternatively, the Cleland Rock col may have already migrated north during prior glaciations, and Cheeseman and Breakneck Runs were dammed directly by a lobe of Titusville ice extending down the Slippery Rock valley. Cheeseman delta builds into Lake Prouty. Divide is that between Cheeseman and Breakneck Runs.

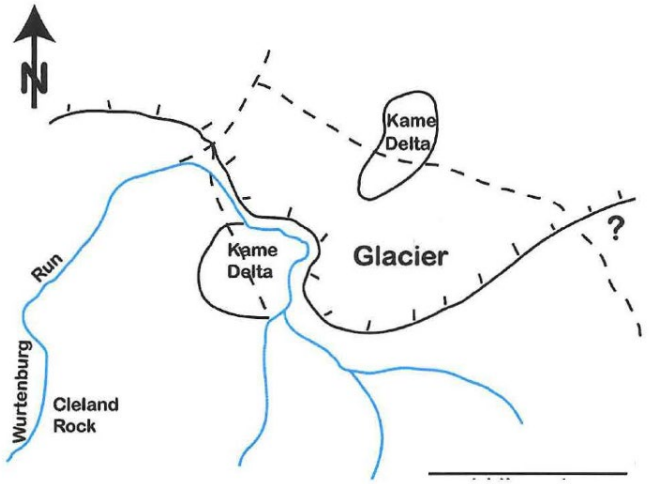

Figure 8.9. B) Maximum advance of glacier. Overridden Cheeseman delta depositing the till at the top. Breakneck delta builds into Lake Prouty. Ice marginal channel forms after Lake Prouty drains, either by migration of the Cleland Rock col or by retreat of the ice lobe in the Slippery Rock kvalley. Dashed lines = former course of pre-glacial Cheeseman and Breakneck Runs.

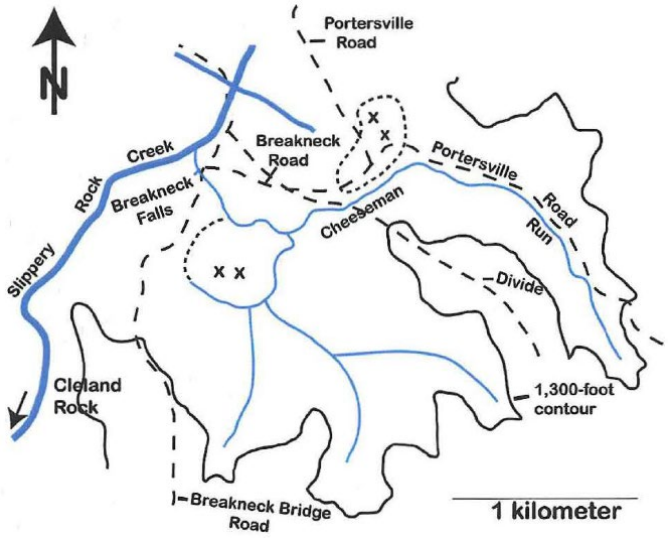

Figure 8.9. C) Present drainage. After retreat of the glacier, Cheeseman Run is diverted into the Breakneck Run valley because it's old course is blocked by the Cheeseman delta. The old course of Breakneck Run is also blocked by the Breakneck delta. The ice marginal channel is maintained. X= gravel pit.

Several questions need to be answered:

1. Do the two deltas (Cheeseman and Breakneck) represent two periods of Lake Prouty formation, or were they deposited during two stages of the same lake? We are currently unable to answer this question.
2. Was Lake Prouty formed between the glacier front to the north and the Cleland rock col to the south, or was it dammed by a lobe of ice extending south in the Slippery Rock Creek/McConnell Run valley past the mouths of Cheeseman and Breakneck Runs? We are currently unable to answer this question.
3. If a lobe of ice dammed the runs, what controlled the lake levels? The col into Grove Run (1268 ft) is 8 feet higher than the top of Breakneck delta (1260) and 18 feet higher than the top of Cheeseman Delta (1250). This col might have controlled the lake when the Breakneck delta was deposited, but this is not as likely for the Cheeseman delta. Grove Run contains no gravel lag or streamlined bedrock that might suggest glacial lake overflow; however, its valley is wider than many Slippery Rock Gorge tributaries and is not so boulder choked.
4. Why is the modern Cheeseman Run valley through Breakneck gorge so wide, largely boulder free, and with a cobble bed?
5. Why did modern Cheeseman Run erode through much more Homewood sandstone than the other falls entering the Slippery Rock Gorge through hanging valleys?

References Cited

D'Urso, Gary J. (2000) Revised glacial margins and Wisconsin meltwater paleoflood hydrology in Slippery Rock Creek basin, central western Pennsylvania, PhD dissertation, West Virginia University, Morgantown, WV, 174 p.

D'Urso, Gary J., Patrick A. Burkhart, Jack Livingston, and Christine Iksic (2004) An examination of field methods for glacial margin mapping and paleoflood reconstruction in Slippery Rock Creek basin, western Pennsylvania, Pittsburgh Geological Society field trip guidebook, 28 p.

Fleeger, Gary M. (1984) Dating the formation of the Slippery Rock Gorge, PA Geology, v. 15, no. 3, pp. 8 – 12

Fleeger, Gary M. (2022) Dating Pleistocene Deposits of Northwestern Pennsylvania and Northeastern Ohio*, in,* Dating in the Pleistocene, 86th Annual Field Conference of Pennsylvania Geologists, Titusville, PA, this guidebook.

Preston, Frank W. (1950) Tour II- Glacial foreland of northwest Pennsylvania, Field Conference of Pennsylvania Geologists, 16th annual meeting, Pittsburgh, PA, pp. 11 - 36.

Preston, Frank W. (1977) Drainage changes in the late Pleistocene in central western Pennsylvania, Carnegie Museum of Natural History, 56 p.

Richardson, G.B. (1936) Geology and mineral resources of the Butler and Zelienople quadrangles, Pennsylvania, USGS Bulletin 873, 93 p.

Shepps, V.C, G.W. White, J.B. Droste, and R.F. Sitler (1959) Glacial geology of northwestern Pennsylvania, Pennsylvania Geological Survey, 4th series, General Geology Report 32, 59 p.

Simoneau, Michael, F.J. Pazzaglia, and G.M. Fleeger (2022) Pleistocene drainage reversals and gorge cutting at the Laurentide ice margin in northwestern Pennsylvania interpreted from new cosmogenic exposure and luminescence ages, *in,* Dating in the Pleistocene, guidebook, 86th Annual Field Conference of PA Geologists, Titusville, PA, this guidebook.

Sitler, Robert F. (1957) Glacial geology of a part of western Pennsylvania, PhD dissertation, University of Illinois at Urbana-Champaign, 120 p. PhD thesis

Totten, Stanley M and John P. Szabo (1987) Stop 5: Mt. Gilead Fairgrounds section, in, Stanley M. Totten and John P. Szabo, eds, Pre-Woodfordian stratigraphy of north-central Ohio, Midwest Friends of the Pleistocene 34th Field Conference, pp. 63 – 67.

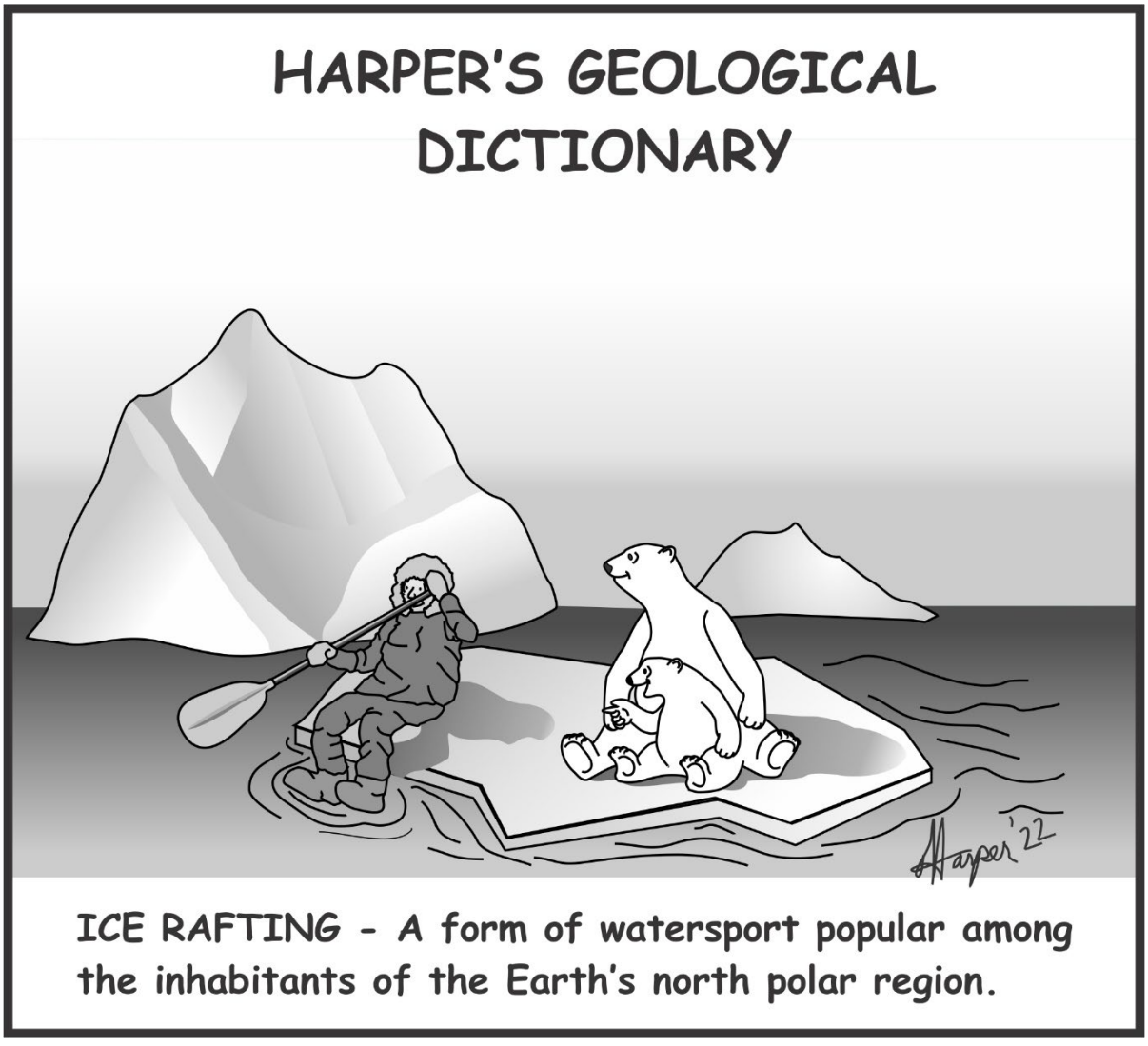

STOP 9: SEDIMENTOLOGY OF THE JACKSONVILLE ESKER – DELTA COMPLEX IN WESTERN PENNSYLVANIA

KATHRYN TAMULONIS – Allegheny College
JOCELYN SPENCER – SNYDER BROTHERS, INC.
FRANK PAZZAGLIA – LEHIGH UNIVERSITY
CONTRIBUTORS:
NOELLE KID, ZACHARY COLE, AND GARY FLEEGER – PENNSYLVANIA GEOLOGICAL SURVEY (RETIRED)

41.0047023 / -80.08402586

Introduction

The Jacksville esker-delta complex is located south of Slippery Rock, Pennsylvania and is composed of the 14.5-km-long Wisconsinan Jacksville Esker (also called the Miller or West Liberty Esker) that enters a kame delta. These delta deposits extend across Black Run Valley, and lacustrine sediments are located south of the delta. The complex was deposited approximately 23,000 years ago during the Kent glaciation (**Figure 9.1**; Fleeger and Lewis-Miller, 2011).

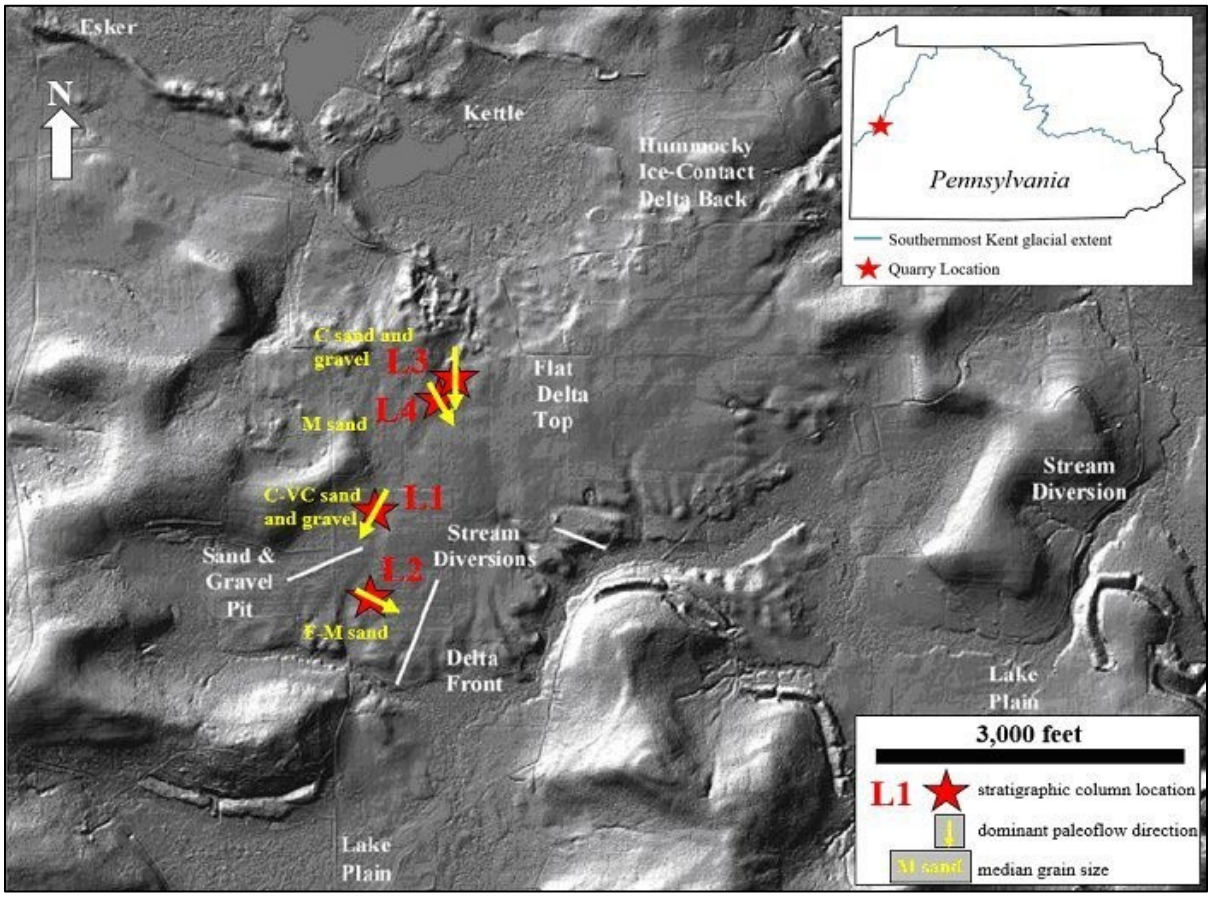

Figure 9.1. *Locations of the Glacial Sand and Gravel Quarry and sample locations (L1-L4) within the quarry pit. The dominant paleoflow direction and mean grain size for each stratigraphic column are represented by yellow arrows and yellow text, respectively. F = fine sand, M = medium sand, C = coarse sand, VC = very coarse sand.*

The objectives of this on-going study include:

1. Determining the esker/delta complex sediment distribution at proximal and distal locations (relative to the retreating glacier),
2. Identifying the sedimentary environments that composed the complex,
3. Interpreting sediment provenance, and
4. Understanding glacial dynamics and drainage patterns in the study area.

This site was visited by the 2011 NE-NC section of GSA (Fleeger and Lewis-Miller, 2011), and the reader is referred to that guidebook for additional details on the geology of the site.

Lithology

The internal composition and structure of the Jacksville esker-kame delta complex is exposed at the Glacial Sand and Gravel Company quarry, which opened in 2009. Due to the nature of quarry operations, new portions of the complex are continuously exposed as well as removed. Between 2019 and 2021, four separate locations (L1, L2, L3, and L4; **Figures 9.1, 9.2, 9.4, 9.6, and 9.8**) within the exposed kame delta sediments in the quarry were described, sampled, and analyzed. At each location, samples within individual beds were collected and sieved for sediment size distribution, and the lithology of the gravel fraction was identified. Delta foreset bed orientations were measured to determine paleoflow direction, and stratigraphic columns were generated (**Figures 9.3, 9.5, 9.7, and 9.9**). **Table 9.1** summarizes the sampling frequency, median grain size, foreset bed orientation, and dominant gravel lithology for each of the sample locations. For this stop, the stratigraphic columns are described from the most proximal sample location (L3) to the most distal location (L2).

Figure 9.2. *The proximal L3 sample location with gravel and sand delta forest beds overlain by bed that fines upward from gravel to sand and silt.*

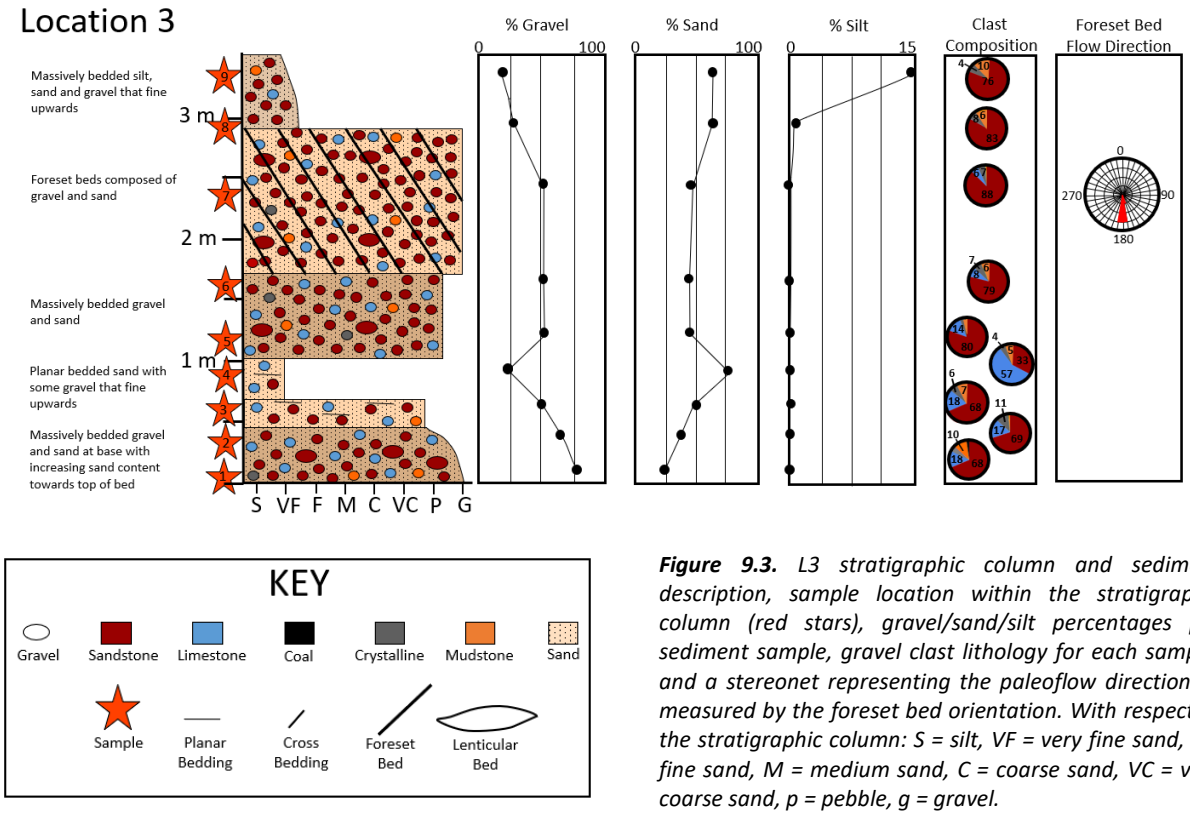

Figure 9.3. *L3 stratigraphic column and sediment description, sample location within the stratigraphic column (red stars), gravel/sand/silt percentages per sediment sample, gravel clast lithology for each sample, and a stereonet representing the paleoflow direction as measured by the foreset bed orientation. With respect to the stratigraphic column: S = silt, VF = very fine sand, F = fine sand, M = medium sand, C = coarse sand, VC = very coarse sand, p = pebble, g = gravel.*

L3 is primarily composed of medium to coarse-grained sand with some gravel dominated beds, and the gravel fraction lithology is dominated by sandstone. Sedimentary structures include foreset beds, fining upward sequences, massive bedding, and planar bedding. The paleoflow directions at L3, as recorded by the foreset bed orientation, is due south (**Figures 9.1, 9.2 and 9.3; Table 9.1**). Crystalline (igneous and metamorphic) clasts do not exceed 11% and generally decrease up-section.

Figure 9.4. *L4 sample location with medium-grained sand and coal gravel of the delta forest beds. Note the relatively abundant bird nests at the top of the exposure.*

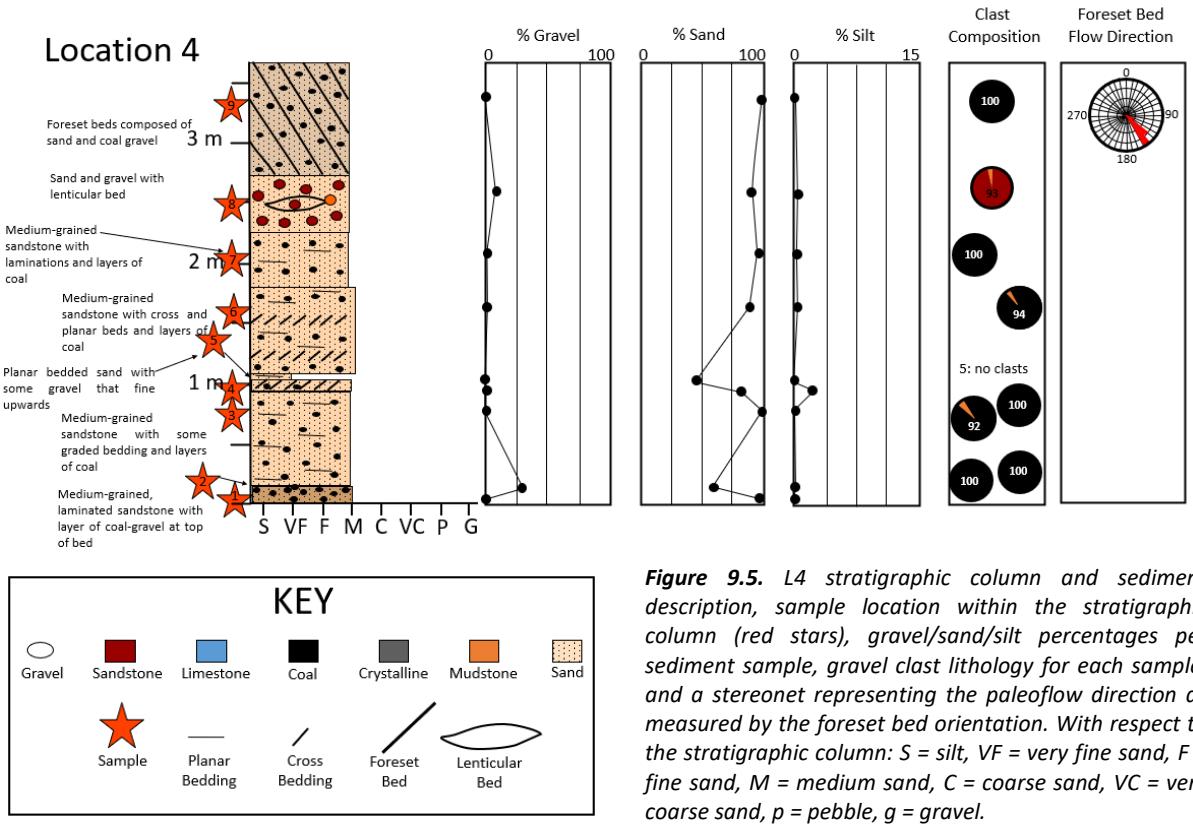

Figure 9.5. *L4 stratigraphic column and sediment description, sample location within the stratigraphic column (red stars), gravel/sand/silt percentages per sediment sample, gravel clast lithology for each sample, and a stereonet representing the paleoflow direction as measured by the foreset bed orientation. With respect to the stratigraphic column: S = silt, VF = very fine sand, F = fine sand, M = medium sand, C = coarse sand, VC = very coarse sand, p = pebble, g = gravel.*

L4 is the second most-proximal location and is composed of very fine to medium-grained sand and gravel. Sedimentary structures observed at this location include laminations, cross beds, a lenticular bed, planar beds, and foreset beds. The gravel fraction lithology is nearly all coal except for the lenticular bed near the top of the outcrop that is primarily composed of sandstone gravel. The paleoflow direction is to the southeast (**Figures 9.1, 9.4 and 9.5; Table 9.1**).

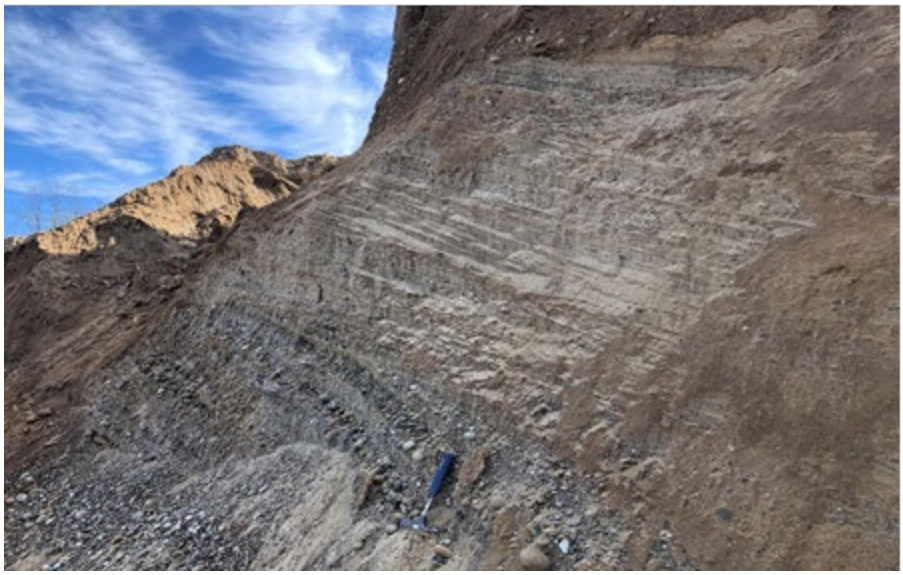

Figure 9.6. *L1 sample location with a lenticular gravel bed overlain by delta forest beds composed of medium to coarse sand. Note rock hammer for scale.*

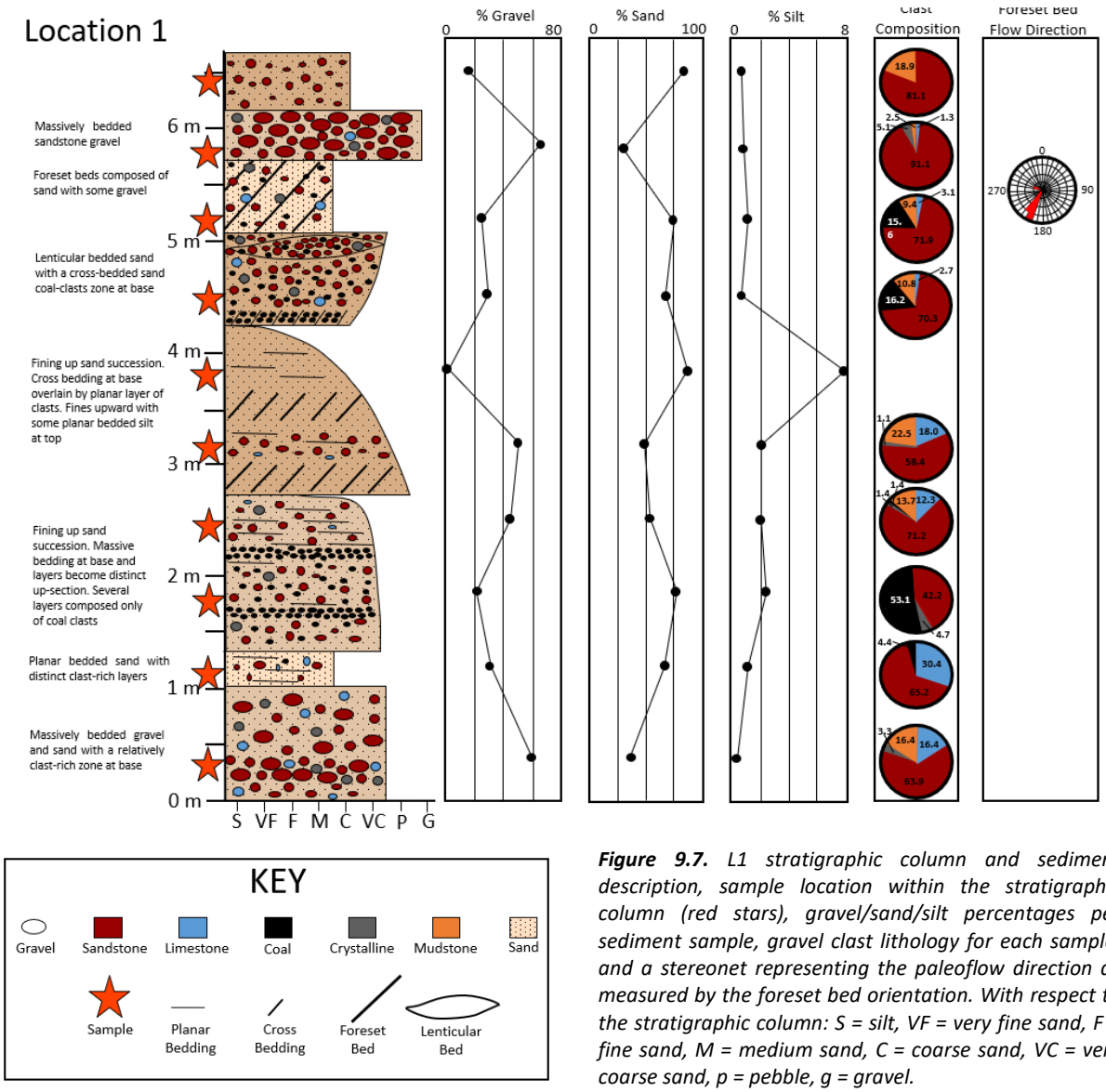

Figure 9.7. *L1 stratigraphic column and sediment description, sample location within the stratigraphic column (red stars), gravel/sand/silt percentages per sediment sample, gravel clast lithology for each sample, and a stereonet representing the paleoflow direction as measured by the foreset bed orientation. With respect to the stratigraphic column: S = silt, VF = very fine sand, F = fine sand, M = medium sand, C = coarse sand, VC = very coarse sand, p = pebble, g = gravel.*

L1 is a relatively distal sample location and resembles L3, as it is primarily composed of medium to coarse-grained sand with some gravel dominated beds (**Figures 9.1, 9.6 and 9.7; Table 9.1**), and the gravel lithology throughout the entire stratigraphic column is primarily sandstone. L1 has three beds with distinct layers composed solely of pebble-sized coal clasts, some of which are imbricated. Crystalline clasts do not exceed 5%. This stratigraphic column has the highest limestone gravel lithology occurrence at 30% and distinct layers within beds that are composed solely of coal gravel. The paleoflow direction at L1 is to the southwest (**Figures 9.1, 9.6 and 9.7; Table 9.1**).

Figure 9.8. *(Right) The distal L2 sample location with medium-grained delta forest sand with layers of gravel, including coal. Note grain-size card for scale.*

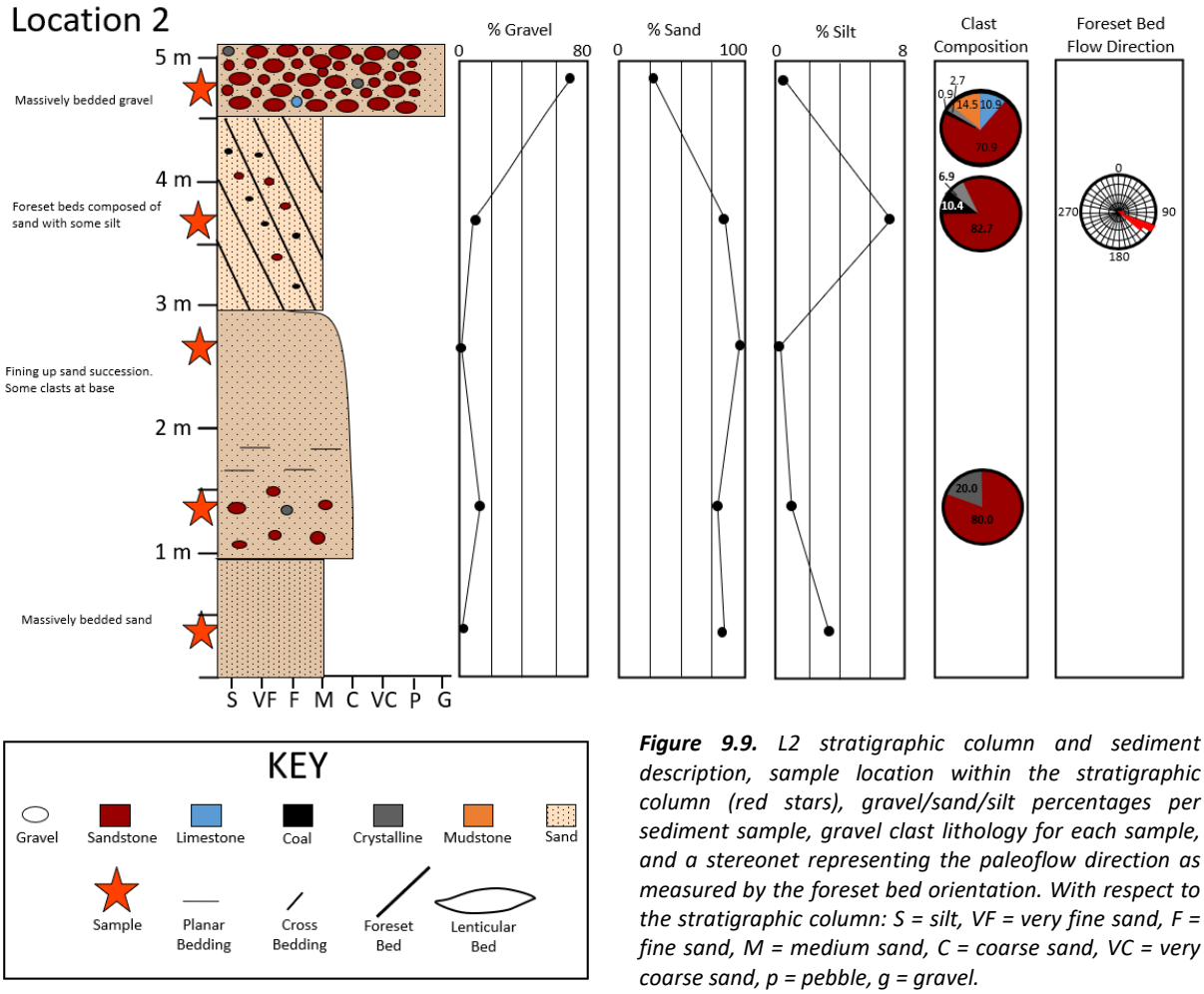

Figure 9.9. *L2 stratigraphic column and sediment description, sample location within the stratigraphic column (red stars), gravel/sand/silt percentages per sediment sample, gravel clast lithology for each sample, and a stereonet representing the paleoflow direction as measured by the foreset bed orientation. With respect to the stratigraphic column: S = silt, VF = very fine sand, F = fine sand, M = medium sand, C = coarse sand, VC = very coarse sand, p = pebble, g = gravel.*

L2 is the most distal sample location and is primarily composed of medium-grained sand with a gravel bed at the top of the outcrop. Gravel lithology is primarily sandstone, though crystalline clasts compose 20% of the gravel fraction near the base of the outcrop. The paleoflow directions at L2 is southeast (**Figures 9.1, 9.8, and 9.9; Table 9.1**).

Table 9.1. Summary of sample locations L1-L4 (see **Figure 9.1** for locations). F = fine sand, M = medium sand, C = coarse sand, VC = very coarse sand.

Location	Outcrop height (m)	Number of Samples	Median Grain Size	Dominant Gravel Lithology	Dominant Foreset Bed Flow direction
L1	~6.5	9	C-VC sand and gravel	sandstone	SW
L2	~5.0	5	F-M sand	sandstone	SE
L3	~3.5	9	C sand and gravel	sandstone	S
L4	~3.5	9	M sand	coal	SE

Deposition

Due to the varying orientations of the foreset beds, it likely that numerous outwash sources entered the kame-delta complex and/or the delta lobes changed orientation over time. Due to the dynamic nature of the quarry, the temporal relation among the stratigraphic columns has not yet been determined. Despite the proximity of L3 and L4, the contact between the respective foreset beds was not visible during field work. The differences between grain size, gravel lithology, and foreset bed orientation at L3 and L4 suggest that two separate lobes sourced the sediment despite the sample locations proximity.

The presence of coal pebble layers, abundant sandstone clasts, and general lack of crystalline clasts indicate that glacial drainage was locally organized around the ice margin, and erratics did not significantly contribute to the sediment load deposited during glacial retreat. Crystalline gravel lithologies do not exceed 11% and generally decrease up-section at L1, L2, and L3, suggesting that glacial erractic deposition decreased throughout the duration of the kame-delta complex deposition. Gross (1967) concludes that 50% of till material in northwest Pennsylvania is derived within 25 miles of the site of deposition, which is supported by the stratigraphic columns described in this study. The presence of coal pebble layers implies that coal gravel and sand are hydraulically equivalent, and the dominance of coal gravel and lack of crystalline gravel at L4 indicate that lobe of the kame-delta complex was locally sourced. The sediment size distribution trends do not follow the coarse to fine trend expected in a simple, single prograding delta scenario, though the most distal sediment at L2 is composed of relatively finer grained sediment. The varying foreset bed orientations support either or a combination of the following hypotheses: 1) a numerous outwash sources entered the delta complex, 2) these sources likely changed with time, and 3) several lobes composed the delta complex.

OSL Dating

In 2019, this site was sampled for OSL dating. Three samples were taken, two of which were dated (**Figure 9.10**), near L1 and L2.

The OSL ages obtained here are stratigraphically reversed (**Table 9.2, Figure 9.10**), caused by one or more of several possible reasons.

- incomplete bleaching and the grains carrying inheritance.
- WL-1 might have been from a higher delta lobe. Exposures in 2009 showed two superimposed sets of topsets-foresets (**Figure 9.11**). WL-3 may have therefore been deposited first in a lower set, and WL-1 later at a higher level over the older delta lobes. The sedimentological analysis has demonstrated no trend in grain size from proximal to distal, and varying foreset orientations, some of which do not come from the direction of the esker mouth, possibly because different delta lobes were being analyzed.
- Because of the OSL date uncertainties, it is possible that they are not actually reversed. Because of the uncertainties, WL-1 could be as old as 24.78 ka, and WL-3 could be as young as 20.8 ka.

The uncertainties are overlapping, so essentially OSL is here giving us the same age – LGM.

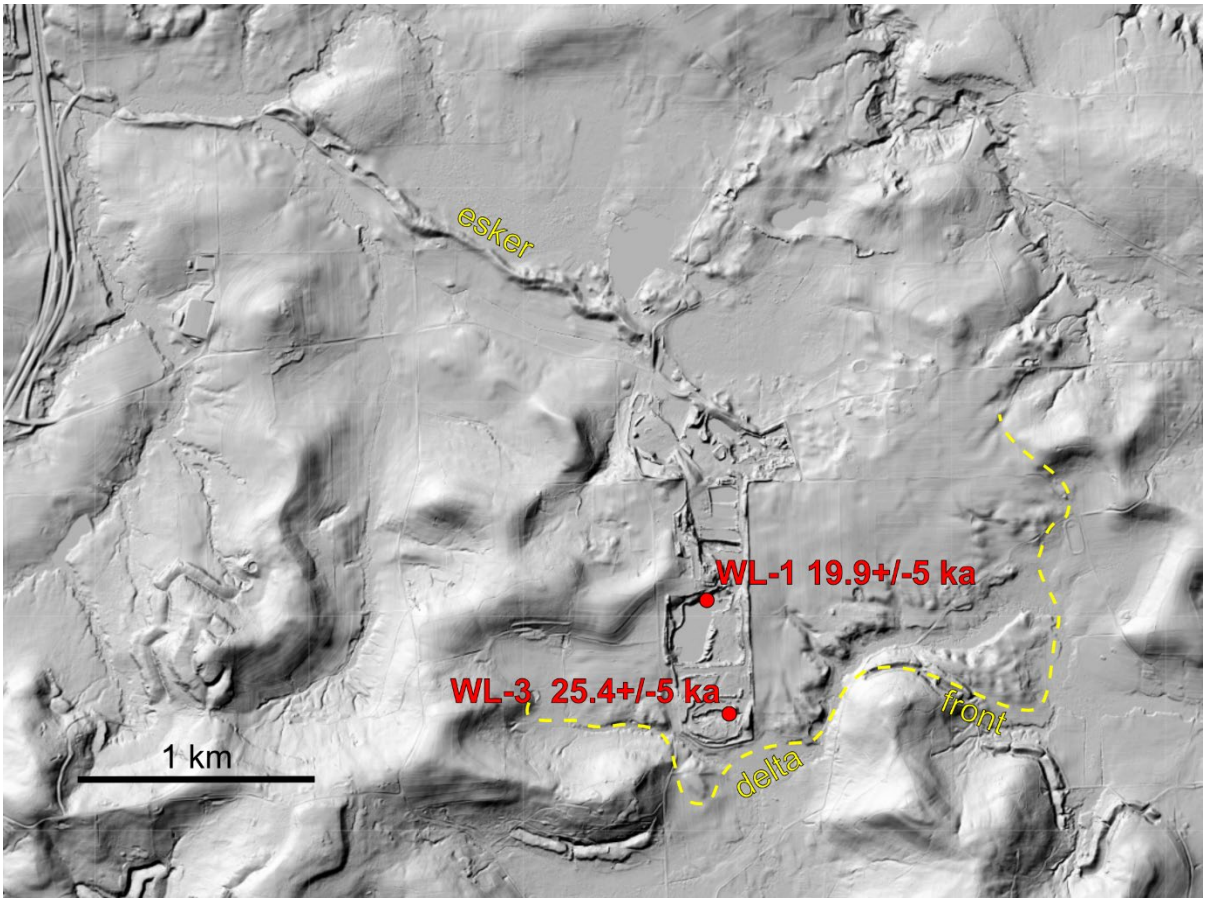

Figure 9.10. *Location of the OSL samples.*

Figure 9.11. *2009 photo of superimposed topset-foreset pairs.*

Table 9.2. *A) Luminescence Age Information.*

Sample	USU number	Lat	Long	Elev (m)	Method[1]	Number of aliquots[1]	Dose rate (Gy/kyr)	Fading Rate g_{2days} (%/decade)	Equivalent Dose[2] ±2σ (Gy)	Age[3]±2σ(kyr)
MMC	USU-2981	40.93933	-80.16634	375	IRSL	16(18)	2.85±0.13	2.4±0.3	316.1±44.0	140 ± 23
WL-1	USU-3550	40.99696	-80.08162	382	OSL	20(35)	0.9±0.04	N/A	17.89±7.78	19.94 ± 4.84
WL-3	USU-3551	40.99261	-80.07931	388	OSL	35(53)	0.91±0.04	N/A	23.0±5.66	25.41 ± 4.61

1 = Age analysis using the single-aliquot regenerative-dose procedure of Murray and Wintle (2000) on 1-2 mm small-aliquots of quartz sand.
Number of aliquots used in age calculation and number of aliquots analyzed in parentheses.

2 = Equivalent dose (De) calculated using the minimum age model (MAM) of Galbraith and Roberts (2012).

3 = IRSL age on each aliquot corrected for fading following the method by Auclair et al., (2003) and correction model of Huntley and Lamothe (2001).

Table 9.2. *B) Dose Rate Information.*

Sample	USU number	Depth (m)	In-situ H2O (%)[1]	Grain size (μm)	K(%)[2]	Rb (ppm)[2]	Th (ppm)[2]	U(ppm)[2]	Cosmic (Gy/ka)
MMC	USU-2981	5	3.6	125-212	0.87±0.02	37.5±1.5	6.3±0.6	1.6±0.1	0.12±0.01
WL-1	USU-3550	15	3.6	150-250	0.5±0.01	22.1±0.9	3.1±0.3	0.87±0.02	0.047±0.005
WL-3	USU-3551	15	3.4	150-250	0.52±0.01	20.9±0.8	3.0±0.3	0.87±0.02	0.047±0.005

1 = Assumed 5.0±2.0% for samples as moisture content over burial history.

2 = Radioelemental concentrations determined using ICP-MS and ICP-AES techniques; dose rate is derived from concentrations by conversion factors from Guerin et al. (2011).

References

Fleeger, G.M., and Lewis-Miller, J. 2011. Stop 1: Jacksville Esker, Delta, Lake Plain and Drainage Diversion Complex. in Szabo, J. Supplement to Geological Society of America Field Guide 20: Quaternary Geology of Northwestern Pennsylvania, p. 1-8.

Gross, D.L. and S.M. Moran (1971) Grain-size and mineralogical gradations within tills of the Allegheny Plateau, in Till/A Symposium, Ohio State University Press, pp. 251 - 274.

Point of Interest: This image shows Carnegie Museum botanist Otto Emery Jennings (1877-1964), for whom the Jennings Environmental Education Center is named. He is shown here with his wife, Grace Kinzer Jennings (d. 1957). Grace worked as a botany assistant at the Carnegie Museum. After they were wed, Otto and Grace accompanied one another on nearly every field excursion.

POI Source:

Smithsonian Libraries and Archives, n.d., Otto Emery Jennings (1877-1964) and Grace Emma Kinzer (d. 1957), https://www.si.edu/object/siris_arc_297448.

POI Figure Source:

Smithsonian Libraries and Archives, n.d., Otto Emery Jennings (1877-1964) and Grace Emma Kinzer (d. 1957), https://www.si.edu/object/siris_arc_297448

We would like to acknowledge our generous donors

Stephen Peterson
Dru Germanoski
Jim Shaulis
Gary Kribbs
Andrew Fetterman
Kent V. Littlefield
Mark B. Ioos, P.G.
Ed Meiser
Patrick Bowling
Natalie Thomas
Alexander J. Zdzinski
Tamra Schiappa
John Stiteler
Chris Oest
Joel Fradel
Fred Zelt
Tony Deluca
Jeff Ciocco
Barbara Rudnick
Mark Keim
Mark Bowers
Tim Davis
Michael Layton
Beverly Phillips
Bill Matulewicz
Christoper Duerr
Joan Hawk
Joe Lee
Bill Bragonier
Jackie Hokenberry
Tony Belfield
Jeff Walsh
Donald E. Wandling
Andrew Frishkorn
Rich Sichler
Dan Cross
Phil Getty
Dennis Noll
Jonathan Wallace
Bill Kochanov
Frank J Pazzaglia
Ed Layton
Lee Nageotte
Dan Martt

FCOPG THANKS YOU!

2022